

Dissertation zur Erlangung des Doktorgrades
der Fakultät für Chemie und Pharmazie
der Ludwig-Maximilians-Universität München

**INDUSTRIAL RAM EXTRUSION AS INNOVATIVE TOOL
FOR THE DEVELOPMENT OF BIODEGRADABLE
SUSTAINED RELEASE IMPLANTS**

Martina Sprengholz

aus

Eggenfelden

2014

Erklärung

Diese Dissertation wurde im Sinne von § 7 der Promotionsordnung vom 28. November 2011 von Herrn Prof. Dr. Gerhard Winter betreut.

Eidesstattliche Versicherung

Diese Dissertation wurde eigenständig und ohne unerlaubte Hilfe erarbeitet.

Waldkraiburg, 25. Mai 2014

Martina Sprengholz

Dissertation eingereicht am	03.06.2014
1. Gutachter	Prof. Dr. Gerhard Winter
2. Gutachter	Prof. Dr. Wolfgang Frieß
Mündliche Prüfung am	03.07.2014

FÜR MEINE ELTERN

ACKNOWLEDGMENTS



Lieber Herr **Prof. Dr. Gerhard Winter**, Sie waren in den letzten Jahren mein roter Faden. Unsere regelmäßigen fachlichen Gespräche haben mich motiviert und mir oftmals neue Perspektiven aufgezeigt. Ich danke Ihnen für Ihr Vertrauen und die Zeit, die Sie sich für mich und meine Arbeit genommen haben. Ich habe viel gelernt und mich - nicht nur in fachlicher Hinsicht - weiterentwickelt. Gerade in den letzten Monaten, die aufgrund der Doppelbelastung umso schwerer waren, haben Sie dafür gesorgt, dass ich mein Ziel nicht aus den Augen verliere. Vielen herzlichen Dank dafür!

Liebe **Kolleginnen und Kollegen aus München**, auch wenn ich nur gelegentlich „vorbeigeschaut“ habe - ihr habt mir immer das Gefühl gegeben, willkommen zu sein. Ihr seid mir mit Rat und Tat zur Seite gestanden und habt mir gezeigt, wie viel ein „Jetzt komm erst mal rein und mach die Tür hinter dir zu“ eigentlich bedeutet. Davon abgesehen danke ich euch für die „Ausflüge“ nach Malta und Istanbul und die wunderbare Zeit in den Bergen.

Lieber Herr **Christian Minke**, lieber Herr **Wolfgang Wünschheim**, ich danke Ihnen für die freundliche Unterstützung (und die flexible Terminfindung) bei den Versuchen am Rasterelektronenmikroskop und dem Röntgendiffraktometer.

Lieber **Thomas Bosch**, ich glaube, dir bin ich zu ganz besonderem Dank verpflichtet. Du warst mein „Ansprechpartner der Wahl“ für Proteine, Gefrier-trocknung und BET-Messungen und hast mich unterstützt, wo es nur ging. Schade, dass nur so wenige unserer gemeinsamen Versuche Eingang in diese Arbeit gefunden haben.

Lieber **Philipp Matthias**, ich danke dir für die Geduld und Gelassenheit, mit der du jede (!) meiner Fragen zum Thema DoE beantwortet hast.



Liebe **Dr. Nicoline Vermeulen**, als „direkte Betreuerin“ warst du von Anfang an für mich und meine Arbeit da. Ich danke dir für unseren Jour Fixe und dein offenes Ohr, wann immer es vonnöten war.

Lieber Herr **Dr. Heiko Spilgies**, liebe Frau **Dr. Sabine Hauck**, Sie haben (nacheinander) meine Arbeit von Seiten der Acino betreut. Ich bedanke mich für die zahlreichen fachlichen Gespräche und die Freiheit, die Sie mir beim Planen und Durchführen meiner Versuche gelassen haben - in einer Industriekooperation ist das nicht selbstverständlich.

Lieber **Alexander Blaß**, lieber **Michael Havemann**, liebe **Christiane Heß**, lieber **Martin Keller**, liebe **Lisa Rösler**, ihr alle wart mir in den letzten Jahren eine große Unterstützung. Ich habe gerne mit euch zusammengearbeitet und viel von euch gelernt. Für die Zukunft wünsche ich euch nur das Beste - egal, ob mit oder ohne GOXIMP und Konsorten.

Lieber **Stephan Kiendl**, du und dein Team, ihr wart das Tüpfelchen auf dem i. Jedes „Ich hab dir die Kryoröhrchen in die Schleuse gelegt“ war eine riesige Erleichterung, weil ich mir so den Umweg über die Produktion sparen konnte. Danke dafür! **Daniela Fischhaber, Alexandra Holzner, Angela Kemmer, Heidi Maier** und **Carola Schuster**, vielen herzlichen Dank für eure großartige Unterstützung, insbesondere auch bei den 39 Extrusionen, die für das DoE absolut unerlässlich waren.

Liebe **Irene Amann**, liebe **Constanze Henkel**, wenn ich in der Gestaltung meiner „Acknowledgments“ nicht so konsequent wäre, würde ich eure Namen sicherlich besonders hervorheben. Ich weiß nicht, wie viele Stunden wir beim gemeinsamen Pipettieren verbracht haben, aber es waren genug, um eine wunderbare Freundschaft entstehen zu lassen. Gerade zum Ende hin wart ihr Gold wert (und seid es noch immer).

Liebe **Kolleginnen und Kollegen der Acino**, ihr wart auf so vielfältige Art und Weise am Gelingen dieser Arbeit beteiligt. Ihr habt mich unermüdlich geschult, mir geduldig Geräte erklärt und mir Zeitfenster eingeräumt, die nie existiert haben. Dafür danke ich euch!

Liebe **Barbara Sprengholz**, lieber **Bernd Sprengholz**, liebe Mum, lieber Paps, euch ist diese Arbeit gewidmet - ohne Wenn und Aber und von ganzem Herzen. Ich danke euch für so vieles: Liebe, Vertrauen, Unterstützung, Geduld. Nicht zuletzt für ein Zuhause, in dem ich so unglaublich gerne bin, weil es meilenweit von „biodegradable sustained release implants“ entfernt ist.

Lieber **Ralph Sprengholz**, lieber Drops, einen besseren Bruder als dich könnte ich mir nicht vorstellen. Ich danke dir für die abendlichen Spaziergänge während meiner „ersten Schreibphase“ - es tut verdammt gut, zwischendurch Luft zu holen!

Liebe **Freunde**, liebe **Familie**, liebe **Kolleginnen und Kollegen der Aenova**, vielen ist es vielleicht gar nicht bewusst, aber ihr alle habt zum Gelingen dieser Arbeit beigetragen - auf welche Art und Weise auch immer (Spieleabende und stundenlange Gespräche am Telefon eingeschlossen). Schlicht und einfach, aber nicht weniger herzlich: DANKE!

Lieber **Jan Keller**, lass es mich mit den Worten der Sportfreunde sagen: „Will ich mal wieder mit dem Kopf durch die Wand, legst du mir Helm und Hammer in die Hand.“ Dafür (und für vieles mehr) danke ich dir von Herzen! Ich liebe dich.

Liebe Frau **Gerda Eibl**, bei Ihnen habe ich weit mehr gefunden als ein Dach über dem Kopf. Ich danke Ihnen für Ihre Herzlichkeit, Ihr Feingefühl und so manches Stück Kuchen. Wenn ich an meine Zeit in Schliersee zurückdenke, dann mit einem Lächeln im Gesicht.

TABLE OF CONTENTS

Chapter I Introduction	1
1 Overview of parenteral controlled release systems	1
1.1 Historical background	2
1.2 Different types	4
1.2.1 Implants	4
1.2.2 Microparticles	7
1.2.3 Nanoparticles	8
1.2.4 Oily solutions and suspensions	9
2 Poly(lactide-co-glycolide) - a magic (matrix) material?	11
2.1 Synthesis	11
2.2 Different types and their physico-chemical properties	13
2.3 Drug release from PLGA-based drug delivery systems	15
2.4 Biocompatibility	18
2.5 Current market situation	18
3 Lipids as alternative matrix materials?	21
3.1 Advantages and limitations in comparison to PLGA-based systems	22
3.2 Drug release from lipid-based drug delivery systems	24
3.3 Biodegradation	26
3.4 Biocompatibility	27
4 Overview of implant manufacturing techniques	29
4.1 Compression	29
4.2 Hot melt extrusion	29
4.2.1 Screw extrusion	30
4.2.2 Ram extrusion	31
4.3 Injection molding	32
4.4 Compression molding	33
4.5 Solvent casting	34
Chapter II Aims of the thesis	35

Chapter III Materials and methods	37
1 Materials	37
1.1 Oxybutynin	37
1.2 Polymers	37
1.3 Lipids	38
1.3.1 Triglycerides.....	38
1.3.2 Hydrogenated cocoglycerides.....	38
1.3.3 Monoglycerides	39
1.3.4 Acetylated glycerides.....	39
1.3.5 Macroglycerides.....	39
1.3.6 Phosphatidylcholines.....	40
1.4 Chemicals	40
1.4.1 Acids and bases	40
1.4.2 Buffers	40
1.4.3 Dyes.....	41
1.4.4 Standard substances.....	41
1.4.5 Immersion oil.....	41
1.4.6 Solvents	41
1.4.7 Gases	42
1.4.8 Ultrapure water	42
2 Methods.....	43
2.1 Implant manufacturing.....	43
2.1.1 Cryogenic grinding.....	43
2.1.2 Hot melt extrusion.....	43
2.1.3 Compression.....	44
2.1.4 Alternative manufacturing strategies	44
2.1.5 Sterilization.....	46
2.2 Concentration of oxybutynin.....	46
2.3 <i>In vitro</i> release studies.....	46
2.4 Investigations on the release mechanisms.....	47
2.4.1 pH measurements	47
2.4.2 Water uptake and mass loss.....	47
2.5 Mechanical properties.....	48

2.6	Investigations on surface morphology.....	48
2.6.1	Macroscopic appearance.....	48
2.6.2	Digital microscopy.....	48
2.6.3	Scanning electron microscopy.....	48
2.7	Thermo-optical analysis.....	48
2.8	Differential scanning calorimetry.....	49
2.9	Size exclusion chromatography.....	49
2.10	Gas chromatography.....	50
2.11	Wide-angle x-ray scattering.....	50
2.12	Saturation limits.....	51
2.13	Stability of oxybutynin.....	51
2.14	Interaction studies.....	51
2.15	Specific surface areas.....	52
2.16	Determination of the particle size.....	53
Chapter IV Optimization of the extrusion process.....		55
1	Industrial ram extrusion.....	55
1.1	Fine-tuning of the process.....	57
1.2	Influence of the process on the integrity of the implant materials.....	62
2	Factorial design of experiments.....	66
2.1	Preliminary studies.....	66
2.2	Rechtschaffner design.....	69
2.3	Verification of the prediction.....	73
3	Further steps towards an optimized process.....	77
3.1	Investigations on the number of die orifices.....	77
3.2	Reduction of the cutting interval.....	79
3.3	Up-scaling of the batch size.....	81
4	Summary.....	83
Chapter V Mechanisms controlling drug release.....		85
1	Influence of the type of drug.....	85
1.1	Insight into the manufacturing process.....	85
1.2	<i>In vitro</i> release studies.....	92

1.3	Studies on the release mechanism	96
2	Influence of the type of polymer	103
2.1	Insight into the manufacturing process	103
2.2	<i>In vitro</i> release studies.....	106
3	Development of innovative release strategies	108
4	Investigations on the interaction of drug and polymer	112
5	Summary	120
Chapter VI Lipids as innovative excipients		123
1	Lipid screening	123
1.1	Insight into the manufacturing process	124
1.2	Determination of mechanical properties.....	125
1.3	<i>In vitro</i> release studies.....	127
1.4	Investigations on the interaction of lipid and polymer	130
2	Homogeneous implants	134
2.1	Dynacet 211 P as excipient	134
2.1.1	Influence on the manufacturing process	134
2.1.2	<i>In vitro</i> release studies.....	139
2.1.3	Studies on the release mechanism	141
2.1.4	Alternative manufacturing strategies	143
2.2	Gelucire 50/13 as excipient	149
2.2.1	Influence on the manufacturing process	149
2.2.2	<i>In vitro</i> release studies.....	153
2.2.3	Studies on the release mechanism	155
3	Heterogeneous implants - core-shell implants	160
3.1	Influence on the manufacturing process	160
3.2	Investigations on the structure.....	164
3.3	<i>In vitro</i> release studies.....	165
3.4	Studies on the release mechanism	167
4	Summary	171
Chapter VII Final summary		175

LIST OF ABBREVIATIONS

API	active pharmaceutical ingredient
BET	Brunauer-Emmett-Teller
BSA	bovine serum albumin
CMC	critical micelle concentration
DoE	design of experiments
DSC	differential scanning calorimetry
FDA	Food and Drug Administration
GRAS	generally recognized as safe
HPLC	high performance liquid chromatography
ICH	International Conference on Harmonization
PEG	poly(ethylene glycol)
PLA	poly(lactide)
PLGA	poly(lactide-co-glycolide)
SEM	scanning electron microscopy
T_g	glass transition temperature
T_m	melting temperature

Chapter I | Introduction

This chapter is intended to provide background information on parenteral controlled release systems in general. It highlights the historical background and introduces implants, micro- and nanoparticles, and oil-based depots as innovative dosage forms, especially for the administration of highly effective drugs. The copolymer poly(lactide-co-glycolide) is presented as biodegradable matrix material, and the question whether it is magic or not is discussed. Next, an upcoming alternative is focused: lipidic matrices. Advantages and limitations in comparison to PLGA-based systems are pointed out. Finally, the most important implant manufacturing techniques are briefly described.

1 Overview of parenteral controlled release systems

It is still common practice that most pharmaceuticals are administered orally, most often in the form of tablets. However, in recent years, more and more drugs have been developed that necessitate another route of administration. Polypeptides and proteins, for example, are rapidly degraded and deactivated by proteolytic enzymes in the gastrointestinal tract. Even if this would not occur, the high molecular weights would prevent the APIs from being absorbed through the intestinal wall. As a consequence, such biopharmaceuticals are usually administered via the parenteral route, especially by intravenous, intramuscular, or subcutaneous injection. Since the elimination half-lives of polypeptides and proteins are known to be very short, frequent injections are required for an effective therapy [1-6]. For the patient compliance, this is of course detrimental. Parenteral controlled release systems that are capable of releasing an API over a period of weeks, months or even years might overcome this problem [2, 3]. They are commonly associated with a number of advantages [1, 7]:

- ✓ The plasma concentrations are maintained within the therapeutic range over an extended period of time.
- ✓ The first-pass metabolism is avoided.
- ✓ Compared to oral delivery systems, the total amount of the drug can be reduced. That way, harmful side effects are prevented, and the cost efficiency is increased.
- ✓ Drugs with short *in vivo* half-lives can be protected from degradation.
- ✓ The patient compliance is improved.
- ✓ In under-privileged areas where good medical supervision is not available, the drug administration is facilitated.

Certainly, these benefits have to be weighed against the potential disadvantages [1, 7-9]:

- ✘ Biocompatibility problems might arise from the carrier material. In the case of biodegradable depot systems, harmful byproducts might additionally be produced.
- ✘ Surgical operations are deemed necessary for the administration and/or removal of some of these delivery systems. Pain might also be caused by the presence of the device during the whole release period (or even longer).
- ✘ Adequate safety features have to be assured so that leaks or other problems that might lead to an over- or underdosing are circumvented.
- ✘ After administration of the depot system, it is difficult or even impossible to stop drug release.
- ✘ The production costs might be increased due to expensive carrier materials and highly sophisticated manufacturing techniques. Furthermore, sterility of the devices has to be guaranteed.

In the development of new controlled release systems, these restrictions have to be overcome. It is important to keep in mind that the parenteral route is still the only chance for an adequate delivery of most therapeutic macromolecules. Beyond that, it might also be of interest for bioactive small molecules that are characterized by a low oral bioavailability.

In the following, the interesting historical background is briefly outlined, and an overview of the most important dosage forms is given.

1.1 Historical background

The origin of controlled drug delivery systems can be dated back to the 1960s when Folkman et al. were circulating rabbit blood inside a Silastic® arterio-venous shunt. They found out that the rabbits would fall asleep if they exposed the silicone rubber tubing to anesthetic gases on the outside [10, 11]. As a consequence, Folkman and Long developed sealed Silastic® capsules that were loaded with different drug molecules. Dogs with surgically induced heart block were anesthetized, and the capsules were implanted in the myocardium. After a few hours, new pacemaker activity could be measured by periodic electrocardiograms. As fibrous tissue was formed at site of implantation, the therapeutic effect was observed to disappear after four to six days [12]. Nevertheless, the very first prolonged delivery device was born that way.

Inspired by the work of Folkman and stimulated by his own vision, Alejandro Zaffaroni founded a company focused on the concept of controlled drug delivery in the late 1960s. He called it Alza, after the first two letters of his first and last name. Folkman and Takeuchi Higuchi, another scientifically recognized researcher, soon decided to join the company. Ocusert[®], an ophthalmic insert, and Progestesert[®], an intrauterine device, count among the first long-acting pharmaceuticals that were designed and marketed by Alza [10]. Later, the Population Council developed a levonorgestrel-loaded subcutaneous implant that comprised of six tiny silicone rubber tubes. Norplant[®] can be regarded as direct extension of Folkman's findings from 1964 [10, 12, 13], and it is one of the first parenteral depot systems that became commercially available. Another milestone was reached in the 1970s when Folkman and Langer, his former postdoc, published a paper on the use of hydrophobic, non-degradable polymers for the sustained release of proteins and other macromolecules [10, 14]. Almost at the same time, namely in the late 1960s and early 1970s, biodegradable sutures made from polymers based on lactide and/or glycolic acid came up [15]. It was not long until this material was also focused for drug delivery purposes. As early as in 1986, Decapeptyl[®] was launched in Europe for the treatment of prostate cancer. This microparticulate system contains the gonadotropin-releasing hormone agonist triptorelin in a matrix of poly(lactide-co-glycolide). It was the first injectable and degradable microparticle depot that was clinically approved, and it is still on the market today [10]. Meanwhile, its indication has been extended to the field of assisted reproduction. Three years later, in 1989, AstraZeneca received the FDA approval for Zoladex[®] (➡ Figure 1), a cylindrical subcutaneous implant loaded with goserelin [16]. Depending on the initial drug loading and the composition of the copolymer (PLGA was used again), dosing intervals of one and three months could be realized. In parallel with these developments, further injectable release systems have been investigated, among those nanoparticles, *in situ* forming implants, liposomal formulations, polymeric micelles, and oily solutions/suspensions [9, 10].



Figure 1 | Single-dose syringe applicator for Zoladex[®] [17].

Today, 50 years after the publication on the Silastic[®] capsules, it is not possible to imagine drug delivery without parenteral depots. The progress in biotechnology and genetic engineering leads to an increasing number of potential therapeutic biomacromolecules, above all proteins [18-20]. As such compounds are usually ineffective by the oral route, parenteral administration is most often

required [2]. This is the main reason why injectable controlled release systems are still of growing interest. Every year, hundreds of papers and patents are published by researchers all over the world.

1.2 Different types

At this point, it is important to mention that a huge number of parenteral controlled release systems is available so far. The information below does not claim to be comprehensive. It rather provides an overview of the dosage forms that are (more or less) related to the context of this work.

1.2.1 Implants

In general, implants are defined as dosage forms that are subcutaneously placed with the aid of minor surgery or a hypodermic needle [21, 22]. They are most often associated with contraceptives such as Implanon[®] that is comprised of a single rod based on the copolymer ethylene vinyl acetate. The rod has a length of 4 cm and a diameter of 2 mm, and it is inserted in the non-dominant upper arm [23]. Implanon[®] delivers etonogestrel at a dose sufficient to suppress ovulation in every cycle throughout three years [24]. Another well-known example is Zoladex[®] (☞ I, 1.1) that is used for the treatment of breast and prostate cancer [25, 26]. However, not every implant is cylindrical in shape. Takahashi et al., for instance, developed biodegradable compressed tablets of 30 mg weight that were intended to provide drug release over a period of one week [27]. Dorta et al. investigated both disk-shaped monolithic films and multilayered systems based on PLGA. The release behavior of 5-fluorouridine and a vaccine against malaria was extensively studied [28].

Solid implants can easily be categorized - either as reservoir- or matrix-based systems. The former are characterized by an inert membrane that encloses the API and mediates the diffusion into the surrounding medium. As long as the reservoir is saturated, a constant concentration gradient is maintained, and zero-order release is achieved. This is of course highly advantageous. However, the manufacturing of such systems turned out to be difficult. Pinhole defects and cracks in the membrane cannot be avoided at 100% and carry the risk of dose dumping. Monolithic matrix-based systems overcome these problems [29] and are therefore more widespread. Ideally, they consist of only two components: the drug and the carrier material. If the latter is biodegradable, the following release mechanisms might be involved:

✓ **Diffusion through water-filled pores**

Pores are commonly formed by water absorption and by degradation/erosion of the matrix [30-33]. If the incorporated drug itself is hydrophilic, it is immediately dissolved upon contact with water. That way, the porosity of the carrier is increased, and further water uptake is facilitated. This is especially relevant for the so-called initial burst that occurs in the early stages of the release period during which non-encapsulated drug particles at the surface or in near-surface areas are washed off [28, 34-37]. Apart from that, the intrusion of water is known to trigger the degradation of a number of synthetic matrix materials by cleaving hydrolytically sensitive bonds. Degradation products of low molecular weight are formed and released, thereby creating new diffusional pathways for the API [38-40]. This is also true for natural biomaterials that undergo enzymatic degradation [39].

✓ **Diffusion through the carrier material**

This release mechanism is limited to small hydrophobic drugs [41, 42] and does not necessarily depend on the implant porosity. However, since the API needs to be dissolved before being released, a high surface area is not detrimental. The rate of diffusion is also influenced by the physical state of the carrier. For some polymers, it was shown to increase substantially at the transition from the vitreous to the rubbery state [34, 43].

✓ **Osmotic pumping**

As its name implies, osmotic pumping occurs when osmotic pressure caused by the absorption of water is responsible for the transport of the drug molecules. In this case, the mechanism of action is convection [34, 44]. For modified reservoir-based systems, osmotic pumping plays a major role than for monolithic depots. The latter usually tend to swell, thereby compensating the osmotic pressure [4, 45].

✓ **Degradation/erosion of the matrix**

Erosion is one of the fundamental processes controlling drug release from biodegradable matrices [46]. It describes the phase during which mass loss can be observed due to degradation products leaving the implant [38, 47]. Given that the API is homogeneously distributed, both drug release and matrix erosion result in identical profiles.

In most cases, more than one release mechanism is present at the same time, and it is not unusual that the dominating mechanism changes [34]. With regard to non-degradable monolithic implants,

this rule can be simplified since diffusion is then the key process. It is important to keep in mind that such depots have to be removed by a second surgical intervention once the therapeutic effect comes to an end [48].

As already mentioned, polymers such as poly(lactide-co-glycolide) or ethylene vinyl acetate count among the most attractive implantable carrier materials [49, 50]. In recent years, lipids have been identified as promising alternative [4, 51-53]. In the chapters 1, 2 and 1, 3, these matrix materials are discussed in detail, and potential advantages and limitations are outlined. Chapter 1, 4 finally summarizes the implant manufacturing techniques.

Over the last few decades, *in situ* forming implants have gained more and more attention [54]. Compared to solid implants, their application is less painful and invasive since a liquid formulation is injected that converts into a (semi-)solid depot upon administration. That way, much smaller needles can be applied, and local anesthesia is not necessary any more [55]. However, *in situ* systems are still associated with a number of problems: first, the implant shape and structure is variable and depends on the attending physician. Second, the formation of the depot leads to comparatively high initial bursts, and third, toxicity issues have to be considered [56], especially for the solvents. Eligard® is one of the few products that have successfully overcome these challenges, and it is now commercially available [57]. Similar to Zoladex® and Decapeptyl® (☞ 1, 1.1), it contains a luteinizing hormone-releasing hormone agonist (leuprorelin), and it has been approved for the long-term treatment of prostate cancer [58]. Including the API, the formulation consists of only three components. Poly(lactide-co-glycolide) serves as depot-forming agent, and methylpyrrolidone is used as solvent [59]. When the solution is injected, the latter is exchanged by tissue fluids, which leads to the precipitation of the polymer. More precisely, PLGA solidifies due to the fact that it is insoluble in water [55]. Currently, new materials and approaches enter the preclinical and clinical phases. It is therefore likely that *in situ* forming implants will gain further importance within the next years [56]. According to their mechanism of depot formation, such systems are commonly distinguished in the following six categories: thermoplastic pastes, *in situ* cross-linked polymer systems, polymer precipitates, temperature-dependent gelling systems, pH-dependent depots, and cubic phases [55, 56, 60]. Each of them is a science unto itself with its individual manufacturing techniques and release properties.

1.2.2 Microparticles

Microparticles are simply defined as particles with a size in the range of 1 μm to 1000 μm [61]. For the use in parenteral drug delivery systems, diameters in between 10 μm and 50 μm are recommended. The lower boundary results from the fact that smaller particles are known to be cleared from the injection site by phagocytosis. In contrast, the upper boundary is comparatively low in order to obtain a sufficient syringability and hence an improved patient compliance [62]. Before administration, the microparticles are usually dispersed in an isotonic and non-irritating solution. The resulting suspension is injected intramuscularly or subcutaneously [63]. Throughout the past decades, several microparticulate products have been approved by the authorities, among those Lupron Depot[®] and Risperdal Consta[®] [62]. The latter consists of risperidone-loaded biodegradable microspheres made from the copolymer PLGA. It is indicated for the treatment of schizophrenia. Interestingly, the release profile is characterized by an initial release of approximately 3.5%, followed by a lag phase of two weeks. In order to bridge this time gap, the patients additionally have to take oral antipsychotic drugs. Between four and five weeks, an increased release rate can be observed [64-66]. This can primarily be attributed to the erosion of the matrix material. In general, the release mechanisms that have already been described for monolithic implants (➔ I, 1.2.1) apply equally to long-acting matrix-based microparticles. Since the latter cannot be removed after the release period, preference is given to biodegradable carrier materials such as poly(lactide-co-glycolide). So far, a number of microencapsulation techniques have been developed. The most established ones include solvent evaporation/extraction (single and double emulsion processes), coacervation (phase separation), and spray drying. The choice of the manufacturing method depends on the nature of the raw materials, the intended use, and the duration of therapy [15, 67, 68]. It is crucial to control the process such that uniform particles of a narrow size distribution are obtained [62]. If, for example, a high fraction of particles is much smaller than the average, the encapsulation efficiency might significantly be reduced. In addition, an unwanted burst release might be caused [62, 69].

In general, the terminology that is used to describe microparticulate formulations is sometimes inconsistent and confusing. The term 'microparticle' basically refers to both microspheres and microcapsules. The inner structure of the former can be compared to monolithic matrix-based implants whereas the latter are defined as reservoir-based systems consisting of a core-shell structure [70]. The same holds true for nanoparticles that are equally categorized into nanospheres and nanocapsules (➔ I, 1.2.3).

1.2.3 Nanoparticles

Nanoparticles may principally result from the same preparation techniques that microspheres do. The manufacturing parameters are simply adjusted [15, 68] so that particles with a size in the range of 10 nm to 1000 nm are attained. It is worth noting that controlled drug delivery systems often require particle diameters of more than 100 nm. This relates to the fact that otherwise a sufficient drug loading would not be possible [71]. As opposed to microparticles, nanoparticles are suitable for intravenous administration. Their circulation half-life and stability (against immunogenic recognition and/or enzyme attack) can be enhanced by PEGylation [10, 72]. In addition, cell membrane receptor antibodies, peptides or small molecule ligands that are conjugated to the carrier surface offer the possibility of an active drug targeting. The last reason that stimulates the development of further nano-scaled delivery systems is the enhanced permeability and retention effect - also known as passive targeting - that describes the accumulation of submicron particles within fast-growing tumors that are characterized by a leaky vasculature [10, 73]. Obviously, nanoparticulate formulations occupy a special position within the field of controlled release parenterals. Once administered, they do not necessarily form a static depot at the site of injection. They are rather intended for circulating in the blood stream, thereby releasing the entrapped API at a constant rate. In contrast, localized drug delivery can be achieved if the nanoparticles are directly transported to the target tissue where they might enter the cells via micropinocytosis [74].

Apart from nanospheres and nanocapsules, liposomes and polymeric micelles also belong to the group of nanoparticles [10]. The former are defined as vesicles in which an aqueous volume is entirely surrounded by a (phospho)lipid membrane [75, 76]. Hydrophilic drugs are commonly loaded into the core whereas hydrophobic drugs are dissolved in the bilayer. As liposomes are mainly composed of naturally occurring substances, they have the distinct advantage of being non-toxic and biodegradable [77]. The release mechanism is as simple as possible: the lipid bilayer fuses with the cell membrane and hence the drug molecules are released into the cell [78]. For the preparation of liposomes, various methods have been reported, for instance reverse-phase evaporation [79], ethanol injection [80], or high-pressure homogenization [81]. In 1995, Doxil[®], a PEGylated liposomal formulation containing doxorubicin was approved by the FDA [10]. It was the first product that reached market readiness, and it is still used for the treatment of ovarian cancer, sarcoma and multiple myeloma [82]. In the last decades, more and more liposome-based drug delivery systems became commercially available, among those AmBisome[®], DaunoXome[®] and Visudyne[®] [83]. Current research is focused on stimuli-responsive liposomes that provide both site-specific and triggered

drug release. To date, temperature-, pH- and ultrasound-sensitive particles have already shown potential [76, 84, 85].

Apart from this, polymeric micelles have gained considerable attention in the last years. These nanoparticles are generally described as self-assembled core-shell structures that are spontaneously formed in an aqueous solution consisting of amphiphilic block copolymers [86-88]. As soon as the concentration of the polymer increases above the critical micelle concentration, the hydrophobic segments start to associate in order to minimize the contact with the water molecules. Consequently, a hydrophobic core that is particularly suitable for the encapsulation of poorly water-soluble drugs is formed. The drug loading is typically realized by one of the following methods: dialysis, oil-in-water emulsion solvent evaporation or solid dispersion [86, 89, 90]. Remarkably, polymeric micelles are much more stable than micelles prepared from detergents, which can be attributed to their (very) low CMC [10, 91]. Pluronics® and PEG-phospholipid conjugates rank among the most promising carrier materials for such delivery systems [92]. Drug release was found to be controlled by the breakup of the micelles and, to a lesser extent, by diffusional processes [93]. Assuming that the surface of the nanoparticles is appropriately functionalized, it can additionally be triggered by internal and external stimuli such as pH [94] or temperature [95]. Similar to liposomes, polymeric micelles combine a number of advantages. They may circulate for prolonged periods in blood, thereby evading host defenses [92]. Furthermore, they are capable of an active (and passive) tumor targeting [96]. Many micellar formulations containing low molecular weight drugs are now in clinical trials [10].

1.2.4 Oily solutions and suspensions

In hormone replacement therapy and for the treatment of schizophrenia, long-acting oily solutions have been in clinical use for more than three decades [97-100]. Ideally, such systems consist of only two components: a lipophilic (pro)drug and an oily carrier such as sesame oil or cottonseed oil [97, 101]. In order to improve the viscosity and hence the syringability, benzyl benzoate or ethanol might be added [102]. Nebido®, for example, contains testosterone undecanoate that is dissolved in a mixture of castor oil and benzyl benzoate. It is intended for the treatment of hypogonadism in males and has to be injected intramuscularly every three months [103]. Interestingly, the underlying *in vivo* drug release mechanisms for such depot injections are not fully understood yet. However, two major contributing processes seem to be identified. The first one describes the diffusion of the drug molecules to the oil-tissue interface and the subsequent transition into the surrounding aqueous phase that is governed by the partition coefficient of the API. The second one refers to the

'disappearance' of small oil droplets from the injection site and their recovery in the lymphatic system [104-107] or in so-called second depots including the fatty tissue and the entero-hepatic circulation [97, 108-110]. Moreover, the biodegradation of the oily carrier has to be considered [102]. Compared to other parenteral depots, the manufacturing of lipophilic solutions (including terminal sterilization) is uncomplicated and inexpensive [97, 102]. Nonetheless, oily injectables have become less and less important over the last years.

Of course, this holds also true for lipophilic suspensions in which the drug particles are thinly dispersed. Such systems are especially suitable for APIs that are insoluble or instable in conventional solvents. In addition, they allow for an elongation of the depot effect [63, 102, 111]. The latter can be achieved since the dissolution of the drug molecules at the oil-tissue interface is now the rate-limiting step [101]. Further drug release occurs as in the case of oily solutions. In general, suspensions are per se instable, and sedimentation is one of the most challenging factors in the development and manufacturing of these parenterals [102]. It is absolutely necessary that the drug particles can easily be resuspended, and that they do not settle rapidly after shaking [63]. Otherwise, it cannot be guaranteed that the correct dose is administered to the patient.

2 Poly(lactide-co-glycolide) - a magic (matrix) material?

Poly(lactide-co-glycolide) is a synthetic copolymer consisting of monomers of lactic acid and glycolic acid that are connected by ester bonds [112]. As lactic acid contains an asymmetric α -carbon, two enantiomeric forms have to be distinguished: D- and L-lactic acid [49]. PLGA is most often prepared from the racemic mixture, which leads to copolymers that are amorphous over a wide range of composition [1, 49].

Originally developed as suture material (☞ I, 1.1), poly(lactide-co-glycolide) has soon become an attractive candidate for controlled release applications [49]. For the delivery of peptides and proteins, it is nowadays the most frequently used biodegradable carrier material [30]. Beyond that, PLGA has demonstrated potential in the field of tissue engineering and orthopedic fixation [113-115]. The reasons for this widespread use can be summarized as follows: first of all, the polymer is 'generally recognized as safe' by the FDA [116]. This is most probably related to the fact that it shows an excellent biocompatibility and biodegradability [15, 30, 117]. In addition, PLGA is available with different physico-chemical properties such as molecular weight, end-capping or lactic to glycolic acid ratio. By this means, the rate of degradation can easily be controlled, and in the case of parenteral depot formulations, a broad range of release profiles can be realized [34, 49, 118-120].

Although poly(lactide-co-glycolide) is a versatile and somehow fascinating (matrix) material, it is far from being magic. As early as in the 1980s, the first controlled release systems based on PLGA have been approved for clinical use (☞ I, 1.1). Almost 30 years later, both Decapeptyl® and Zoladex® are still on the market. This underlines the aforementioned GRAS status and indicates that the underlying drug release mechanisms have extensively been studied over the last years. Thus, PLGA is today anything but new.

The following chapters introduce its synthesis and provide a comprehensive overview of the different types and their individual physico-chemical properties. Detailed information is given on both biodegradability/drug release and biocompatibility. Finally, the current market situation is briefly outlined.

2.1 Synthesis

Poly(lactide-co-glycolide) is either synthesized by direct polycondensation or by ring-opening polymerization [121] (☞ Figure 2). The former leads to polymers with a molecular weight

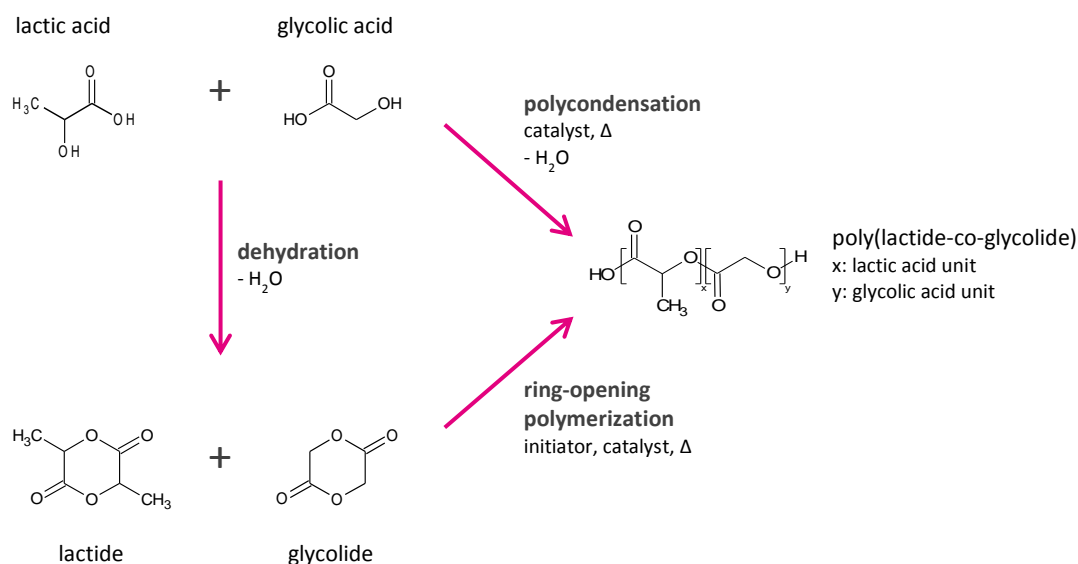


Figure 2 | Schematic representation of PLGA synthesis by direct polycondensation or ring-opening polymerization [121].

ranging from less than 5,000 g/mol [122] to about 10,000 g/mol [123, 124]. As these polymers are characterized by substandard mechanical properties, they are not suitable for many applications [125]. For this reason, ring-opening polymerization has become the method of choice. It yields higher molecular weight PLGA [121, 124] with an increased mechanical stability. As illustrated in Figure 2, the manufacturing process has to be divided into two steps. The first one includes the conversion of lactic acid and glycolic acid into cyclic dimers by dehydration. The purification of lactide and glycolide is time-consuming, requires a great quantity of organic solvent and results in low yields. This makes the PLGA products comparatively expensive [126]. The second step is the bulk copolymerization in which successive monomeric units (of lactic acid and glycolic acid) are linked together by ester bonds, thus forming a linear, aliphatic polyester [127]. The chain length and hence the molecular weight can be controlled by the concentration of the initiator and the catalyst, the reaction temperature, the process time, and the degree of vacuum. Another possibility is the addition of a molecular weight controller. Lauryl alcohol, for example, reacts with the carboxylic end groups of the growing polymer chains and blocks them for propagation [124, 128]. The physico-chemical properties of the resulting polymer can additionally be influenced by the lactide to glycolide ratio or the introduction of specific end groups. Ring-opening polymerization is commonly catalyzed by tin-based compounds such as stannous octoate that is permitted as food additive in numerous countries [126, 127, 129]. Other metal-containing catalysts including zinc and aluminum alkoxides have also been reported. However, some of these compounds are associated with health safety concerns. This is why enzymes have been investigated as promising alternative [130, 131]. Apart

from that, lauryl alcohol [124] and 1,10-decanediol [132] need to be mentioned since they are typically used as starter molecules, so-called initiators.

2.2 Different types and their physico-chemical properties

With regard to the development of new drug delivery systems, the knowledge of the most important PLGA types and the understanding of their physico-chemical properties is absolutely necessary [15]. In general, the copolymers can be distinguished by means of their molecular weight and/or lactic to glycolic acid ratio. Furthermore, they might be equipped with different end groups such as free carboxylic acids or alkyl esters. Each of these properties has an influence on the rate of degradation and hence on the release kinetics [34].

The mechanical strength of the polymer and its ability to be formulated as controlled release system depend primarily on the molecular weight and the corresponding polydispersity index [15, 133, 134]. Commercially available PLGA types are usually characterized in terms of intrinsic viscosity which is directly related to the molecular weight [49]. The values reported by Evonik, one of the world's largest manufacturers, range from 0.05 dL/g to 1.7 dL/g (measured at 0.1% in chloroform at 25 °C with an Ubbelohde glass capillary viscometer). The lower boundary refers to a 50:50 polymer that is terminated with an acid end group whereas the upper boundary reflects a 85:15 polymer with an ester end group. As might be imagined, higher molecular weight PLGA types are more resistant to hydrolytic degradation than their short-chain equivalents [34, 135]. This behavior can also be related to the glass transition temperature that describes the transition from the rigid glassy state to the mobile rubbery state. With decreasing molecular weight, more chain ends are present and more free volume is generated. Therefore, the polymer chains have more space to move, and the rubbery state is reached earlier/at a lower temperature [136, 137]. Since the T_g is in most cases above the physiological temperature of 37 °C, poly(lactide-co-glycolide) has a fairly rigid chain structure that ensures significant mechanical strength [15, 134]. As soon as the polymer comes in contact with water, the glass transition temperature decreases considerably. Vey et al. studied the degradation mechanisms of cast PLGA films in phosphate buffer and confirmed that the T_g is additionally influenced by the lactic to glycolic acid ratio. It was observed to increase with an increasing number of lactic acid units [136].

This is in good agreement with the fact that lactic acid is more hydrophobic than glycolic acid, which can be attributed to the additional methyl group at the asymmetric α -carbon (\Rightarrow Figure 2). As a consequence, polymers with a high lactic to glycolic acid ratio are less hydrophilic. Compared to

glycolide-rich/er PLGA types, they absorb less water and degrade more slowly [15, 134]. However, this is only half the story. Polymers of a 50:50 ratio have been shown to occupy a special position since they are hydrolyzed much faster than their equivalents at either end of the composition range [15, 39, 133, 138, 139]. At a first glance, this is astonishing because higher degradation rates would have been expected from lactic to glycolic acid ratios below 50:50. A simple explanation is given by the fact that the polymer crystallinity changes with the molar ratio of the individual monomer components [15, 67]. PLGA types containing less than 70% of glycolide have been reported to be amorphous [15, 140]. This leads to the conclusion that copolymers with less than 30% of lactic acid and more than 70% of glycolic acid tend to be crystalline in nature, that way decreasing the rate of degradation [141]. Depending on the field of application, the polymers have to be chosen carefully. For controlled release systems such as implants or microparticles, amorphous PLGA types based on D,L-lactic acid and glycolic acid are preferred. Typically, the monomer ratio does not come below 50:50. Medical devices mainly consist of pure poly(L-lactide), poly(L-lactide-co-D,L-lactide) or poly(L-lactide-co-glycolide) [135]. These polymers are inherently (semi-)crystalline [15, 134], thus resulting in much smaller degradation rates.

Another key parameter that is commonly used to describe the physico-chemical properties of PLGA is the nature of its end groups. The conventional synthesis of the polymer (☞ I, 2.1) - either by polycondensation or by ring-opening polymerization - leads to free carboxyl terminals. In an aqueous environment, these end groups attract water molecules, and the polymer (matrix) starts to swell. Consequently, the hydrolysis of the ester bonds is facilitated. The presence of instantly free carboxyl groups further contributes to the autocatalytic degradation of the polymer. Compared to capped PLGA types bearing an aliphatic group at the end of the polyester chain, the degradation of the matrix proceeds much faster. In other words, the polymer is less hydrophilic and more inert if it exhibits esterified terminals such as methyl, ethyl or lauryl groups [41]. In general, the nature of the end groups plays a major role for low molecular weight polymers that simply have a larger number of chain ends. Apart from that, uncapped carboxyl terminals have been reported to be prone to drug/polymer interactions that might affect the release kinetics [34, 142].

Independent of the molecular weight, the lactic to glycolic acid ratio and the nature of the end groups, poly(lactide-co-glycolide) is soluble in a wide range of common solvents such as tetrahydrofuran, acetone or ethyl acetate [49, 143, 144]. In water, it undergoes (bio)degradation by hydrolysis of its ester bonds [15, 49]. This sounds simple but is quite tricky as soon as PLGA-based drug delivery systems are regarded (☞ I, 2.3).

2.3 Drug release from PLGA-based drug delivery systems

In most cases, drug release from PLGA-based drug delivery systems results in a multi-phase release profile. Zero-order kinetics would of course be preferred but they have rarely been described for such depots [34, 145].

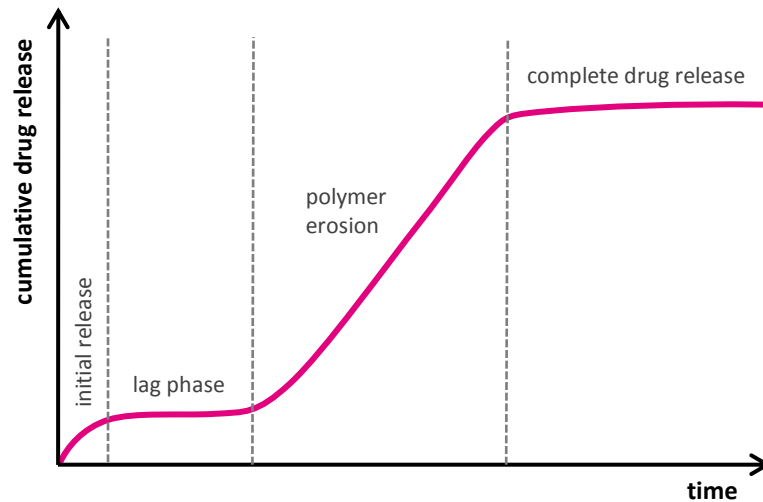


Figure 3 | Schematic representation of a multi-phase release profile that is typically obtained for PLGA-based drug delivery systems.

As displayed in Figure 3, a phase of rapid release is typically obtained within the first day or so. This phenomenon is referred to as initial burst and can be ascribed to non-encapsulated drug particles at the surface or in near-surface areas [34, 35, 146]. The API is released as a function of solubility as well as penetration of water into the polymer matrix [49]. The second phase is a lag phase that is characterized by comparatively small release rates. The drug molecules have been shown to diffuse slowly - either through the relatively dense polymer or through the few existing pores [34]. The random chain scission process significantly decreases the molecular weight of the polymer but no appreciable mass loss can be observed [15, 49]. The next phase is usually a period of faster release, and it is often attributed to the onset of erosion [34]. The latter designates the loss of material that can be related to soluble oligomeric and monomeric products leaving the matrix [15, 38, 49]. Complete drug release is achieved at the latest when the polymer is entirely solubilized. Concerning the degradation *in vivo*, the role of enzymes is unclear. However, most of the literature indicates that no enzymatic activity is involved, and that the chain scission process is purely controlled by hydrolysis [15, 134].

Both diffusion and erosion have been identified as main release mechanisms for PLGA-based drug delivery systems. The former is more relevant throughout the first phases whereas the latter dominates the so-called second burst [34, 37]. A brief explanation of these processes has already been given (☞ I, 1.2.1).

Poly(lactide-co-glycolide) counts among the bulk-eroding polymers, which means that the degradation occurs throughout the whole matrix equally [28, 147-149] (☞ Figure 4). The size of the device remains constant over a considerable period of time. In contrast, surface-eroding polymers lose material from the surface only. The inside of the matrix remains unchanged until the surrounding material has been completely degraded. Therefore, the device gets smaller but keeps its original shape [38, 46, 149]. Surface erosion proceeds at a constant rate at any time [38, 150]. This is advantageous since it allows for the prediction of drug release [38, 151]. For bulk-eroding polymers, the things are more complicated as there is no constant erosion velocity [147, 150]. Burkersroda et al. investigated the erosion behavior of matrices made from PLGA and PLA, respectively. They found out that the erosion mechanism can be changed from bulk to surface erosion, depending on the surrounding conditions and the device geometry. At pH values greater than 13, for example, linear erosion profiles were obtained, and the molecular weights proved to be constant [147].

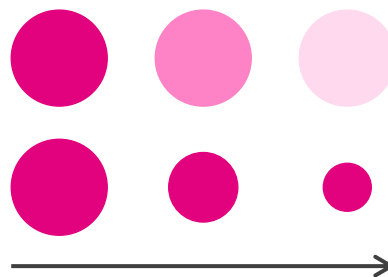


Figure 4 | Top: Bulk erosion. **Bottom:** Surface erosion [147].

The degradation of poly(lactide-co-glycolide) has been studied in detail over the past decades. Today, plenty of literature is available on this topic. Figure 5 shows the reaction schemes for both the normal hydrolytic degradation and the autocatalytic degradation. The former occurs as soon as the polymer comes in contact with water. The ester groups are hydrolyzed, and free carboxyl groups are formed at the chain ends. In the early stages of the degradation process, these lower molecular weight byproducts remain trapped inside the matrix. Consequently, the concentration of acid end

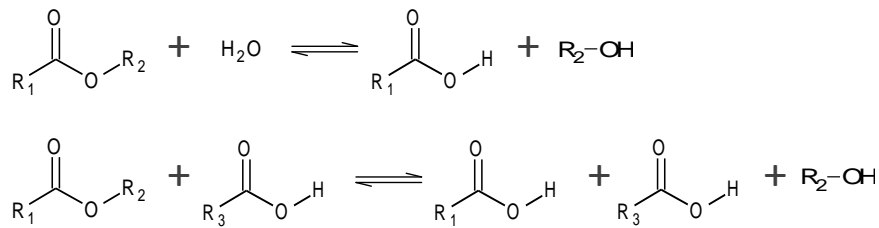


Figure 5 | Top: Hydrolytic degradation of PLGA. **Bottom:** Autocatalytic degradation of PLGA [136].

groups increases rapidly, and the pH drops [136, 34]. Li and Schwendeman developed a quantitative ratiometric method based on laser scanning confocal microscopic imaging that enables the determination of the microclimate pH inside degrading PLGA microspheres. They confirmed that this pH can be much more acidic than the one of the surrounding release medium - even when the particles are as small as 2 μm in diameter [152]. As illustrated in Figure 5, the (acidic) PLGA fragments that are formed upon hydrolysis catalyze further degradation of the polymer. This autocatalytic effect leads to an inhomogeneous degradation of the matrix with the center degrading much faster than the surface [34, 153]. It might only be reduced by neutralizing buffer ions that diffuse from outside into the bulk [136, 37].

In general, the factors that influence the rate of degradation and hence drug release are manifold. First of all, the polymer itself needs to be mentioned. Poly(lactide-co-glycolide) is available with different molecular weights, lactic to glycolic acid ratios and end groups (☞ I, 2.2). These properties allow for realizing a broad range of release profiles. However, the incorporated drug substance is not to be underestimated. Depending on the physico-chemical properties and the initial loading, it might affect the rate of degradation to a greater or lesser extent. The same holds true for additives such as salts, surfactants or plasticizers. Apart from that, the size, shape, porosity and density of the drug delivery system have to be considered. Attention has also to be paid to the surrounding conditions. The composition of the release medium that determines both osmolality and pH might substantially affect hydrolysis of the PLGA chains. Temperature and stirring are further factors that have been reported to influence the *in vitro* release kinetics. Since the physiological conditions are assumed to be constant within a certain range, the situation *in vivo* seems to be less problematic. Despite that, the sink conditions as well as the presence of enzymes and lipids need to be kept in mind. Immune responses might additionally play an important role [34, 49].

Although the development of new drug delivery systems based on PLGA has become routine over the years, it is still a challenge to exactly predict the release rates - both *in vitro* and *in vivo*. This can

probably be attributed to the fact that it is not possible to predict how the erosion process changes when the rate of degradation is altered [147].

2.4 Biocompatibility

Biocompatibility is generally defined as the ability of a material to perform with an appropriate host response in a specific application [154]. Particular attention has to be paid to biodegradable materials since their chemical, physical, mechanical, and biological properties are known to change with time. Degradation products with different levels of tissue compatibility might be produced.

As mentioned before (⇒ I, 2.3), poly(lactide-co-glycolide) undergoes bulk erosion through non-specific hydrolysis of the ester bonds [39, 113]. Acidic oligomers and monomers are formed [38]. These degradation products are non-toxic, and they get eliminated by the normal metabolic pathways [49]. Lactic acid enters the citric acid cycle and is converted to carbon dioxide and water. Glycolic acid either takes the same way or it is excreted unchanged in the urine [15, 67, 113, 134, 155].

Although PLGA is well-tolerated *in vivo*, its injection/implantation entails the risk of local events including acute and chronic inflammation, granulation tissue formation, foreign body reaction, and fibrous encapsulation [156-158].

2.5 Current market situation

PLGA-based medicinal products have a long tradition: the first parenteral controlled release systems reached market readiness as early as in the 1980s (⇒ I, 1.1). Since then, a number of microparticulate formulations and implants have been approved by the regulatory authorities all over the world. Table 1 gives a comprehensive overview of the products that are currently commercially available in Germany. Interestingly, the majority of them contains a gonadotropin-releasing hormone agonist and is intended for the treatment of hormone-dependent diseases such as breast or prostate cancer. Among these formulations, Eligard® that is loaded with leuprorelin acetate in a dosage of 7.5 mg, 22.5 mg or 45 mg takes a special position since it is the only *in situ* forming depot [103] (⇒ I, 1.2.1). Depending on the type of copolymer that is used as matrix material, its duration of action varies between one and six months. More precisely, the lactic to glycolic acid ratio and the type of end group determine the rate of degradation and hence the rate of drug release. PLGA 50:50 that contains free carboxyl end groups provides the shortest dosing interval

whereas PLGA 75:25 and 85:15 - both terminated with alkyl esters - are responsible for the longer dosing intervals [159].

Bydureon® and Sandostatin® have also been designed for the administration of polypeptides. The former contains 2 mg of the glucagon-like peptide-1 agonist exenatide and is used for the treatment of diabetes mellitus type II. It has to be injected subcutaneously once a week. The latter is loaded with 10 mg, 20 mg or 30 mg of octreotide acetate, a somatostatin analog. It is administered every four weeks to patients that suffer from tumors of the gastrointestinal tract or from acromegaly [103].

Table 1 | Overview of commercially available pharmaceuticals containing poly(lactide-co-glycolide) [103].

Trade name	Company	API	Dosage form	Indication
Bydureon®	AstraZeneca/Bristol-Myers Squibb	exenatide	microparticles	diabetes
Decapeptyl®	Ferring	triptorelin	microparticles	precocious puberty, endometriosis, uterine fibroids, assisted reproduction, prostate cancer
Eligard®	Astellas Pharma	leuprorelin	<i>in situ</i> forming implant	prostate cancer
Enantone®	Takeda	leuprorelin	microparticles	precocious puberty, endometriosis, uterine fibroids, breast cancer, prostate cancer
Ozurdex®	Allergan Pharmaceuticals	dexamethasone	implant	macular edema
Pamorelin®	Ipsen Pharma	triptorelin	microparticles	prostate cancer
Profact®	Sanofi/Apogepha	buserelin	implant	prostate cancer
Risperdal Consta®	Janssen-Cilag	risperidone	microparticles	schizophrenia
Salvacyl®	Pfleger	triptorelin	microparticles	sexual drive disorder
Sandostatin®	Novartis Pharma	octreotide	microparticles	tumors of the gastrointestinal tract, acromegaly
Zoladex®	AstraZeneca/TEVA	goserelin	implant	endometriosis, uterine fibroids, breast cancer, prostate cancer

Risperdal Consta® is the only long-acting drug delivery system based on PLGA that has been approved for the treatment of schizophrenia so far. It is available in dosages ranging from 25 mg to 50 mg of risperidone. The microparticles are typically suspended in an isotonic solution and injected deep intramuscularly every two weeks [103].

Ozurdex® is another product that has been developed for the release of a low molecular weight drug. It belongs to the group of solid implants and is loaded with 700 µg of dexamethasone. Its matrix consists of a PLGA mixture with a lactic to glycolic acid ratio of 50:50. The polymer end groups are partially terminated with esters and carboxylic acids. In contrast to the other products that are listed in Table 1, Ozurdex® is injected intravitreally. Thus, the glucocorticoid is released directly inside the eye where it contributes to the reduction of macular edema [103].

3 Lipids as alternative matrix materials?

Lipids are loosely defined as biological substances that are generally hydrophobic in nature and in many cases soluble in organic solvents [160, 161]. Accordingly, they are rather characterized in terms of solubility than in terms of a particular structure [162]. Over the years, different classification systems have been proposed. One of them was published in 2005 by Fahy et al. who introduced eight lipid categories - based on the chemical structure and driven by the distinct hydrophobic and hydrophilic elements that constitute the lipid: fatty acyls, glycerolipids, glycerophospholipids, sphingolipids, sterol lipids, prenol lipids, saccharolipids, and polyketides [160].

In the past years, lipids have gained considerable attention as matrix materials for parenteral controlled release systems. Compared to (approved) polymers such as poly(lactide-co-glycolide), they seem to be a promising alternative, especially for the administration of proteins [5, 6, 52, 53, 163] (☞ I, 3.1).

The use of lipids for implantable devices dates back to the 1970s when Sullivan et al. investigated the release of cyclazocine from a glyceride matrix. Both the modification of the matrix and the manipulation of the drug concentration allowed for controlling the release rates. That way, durations of action between a few days and a month could be realized [164]. Almost at the same time, Joseph et al. published a paper on the *in vivo* release of progesterone from cholesterol pellets. Zero-order release was obtained for approximately 80 d or until about 70% of the available drug were exhausted [165].

As already mentioned, current research is mainly focused on the delivery of proteins. These macromolecules are characterized by a fragile three-dimensional structure which makes them susceptible to a number of chemical and physical degradation pathways [52, 166-168]. Lipid matrices, either in the form of microparticles or implants, have been shown to preserve this structure. Mohl and Winter, for instance, prepared compressed implants consisting of lyophilized rh-interferon α -2a, PEG 6000, and tristearin. They found out that 90% to 95% of the incorporated protein were released continuously over a period of one month. The release rates could be controlled by the amount of poly(ethylene glycol) that was shown to act as pore-forming agent. Remarkably, 85% to 95% of the API were released as native monomer [5]. Similar results were obtained by Koennings et al. who established miniature-sized triglyceride matrices for the long-term delivery of brain-derived neurotrophic factor. *In vitro*, 60% of the incorporated protein were released in a continuous manner over more than 30 d. Only minor aggregates were detected in the end of the release period, indicating that the structural integrity of the API (that was still embedded in the

matrix) was maintained [169]. Another example is given by Maschke et al. who developed a spray congealing process for the preparation of insulin-loaded lipid microparticles. The stability of the protein under release conditions over 28 d was assessed by investigating the residual insulin content. Both desamido insulin and a covalent insulin dimer could be detected. Nevertheless, testing the microparticles in a fibrin gel chondrocyte culture revealed that the released protein was bioactive and had a significant effect on chondrocyte extracellular matrix production [170].

Although lipids have proved to have a great potential as (alternative) matrix materials, their use in microparticulate systems or monolithic implants has not reached market readiness so far. However, the latter might simply be a question of time.

The next chapter highlights the advantages and limitations of lipid-based drug delivery systems and compares them to PLGA-based systems. Thereafter, insight is given into the mechanism/s governing drug release, and the question whether lipidic matrices undergo biodegradation or not is discussed. In addition, the reasons for the excellent biocompatibility of the most lipids are briefly outlined.

3.1 Advantages and limitations in comparison to PLGA-based systems

Although biodegradable synthetic polymers such as PLA or PLGA are nowadays frequently used for the controlled parenteral administration of peptides and small molecules, they seem to be less appropriate for the delivery of proteins and other sensitive drugs [171, 172]. One of the reasons for this assessment is the accumulation of acidic degradation products within the matrix (➡ I, 2.3). As a consequence, the microclimate changes such that the pH drops significantly and/or the osmotic pressure increases [44, 173]. This might induce chemical degradation and - in the case of proteins - unfolding and aggregation [174]. Furthermore, (detrimental) drug/polymer interactions have been reported [34, 171, 173, 175]. In order to overcome at least part of these problems, Zhu et al. investigated the co-incorporation of neutralizing basic salts. The antacid $Mg(OH)_2$, for example, was successfully shown to increase the pH, thereby preventing BSA structural losses and aggregation for more than one month [176, 177]. Another idea was to increase the porosity of the matrix so that the degradation products are washed out rapidly [167, 174]. In contrast to lipidic depots, PLGA-based systems are known to absorb water, that way increasing the protein molecular mobility. Hence, it is likely that protein unfolding and irreversible aggregation take place [174]. The presence of water might additionally cause problems if moisture-sensitive low molecular weight drugs are embedded. In this context, lipidic matrices turned out to be a promising alternative. As they are typically hydrophobic in nature, water is not taken up, and an increased stability of the incorporated drug can

be assumed - even upon *in vivo* administration. The absence of acidic degradation products further contributes to this stabilizing effect [171].

Drug release from PLGA-based systems results most often in multi-phase release profiles consisting of an initial burst that is followed by a lag phase and a second burst (☞ I, 2.3). This is not necessarily disadvantageous but needs to be considered in order to circumvent an over- or underdosing. Risperdal Consta[®], for instance, requires additional intake of oral antipsychotics during the first three weeks of treatment [103] (☞ I, 1.2.2). Lipid-based systems rather tend to provide zero-order constant release, which is of course highly favorable [4, 171] (☞ I, 3.2).

Obviously, poly(lactide-co-glycolide) comes along with a number of drawbacks, especially when compared to lipidic matrices. On the other side, it possesses many positive attributes. As PLGA is available with different physico-chemical properties, drug release can precisely be controlled, and a broad range of release profiles can be realized (without adding further excipients) [173] (☞ I, 2.2). Its biodegradability leads to the great advantage that the device does not have to be removed by a surgical intervention once the therapeutic effect comes to an end. As might be imagined, this is beneficial for the patient compliance. Other reasons for the widespread use of PLGA include its outstanding biocompatibility and the fact that it has been approved by regulatory authorities all over the world [49].

Against all odds, PLGA has several times been investigated as matrix material for the delivery of proteins [178]. Quite good results were attained by Ghalanbor et al. who studied the *in vitro* drug release from lysozyme-loaded cylindrical implants prepared by hot melt extrusion. 100% of the incorporated protein could be liberated within 60 d to 80 d. Losses in the enzymatic activity of the last fraction of released lysozyme were found to be negligible [179].

A major problem that is commonly associated with the use of lipidic matrices is that of polymorphic transformations upon manufacturing and/or storage that might account for changes in the release behavior [174]. Polymorphism is simply defined as the phenomenon wherein the same chemical substance exists in different crystalline forms [180]. For mono-acid triglycerides, three basic polymorphs called α , β' , and β are distinguished. Thermodynamically, the β form is most stable, β' metastable, and α is the least stable form [181]. According to the Ostwald's step rule, it is usually the α polymorph that crystallizes first from a solution or a melt [182]. Therefore, manufacturing processes that comprise a dissolution or a melting step have to be carefully considered since less stable polymorphs are (first) obtained. Upon storage, these α and β' forms typically convert into the

β form. As already mentioned, such a rearrangement might affect the release properties. In addition, changes in the surface morphology of the microparticles or implants might occur [174, 183].

Another shortcoming of lipid-based drug delivery systems is the fact that they do not necessarily degrade *in vivo* (☞ I, 3.3). Especially larger devices based on pure triglycerides need to be removed as soon as the release period is finished [174]. With regard to the patient compliance, this is of course detrimental. However, the non-degradability of the depot might also be advantageous. Once it is desirable to immediately stop the therapeutic effect, the device can simply be removed.

3.2 Drug release from lipid-based drug delivery systems

Despite of the steadily increasing importance of lipid-based drug delivery systems, only little is known about the underlying mass transport mechanisms [4, 53, 171]. This is probably due to the fact that the term 'lipid' refers to a large and rather heterogeneous group of excipients. Hence, countless depot formulations are conceivable, each of them with its individual release kinetics.

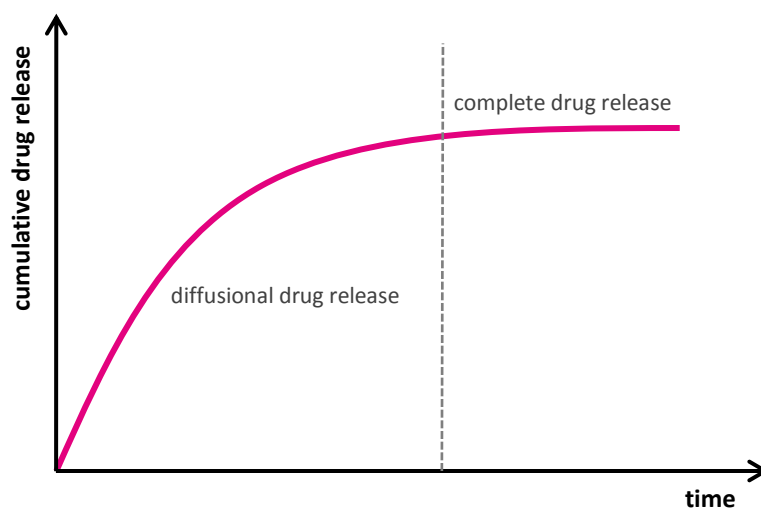


Figure 6 | Schematic representation of a release profile that is typically obtained for lipid-based drug delivery systems.

For non-degradable matrices such as triglycerides, diffusional processes have been shown to play a major role [18, 53, 171]. An example is given by Guse et al. who investigated the release behavior of lysozyme- and pyranine-loaded compressed implants made from different mono-acid triglycerides. Depending on the manufacturing technique, the type of lipid, the drug loading, the particle size, and the addition of a pore-forming agent, a broad range of release profiles was obtained. In many cases, the release could adequately be described by Fick's second law, which means that it is purely

controlled by diffusion [4]. Kreye et al. who prepared propranolol- and theophylline-containing (cast) lipid implants came to a similar conclusion. They emphasized the importance of diffusional processes and explained that the latter might potentially be combined with limited drug solubility effects resulting from the low amounts of water inside the matrix [53].

As displayed in Figure 6, drug release from non-degradable lipidic matrices is less complex than in the case of PLGA-based systems (⇒ I, 2.3). The release rates are comparatively high in the beginning and start to decrease monotonically with time [4]. As long as the diffusion gradient is constant, zero-order release can be achieved. In this respect, perfect sink conditions are a prerequisite. It is further necessary that the concentration of the available API remains unchanged over time. This is the case when the released amount of drug is compensated by the dissolution of formerly non-available drug particles [184].

In general, drug release from non-degradable matrices is assumed to proceed as follows: at first, water penetrates into the system and dissolves the incorporated API as well as potential hydrophilic excipients. Water-filled pores and channels are formed which allow the drug to diffuse out of the matrix (⇒ Figure 7). Due to the geometric characteristics of the pore network (more precisely, the generally restricted diameters and the tortuosity of the channels), drug release is typically sustained. If the drug loading is too low, the pore network is incomplete, and API molecules are (partially) trapped inside the matrix. Consequently, the release does not reach 100% [171, 185]. It might be concluded that diffusion through water-filled pores is the predominating release mechanism. Diffusion through the crystalline lipid can be expected to be negligible [4].



Figure 7 | Formation of an inter-connecting pore network.

In 2012, Sax et al. studied the drug release from rh-interferon α -2a-loaded matrices that were composed of both a high melting mono-acid triglyceride and a low melting mixed-acid triglyceride. As the protein was labeled with a stable fluorescent dye, its release pathways could be tracked by single molecule wide-field fluorescence microscopy. Remarkably, two populations of diffusing proteins were found to be present. The first one was released via water-filled pores whereas the second one was shown to diffuse through a phase of molten lipid. In this case, the matrix can no longer be

considered as being completely inert, it rather acts as a drug reservoir that is slowly depleted upon incubation at temperatures above the melting point of the mixed-acid triglyceride [186].

So far, several mathematical models for quantifying/predicting drug release from triglyceride-based matrices have been developed [4, 6, 53, 171, 174, 187, 188]. One of them refers to an interferon α -loaded system and was described by Siepmann et al. The model takes into account the simultaneous diffusion of multiple compounds including the API and water-soluble excipients such as release modifiers or drug stabilizers. Dynamic changes of the implant - in particular, the formation of a porous network - are considered, resulting in a significant time- and position-dependent mobility of the diffusing species within the system. In addition, the limited solubility of the drug and/or excipients in water-filled channels can be taken into consideration. Importantly, the theory was shown to be in good agreement with the experimentally determined release kinetics. A quantitative prediction of the effects of different formulation and processing parameters on the resulting release profiles was possible [187].

3.3 Biodegradation

Larger matrices based on mono-acid triglycerides can be assumed to reveal no biodegradation [163, 173, 174, 189-192]. This was, for example, confirmed by Vogelhuber et al. who investigated the *in vitro* erosion behavior of compressed implants. For more than six months, no significant water uptake could be observed. The mass of the (dried) matrices remained constant [190]. With the intention to prove the biocompatibility of subcutaneously placed rh-interferon α -2a-loaded tristearin implants, Schwab et al. performed an *in vivo* experiment using rabbits as animal models. In the end of the study, the matrices that appeared to be intact were surgically removed. Indeed, no signs of bioerosion could be detected [163, 192].

In contrast, implants based on lecithin and cholesterol [193] or glyceryl monostearate [194] were found to be degradable. This led to the idea that the erosion behavior of triglyceride matrices could be improved by admixing so-called erosion modifiers [174]. Promising results were published by Guse et al. who prepared tripalmitin-based implants containing different amounts of a phospholipid. After subcutaneous implantation into mice, the matrices showed distinct swelling and erosion, demonstrated through both an increase in wet weight and a mass loss after freeze-drying. Interestingly, the attempt to influence the erosion rate failed when cholesterol was used instead of the phospholipid [173]. Another step towards bioerosion of larger lipid-based implants was reported from Sax et al. who studied the *in vivo* degradation behavior of twin-screw extruded placebo rods

containing a high melting mono-acid triglyceride and a low melting mixed-acid triglyceride. After six months of incubation, only 25% of the matrix could be recovered from the rabbit's subcutaneous tissue, indicating a significant mass loss and a breakdown of the porous implant structure [195].

Even though the *in vivo* stability of mono-acid triglycerides is advantageous in terms of long-term drug delivery, an (accelerated) erosion of the material would be desirable for generating an applicable biodegradable device and for obtaining a greater flexibility concerning the adjustment of the release rates [173].

3.4 Biocompatibility

Bioerosion and biocompatibility are often mentioned in the same breath. This can be ascribed to the fact that it is not only the 'initial device' that needs to be biocompatible but also its degradation products. Against this background, Reithmeier et al. conducted a comparative study on the biocompatibility of glyceryl tripalmitate-based microparticles. Poly(lactide-co-glycolide) was chosen as reference material since it is known to be well-tolerated *in vivo* (☞ I, 2.4). Placebo microparticles made from both the lipid and the polymer were placed subcutaneously into anesthetized mice. At predetermined points of time, two animals of each group were sacrificed, and the tissue at the implantation site was investigated for immunoreactions. After 2 d, a weak proliferation of the connective tissue combined with a slight infiltration of unspecific inflammatory cells such as neutrophil granulocytes or monocytes could be observed for both groups. It was finally concluded that the biocompatibility of the lipid is comparable to the one of the (approved) polymer. Importantly, not only the latter was found to degrade in the subcutaneous tissue [196]. It is likely that the bioerosion of glyceryl tripalmitate can be attributed to the small the size of the microparticles and the presence of enzymes [163]. Concerning the biocompatibility, similar results were obtained by Guse et al. who investigated the *in vivo* behavior of monolithic implants that were prepared from the same triglyceride. Once again, the intensity of the encapsulation into connective tissue was shown to be comparable to the one of PLGA-based matrices. However, the integrity of the implants could be confirmed for the entire observation period of 60 d. When different amounts of cholesterol were added, the biocompatibility remained unaffected. In contrast, when distearoyl-phosphatidylcholine was admixed, distinct signs of degradation were achieved, and a foreign body reaction could be detected [173].

In summary, pure triglycerides can generally be expected to show good biocompatibility [171] - independent of the question whether they undergo biodegradation or not. Other lipids have to be

regarded with skepticism. The administration of fatty acids, for example, has been reported to lead to inflammation and the formation of blisters [163]. In the end, decisions on the suitability of potential matrix materials have to be taken on a case-to-case basis.

4 Overview of implant manufacturing techniques

The following chapter gives an overview of the most important manufacturing techniques that have been described for the production of parenteral implants. More precisely, compression, hot melt extrusion, injection molding, compression molding, and solvent casting are briefly introduced.

4.1 Compression

Compression is generally used for the production of lipidic implants [6, 163, 169, 174, 197] but has also been mentioned in the context of polymeric devices [198, 199]. In the lab scale, hydraulic presses equipped with special compaction tools are commonly employed. Homogeneous powder blends are filled into these compaction tools, and force is applied for a certain time span. The resulting implants are disk-shaped so that a surgical intervention is deemed necessary for their implantation.

4.2 Hot melt extrusion

Within the plastics industry, hot melt extrusion is one of the most widely used processing techniques. Currently, more than half of all plastic products including bags, sheets, and pipes are manufactured by this process [200]. To a lesser extent, it is also utilized in the food industry, for example for the production of cereals [201]. During the past decade, the technology has emerged as a viable platform for pharmaceutical applications [202]. It is nowadays most often associated with the production of solid oral dosage forms. Especially screw extruders are used for the manufacturing of granules or pellets that are further processed into capsules or tablets [200, 203-205]. Prime candidates for such delivery systems are drugs with poor bioavailability, among those numerous new chemical entities [205]. A plethora of these drugs forms solid solutions with the (polymeric) matrix material, that way providing an enhanced bioavailability [206]. For the production of long-acting parenteral implants, hot melt extrusion is used as well. The technique is particularly suitable for the manufacturing of slim cylindrical rods that can be administered by means of a hypodermic needle [205, 207].

In general, hot melt extrusion can be defined as a process that converts a raw material or blend into a product of uniform shape and density by forcing it through a die under controlled conditions such as temperature or pressure [201, 203, 208, 209]. For this purpose, conventional extruders consist of two components: a transport system that may impart a mixing function and a die system that forms the material [174].

4.2.1 Screw extrusion

As their name implies, screw extruders are characterized by at least one rotating screw inside a stationary cylindrical barrel (➡ Figure 8). The latter is often manufactured in sections which are bolted or clamped together. A die that is connected to the end of the barrel determines the shape of the extruded product. Remarkably, up to 80% of the heat that is required to melt or fuse the material (inside the barrel) results from friction. Additional heat may be supplied by electric or liquid heaters [203].

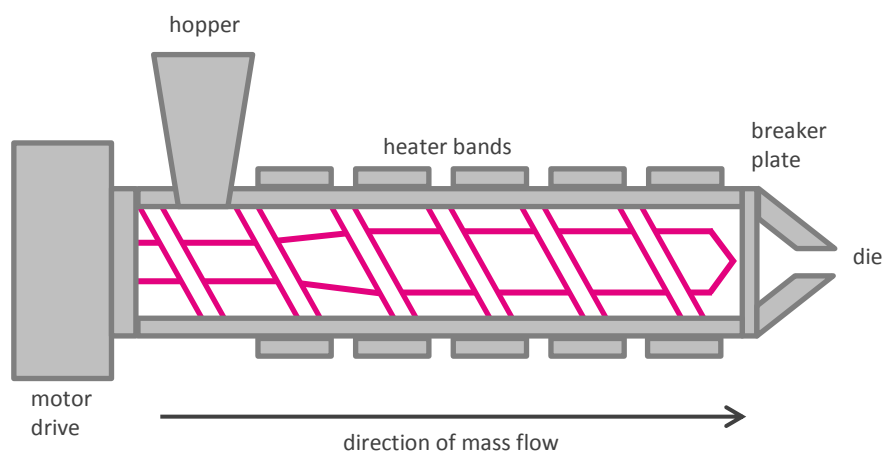


Figure 8 | Schematic representation of a single-screw extruder [203].

The extrusion channel is commonly divided into three sections: feed zone, transition zone, and metering zone. The starting material is fed from a hopper directly into the feed section. As this part of the extruder is of a special geometry, the material is enabled to fall easily into the rotating screw. It is then conveyed along the barrel and reaches the transition zone where it is mixed, compressed, melted, and plasticized. The function of the metering zone to which the material is finally transported as a homogeneous melt is the reduction of the pulsating flow, thus ensuring a uniform delivery rate through the die [203, 209].

Aside from single-screw extruders, twin-screw extruders that consist of two agitator assemblies mounted on parallel shafts have gained considerable attention. The shafts may either rotate in the same or the opposite direction. Counter-rotating extruders are said to have better mixing capabilities as their surfaces move towards each other, thereby squeezing the material through the gap between the two screws. This results in comparatively high shear forces [200, 203, 210]. At the same time, such systems may suffer from air entrapment, the generation of high pressures, and low maximum screw speeds and output [200]. Co-rotating extruders are generally of the intermeshing design which is known to be self-wiping. This ensures almost complete emptying of the barrel, hence minimizing

product wastage on shutdown [200, 203]. In addition, lower screw and barrel wear is generated. As such systems can be operated at high screw speeds, and as they achieve high outputs while maintaining good mixing and conveying characteristics, they are - from an industrial point of view - the most important type of extruder [200].

In 2009, Schulze and Winter investigated the applicability of twin-screw extrusion for the manufacturing of lipid-based implants. At first, they tried to process their standard formulation consisting of 80% of tristearin, 10% of placebo lyophilisate, and 10% of PEG. Importantly, extrusion at various temperatures failed. This was primarily ascribed to the sharp melting point of the lipid. As soon as the process temperature exceeded the melting temperature, a low-viscosity melt inapplicable for extrusion was formed. In contrast, when the temperature was too low, the formulation remained solid, and an adequate feeding of the extruder was not possible. These problems could successfully be overcome by admixing smaller amounts of lipids with a lower melting point. This approach enabled extrusion at temperatures of 40 °C or 45 °C, which is especially advantageous if temperature-sensitive drugs such as proteins are to be embedded [52].

4.2.2 Ram extrusion

At a first glance, ram extrusion seems to be inferior to screw extrusion. This can be attributed to a number of reasons: first, the process cannot be run continuously so that the batch size is limited by the capacity of the barrel. Second, extrudates with lower homogeneity have to be expected as the system does not provide any mixing function. Third, the melting capacity is limited, which causes poor temperature uniformity in the extrudates [200]. However, all of these limitations can be dealt with in practice. Highly sophisticated ram extruders allow for precisely controlling the process (parameters), thus leading to extrudates of a very consistent diameter and with a homogeneous drug distribution. It is hardly surprising that such systems have already found their way into the production of commercially available implants.

As depicted in Figure 9, the setup and operating principle of a ram extruder is as simple as possible. The barrel that is closed with a die at one side is pre-filled with the raw material or blend. It is then mounted into the heating unit that enables a precise temperature control. Finally, the piston moves downwards (assuming that the extruder is of a vertical design), thereby forcing the material through the die.

The process is usually divided into different phases. At first, the material inside the barrel is compressed to a plug, that way removing residual air. In a second step, heating is applied with the

aim of converting the implant formulation to a viscous mass. During the last phase, the extrusion itself takes place. The material is pushed through the die in order to obtain its characteristic shape. This stage of process is either controlled by a constant piston speed or by a constant piston force. A concrete example is given in chapter IV, 1.

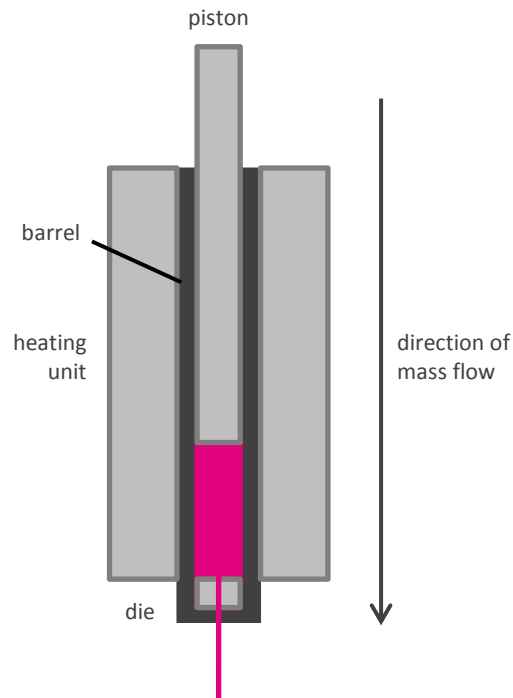


Figure 9 | Schematic representation of a ram extruder.

In the lab scale, syringes are often (mis)used as ‘mini ram extruders’. A self-made syringe-die assembly has, for example, been described by Ghalanbor et al. who worked on protein-loaded implants based on PLGA. The principle is simple: the syringe is filled with the powder mixture and connected to the die. This assembly is then heated at 105 °C for 10 min. Cylindrical matrices are finally formed by moving the plunger towards the die [179, 211].

4.3 Injection molding

Similar to hot melt extrusion, injection molding is a manufacturing technique that originates from the plastics industry. The raw material or blend is fed into a heated barrel, mixed, and forced into a mold cavity where it cools and hardens to the configuration of the cavity. The setup of the machines - typically consisting of a hopper, an injection ram or a screw-type plunger, and a heating unit - can be

compared to hot melt extruders. The only difference is the final shaping of the implant formulation [212, 213].

Rothen-Weinhold et al. used both extrusion and injection molding for the preparation of vapreotide-loaded biodegradable implants. Right after manufacturing, they determined the purity of the peptide. It was found to be significantly decreased in the injection-molded implants. This was ascribed to the presence of high shear forces and comparatively high process temperatures. Apart from that, the *in vitro* release rates were investigated. They were shown to be similar for the first 48 h of incubation, thereafter an increase could be observed for the extruded implants. This was related to the porosity of the matrix and to the crystalline/amorphous ratio which was supposed to be increased for the injection-molded implants. In summary, both techniques proved to be feasible for the production of peptide-loaded implants. However, it was concluded that the injection molding process needs to be optimized, especially with regard to the degradation of the API [207].

4.4 Compression molding

Compression molding is one of the oldest techniques used for processing plastics. Over the past decades, it has to some extent been replaced by injection molding that offers advantages in materials handling and ease of automation. However, compression molding retains a distinct advantage: as there are no regions of very high stress such as at the gate of an injection mold [214], shear-sensitive materials can be processed. For peptides and proteins, this might be of particular importance. The operating principle can be described as follows: a metal mold is filled with the raw material or blend. It is then heated, and pressure is applied until the powder has plasticized completely. The hot mold is finally cooled at a controlled rate, and the sintered implant is demolded [215].

Witt et al. utilized this technique for the production of placebo implants made from pure poly(lactide-co-glycolide) or ABA triblock copolymers consisting of PLGA A-blocks and PEG B-blocks. Independent of the type of polymer, the resulting tablets were characterized by an average diameter of 7.28 mm and a height of 2.13 mm. For comparison purposes, rod-shaped implants manufactured by ram extrusion were additionally investigated. This time, the dimensions were found to strongly depend on the polymer. Implants prepared from ABA were 87.0 mm in average length and 1.04 mm in average diameter whereas the average length of PLGA implants was 54.0 mm, and the average diameter was 1.44 mm [216]. This example clearly illustrates one of the benefits of compression

molding: the shape of the resulting devices remains unchanged, even if polymers of different physico-chemical properties are used.

4.5 Solvent casting

As opposed to the aforementioned methods, solvent casting comes along with the disadvantage of involving large amounts of organic solvents. Nevertheless, it is still often used, especially for the lab-scale manufacturing of PLGA-based implants [28, 217-220]. The polymer is typically dissolved in an appropriate solvent such as dichloromethane or acetone. The drug is added, and the mixture is carefully homogenized. Thereafter, it is poured into three-dimensional molds or cast onto glass plates. The solvent is finally allowed to evaporate. This stage of the process might require several weeks and can therefore be seen as additional disadvantage [220].

In 2010, Wang et al. tried to translate a laboratory solvent casting process into a continuous and more scalable extrusion process. For this purpose, haloperidol-loaded implants based on poly(lactide-co-glycolide) were focused. The extrusion temperature, the screw speed, and the resulting pressure were shown to influence the surface morphology and hence the release rates. Although the process was optimized in several steps, the release profile of the solvent-cast pellets could not be matched one-to-one. In particular, the lag phase was found to be longer for the extruded rods. Despite that, extrusion turned out to be a reliable process for the manufacturing of larger batches [220].

Chapter II | Aims of the thesis

For the production of parenteral implants based on poly(lactide-co-glycolide), hot melt extrusion is one of the favorite manufacturing techniques, if not the most important one [200, 203, 205, 207, 209, 221]. Screw systems are still more widespread than ram systems but in the last years, the latter gained more and more importance and evolved into a serious competitor. However, both techniques have a major drawback in common: as relatively high temperatures have to be applied for polymer softening, thermosensitive drugs such as biopharmaceuticals cannot be processed. With regard to the increasing market for these APIs and the need for adequate delivery systems [222], this is not sustainable. Hence, the reduction of the manufacturing temperature was declared as main objective of this thesis. At the same time, it was desired that the characteristic release profiles were maintained.

Acino offered the great opportunity of cooperation so that all experiments could be performed using an industrial ram extruder. Since almost no literature had been available on this topic so far, this work will hopefully close the gap by providing comprehensive information.

A factorial design of experiments including the most important factors - for example, the piston speed or the duration of the heating phases - was intended to clarify whether the temperature could be lowered by precisely adjusting the process parameters (and leaving the formulation unchanged). Additionally, the die geometry and its influence on the extrusion behavior were investigated.

In order to find out whether the extrudability and the release properties are affected by the type of drug and the type of polymer, implants consisting of either oxybutynin hydrochloride or oxybutynin base in PLGA matrices with different physico-chemical properties were produced. The underlying release mechanisms were elucidated by a number of *in vitro* tests whereby a special focus was put on drug/polymer interactions.

At last, the idea that lipidic excipients might act as lubricants or binders, thus facilitating extrusion of PLGA-based formulations, was followed up. A variety of lipids, among those highly hydrophobic and rather amphiphilic ones, was subjected to a screening in which the most promising candidates were identified. With the objective to demonstrate the potential of these excipients, the extrusion temperature was reduced stepwise. Detailed studies on the *in vitro* release were necessary to understand the complex role of the two-component matrix.

Against the background of a process optimization towards lower extrusion temperatures, the aims of this thesis can be summarized as follows:

- ✓ Determination of an optimum parameter set by means of a factorial design of experiments
- ✓ Investigations on the influence of the type of drug and the type of polymer on the extrusion behavior and the release mechanisms
- ✓ Investigations on the influence of different (additional) lipids on the extrusion behavior and the release mechanisms

Chapter III | Materials and methods

1 Materials

The information given in this chapter was summarized from product information sheets, material safety data sheets, certificates of analysis, and personal correspondence with representatives of different manufacturers.

1.1 Oxybutynin

Oxybutynin hydrochloride (☞ Figure 10) was received from Fagron (Barsbüttel, Germany). It is characterized by a molecular weight of 393.95 g/mol and a melting temperature of 124 °C - 129 °C.

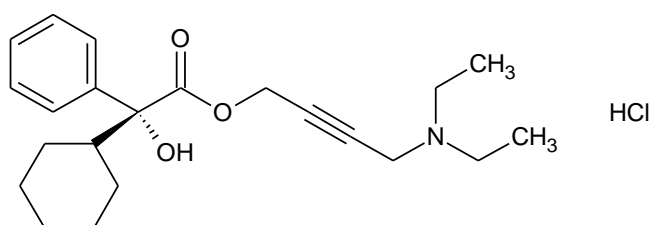


Figure 10 | Chemical structure of oxybutynin hydrochloride.

In contrast, the corresponding base melts in the range of 56 °C to 58 °C and has a molecular weight of 357.49 g/mol.

1.2 Polymers

All poly(D,L-lactide-co-glycolides) and poly(D,L-lactides) were of the Resomer type and purchased from Boehringer Ingelheim (Ingelheim am Rhein, Germany). Their individual properties are summarized in Table 2. The polymers are either terminated with alkyl esters or free carboxylic acids. According to the specifications, the appropriate acid values range from minimum 3 mg KOH/g for RG 503 H and R 203 H to minimum 6 mg KOH/g for RG 502 H and R 202 H to 8 mg KOH/g to 15 mg KOH/g for RG 752 H.

Table 2 | Properties of RG 502, RG 502 H, RG 503, RG 503 H, RG 752 H, R 202 H, and R 203 H.

	Composition	end group	molecular weight [g/mol]	inherent viscosity [dL/g]*	T_g [°C]
RG 502	poly(D,L-lactide-co-glycolide) 50:50	ester	7,000 - 17,000	0.16 - 0.24	42 - 46
RG 502 H	poly(D,L-lactide-co-glycolide) 50:50	acid	7,000 - 17,000	0.16 - 0.24	42 - 46
RG 503	poly(D,L-lactide-co-glycolide) 50:50	ester	24,000 - 38,000	0.32 - 0.44	44 - 48
RG 503 H	poly(D,L-lactide-co-glycolide) 50:50	acid	24,000 - 38,000	0.32 - 0.44	44 - 48
RG 752 H	poly(D,L-lactide-co-glycolide) 75:25	acid	4,000 - 15,000	0.14 - 0.22	42 - 46
R 202 H	poly(D,L-lactide)	acid	10,000 - 18,000	0.16 - 0.24	44 - 48
R 203 H	poly(D,L-lactide)	acid	18,000 - 28,000	0.25 - 0.35	48 - 52

* measured at 0.1% in chloroform (w/v), 25 °C

Resomer Condensate RG 50:50 M_n 2300 was also obtained from Boehringer Ingelheim (Ingelheim am Rhein, Germany). The oligo(D,L-lactate-co-glycolate) 50:50 is characterized by free carboxylic acid end groups, a molecular weight of 2,000 g/mol - 2,500 g/mol, and a glass transition temperature around 30 °C.

1.3 Lipids

1.3.1 Triglycerides

Microcrystalline Dynasan 114 and Dynasan 118 in the stable β modification were a gift from Sasol (Johannesburg, South Africa). Their properties are listed in Table 3.

Table 3 | Properties of Dynasan 114 and Dynasan 118.

	Dynasan 114	Dynasan 118
chemical name	trimyristin	tristearin
acid value [mg KOH/g]	max. 3	max. 3
hydroxyl value [mg KOH/g]	max. 10	max. 10
iodine value [g I₂/100 g]	max. 1	max. 1
saponification value [mg KOH/g]	229 - 238	186 - 192
melting range [°C]	55 - 58	70 - 73

1.3.2 Hydrogenated cocoglycerides

Witepsol H 12, Witepsol W 31, and Witocan 42/44 were kindly provided by Sasol (Johannesburg, South Africa). The lipids comprise a mixture of tri-, di- and monoglycerides of saturated C10 to C18 fatty acids. Their individual properties are summarized in Table 4.

Table 4 | Properties of Witepsol H 12, Witepsol W 31, and Witocan 42/44.

	Witepsol H 12	Witepsol W 31	Witocan 42/44
acid value [mg KOH/g]	max. 0.2	max. 0.3	max. 0.5
hydroxyl value [mg KOH/g]	5 - 15	25 - 35	approx. 15
iodine value [g I₂/100 g]	max. 3	max. 3	max. 2
saponification value [mg KOH/g]	240 - 255	225 - 240	215 - 235
ascending melting point [°C]	32.0 - 33.5	35.5 - 37.0	42 - 44*

* melting range [°C]

1.3.3 Monoglycerides

Imwitor 960 P (F) that belongs to the group of glyceryl stearates was obtained from Sasol (Johannesburg, South Africa). It contains minimum 30% of 1-monoglycerides of palmitic and stearic acid and maximum 7% of free glycerol. Further ingredients are potassium palmitate and stearate. The lipid is characterized by an acid value of maximum 5 mg KOH/g and a saponification value of 150 mg KOH/g to 180 mg KOH/g. Melting occurs around 60 °C.

1.3.4 Acetylated glycerides

Dynacet 211 P and Dynacet 212 P that were received from Sasol (Johannesburg, South Africa) mainly consist of acetylated mono- and diglycerides of palmitic and stearic acid. Their characteristics are summarized in Table 5.

Table 5 | Properties of Dynacet 211 P and Dynacet 212 P.

	Dynacet 211 P	Dynacet 212 P
acid value [mg KOH/g]	max. 2	max. 2
hydroxyl value [mg KOH/g]	135 - 155	75 - 90
iodine value [g I₂/100 g]	max. 3	max. 3
saponification value [mg KOH/g]	270 - 310	300 - 340
melting range [°C]	41 - 47	36 - 44

1.3.5 Macroglycerides

Labrafil M 2130 CS, Gelucire 44/14, and Gelucire 50/13 were a gift from Gattefossé (Saint-Priest, France). The lipids are composed of mono-, di-, and triglycerides as well as fatty acid esters of poly(ethylene glycol). Labrafil M 2130 CS and Gelucire 44/14 count among the lauroyl macroglycerides whereas Gelucire 50/13 belongs to the stearyl macroglycerides. Their individual properties are listed in Table 6.

Table 6 | Properties of Labrafil M 2130 CS, Gelucire 44/14, and Gelucire 50/13.

	Labrafil M 2130 CS	Gelucire 44/14	Gelucire 50/13
acid value [mg KOH/g]	max. 2	max. 2	max. 2
hydroxyl value [mg KOH/g]	65 - 85	36 - 56	36 - 56
iodine value [g I₂/100 g]	max. 2	max. 2	max. 2
saponification value [mg KOH/g]	190 - 204	79 - 93	67 - 81
drop point [°C]	33.5 - 38.0	42.5 - 47.5	46.0 - 51.0

1.3.6 Phosphatidylcholines

All lecithins were kindly provided by Lipoid (Ludwigshafen, Germany). Lipoid S 100 and Lipoid E PC contain at least 94.0% and 98.0% of phosphatidylcholine (in dry matter) that is typically composed of different saturated and unsaturated fatty acids. As indicated by their name, the lipids are extracted from soybean and egg, respectively. The same holds true for the hydrogenated types Lipoid S PC-3 and Lipoid E PC-3 that mainly consist of palmitic and stearic acid-based phosphatidylcholine. Lipoid PC 16:0/16:0 and Lipoid PC 18:0/18:0 are highly purified dipalmitoyl- and distearoyl-phosphatidylcholines with molecular weights of 734 g/mol and 790 g/mol.

1.4 Chemicals

1.4.1 Acids and bases

85% phosphoric acid (H₃PO₄, suitable for use as excipient, EMPROVE exp), trifluoroacetic acid (C₂HF₃O₂, for spectroscopy, Uvasol), and potassium hydroxide pellets (KOH, pure) were received from Merck (Darmstadt, Germany). For the preparation of 5 M KOH solution, 140.26 g of the pellets were dissolved in 0.5 L of ultrapure water.

1.4.2 Buffers

Potassium dihydrogen phosphate (KH₂PO₄, for analysis, EMSURE ISO), potassium hydrogen phosphate (K₂HPO₄, anhydrous, for analysis, EMSURE), and sodium azide (NaN₃, extra pure) were purchased from Merck (Darmstadt, Germany).

✓ 0.1 M phosphate buffer pH 3.0

6.80 g of KH₂PO₄ and 0.10 g of NaN₃ were dissolved in 0.5 L of ultrapure water. The pH was adjusted to 3.0 with 85% phosphoric acid (Orion Star LogR, Thermo Scientific, Waltham, United States).

✓ **0.1 M phosphate buffer pH 6.0**

12.82 g of KH_2PO_4 , 1.01 g of K_2HPO_4 , and 0.20 g of NaN_3 were dissolved in 1.0 L of ultrapure water. The pH was adjusted to 6.0 with 5 M KOH solution and 85% phosphoric acid, respectively (Orion Star LogR, Thermo Scientific, Waltham, United States).

✓ **1.0 M phosphate buffer pH 6.0**

64.09 g of KH_2PO_4 , 5.06 g of K_2HPO_4 , and 0.10 g of NaN_3 were dissolved in 0.5 L of ultrapure water. The pH was adjusted to 6.0 with 5 M KOH solution (Orion Star LogR, Thermo Scientific, Waltham, United States).

✓ **10 mM phosphate buffer pH 6.95**

3.40 g of KH_2PO_4 and 4.36 g of K_2HPO_4 were dissolved in 1.0 L of ultrapure water. If necessary, the pH was adjusted to 6.95 with 5 M KOH solution and 85% phosphoric acid, respectively (Orion Star LogR, Thermo Scientific, Waltham, United States). This 50 mM solution was diluted to 10 mM with ultrapure water.

1.4.3 Dyes

Methylene blue and Sudan red G were received from Merck (Darmstadt, Germany).

1.4.4 Standard substances

Butylated hydroxytoluene was purchased from Merck (Darmstadt, Germany), and a DIN kit with polystyrenes of different molecular weight, namely 162 g/mol, 685 g/mol, 1,470 g/mol, 3,250 g/mol, 9,130 g/mol, 19,600 g/mol, 34,300 g/mol, 100,000 g/mol, 250,000 g/mol, 556,000 g/mol, 851,000 g/mol, and 1,865,000 g/mol, was ordered from PSS (Mainz, Germany).

1.4.5 Immersion oil

Immersion oil type DF was received from Cargille Laboratories (Cedar Grove, United States).

1.4.6 Solvents

Acetone (suitable for use as excipient, EMPROVE exp), acetonitrile (gradient grade for liquid chromatography, LiChrosolv), dimethylformamide (for gas chromatography, SupraSolv), dimethyl sulfoxide (EMPLURA), ethyl acetate (for gas chromatography, SupraSolv), heptane (for liquid

chromatography, LiChrosolv), methylpyrrolidone (EMPLURA), and tetrahydrofuran (for liquid chromatography, LiChrosolv) were obtained from Merck (Darmstadt, Germany).

1.4.7 Gases

Hydrogen, purified compressed air, and nitrogen were produced by a H2PEM-100 Hydrogen Generator (Parker Balston, Haverhill, United States), a 75-83 Zero Air Generator, and a 76-94-220 Nitrogen Generator (both Whatman, Maidstone, United Kingdom), respectively.

1.4.8 Ultrapure water

Ultrapure water was obtained from an in-house generator (Milli-Q Integral 15, Millipore, Billerica, United States).

2 Methods

2.1 Implant manufacturing

2.1.1 Cryogenic grinding

A total of 3.0 g of an implant formulation, for example 2.40 g of RG 502 H and 0.60 g of oxybutynin hydrochloride, was filled into a small polycarbonate center cylinder that was tightly closed with a stainless steel end plug on one side. After addition of a stainless steel impactor, the other side was sealed as well. In order to mill four samples at the same time, a multi-vial adapter was placed in the grinding chamber of the Freezer/Mill 6850 (SPEX SamplePrep, Metuchen, United States). The cylinders were fastened and cooled down in a liquid nitrogen bath for 5.0 min. Thereafter, ten milling cycles were run, each with a duration of 1.5 min and a rate of 30 impacts per second. Every milling cycle was followed by a cooling phase of 1.0 min. For thawing, the cylinders were placed inside a desiccator for at least 2 h. The powders were used immediately or they were transferred into amber glass bottles that were stored at 2 °C to 8 °C.

2.1.2 Hot melt extrusion

A Rheograph 25 E II (Göttfert, Buchen, Germany) equipped with dies of different geometry (standard die: 21.0 mm length, 1.15 mm diameter) was used for extrusion purposes. Unless otherwise stated, 1.5 g of a pulverized implant formulation were filled into the barrel that was closed with a die and an appropriate stopper at the lower end. The barrel was mounted into the heating unit, and the piston was positioned. Then, the standard program (↪ Table 7) was started. Straight before extrusion, the stopper was removed. The strand was cut by hand into pieces of a length of approximately 10 cm.

Table 7 | Standard extrusion program.

	temperature [°C]	piston force [N]	piston speed [mm/s]	time [min]
compression phase	room temperature	2,000	0	10
first heating phase	room temperature - 75*	250	0	10
second heating phase	75*	250	0	10
temperature control	75*	250	0	0.5
extrusion	75*	variable	0.010	variable
cooling	75* - 10	0	0	variable

* If necessary, the temperature was adapted to the formulation.
 These parameters were modified during process optimization.

These pieces were stored in centrifuge tubes at 2 °C to 8 °C. Collected data were evaluated using LabRheo and WinRheo II software (Göttfert, Buchen, Germany).

✓ **Process optimization**

Within the scope of a process optimization, the parameters marked pink in Table 7 were modified. A factorial design of experiments was calculated, carried out, and then analyzed using MODDE 9 software (Umetrics, Umeå, Sweden).

✓ **Influence of the die geometry**

Dies with a diameter of 1.08 mm, 1.15 mm, or 1.46 mm were used. Their length was either 14.2 mm or 21.0 mm, and the number of orifices was one, two, or four (Göttfert, Buchen, Germany; Schönbach, Fischbachau, Germany; Senss, Reinach, Switzerland).

✓ **Determination of strand diameters**

In the case of one- and two-holed dies, strand diameters were recorded automatically by LabRheo (Göttfert, Buchen, Germany) every 2 s. When four-holed dies were employed, the diameters had to be determined by hand. A caliper rule (Helios DIGI-MET, Preisser Messtechnik, Gammertingen, Germany) was used to measure them approximately every 0.3 mm.

2.1.3 Compression

Approximately 80 mg of a pulverized implant formulation consisting of 80% of RG 502 H and 20% of oxybutynin (w/w) were filled into the cylindrical matrix of a compaction tool with a diameter of 13 mm (Maassen, Reutlingen, Germany). A plunger was carefully positioned onto the powder, and a pressure of 3 bar was applied for 30 s (5-T-PRESSE manuell, Maassen, Reutlingen, Germany). The resultant platelets were divided into four parts of almost the same size, each with a mass of 20 mg.

2.1.4 Alternative manufacturing strategies

Alternative manufacturing strategies mainly concerning the workflow prior to extrusion were developed for implant formulations containing 70% of RG 502 H, 20% of oxybutynin hydrochloride, and 10% of Dynacet 211 P (w/w). Grinding and extrusion were performed as described before (➔ III, 2.1.1 and 2.1.2).

2.1.4.1 Heptane dispersion

RG 502 H and oxybutynin were dispersed in 10.0 mL of heptane. After shaking at 300 rpm for 20 min (KS 260 basic, IKA, Staufen, Germany), the suspension was transferred into a shallow pan made from aluminum, and the solvent was allowed to evaporate at room temperature for at least 2 h. Thereafter, the formulation was dried to constant weight at 37 °C (ED 115, Binder, Tuttlingen, Germany). Dynacet 211 P was added, and cryogenic grinding was performed before the mixture was extruded at 55 °C.

2.1.4.2 Solvent casting

RG 502 H and oxybutynin were dissolved in 5.0 mL of an appropriate solvent, for example acetonitrile. Shaking at 300 rpm was applied for at least 30 min (KS 260 basic, IKA, Staufen, Germany). In aliquots of 50 µL, the clear solution was pipetted onto a synthetic foil with lotus effect. In order to prevent coalescence, enough space had to be left between the individual droplets. The solvent was allowed to evaporate overnight before the platelets were dried to constant weight at 37 °C (ED 115, Binder, Tuttlingen, Germany). Dynacet 211 P was added, and cryogenic grinding was performed. The mixtures were extruded at 55 °C and lower.

For comparison purposes, lipid-free films of the same drug to polymer ratio were prepared.

2.1.4.3 Compression

RG 502 H and oxybutynin were pulverized and compressed at 10,000 N for 10 min (Rheograph 25 E II, Göttfert, Buchen, Germany). After addition of Dynacet 211 P, the formulation was ground again. Extrusion was performed at 55 °C.

2.1.4.4 Threefold grinding

The formulation was ground three times so that a total of 30 milling cycles was run. Extrusion was performed at 55 °C.

2.1.4.5 Double extrusion

Grinding and extrusion were done twice in a row at the same conditions. The extrusion temperature was adjusted to 55 °C.

2.1.5 Sterilization

For sterilization purposes, implant strands were packed into centrifuge or safe-lock tubes. Sealing film was used to tightly close the tubes. In aluminum pouches without a desiccant capsule, they were sent to Isotron (Allershausen, Germany) where gamma sterilization was performed at 28 kGy.

2.2 Concentration of oxybutynin

The concentration of oxybutynin that was, for example, present in the samples of the release tests was determined by reverse phase chromatography. An UltiMate 3000 system comprising a SRD-3400 solvent rack, a LPG-3400 pump, a WPS-3000 sampler, a TCC-3000 column oven, and a DAD-3000 detector (all Dionex, Sunnyvale, United States) was equipped with a SecurityGuard Standard C8 precolumn (3.0 mm x 4 mm) (Phenomenex, Torrance, United States) and a XTerra Shield RP18 column (125 Å, 3.5 µm, 3.9 mm x 100 mm) (Waters, Milford, United States). The mobile phase that consisted of 55% of acetonitrile and 45% of 10 mM phosphate buffer pH 6.95 (v/v) (☞ III, 1.4.2) was automatically mixed and degassed. At a flow rate of 1.0 mL/min, sample volumes of 10 µL were injected. UV absorption was measured at 210 nm for 7.0 min. Sampler and oven were run at 20 °C and 25 °C, respectively. The chromatograms were analyzed using Chromeleon software (Dionex, Sunnyvale, United States).

The same method was used for determining the amount of incorporated oxybutynin. Entire implants or implant fragments of 20 mg weight were placed in headspace vials, and 3.0 mL of acetonitrile were added. After shaking at 300 rpm for 20 min (KS 260 basic, IKA, Staufen, Germany), 150 µL of the clear solutions were diluted with 850 µL of fresh acetonitrile. The samples were analyzed immediately or they were frozen at -20 °C.

For the determination of homogeneity, six samples per batch were compared. In the case of batches that were macroscopically inhomogeneous, implants or fragments of different appearance were intentionally chosen. For example, opaque and almost transparent rods were investigated.

2.3 *In vitro* release studies

At first, length and diameter of implants of 20 mg weight were determined so that their density could be calculated. The rods were placed in amber glass bottles, and 10.0 mL of 0.1 M phosphate buffer pH 6.0 (☞ III, 1.4.2) were added. The bottles were stored in a compartment dryer (ED 115, Binder, Tuttlingen, Germany) at 37 °C until samples were drawn at predetermined points of time. After 1 d,

4 d, 7 d, 11 d, 14 d, 18 d, 21 d, 25 d, 28 d, and 32 d the bottles were removed and carefully shaken by hand. 1.0 mL of each sample was pipetted into a vial which was either analyzed immediately (☞ III, 2.2) or which was frozen at -20 °C. Removed buffer solution was replaced by fresh one before the bottles were shaken again and put back into the dryer.

✓ **Influence of the molarity of the release medium**

1.0 M phosphate buffer pH 6.0 (☞ III, 1.4.2) was used.

✓ **pH measurements**

After 32 d of incubation, the pH values were measured with a mobile pH meter (pH 315i, WTW, Weilheim, Germany).

2.4 Investigations on the release mechanisms

Similar to the *in vitro* release studies (☞ III, 2.3), implants of 20 mg weight were placed in amber glass bottles, and 10.0 mL of 0.1 M phosphate buffer pH 6.0 were added. The bottles were stored in a compartment dryer (ED 115, Binder, Tuttlingen, Germany) at 37 °C. At predetermined points of time, namely after 1 d, 4 d, 7 d, 11 d, 14 d, 18 d, 21 d, and 25 d, they were removed, carefully shaken by hand, and allowed to stand until room temperature was reached.

2.4.1 pH measurements

The pH values were measured with a mobile pH meter (pH 315i, WTW, Weilheim, Germany).

2.4.2 Water uptake and mass loss

The buffer was carefully discarded, and the implant residues were twice washed with 5 mL of ultrapure water. Lint-free tissue paper was used to gently remove excess surface water. The implants were accurately weighed and dried to constant weight at 37 °C (ED 115, Binder, Tuttlingen, Germany) before their masses were determined again. In order not to damage them, sticky or fragile implants were usually left in the bottles. In this case, the tare weights had to be determined as well.

$$\text{water uptake [\%]} = \left(\frac{m_w - m_d}{m_d} \right) \cdot 100 \quad \{1\}$$

$$\text{mass loss [\%]} = \left(\frac{m_0 - m_d}{m_0} \right) \cdot 100 \quad \{2\}$$

Water uptake and mass loss were calculated with equations {1} and {2} where m_0 is the initial mass and m_w and m_d are the wet and the dry mass after exposure to the release buffer.

2.5 Mechanical properties

An EZ Test 500 N equipped with a 20 N measuring cell (both Shimadzu, Kyoto, Japan) was employed to determine the tensile strength. An implant of 2 cm was fixed in a custom-made holder with locking screws at both ends (Schönbach, Fischbachau, Germany) (uncovered part: 0.4 cm). A link chain that was connected to the measuring cell was attached to the middle of the implant. It was raised with a constant speed of 10 mm/min for maximum 60 s until the implant was broken or completely deformed. Anwendungssoftware für Universalprüfmaschinen was used for data acquisition.

2.6 Investigations on surface morphology

2.6.1 Macroscopic appearance

A Lumix DMC-TZ7 camera (Panasonic, Osaka, Japan) was used to take pictures.

2.6.2 Digital microscopy

A VHX-500FD digital microscope equipped with a VH-Z20R or a VH-Z100R zoom lens (all Keyence, Osaka, Japan) was used. When the depth composition mode was applied, at least five pictures with different sharpness were taken.

2.6.3 Scanning electron microscopy

Implant fragments were fixed on specimen holders with conductive adhesive tape. Under vacuum and with an acceleration voltage of 2 kV, the surface morphology was studied at different magnifications (JSM-6500F, JEOL, Akishima, Japan). The implants were not subjected to a coating step.

2.7 Thermo-optical analysis

Raw materials or thin implant cross sections were investigated under a BX51 microscope that was connected to a U-CMAD3 digital color camera (both Olympus, Tokyo, Japan). The samples were heated from 25.0 °C to 90.0 °C with a rate of 10.0 K/min (hot stage FP82HT, Mettler-Toledo,

Greifensee, Switzerland). Pictures were taken every 2.0 K up to 60.0 °C and every 5.0 K up to 90.0 °C (analySIS software, Olympus, Tokyo, Japan).

2.8 Differential scanning calorimetry

Samples of 5 mg of raw materials, powder mixtures, unmodified or degraded implants were accurately weighed and sealed in 40 µL aluminum crucibles. An empty but closed crucible was used as reference. All samples were subjected to the following temperature program (DSC821^e, Mettler-Toledo, Greifensee, Switzerland): after insertion at 25 °C, the crucibles were cooled down to -10 °C. This temperature was maintained for 2 min. Then, heating was applied at a constant rate of 10 K/min. As soon as 160 °C were reached, a second isothermal phase of 2 min followed. Principally, only one heating cycle was run. The thermograms were analyzed for glass transition and melting temperatures using STAR^e software (Mettler-Toledo, Greifensee, Switzerland).

2.9 Size exclusion chromatography

The molecular weight of RG 502 H and its degradation products was determined by size exclusion chromatography. A system comprising a P680 ISO isocratic pump, a Gina 50 sampler, a STH 585 column oven (all Dionex, Sunnyvale, United States), and a Shodex RI-71 refractive index detector (Shoko Scientific, Yokohama, Japan) was equipped with a GPC precolumn PSS SDV analytical (5 µm, 8.0 mm x 50 mm) and three GPC columns PSS SDV analytical (5 µm, 8.0 mm x 300 mm) with increasing porosity (100 Å, 1,000 Å and 100,000 Å) (all PSS, Mainz, Germany) that were connected in series. The mobile phase consisted of tetrahydrofuran which was acidified with 0.01% (v/v) of trifluoroacetic acid. At a flow rate of 1.0 mL/min, sample volumes of 100 µL were injected. The oven temperature was adjusted to 30 °C. Each run had a duration of 35 min. The chromatograms were analyzed using WinGPC software (PSS, Mainz, Germany).

Pure polymer, polymer-containing powders, unmodified implants of 20 mg weight or degraded implant residues that were dried to constant weight at a temperature of 37 °C (ED 115, Binder, Tuttlingen, Germany) were dissolved in 1.0 mL of a 0.20 mg/mL solution of butylated hydroxytoluene in tetrahydrofuran (internal standard solution). Ultrasound (5510-MT, Branson, Danbury, United States) was applied for 20 min. The samples were directly filled into vials and analyzed immediately or they were stored at -20 °C.

In addition, a 10 mg/mL reference solution of R 202 H in the aforementioned internal standard solution was prepared.

Polystyrene standards were used for calibration purposes. 50 mg of the following molecular weights were all together dissolved in 50 mL of the internal standard solution: 162 g/mol, 1,470 g/mol, 9,130 g/mol, 34,300 g/mol, 250,000 g/mol, and 851,000 g/mol. Another polystyrene solution contained the following molecular weights: 685 g/mol, 3,250 g/mol, 19,600 g/mol, 100,000 g/mol, 556,000 g/mol, and 1,865,000 g/mol. For 1,865,000 g/mol, 25 mg were weighed out instead of 50 mg.

2.10 Gas chromatography

The content of residual acetonitrile was determined by gas chromatography. A 6890 system with flame ionization detector (Agilent Technologies, Santa Clara, United States) and CTC Combi PAL sampler (Leap Technologies, Carrboro, United States) was equipped with a Zebron ZB-624 capillary GC column (3.0 μ m, 0.53 mm x 60 m) (Phenomenex, Torrance, United States). Nitrogen was used as carrier gas. Samples of 2 μ L were injected at 180 °C (split: 1:5, equilibration time: 1 min). The column pressure was adjusted to 0.5 bar. An oven temperature of 40 °C was maintained for the first 15.0 min. Then, a gradient up to 260 °C was run for 16.0 min, followed by a second one up to 265 °C for 4.0 min. This temperature was maintained for 10.0 min. 265 °C was also the detector temperature. The chromatograms were analyzed using Chromeleon software (Dionex, Sunnyvale, United States).

Implants of 20 mg weight were placed in safe-lock tubes. 1.0 mL of dimethylformamide was added. After shaking at 300 rpm for 30 min (MHR 23, HLC BioTech, Bovenden, Germany), the samples were directly filled into vials and analyzed immediately.

2.11 Wide-angle x-ray scattering

Less than 0.5 g of raw materials, powder mixtures, or pulverized implants were filled into sample holders with a diameter of 20 mm and a depth of 0.5 mm. The surface of each sample was smoothed with a glass slide. The x-ray diffractometer XRD 3000 TT (Seifert, Ahrensburg, Germany) that was equipped with a copper anode (40 kV, 30 mA, 0.154178 nm) was run with the following parameters: in 0.05° (2 θ) steps, a range from 5° to 40° was scanned. Each step was performed within a time span of 2 s.

2.12 Saturation limits

The saturation limits for oxybutynin, either as hydrochloride or free base, were determined in 0.1 M phosphate buffer pH 3.0 and pH 6.0 (☞ III, 1.4.2). An excess of oxybutynin was added to headspace vials that were filled with 2.0 mL of the buffer. As soon as a clear solution was obtained, more oxybutynin was added. The vials were shaken at 500 rpm for 24 h (MHR 23, HLC BioTech, Bovenden, Germany). After another 24 h without shaking, 500 µL of the supernatants were pipetted into safe-lock tubes. The tubes were centrifuged at 14,000 rpm for 5 min (5424, Eppendorf, Hamburg, Germany). Hydrochloride-containing solutions were diluted 1:100 with the appropriate buffer whereas base-containing solutions were diluted 1:10. The samples were analyzed immediately (☞ III, 2.2) or they were frozen at -20 °C.

2.13 Stability of oxybutynin

4.0 mL of a 1.0 mg/mL stock solution of oxybutynin hydrochloride in 0.1 M phosphate buffer pH 3.0 or pH 6.0 (☞ III, 1.4.2) were diluted with 6.0 mL of the appropriate buffer. Further treatment of the samples was consistent with the *in vitro* release studies described before (☞ III, 2.3).

Additionally, 400 µL of the stock solutions were directly filled into vials and diluted with 600 µL of the appropriate buffer. The samples were analyzed immediately (☞ III, 2.2) or they were frozen at -20 °C.

2.14 Interaction studies

Unless otherwise stated, the interaction of oxybutynin with different polymers and/or lipids was investigated as follows: the excipients were accurately weighed and dispersed in 6.0 mL of 0.1 M phosphate buffer pH 6.0 (☞ III, 1.4.2). 4.0 mL of a 1.0 mg/mL stock solution of oxybutynin hydrochloride in the same buffer were added. Further treatment of the samples was consistent with the *in vitro* release studies described before (☞ III, 2.3).

✓ Influence of the polymer type

16 mg of the following polymer types were investigated: Condensate RG 50:50, RG 502, RG 502 H, RG 503, RG 503 H, RG 752 H, R 202 H, and R 203 H. All polymers were used as received.

✓ **Influence of the polymer mass**

RG 502 H was ground in a mortar. The following masses were investigated: 4 mg, 8 mg, 16 mg, 32 mg, 64 mg, and 128 mg. After 39 d, the experiment was stopped, and the pH values were determined (pH 315i, WTW, Weilheim, Germany).

✓ **Influence of the surface area of the polymer**

16 mg of RG 502 H, either as raw material or pulverized in a mortar, were used.

✓ **Influence of degraded and non-degraded placebo implants**

Placebo strands made from RG 502 H were cut into pieces of 16 mg. The implants were allowed to degrade in 10.0 mL of 0.1 M phosphate buffer pH 6.0 at 37 °C (ED 115, Binder, Tuttlingen, Germany). After 10 d of incubation, the buffer was carefully discarded, and the implant residues were washed with 5 mL of ultrapure water. 6.0 mL of 0.1 M phosphate buffer pH 3.0 or pH 6.0 (☞ III, 1.4.2) and 4.0 mL of an appropriate 1.0 mg/mL oxybutynin stock solution were added.

Non-degraded implants were investigated as well.

✓ **Influence of the pH**

16 mg of RG 502 H and 4 mg of oxybutynin hydrochloride were dispersed in 10.0 mL of 0.1 M phosphate buffer pH 3.0 (☞ III, 1.4.2).

✓ **Influence of oxybutynin base**

16 mg of RG 502 H and 4 mg of oxybutynin base were dispersed in 10.0 mL of 0.1 M phosphate buffer pH 6.0 (☞ III, 1.4.2).

✓ **Influence of different lipids**

The influence of the following lipids was investigated: Dynacet 211 P, Dynasan 118, Imwitor 960 P (F), Gelucire 50/13, Lipoid S 100, and Witepsol H 12. 2 mg or 14 mg were incubated together with 14 mg of RG 502 H that were ground in a mortar.

For comparison purposes, selected experiments were repeated without RG 502 H.

2.15 Specific surface areas

For the determination of specific surface areas by gas adsorption, an Autosorb-1-MP (Quantachrome, Boynton Beach, United States) was used. At least 200 mg of RG 502 H, either as coarse raw material

or pulverized in a mortar, were investigated. The samples were degassed under vacuum at 25 °C for at least 2 h. Then, krypton adsorption at 77.3 K was recorded over a relative pressure range of 0.05 to 0.23. The data of altogether eight measuring points were finally fitted to the Brunauer-Emmett-Teller equation with AS1Win software (Quantachrome, Boynton Beach, United States).

2.16 Determination of the particle size

A small amount of oxybutynin was placed on a microscope slide and dispersed in a droplet of immersion oil. Particle sizes were estimated immediately with a VHX-500FD digital microscope equipped with a VH-Z100R zoom lens (both Keyence, Osaka, Japan).

Chapter IV | Optimization of the extrusion process

This chapter gives an introduction into pharmaceutical ram extrusion as innovative tool for the production of biodegradable oxybutynin-loaded implants. It highlights the single process parameters and provides an overview of the fine-tuning possibilities. Changes in the integrity of the implant materials that occur during manufacturing are presented. However, the focus is on the optimization of the extrusion process where the reduction of the temperature is crucial. A factorial design of experiments, the so-called Rechtschaffner design, is used for the determination of an optimum parameter set. On this basis, the influence of the die geometry, the reduction of the cutting intervals, and the up-scaling of the batch size are investigated.

1 Industrial ram extrusion

Initially developed as high pressure capillary rheometer, the Rheograph 25 E II (☞ Figure 11) was intended to determine the flow behavior and the viscosity of thermoplastic materials. Meanwhile, it is also used for the production of pharmaceutical implants, even under cleanroom conditions. Small batch sizes that are distinctive of research and development can be processed as well as regular industrial batch sizes [223].



Figure 11 | Left: Piston and barrel with die, nuts, and stopper. **Center:** Barrel screwed with die and stopper. **Right:** Ram extruder Rheograph 25 E II.

With piston, barrel, and die as key elements (☞ Figure 11), the construction of the extruder is as simple as possible (☞ I, 4.2.2). The implant formulation, usually milled and homogenized by cryogenic grinding, is filled into the barrel that is closed with a die and an appropriate stopper at the lower end. The barrel is mounted into the surrounding heating unit which allows for precise temperature control. When the piston is finally positioned in the upper part of the Rheograph 25 E II, the extrusion program can be started. As it is script-controlled, production procedures and measurements can exactly be defined and continuously monitored [223].

The standard program that is characterized by the following settings provided the basis for this work:

✓ **Compression**

The compression phase is essential for removing entrapped air from the implant formulation. With a piston force of 2,000 N (applied to a barrel diameter of 20 mm), the material is compacted at room temperature for 10 min. Residual air is able to leave along the small distance between the piston and the barrel.

✓ **First heating phase**

The first heating phase demands another 10 min and is intended to heat the material inside the barrel from room temperature to 75 °C, that way inducing softening of the polymer in the implant formulation. In order to prevent liquidized material to leak, the piston force is reduced to 250 N.

✓ **Second heating phase**

During the second heating phase that takes 10 min again, the desired temperature (of 75 °C) is kept constant. In addition, the piston force remains unchanged at 250 N. This phase is necessary to ensure consistent heat distribution, even in the center of the barrel.

✓ **Temperature control**

In the best case, the temperature control requires only 0.5 min. During this time, the temperature is measured at two positions of the heating unit. If it corresponds to the desired value of 75 °C, extrusion is started. Otherwise, the control loop starts from the beginning.

✓ **Extrusion**

For extrusion, the stopper at the lower end of the barrel is taken off. At a constant speed of 0.010 mm/s, the piston is moved down, thus pressing the material through the die. The

resulting strand is cut by hand into pieces of approximately 10 cm. The temperature is held constant at 75 °C, whereas both piston force and duration of the extrusion phase are variable and depend on the implant composition.

✓ **Cooling**

For cooling purposes, the heating unit is flooded with cold water until a temperature of $10\text{ °C} \pm 10\text{ °C}$ is reached. The next extrusion can be started immediately.

INFO BOX #1

'Constant speed' or 'constant force' - which extrusion mode is the preferable one?

In this work the 'constant speed mode' was applied without exception. It allows for detailed investigations on the piston force and, from a practical point of view, the likelihood for a process-related termination is low and can be easily controlled, even if materials of unknown properties are used. Extrusion results in a so-called overload as soon as a piston force of 25 kN is exceeded. When piston speed and temperature are chosen properly, this is highly improbable.

In contrast, processes that are run in the 'constant force mode' do not lead to an overload. They rather have to be interrupted or stopped due to inappropriate predefined values for the piston force. If such values are, for example, too low, extrusion does not even start. The other way around, higher values might provoke extrusion although the desired piston force is not yet reached.

However, with a certain degree of experience both 'constant speed' and 'constant force' can be successfully applied for the production of biodegradable sustained release implants. Consequently, a preferable extrusion mode does not exist.

1.1 Fine-tuning of the process

The Rheograph 25 E II offers numerous possibilities to adapt and fine-tune the extrusion parameters. Piston force, temperature, piston position, piston speed, and implant diameter are monitored over the whole process, that way allowing for precise control and detailed analysis.



Figure 12 | Implants consisting of 80% of RG 502 H and 20% of oxybutynin hydrochloride that were cut to a weight of 20 mg.

In order to gain deeper insight into the manufacturing process, 1.5 g of a ground implant formulation consisting of 80% of RG 502 H and 20% of oxybutynin hydrochloride were extruded with the standard program described before (➔ IV, 1). A one-holed die with a length of 21.0 mm and a diameter of 1.15 mm was used without exception. After solidification at room temperature, the strands were cut into pieces of 20 mg weight (➔ Figure 12) - the final dosage form.

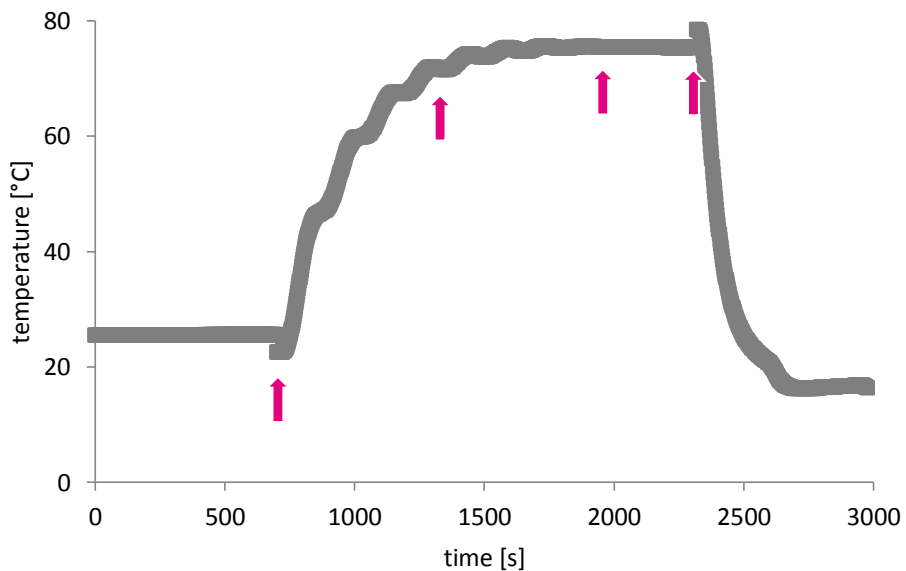


Figure 13 | Temperature during the extrusion (standard program) of a formulation consisting of 80% of RG 502 H and 20% of oxybutynin hydrochloride. Arrows indicate the beginning of the following phases: first heating phase, second heating phase, extrusion, and cooling.

The adjustment of the temperature is effected by means of two separate heating circuits. The temperature is continuously measured via Pt100 sensors [223] at two positions inside the heating unit - one in the upper part and one in the lower part. As the heat has to be transferred to the barrel and the material inside, none of these values reflects exactly the temperature of the implant formulation. However, during extrusion, the temperature (inside the heating unit) is usually constant within a range of $\pm 1\text{ }^{\circ}\text{C}$, which indicates that the heat transfer was complete. Since it is more relevant for smaller batch sizes, Figure 13 displays the temperature curve of the lower measuring point only. Besides, the curve of the upper one is almost identical. As can be seen, the process is started at room temperature. After the first 10 min, heating is applied, which results in a strong oscillating increase. Approximately $72\text{ }^{\circ}\text{C}$ are reached at the beginning of the second heating phase. During the next 10 min, the temperature levels off at $75\text{ }^{\circ}\text{C}$, and the oscillating effect disappears. Extrusion is then performed at a constant temperature. In the end, cooling is applied so that the Rheograph 25 E II is immediately ready for the next production.

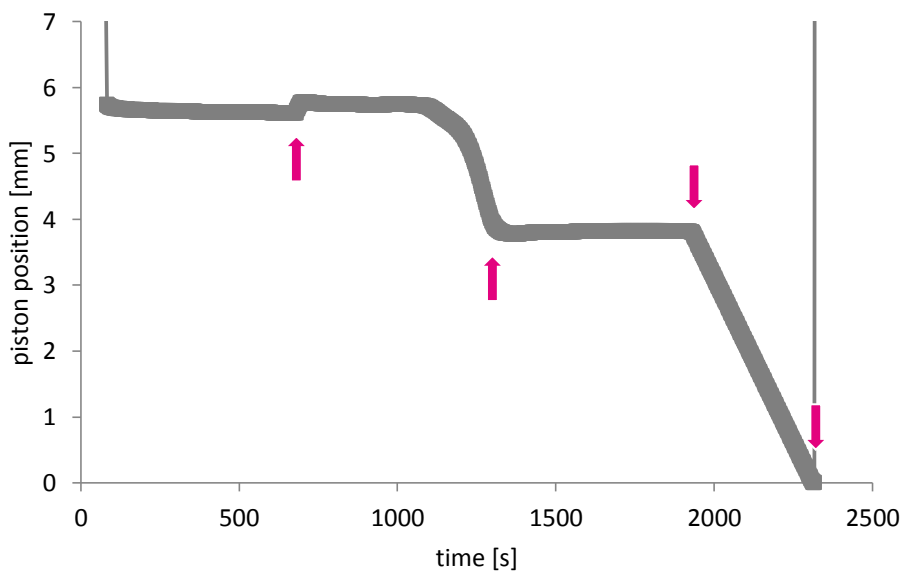


Figure 14 | Piston position during the extrusion (standard program) of a formulation consisting of 80% of RG 502 H and 20% of oxybutynin hydrochloride. Arrows indicate the beginning of the following phases: first heating phase, second heating phase, extrusion, and cooling.

As its name implies, the piston position is a measure for the position of the piston inside the barrel. A value of 0 indicates the end of the extrusion when piston and die come in contact. Higher values can be attributed to the fill level of the material. In Figure 14, for example, the compression phase starts at 5.74 mm and ends at 5.61 mm. This corresponds to a decrease of 2.3%. As mentioned

before (➡ IV, 1), entrapped air is removed during this phase. The step that can be observed at the beginning of the first heating phase reveals the reduction of the piston force from initially 2,000 N to 250 N. With increasing temperature, the polymer softens. It turns from a rigid glassy state to a mobile rubbery state [136], thereby losing volume. The piston position is continuously adapted and results in a distinctive decrease in the end of the first heating phase. Within the last minutes before extrusion, the piston position is stable with hardly any fluctuations. This plateau phase suggests that the temperature distribution is uniform, even in the middle of the implant formulation. Since extrusion is finally performed in the 'constant speed mode', the piston position decreases in a linear manner.

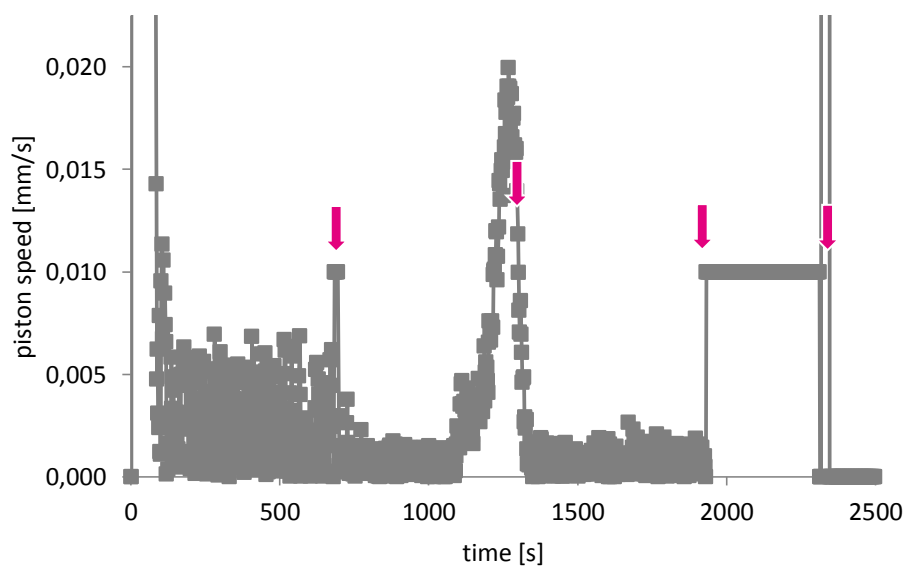


Figure 15 | Piston speed during the extrusion (standard program) of a formulation consisting of 80% of RG 502 H and 20% of oxybutynin hydrochloride. Arrows indicate the beginning of the following phases: first heating phase, second heating phase, extrusion, and cooling.

Both piston position and piston speed provide similar information. As shown in Figure 15, the piston speed fluctuates strongly in the compression phase. This is related to the high predefined piston force. In contrast, when 250 N are applied in the heating phases (instead of 2,000 N during compression), the range of fluctuations declines immediately. In the end of the first heating phase, a maximum of 0.020 mm/s can be detected. This is an indicator for the exceeding of the glass transition temperature of the polymer. The material inside the barrel which mainly consists of poly(D,L-lactide-co-glycolide) softens and decreases in volume, thereby inducing an increase in piston speed. With the exception of the extrusion phase, the piston speed is automatically adjusted and

depends on the piston force and the melting or softening behavior of the implant formulation. As can be seen, a constant value of 0.010 mm/s is preset for extrusion.

Monitoring of the piston force is one of the key elements of this work since it enables the identification of the maximum piston force. This value pertains to the extrusion phase and is essential for the implementation of modifications concerning either the implant formulation or the process itself. As soon as the force transducer records a piston force of more than 25 kN, extrusion is stopped. Therefore, it is absolutely necessary not to exceed this upper limit. Figure 16 displays the piston force during the whole extrusion process. As expected, the values that were adjusted beforehand for compression and heating, in particular 2,000 N and 250 N, correspond exactly to the measured ones. In the beginning of the extrusion phase, a strong increase of the piston force can be observed. This is due to the force transmission from the cross section of the barrel to the cross section of the die. Commonly, it takes a few seconds until the first implant strand becomes visible. In this example, the maximum is achieved at approximately 18 kN, followed by a decrease that ends abruptly when the piston reaches its lowest position. The piston force jumps from initially 15 kN to 0 kN.

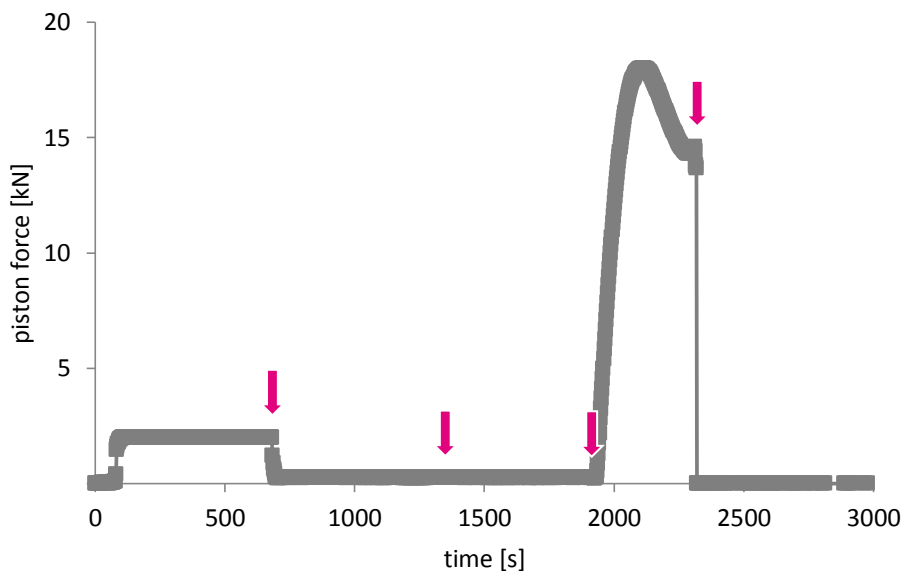


Figure 16 | Piston force during the extrusion (standard program) of a formulation consisting of 80% of RG 502 H and 20% of oxybutynin hydrochloride. Arrows indicate the beginning of the following phases: first heating phase, second heating phase, extrusion, and cooling.

Another parameter that is of major importance for this work is the implant diameter. Laser technology with a resolution of 7 μm is used to measure it [223]. As demonstrated in Figure 17, a

zigzag curve is obtained for the extrusion of the so-called standard formulation. This is due to the fact that the material does not immediately solidify at room temperature. With increasing weight, it becomes thinner at the exit of the die. Once the strand is cut (this is usually done with household scissors), the diameter increases again. As comparatively large pieces of about 10 cm were prepared in this example, the zigzag characteristics are highly pronounced. In spite of that, mean and diameter are acceptable with $1.27 \text{ mm} \pm 0.03 \text{ mm}$. Interestingly, the measured diameter is much higher than the one of the die orifice that has 1.15 mm. This can be attributed to the expansion of the material which was subjected to high pressure before.

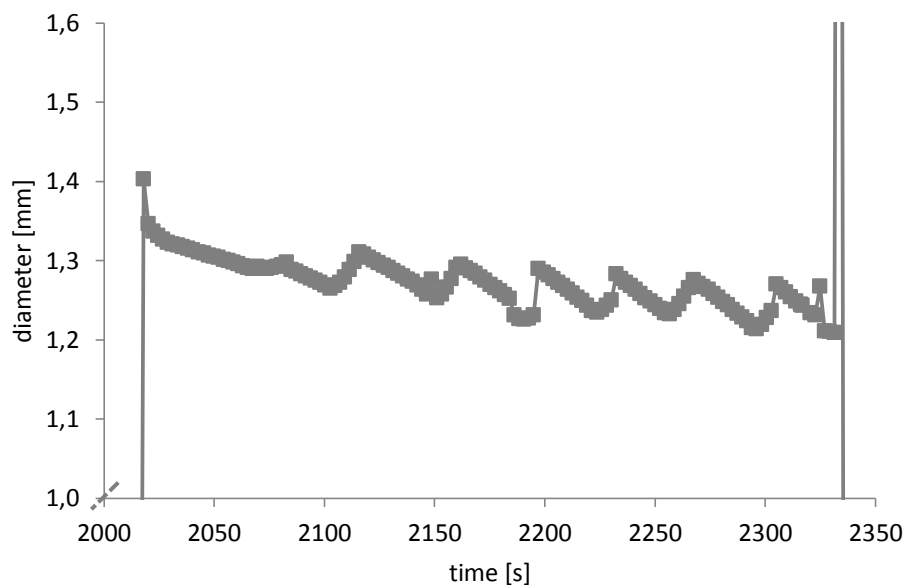


Figure 17 | Implant diameter during the extrusion (standard program) of a formulation consisting of 80% of RG 502 H and 20% of oxybutynin hydrochloride.

All in all, the diameter is a measure for the quality of the implants. For packaging purposes, the rods have to be fixed in a cannula, either using an O-ring or a shrink tubing. This is certainly facilitated by constant diameters. In addition, automatic cutting to a predefined length which corresponds to the final dosage form makes only sense if the weight for every implant is equal at 20 mg. This cannot be guaranteed in the case of fluctuating diameters but would be helpful for future productions. The manual cutting process could be skipped then.

1.2 Influence of the process on the integrity of the implant materials

The influence of the production process, including both cryogenic grinding and extrusion, on the integrity of the implant materials was investigated. Weight average molecular weight of the polymer

was determined by size exclusion chromatography against polystyrene standards. The results are illustrated in Figure 18. As can be seen, the molecular weight decreases from initially 13,011 g/mol in the raw material to 12,140 g/mol in the final product. Even when oxybutynin hydrochloride and RG 502 H are physically mixed, a slight decrease can be observed. This might be due to the stress in

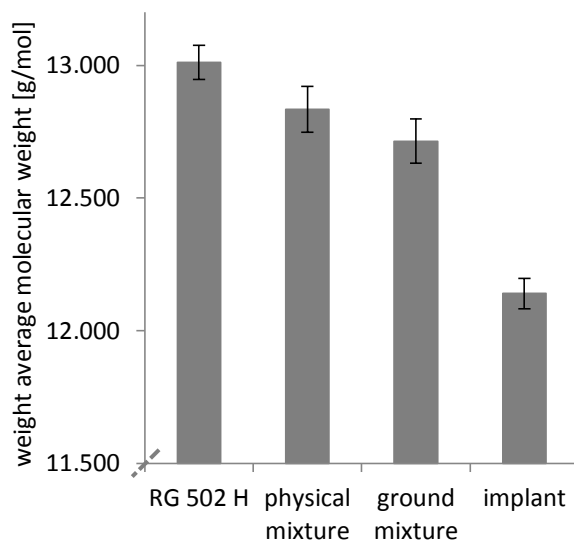


Figure 18 | Weight average molecular weight of RG 502 H before and after physical blending with oxybutynin hydrochloride, cryogenic grinding, and extrusion (mean \pm standard deviation, $n = 3$).

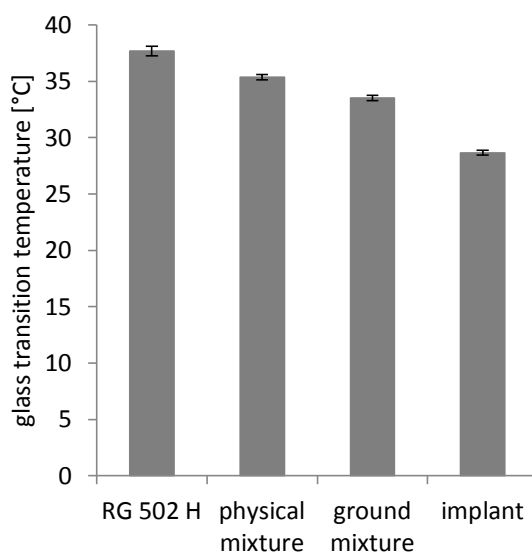


Figure 19 | Glass transition temperature of RG 502 H before and after physical blending with oxybutynin hydrochloride, cryogenic grinding, and extrusion (mean \pm standard deviation, $n = 3$).

the mortar that the materials were subjected to. However, this step does not belong to the common extrusion process and was analyzed to get further information only. In general, RG 502 H seems to be prone to stress. Cryogenic grinding, for example, is performed in liquid nitrogen at $-196\text{ }^{\circ}\text{C}$. Additionally, strong mechanical forces are directly applied by the steel impactor. During extrusion, the implant formulation is first compressed by a force of 2,000 N and then heated up to $75\text{ }^{\circ}\text{C}$. While it passes the die, high frictional forces occur, especially along the walls. All these factors might be responsible for the degradation of the polymer. Similar results were obtained by Rothen-Weinhold et al. who prepared vapreotide-loaded extrudates with different PLGA matrices. The weight average molecular weight was found to decrease by up to 5% during extrusion [224].

The results of the T_g measurements that are depicted in Figure 19 confirm the aforementioned findings. Each of the manufacturing steps leads to a further reduction of the glass transition temperature. More precisely, the T_g decreases from $37.7\text{ }^{\circ}\text{C}$ in the raw material to $33.5\text{ }^{\circ}\text{C}$ in the ground mixture to $28.6\text{ }^{\circ}\text{C}$ in the extrudate.

INFO BOX #2

Why does the measured T_g for RG 502 H differ from literature?

In literature, a glass transition temperature of $42\text{ }^{\circ}\text{C}$ to $46\text{ }^{\circ}\text{C}$ is found for RG 502 H (☞ Table 2). In contrast, $38\text{ }^{\circ}\text{C}$ were obtained from the DSC measurements that were carried out in the context of this thesis. This decrease might be attributed to the hydration of the polymer by water vapor of the air [225]. It is important to keep in mind that once the original packing of the raw material is opened, the polymer is subjected to the surrounding conditions. For this reason, storage in a desiccator in a cool place is advisable.

Wide-angle x-ray scattering was performed in order to gain information on the crystallinity of oxybutynin hydrochloride in the polymer matrix. As RG 502 H is amorphous, it gives no peak signals in the diffractogram (☞ Figure 20). In contrast, the drug substance reveals a distinct peak at 18.9° (2θ). Smaller characteristic peaks are particularly found in between 10° (2θ) and 30° (2θ). The diffractogram of a physical blend consisting of 80% of the polymer and 20% of oxybutynin hydrochloride repeats the most important peaks, thus indicating that the structure of the solids remains unaffected. The same holds true after cryogenic grinding, although the peaks are less pronounced then. The diffractogram of extruded implants is similar to the one of pure RG 502 H, which suggests that the drug substance is in the amorphous state [226]. However, as melting peaks

are found in the corresponding DSC thermograms (data not shown), at least part of the API must be crystalline.

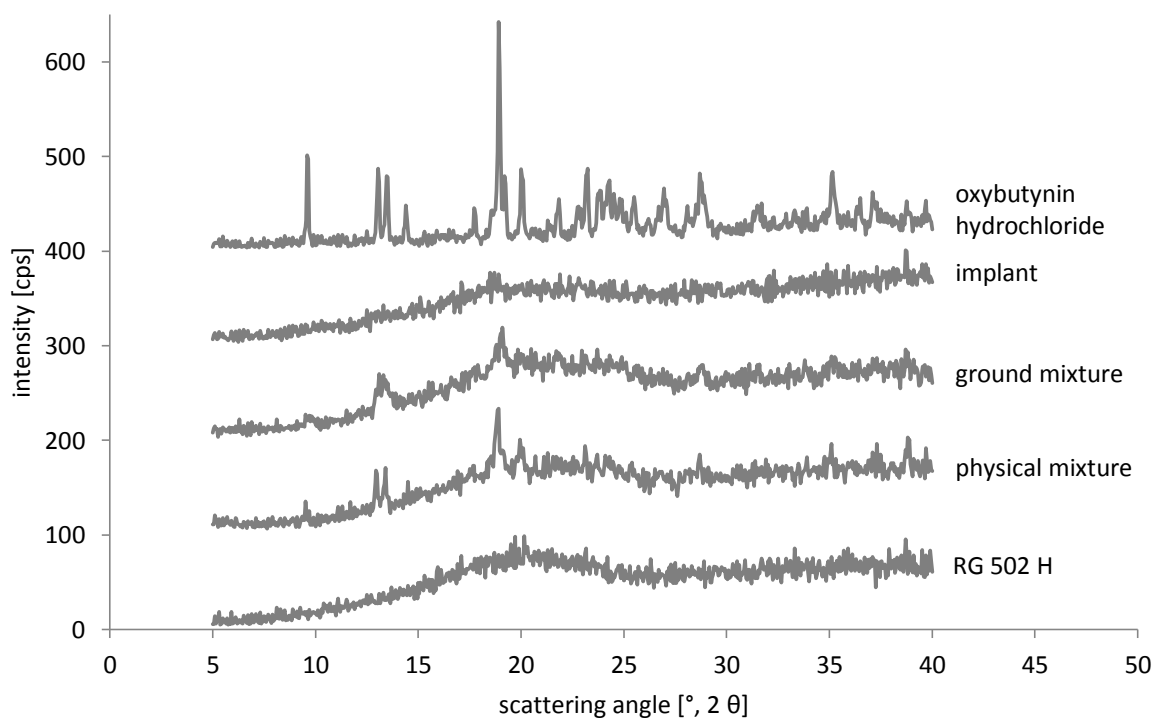


Figure 20 | Wide-angle x-ray analysis of RG 502 H, oxybutynin hydrochloride, and formulations consisting of 80% of RG 502 H and 20% of oxybutynin hydrochloride after physical blending, cryogenic grinding, and extrusion.

2 Factorial design of experiments

For the optimization of production processes, the factorial design of experiments is a helpful tool. In contrast to conventional studies that consider only one factor at a time, the DoE systematically combines different factors in one experiment. That way, the total number of experiments can be drastically reduced [227].

Concerning implant manufacturing with the Rheograph 25 E II, the following seven parameters were defined as variables:

- ✓ Time for the compression phase [min]
- ✓ Piston force during the compression phase [N]
- ✓ Time for the first heating phase [min]
- ✓ Time for the second heating phase [min]
- ✓ Piston force during the heating phases [N]
- ✓ Temperature [°C]
- ✓ Piston speed [mm/s]

The major goal was to investigate their influence on the extrusion process, primarily on the maximum piston force that is known to be directly related to the temperature. A reduction of the temperature is absolutely essential for the process optimization since it offers the possibility of embedding of thermosensitive drugs.

As in the preceding chapter, the standard formulation consisting of 80% of RG 502 H and 20% of oxybutynin hydrochloride was used without exception.

2.1 Preliminary studies

Preliminary studies were necessary in order to define the constants as well as the lower and upper limits for the extrusion parameters, thus minimizing the number of experiments. Regarding the die, a large choice is given. The dies are typically characterized by different diameters and heights and they



Figure 21 | **Left:** Dies with diameters of 1.08 mm, 1.15 mm, and 1.46 mm. **Center:** Dies with a height of 14.2 mm and 21.0 mm. **Right:** One- and two-holed dies.

comprise one or more orifices (☞ Figure 21). Since they are mainly custom-made, almost every design can be realized.

As illustrated in Figure 22, both maximum piston force and implant diameter are influenced by the die geometry. The orifice diameter is expectably the determining factor for the implant thickness. However, it turned out to be smaller than the corresponding measured values, which can be attributed to the relaxation of the polymer (☞ IV, 1.1). The 1.08 mm die, for example, results in strands of 1.20 mm thickness. This effect is less pronounced for larger die orifices. The standard deviations are greater then, which is due to the implant strand that gains more weight in a shorter time, thereby stretching the material that has already left the die. In contrast, the maximum piston force increases with decreasing orifice diameter. For the 1.08 mm die, 23 kN were measured whereas the 1.46 mm die leads to only 7 kN. As the translation from the diameter of the barrel to the one of die is more distinct for smaller die orifices, the frictional forces along the walls are more effective than in the case of larger die orifices. Hence, higher values for the maximum piston force can be expected. The same holds true for dies with a height of 21.0 mm compared to 14.2 mm. Since the orifice diameters are equal at 1.15 mm, the translation from the barrel to the die is not affected. Despite of that the friction is higher because of the longer material pathway. Additionally, the

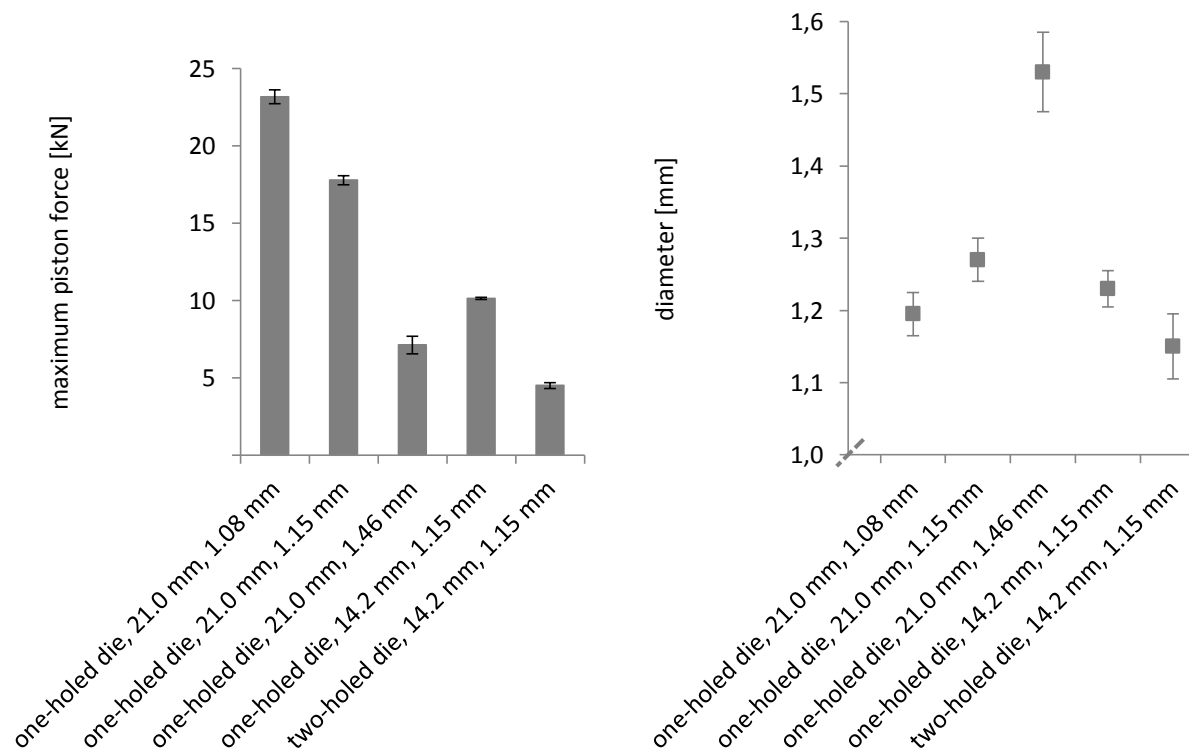


Figure 22 | Influence of the die geometry during the extrusion (standard program) of a formulation consisting of 80% of RG 502 H and 20% of oxybutynin hydrochloride (mean \pm standard deviation, $n = 2$). **Left:** Influence on the maximum piston force. **Right:** Influence on the implant diameter.

number of die orifices was investigated. As can be seen in Figure 22, the lowest maximum piston force was observed for two-holed dies with a diameter of 1.15 mm and a height of 14.2 mm. In comparison to the corresponding one-holed die, the maximum piston force was more than halved. A value of 5 kN was recorded. Regarding the diameters of the resulting extrudates, it is obvious that they relate to the maximum piston force. With increasing force, the implants become thicker. Once more, this can be related to the expansion of the material that is more pronounced when higher forces are applied (➡ IV, 1.1).

Finally, a one-holed die with a diameter of 1.15 mm and a height of 14.2 mm was chosen as constant factor. With regard to the results this might be surprising. Both a diameter of 1.46 mm and two die orifices instead of one seem to be more favorable since they reduce the maximum piston force to a greater extent. However, thicker implants require larger needles and are therefore less patient-friendly. Due to practical reasons, a two-holed die was neither used. As soon as two strands are extruded at the same time, the handling of the process becomes more complicated, especially at higher temperatures.

Table 8 | Experimentally determined requirements for the extrusion parameters.

parameters	
time/compression phase [min]	variable
piston force/compression phase [N]	variable
time/first heating phase [min]	≥ 10
time/second heating phase [min]	≥ 10
piston force/heating phases [N]	variable
temperature [°C]	≥ 75
piston speed [mm/s]	> 0 and ≤ 0.0125

Table 8 summarizes the experimentally determined requirements for the single extrusion parameters. Time and piston force are variable for the compression phase. In order to ensure complete heat transfer from the heating unit to the material inside the barrel, the time for each heating phase has to be at least 10 min. Otherwise, the absence of an overload (➡ IV, 1) cannot be guaranteed. The piston force, in contrast, is variable again. However, values as high as during the compression phase should be avoided to prevent leakage of the liquidized implant formulation. The temperature turned out to result in an overload at 70 °C. Therefore, at least 75 °C are recommended for an error-free process. Regarding the piston speed, at most 0.0125 mm/s are realizable. At higher values, the piston force leads to an overload, thus stopping extrusion.

2.2 Rechtschaffner design

The Rechtschaffner design is known as saturated statistical design in which main effects and two-factor interactions are estimable if three-factor and higher order interactions are negligible [228]. It was used for the process optimization since it reduced the number of experiments to a minimum. For the investigation of seven quantitative factors (⇒ Table 9), 39 runs were calculated. Conventional one factor at a time tests would have required at least $2^7 = 128$ runs, if only two different settings were analyzed [227]. The ambient conditions were assumed to be constant during extrusion, and the die geometry was not changed. The experiments were performed in a random order.

Table 9 | Overview of the factors included in the Rechtschaffner design.

parameters	lower limit	mean	upper limit
time/compression phase [min]	2	11	20
piston force/compression phase [N]	1000	2500	4000
time/first heating phase [min]	10	15	20
time/second heating phase [min]	10	15	20
piston force/heating phases [N]	125	312.5	500
temperature [°C]	75	82.5	90
piston speed [mm/s]	0.0025	0.0075	0.0125

Table 9 gives an overview of the factors that were included in the DoE. The lower and upper limits mainly resulted from the preliminary studies (⇒ IV, 2.1). For the time of the compression phase a lower limit had to be introduced in order to keep the number of parameters constant. When the time would have been 0, the complete compression phase comprising two factors would have been lost. The limits for the piston force were chosen close to the values of the standard extrusion program (⇒ IV, 1). The lower limit was obtained by dividing the standard value by two, and the upper limit by multiplying the standard value by two. Concerning the temperature, an upper limit of 90 °C was fixed. This can be attributed to the softening behavior of the polymer. With a temperature far above the glass transition, the material becomes almost liquid and can hardly be extruded to uniform strands. The complete manufacturing schedule is outlined in Table 11 in the supplement.

During the 39 extrusions, it became clear that the quality of the implants strongly depends on the process temperature. At 90 °C, thin extrudates with an inconstant diameter were obtained. This can primarily be attributed to the comparatively low viscosity of the material inside the barrel. Exactly the opposite was true when the formulation was processed at 75 °C. The strand diameters were found to be constant with a very small standard deviation. As the main aim of the DoE was to further reduce the manufacturing temperature, it was not decisive whether fluctuating diameters were observed at the other end of the temperature range.

As the maximum piston force is essential for the optimization of the extrusion process, it was the only response that was investigated in detail. At first, non-significant model terms of which the error bars crossed the x-axis were removed from the coefficient plot (⇒ Figure 23). Apparently, the compression phase represented by time and piston force seems to have no influence on the maximum piston force. The same holds true for the piston force during the heating phases. These factors are exactly the same that were supposed to be variable in the preliminary studies (⇒ IV, 2.1). As expected, the temperature has the strongest influence on the maximum piston force, followed by the piston speed. The time of the heating phases is also a significant model term although its influence is less distinct. Two-factor interactions can, for example, be observed for piston speed and temperature. At higher temperatures, the effect of the piston speed is less relevant than at lower temperatures. The other way around, the influence of the temperature is more pronounced at higher piston speeds than at lower ones. As can be seen, significant self-interactions occur additionally. The piston speed, for instance, affects the maximum piston force to a greater extent if it increases to higher values.

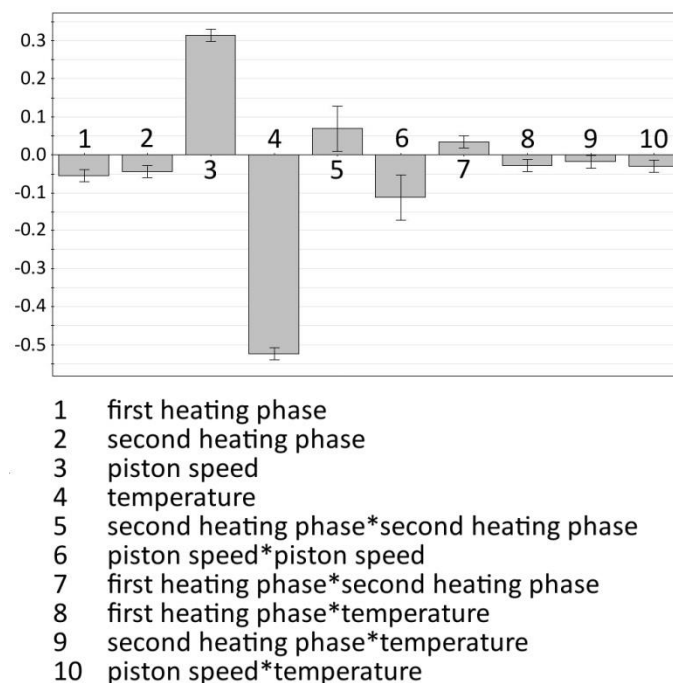


Figure 23 | Coefficient plot referring to the response of the maximum piston force (non-significant model terms were removed).

The summary plot that is illustrated in Figure 24 resulted from the correction of the coefficient plot. It assembles the basic model statistics in four parameters - R², Q², model validity, and reproducibility. For each parameter, a value of 1.0 is considered to be perfect. Q² which is an

estimate for the future prediction precision is the best and most sensitive parameter, followed by the model fit R^2 . The model validity hints at diverse model problems such as the presence of outliers or an incorrect model if the value is smaller than 0.25. The reproducibility shows the variation of the replicates compared to the overall variability. In this case a value greater than 0.5 is warranted [229]. For the optimization of the extrusion process, a reliable model was built on four out of seven parameters. The values for R^2 , Q^2 and the reproducibility are close to 1.0, and the value for the model validity is greater than 0.8. In other words, the model was found to have excellent performance indicators. On this basis, a variety of plots was compiled and evaluated.

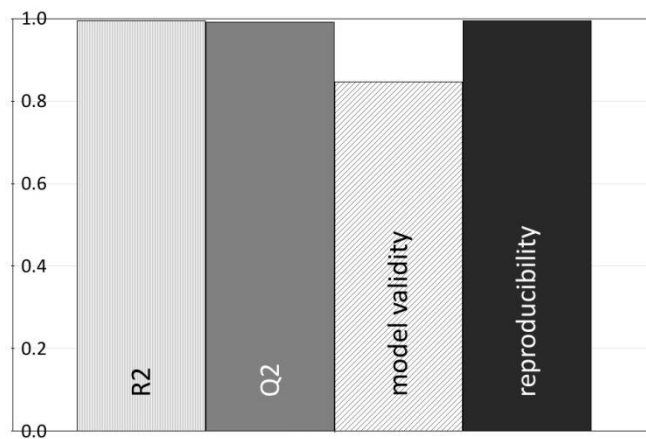


Figure 24 | Summary plot referring to the response of the maximum piston force (R^2 = model fit, Q^2 = estimate of the future prediction precision).

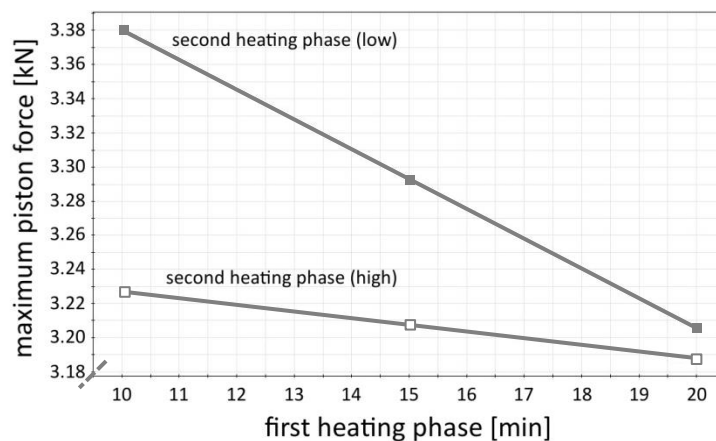


Figure 25 | Interaction plot for the time of the first and the second heating phase referring to the response of the maximum piston force.

An interaction plot is, for example, shown in Figure 25. If the time for the second heating phase is short (upper line), the effect of the first heating phase on the maximum piston force is more pronounced than in the case of a longer second heating phase (lower line). In other words, when the first heating phase takes 20 min, the impact of the second heating phase is almost negligible. In contrast, the maximum piston force strongly depends on the duration of the second heating phase if the first one is short. In conclusion, the total time that is required for heating plays a major role than its splitting in first and second heating phase. Figure 25 clearly demonstrates that there is only a slight difference if 10 min and 20 min or 20 min and 10 min are used.

The coefficient plot (➔ Figure 23) already revealed a strong relationship between the maximum piston force and the temperature. This is confirmed by the main effects plot that is depicted in Figure 26. A linear decrease from 3.70 kN to 2.65 kN can be observed while the temperature increases from 75 °C to 90 °C. However, the suggestion that the line can be extrapolated in both directions is wrong. At lower temperatures the polymer does not soften enough or it remains completely unchanged. Hence, the maximum piston force increases rapidly and results quite often in an overload. In contrast, it cannot come below 0 - even if the material is completely liquidized.

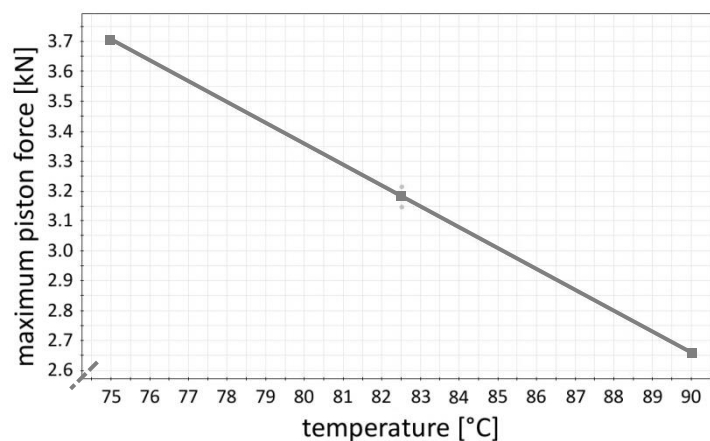


Figure 26 | Main effects plot for the temperature referring to the response of the maximum piston force.

In order to optimize the extrusion process, the following challenge had to be overcome: a reduction of the temperature was absolutely necessary in respect of thermosensitive drugs but at the same time an increase of the maximum piston force above 25 kN had to be circumvented. The influence of all significant parameters on the maximum piston force was evaluated in a sweet spot plot (➔ Figure 27). Model terms that turned out to be non-significant were set to constant values. The piston force during the compression phase and the heating phases was adjusted to 2,000 N and 250 N,

respectively. The time for the compression phase was reduced to a minimum of 2 min. Dark grey areas cover the values that were experimentally determined, and light grey areas display calculated values. Both areas refer to a maximum piston force in between 0 and 25 kN - the so-called sweet spot. Regarding the minimum temperature that is reached at piston speeds close to 0, all diagrams seem to be equal at a first glance. However, slight differences can be detected. The best performance is obtained when the first heating phase takes 10 min, followed by the second heating phase with 15 min. As the piston speed strongly affects the maximum piston force, it has to be reduced to a minimum. At values close to 0, the sweet spot plot predicts temperatures as low as 58 °C. For the following optimized extrusions, the piston speed was adjusted to 0.0025 mm/s. This is a quarter of the value of the standard program. It is important to be aware that such a reduction results in a quadruplication of the extrusion time. The optimized process requires 27 min prior to extrusion compared to 30 min for the standard program. Thus, it is the piston speed and its influence on the extrusion phase that decides on the total process time. Since the reduction of the temperature was the major goal of this thesis, an increase of the process time was accepted.

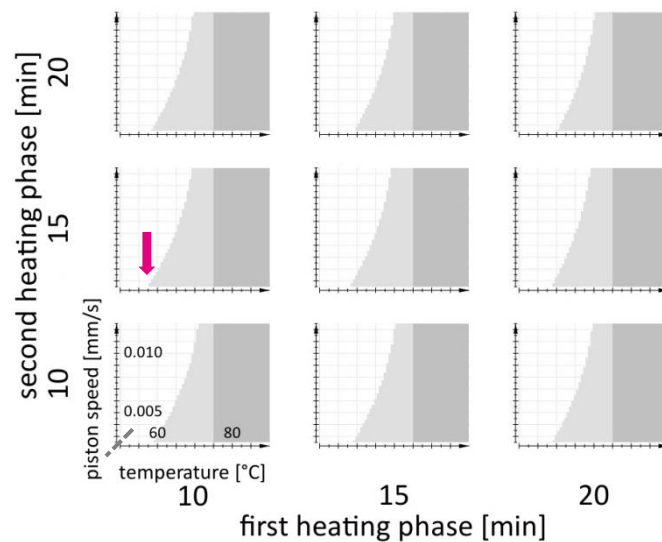


Figure 27 | Sweet spot plot (sweet spot = maximum piston force in the range of 0 - 25 kN; light grey: calculated values, dark grey: experimentally determined values). The piston force during the compression phase and the heating phases was set to 2,000 N and 250 N, respectively. The duration of the compression phase was 2 min.

2.3 Verification of the prediction

The prediction of the Rechtschaffner design was verified by reducing the temperature in steps of 5 °C. All other parameters remained unchanged at the values that were specified before (➔ IV, 2.2).

Figure 28 reveals an increase of the maximum piston force from initially 1 kN at 75 °C up to 6 kN at 65 °C. At a temperature of 60 °C, the process was stopped due to an overload. Thus, the smallest possible extrusion temperature is 65 °C. The difference to the predictive value of approximately 58 °C can potentially be attributed to the piston speed that was set to 0.0025 mm/s instead of a value closer to 0. For comparison purposes, the maximum piston force for the standard process (using the 21.0 mm die) was also determined. With 18 kN, it is much higher than the value for the optimized process. Although the die was not changed when the optimized process was run, different implant diameters were obtained. As previously mentioned, this depends on the maximum piston force (➔ IV, 2.1). In addition, it can be related to the temperature if one and the same extrusion program is used. Higher temperatures lead to lower implant diameters and the other way around. For example, 1.11 mm were measured at 75 °C whereas 1.23 mm were monitored at 65 °C. As can be seen, the expansion of the polymer does not play a role when the optimized process is run at 75 °C. In this case, the measured diameter is smaller than the one of the die orifice. Advantageously, the standard deviations become smaller with decreasing temperature. This is because of the fact that the material solidifies earlier at temperatures closer to the T_g of the polymer. Hence, the thinning trend concomitant with the fluctuations of the implant thickness is reduced.

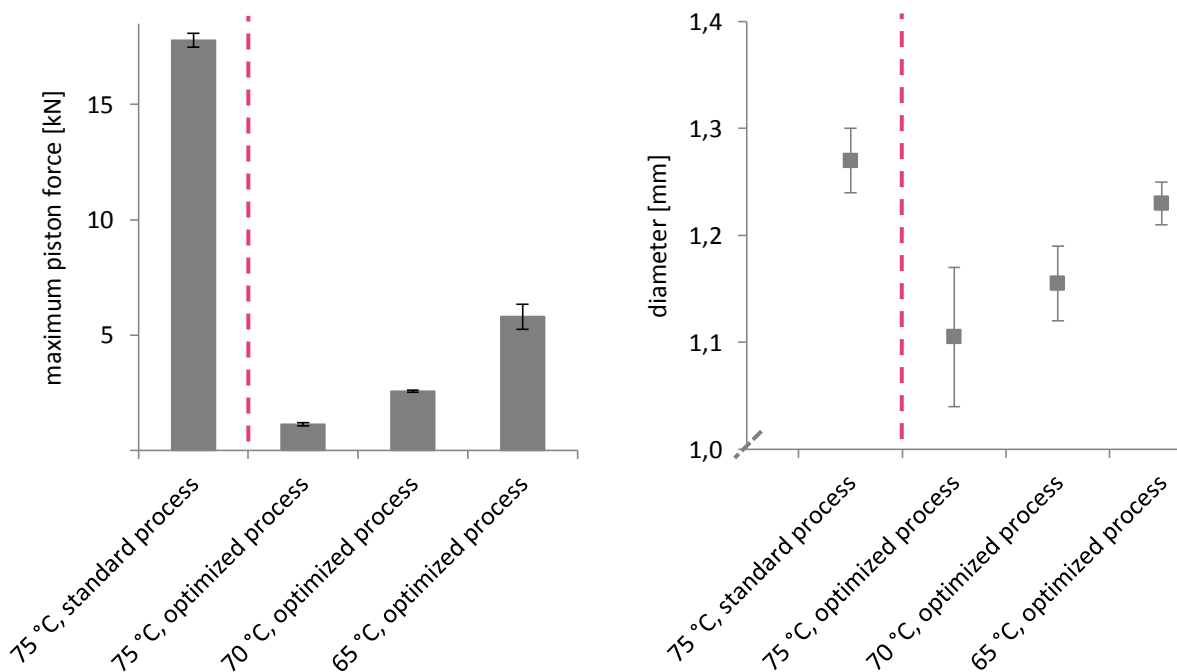


Figure 28 | Influence of the extrusion program and the temperature. The implants consisted of 80% of RG 502 H and 20% of oxybutynin hydrochloride (mean ± standard deviation, n = 2). **Left:** Influence on the maximum piston force. **Right:** Influence on the implant diameter.

As implants are primarily intended for controlled drug release over a prolonged period of time, it is important to investigate if their release profile is affected by changes in the extrusion process. Figure 29 shows the cumulative release of oxybutynin hydrochloride-containing implants that were either produced by the standard process at 75 °C or the optimized process at 65 °C. The tests were performed *in vitro* in 0.1 M phosphate buffer pH 6.0 at 37 °C. Both curves are almost identical, thus indicating that the extrusion process has no influence on the release profiles. In terms of the process optimization, this is crucial.

Drug release from PLGA matrices is typically divided into different phases (☞ I, 2.3). Usually, the first one is described as burst release and can be attributed to API molecules located at the surface or in near-surface areas that are easily accessible for hydration [34, 35]. Interestingly, such an initial burst is not observed for implants made from the standard formulation. Maximum 0.8% of the API are released within the first 24 h. This phenomenon will be discussed later (☞ V, 4). As can be seen, the first 4 d are characterized by a lag phase in which almost no release occurs. The polymer swells and starts to degrade. Diffusion, either through the relatively dense matrix or through the few existing pores, is the prevalent release mechanism. The beginning of the following phase is characterized by an increase of the release rates, which is most often due to the onset of erosion [34, 38]. Drug release is nearly linear during the next 21 d. After 28 d, almost 100% of the API are released. At this point in time, only a small fragile bead of the initially rod-shaped implant is left.

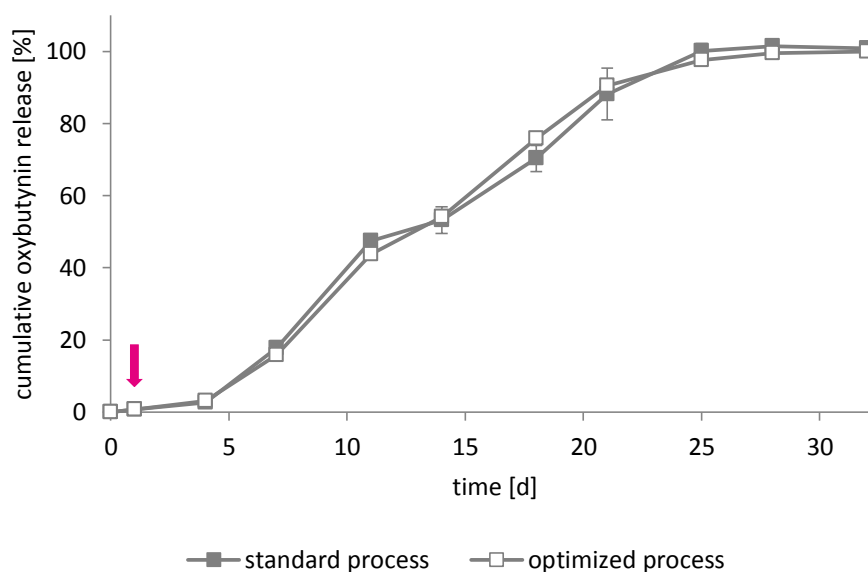


Figure 29 | *In vitro* drug release from implants consisting of 80% of RG 502 H and 20% of oxybutynin hydrochloride in 0.1 M phosphate buffer pH 6.0 at 37 °C. Influence of the extrusion program and the temperature (mean \pm standard deviation, $n = 3$).

INFO BOX #3

Why are the release tests performed at pH 6.0?

In general, a physiological pH of 7.4 is more favorable for *in vitro* drug release tests since it simulates the conditions *in vivo* [21]. However, the solubility of oxybutynin in aqueous solutions is inversely related to the pH. This means that the API is more soluble in acidic solutions than at neutral or even basic pH [230]. In order to guarantee sink conditions for the complete release period, an optimum pH of 6.0 was experimentally determined and finally chosen.

In summary, the ‘translation’ of the standard process into the optimized process was quite successful. A temperature reduction from initially 75 °C to 65 °C could be achieved without affecting the release kinetics. Apart from that, the maximum piston force could be lowered which implies that the frictional forces along the walls of the barrel and the die are less pronounced.

3 Further steps towards an optimized process

On the basis of the parameters that were previously determined in the factorial design (➔ IV, 2.2), the process was further optimized with regard to the number of die orifices, the cutting interval, and the batch size.

3.1 Investigations on the number of die orifices

In the preliminary studies, a 14.2 mm die with two orifices was found to be superior to a one-holed die. For the standard extrusion program, the maximum piston force could be reduced from 10 kN to 5 kN (➔ IV, 2.1). However, due to practical reasons, the DoE experiments were run with a one-holed die.

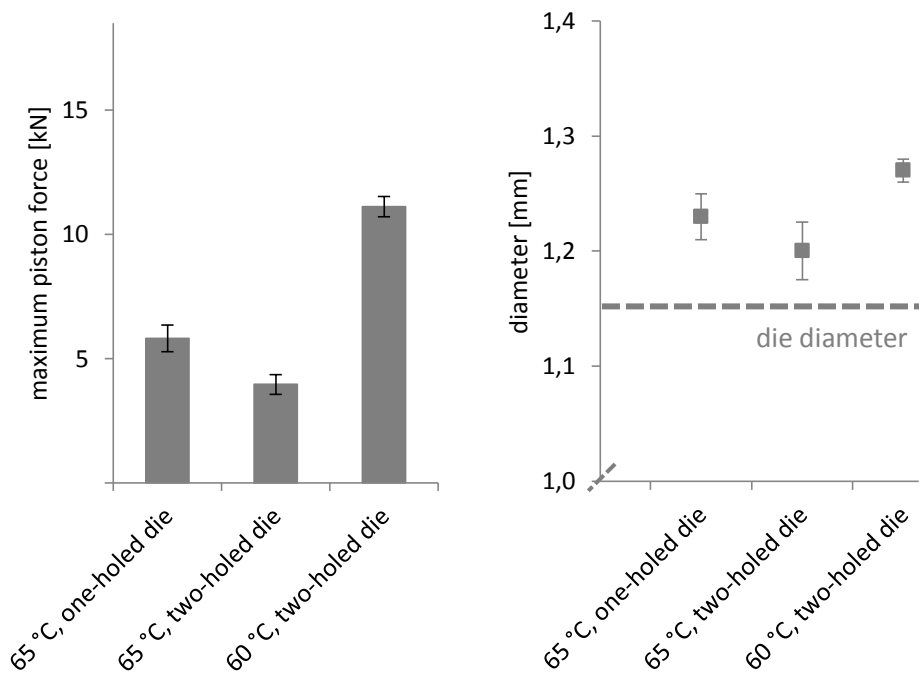


Figure 30 | Influence of the temperature and the number of die orifices. The implants consisted of 80% of RG 502 H and 20% of oxybutynin hydrochloride, and they were extruded using the optimized program (mean \pm standard deviation, $n = 2$). **Left:** Influence on the maximum piston force. **Right:** Influence on the implant diameter.

Together with the optimized process, the influence of the number of die orifices was investigated again. The results are presented in Figure 30. When the process is run at 65 °C, the maximum piston force can be decreased from 6 kN with the one-holed die to 4 kN with the two-holed die. Advantageously, this enables further reduction of the extrusion temperature by another 5 °C to 60 °C. The maximum piston force is then 11 kN and the implant diameter is 1.27 mm with a standard

deviation of only 0.01 mm. As can be concluded from Figure 29 and Figure 33, the drug release profiles are not affected by this modification.

In order to further optimize the process, a four-holed die was custom-made (⇒ Figure 31). Extrusion was performed using the same parameters as before. Figure 32 illustrates the piston force, both for two-holed and four-holed dies. The curves for the complete extrusion phase are represented since maximum values could not be detected for every run. If the two-holed die is exchanged by a four-holed one, the piston force is clearly reduced. Kind of a plateau is formed around 5 kN instead of



Figure 31 | Extrusion using a custom-made four-holed die.

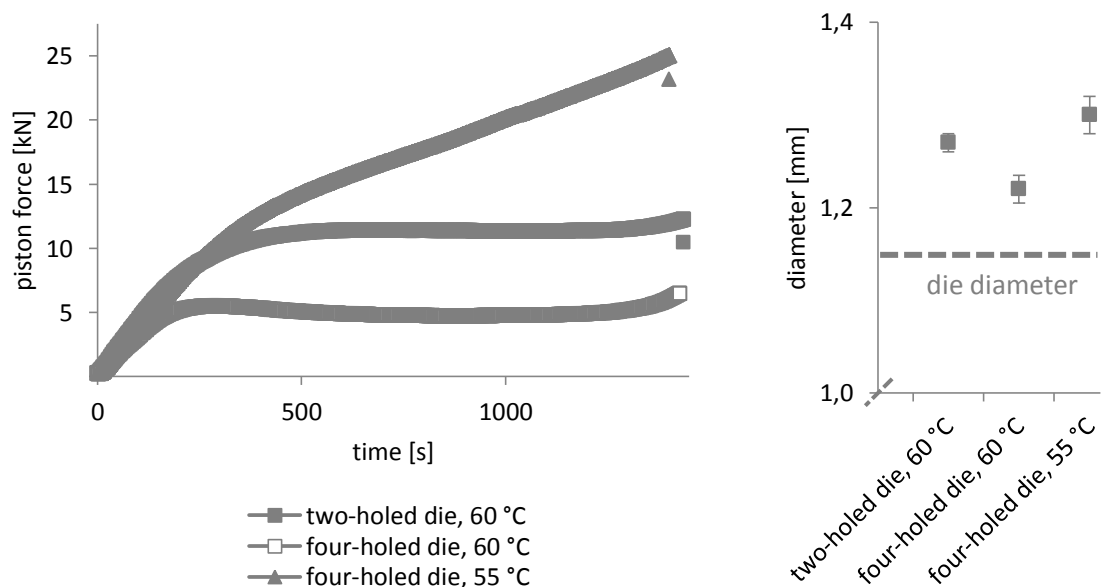


Figure 32 | Influence of the number of die orifices and the temperature. The implants consisted of 80% of RG 502 H and 20% of oxybutynin hydrochloride, and they were extruded using the optimized program. **Left:** Influence on the piston force ($n = 1$). **Right:** Influence on the implant diameter (mean \pm standard deviation, $n = 2$).

11 kN. At a temperature of 55 °C, the piston force increases linearly. Although 25 kN are reached quite at the end of the process, it could be finished without an overload. However, this indicates that further optimization is not possible. As the laser system is not able to measure the thickness of more than two strands at the same time, the implant diameters have to be determined by hand. Once more, they relate to the piston force (☞ IV, 2.1). The die comprising four orifices leads to rods of $1.30 \text{ mm} \pm 0.02 \text{ mm}$ (when extrusion is performed at 55 °C) which is so far the greatest value that was obtained for a 1.15 mm die. As can be seen in Figure 33, the number of die orifices and the temperature do not influence the release profiles.

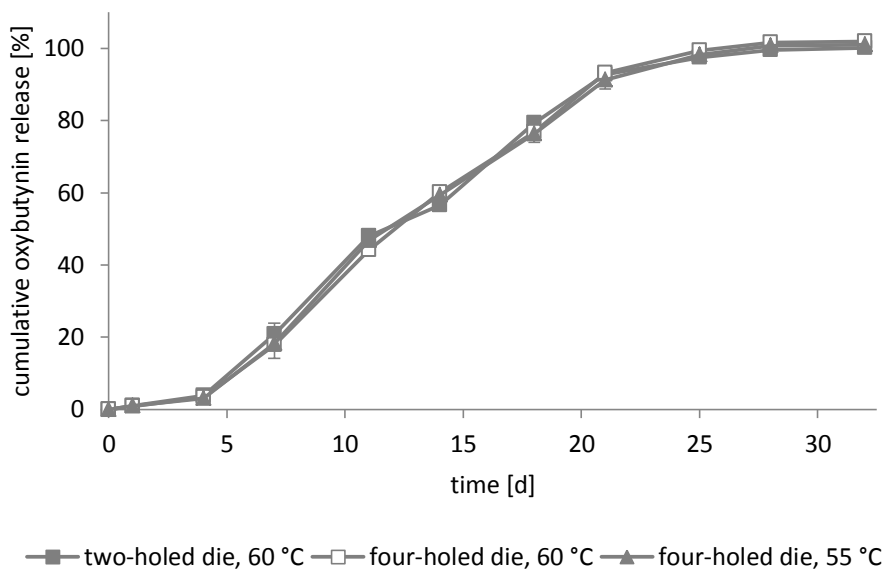


Figure 33 | *In vitro* drug release from implants consisting of 80% of RG 502 H and 20% of oxybutynin hydrochloride in 0.1 M phosphate buffer pH 6.0 at 37 °C. Influence of the number of die orifices and the temperature (mean \pm standard deviation, $n = 3$).

3.2 Reduction of the cutting interval

As mentioned before (☞ IV, 1.1), the monitoring of the implant diameters results in typical zigzag curves. This can be attributed to the thinning of the material that leaves the die. In order to further improve the extrusion process, the reduction of the standard deviations referring to the thickness of the implants was focused. For that, the cutting interval was decreased from initially 10.0 cm to 5.0 cm and 2.5 cm. The extrusions were run using the optimized parameters (☞ IV, 2.2), either with a one-holed die at 75 °C or with a two-holed die at 60 °C. Figure 34 summarizes the results. Expectably, the zigzag characteristics are much more pronounced at higher temperatures. A diameter of $1.12 \text{ mm} \pm 0.06 \text{ mm}$ was, for example, measured for a cutting interval of 10.0 cm. With decreasing

cutting intervals, the implant thickness increases, and the corresponding standard deviations become smaller. This can be explained by the declining weight of the strands which reduces the thinning trend, thereby smoothing the zigzag curve. A cutting interval of 2.5 cm leads to implant strands of $1.19 \text{ mm} \pm 0.03 \text{ mm}$. When the temperature is additionally reduced to $60 \text{ }^\circ\text{C}$, strands of $1.28 \text{ mm} \pm 0.00 \text{ mm}$ thickness are obtained. Such small standard deviations are favorable for future productions since they enable automatic cutting processes. In the best case, the implants can be cut to their final weight, and the manual cutting step can be skipped. It is important to keep in mind that

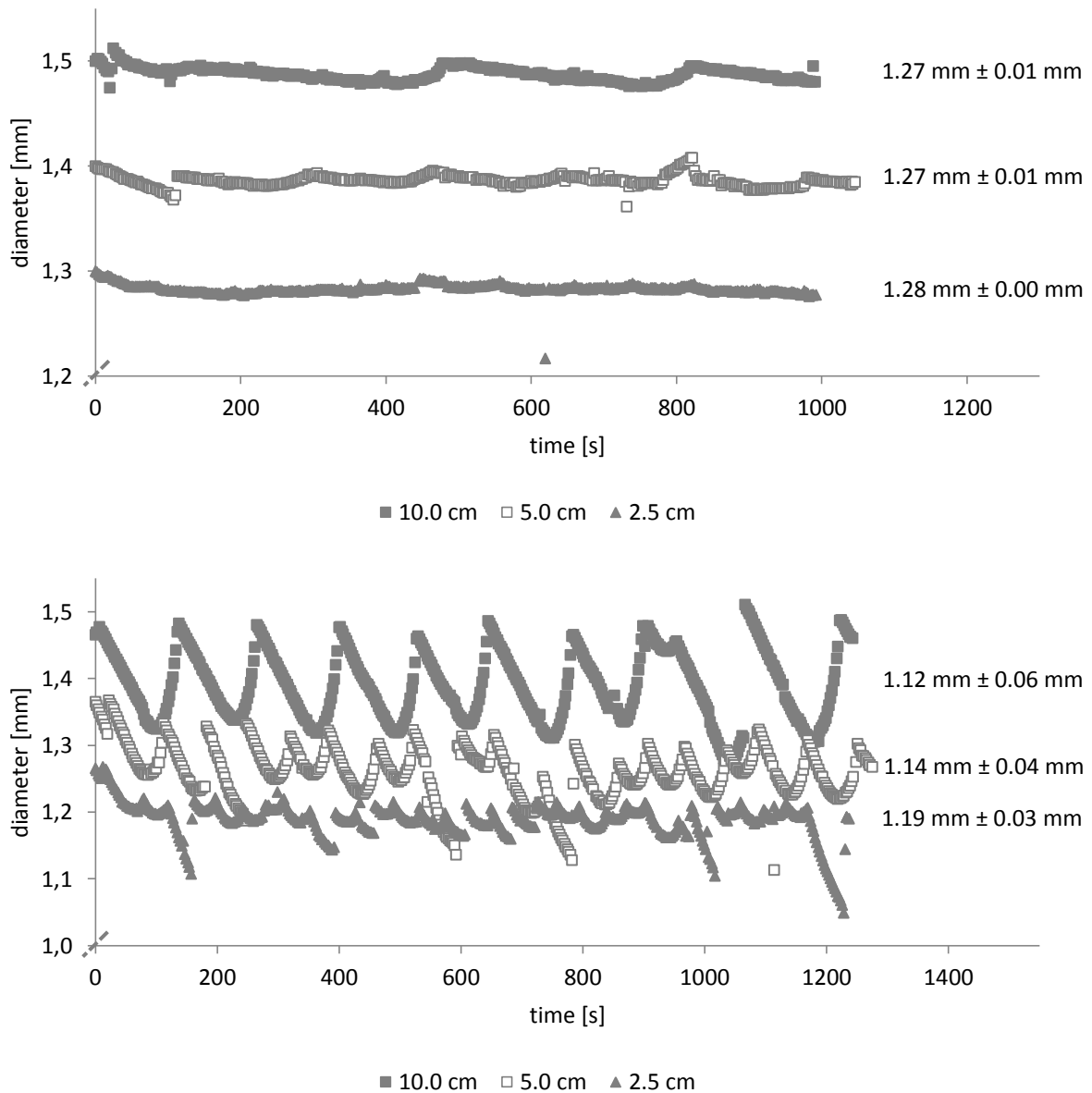


Figure 34 | Influence of the cutting interval on the implant diameter. The implants consisted of 80% of RG 502 H and 20% of oxybutynin hydrochloride. **Top:** Extrusion was performed using the optimized program together with a two-holed die at a temperature of $60 \text{ }^\circ\text{C}$. **Bottom:** Extrusion was performed using the optimized program together with a one-holed die at a temperature of $75 \text{ }^\circ\text{C}$.

a two-holed die was used for the experiments at 60 °C. As the piston speed remained unchanged at 0.0025 mm/s, the time for the extrusion of a single strand was duplicated compared to a one-holed die. The distance between the waves is therefore greater.

3.3 Up-scaling of the batch size

In a final step, an up-scaling of the batch size from initially 1.5 g to 3.0 g and 6.0 g was investigated. For cost reasons, commercial batch sizes in the range of 25 g were excluded from this thesis. The process was performed according to the optimized program (↻ IV, 2.2) at a temperature of 60 °C. A die with two orifices was used.

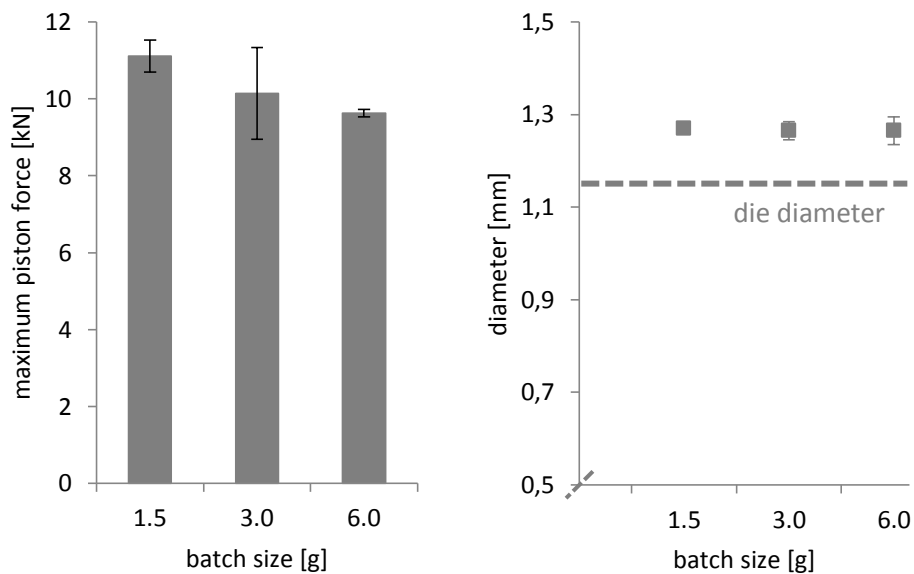


Figure 35 | Influence of the batch size. The implants consisted of 80% of RG 502 H and 20% of oxybutynin hydrochloride, and they were extruded using the optimized program (mean \pm standard deviation, $n = 2$). **Left:** Influence on the maximum piston force. **Right:** Influence on the implant diameter.

As displayed in Figure 35, the implant diameter remains constant at 1.27 mm whereas the maximum piston force decreases slightly with increasing batch size. This relates to the percentage reduction of the fill level inside the barrel, both during the compression phase and the heating phases (↻ Figure 36). At a batch size of 6.0 g, the fill level is reduced by 3.9% during the compression phase and by 35.5% during the heating phases. In contrast, values of 1.5% and 31.5% are obtained for the standard batch size of 1.5 g. Since the material is less densified then, the piston force increases to a greater extent. If higher forces were applied prior to extrusion of smaller batch sizes, this trend could probably be counteracted.

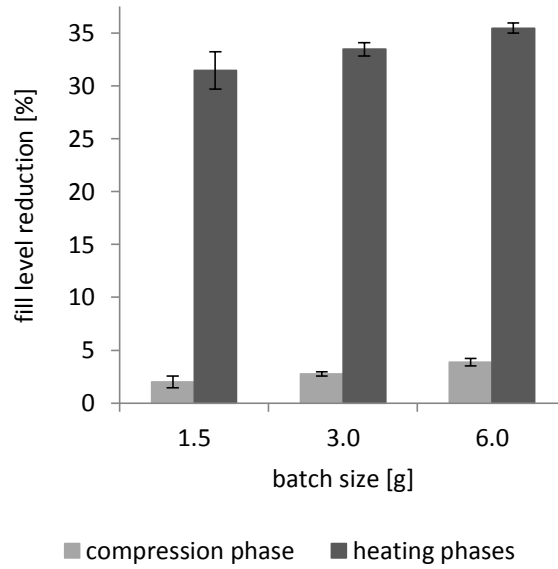


Figure 36 | Influence of the batch size on the fill level reduction. The implants consisted of 80% of RG 502 H and 20% of oxybutynin hydrochloride, and they were extruded using the optimized program (mean \pm standard deviation, n = 2).

The *in vitro* release profiles were found not to be affected by an up-scaling of the batch size although the total extrusion time increased markedly from less than 60 min (1.5 g) to more than 2 h (6.0 g). The API turned out to be stable during the whole manufacturing process and the following release period.

4 Summary

The aim of this chapter was the optimization of the extrusion process that is used for the manufacturing of biodegradable implants based on poly(lactide-co-glycolide). Such implants are interesting candidates for the permanent administration of highly efficient drugs, among those low molecular weight molecules as well as peptides or proteins. However, this process is to date restricted to thermostable drugs since extrusion temperatures of 90 °C and more are applied [179, 231]. Hence, a reduction of the temperature was defined as major goal for this chapter. As the maximum piston force relates inversely to the temperature, it was also focused.

At first, a standard mixture consisting of 80% of poly(lactide-co-glycolide) and 20% of oxybutynin hydrochloride was prepared by cryogenic grinding and extruded with the Rheograph 25 E II. For this formulation, a minimum temperature of 75 °C was obtained with the standard program. Size exclusion chromatography, wide-angle x-ray scattering, and differential scanning calorimetry were used to investigate the integrity of the implant materials. Both weight average molecular weight and glass transition temperature of RG 502 H were observed to decrease during production. This indicates slight degradation of the polymer. Concerning the crystallinity of the API, the decisive peaks disappeared in the diffractogram of the implant. Thus, at least part of oxybutynin hydrochloride switched to an amorphous form.

Within the scope of a factorial design of experiments, the influence of seven process parameters on the maximum piston force was determined. Preliminary studies were necessary to decide on the die geometry and to ascertain lower and upper limits. In total, 39 extrusions were required. The time and the piston force of the compression phase were shown to be non-significant model terms. The same holds true for the piston force during the heating phases. Hence, a prediction plot based on these factors as constants was calculated. The combination of the following parameters turned out to have the highest potential for a reduction of the maximum piston force:

- ✓ Time for the compression phase: 2 min
- ✓ Piston force during the compression phase: 2,000 N
- ✓ Time for the first heating phase: 10 min
- ✓ Time for the second heating phase: 15 min
- ✓ Piston force during the heating phases: 250 N
- ✓ Piston speed: 0.0025 mm/s

Indeed, a value of 1 kN (instead of 18 kN) could be achieved when the process was run at 75 °C. This formed the basis for a stepwise reduction of the extrusion temperature. Finally, 65 °C were reached.

In order to further optimize the process, the influence of the number of die orifices was investigated again. A two-holed die enabled extrusion at 60 °C, and a temperature of 55 °C was possible with a four-holed die. However, in this case, the maximum piston force ranged around 25 kN in the end of the process, thus indicating that larger batch sizes would cause an overload.

As the cutting interval is mainly responsible for the fluctuations of the implant diameters, it was stepwise reduced. In the best case, a standard deviation of practically 0 was obtained. With regard to automatic cutting processes, this is highly beneficial.

In a final step, an up-scaling of the batch size was performed. Larger batch sizes were observed to lead to a slight decrease in the maximum piston force. This correlates inversely to the reduction of the fill level inside the barrel, both during the compression phase and the heating phases. However, an influence on the implant diameter was not detected.

Importantly, all modifications that were made in the context of the process optimization turned out to have no influence on the *in vitro* release profiles. This is highly advantageous because it means that the extrusion parameters and the die can be chosen without any restrictions (regarding the quality of the rods). That way, the manufacturing temperature can easily be shifted towards lower values. As already mentioned, for the investigated formulation, the lowest possible extrusion temperature was found to be as low as 55 °C - this is 20 °C below the value that was formerly obtained for the standard program.

Chapter V | Mechanisms controlling drug release

This chapter provides detailed information on the mechanisms controlling oxybutynin release from PLGA-based implants. The influence of the type of drug and the type of polymer on the manufacturing process and the release profiles is discussed. On this basis, innovative release strategies are developed. Interactions of drug and polymer are also focused since their impact on the release profiles is not to be underestimated.

1 Influence of the type of drug

As already reported in literature, it is not unusual that the type of drug affects the release kinetics from PLGA-based drug delivery systems such as microparticles, films, or implants. For instance, Siegel et al. compared the release rates of six different drugs from pellets. Although polymer matrix and drug loading were the same for all APIs, the rate of polymer degradation and the release profiles differed significantly [232]. Similar results were obtained from Miyajima et al. who studied the effect of acidic, neutral, and basic drugs on their release behavior from PLGA rods [233]. Frank et al. prepared lidocaine-loaded polymer films and investigated the influence of base and salt form of the drug. They found out that the base has an accelerating effect on the matrix degradation, thereby substantially changing the release characteristics [219].

In this thesis, oxybutynin hydrochloride and oxybutynin base were used as model drugs. Unless otherwise stated, 20% of the API and 80% of RG 502 H were ground in a cryogenic mill and extruded to implant strands that were subsequently cut to a weight of 20 mg. For extrusion, the standard program was applied with individually adjusted temperatures (☞ IV, 1).

1.1 Insight into the manufacturing process

Prior to cryogenic grinding, the particle size of both drug types was determined by digital microscopy (☞ Figure 37). In contrast to oxybutynin hydrochloride, the base tends to agglomerate. However, the mean particle sizes turned out to be similar with $29.3 \mu\text{m} \pm 7.6 \mu\text{m}$ and $33.2 \mu\text{m} \pm 10.5 \mu\text{m}$. For the following experiments, this is decisive as the initial particle size can be excluded as influencing factor.

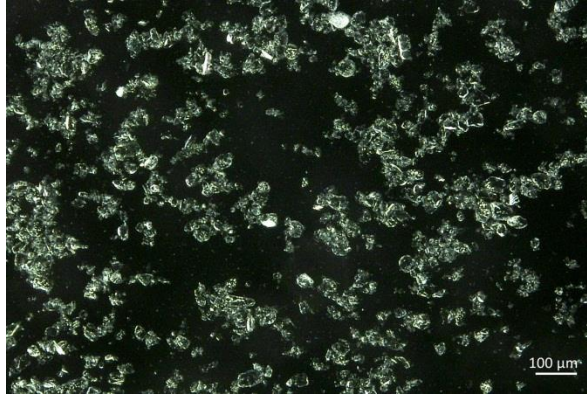


Figure 37 | Digital microscopy of oxybutynin hydrochloride.

Before extrusion, the API and the polymer were subjected to a milling/mixing step that is intended to destroy possible polymer aggregates and to homogeneously distribute the drug particles. At a temperature of 75 °C, the implants containing either the hydrochloride or the base were finally extruded using a die of 21.0 mm length. Figure 38 shows their macroscopic appearance. As can be seen, the hydrochloride leads to white opaque rods whereas the base results in more transparent rods. The diameters greatly differ although the same 1.15 mm die was used. Exceptionally, the strands were cut to approximately the same length (and not to the same weight).



Figure 38 | Comparison of implants consisting of 80% of RG 502 H and 20% of oxybutynin hydrochloride (left) or oxybutynin base (right).

Figure 39 displays the behavior of the piston force during the extrusion phase. As already mentioned (☞ IV, 1.1), a maximum of 18 kN is found for the hydrochloride-containing formulation. In contrast, for the base-containing formulation a zigzag curve with maximum values around 3 kN is

obtained. Only in the end, the piston force increases to 6 kN. During extrusion, the strand was observed to leave the die in a stop-and-go manner whereas the other formulation was extruded continuously. In both cases, the piston speed was not changed. Remarkably, significant differences in the density of the resulting rods could not be detected.

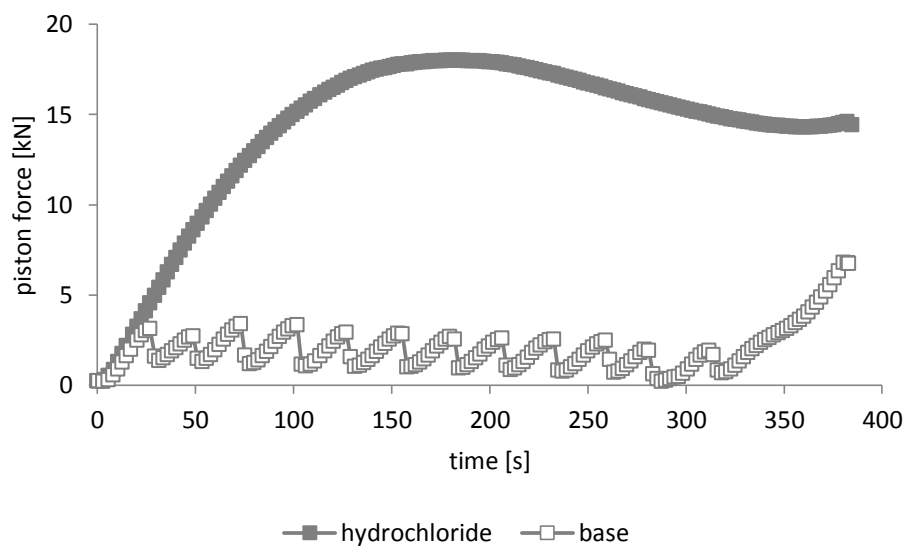


Figure 39 | Influence of the type of drug on the piston force during the extrusion (standard program) of formulations consisting of 80% of RG 502 H and 20% of oxybutynin.

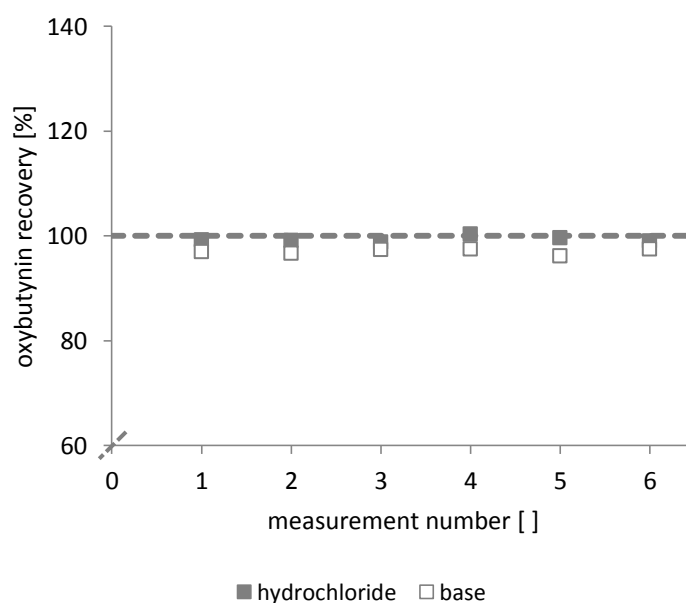


Figure 40 | Homogeneity of implants consisting of 80% of RG 502 H and 20% of oxybutynin hydrochloride or oxybutynin base (n = 6).

Due to the different melting points of the drugs (124 °C to 129 °C for the hydrochloride [234] and 56 °C to 58 °C for the base [235]), kind of a phase separation between the API and the polymer could not be excluded. Hence, the homogeneity of the implants was investigated (⇒ III, 2.2) (⇒ Figure 40). Interestingly, approximately 100% of the drug substances were recovered from the implants, independent of the type of drug. The standard deviations were smaller than 0.6%. This indicates that the API is homogeneously distributed within the polymer matrix.

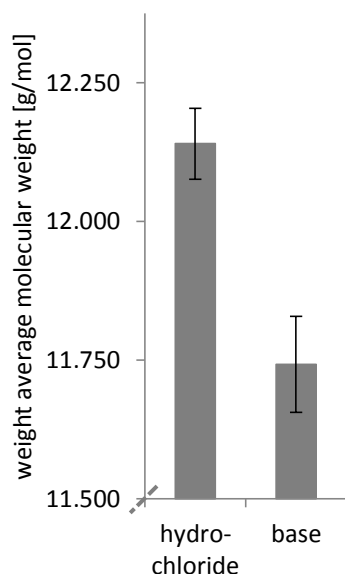


Figure 41 | Weight average molecular weight of RG 502 H in implants consisting of 80% of the polymer and 20% of oxybutynin hydrochloride or oxybutynin base (mean ± standard deviation, n = 3).

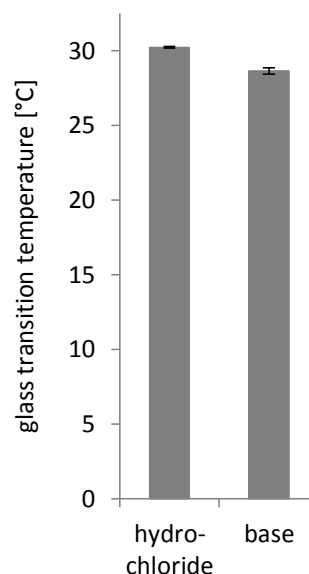


Figure 42 | Glass transition temperature of RG 502 H in implants consisting of 80% of the polymer and 20% of oxybutynin hydrochloride or oxybutynin base (mean ± standard deviation, n = 3).

In order to get more information on the different extrusion behavior of the hydrochloride and the base, weight average molecular weight and glass transition temperature of the polymer were determined (⇒ Figure 41 and Figure 42). Both values were found to be slightly smaller for the implants with the base. A molecular weight of 12,140 g/mol was obtained for the hydrochloride-containing polymer whereas the base-containing one exhibits 11,743 g/mol. The T_g values which are 30.2 °C and 28.6 °C differ by 1.6 °C. This suggests that the base accelerates the degradation of RG 502 H, even during implant manufacturing. In spite of that, the differences are judged too small to have an influence on the extrusion process.

In the following, the extrusion temperature for the base-containing formulation was reduced in steps of 5 °C (☞ Figure 43). At 70 °C, the maximum piston force decreases to a minimum of less than 1 kN. This value goes up to 2 kN at a temperature of 65 °C and induces an unexpected overload at 60 °C. With the optimized process in combination with a two-holed die, 60 °C can be reached. As soon as the temperature comes below the T_m of the drug substance, the process is automatically stopped due to piston forces greater than 25 kN. The zigzag characteristic of the piston force diminishes with decreasing temperature, thus resulting in a typical curve with a maximum when extrusion is, for example, performed at 65 °C (data not shown). At this temperature, oxybutynin base is assumed to be completely molten. However, the polymer might stabilize the process since it is not as liquid as at 75 °C. Despite that, it remains surprising that the homogeneity of the implants is not touched at higher temperatures.

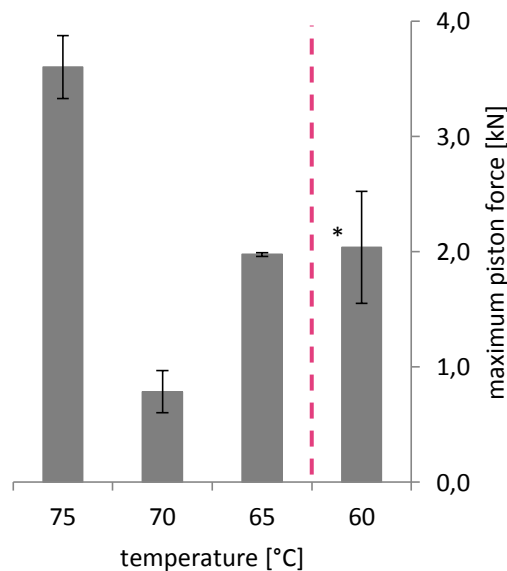


Figure 43 | Influence of the temperature on the maximum piston force during the extrusion (standard program, * optimized program in combination with a two-holed die) of formulations consisting of 80% of RG 502 H and 20% of oxybutynin base (mean \pm standard deviation, $n = 2$).

Regarding the implant diameters (☞ Figure 44), it is not surprising that the hydrochloride leads to compact rods of $1.27 \text{ mm} \pm 0.03 \text{ mm}$ whereas the base-containing implants are thin with an inconstant diameter of $0.88 \text{ mm} \pm 0.15 \text{ mm}$ (both values refer to an extrusion temperature of 75 °C). This indicates that the formulation with the base becomes too liquid during heating. When the temperature is reduced to 70 °C or 65 °C, the standard deviation is considerably improved, which can

be attributed to the more solid consistency of the material inside the barrel. With $1.14 \text{ mm} \pm 0.03 \text{ mm}$ and $1.22 \text{ mm} \pm 0.03 \text{ mm}$, the resulting strands remain thinner than the corresponding hydrochloride-containing ones, but their quality is comparable. For base-loaded implants, it cannot be concluded that the diameter directly relates to the maximum piston force. This is due to the uncharacteristic stop-and-go extrusion behavior which results in a zigzag curve for the piston force.

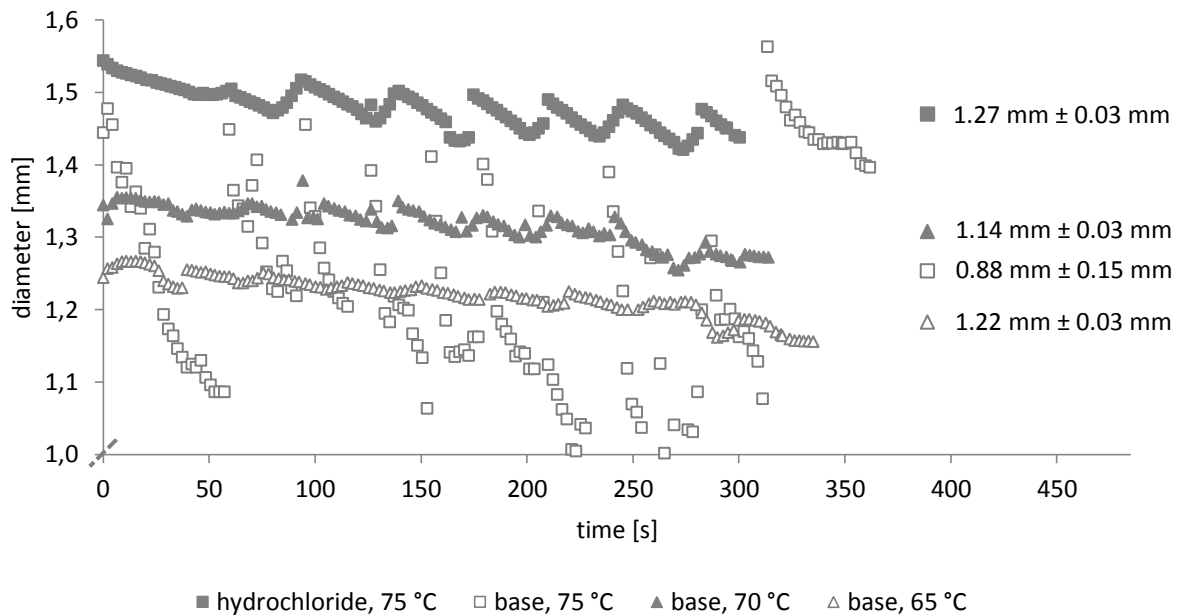


Figure 44 | Influence of the type of drug and the temperature on the implant diameter. The implants consisted of 80% of RG 502 H and 20% of oxybutynin hydrochloride or oxybutynin base. Extrusion was performed using the standard program.

Finally, the influence of different fractions of oxybutynin hydrochloride or oxybutynin base on the maximum piston force was investigated. The results are presented in Figure 45. If the hydrochloride is used in percentage amounts of 5%, 10%, and 15%, the maximum piston force is reduced to values in the range of 7 kN to 10 kN. At 20%, 18 kN are obtained. As the drug substance does not melt during extrusion, the solid content in the softened polymer increases with the amount of the API. This leads to an increase of the viscosity and results in higher frictional forces along the walls of the barrel and the die. By way of illustration, when the polymer is completely replaced by the hydrochloride, the process would certainly be stopped due to an overload. Interestingly, 20 kN were found to be necessary for the extrusion of pure RG 502 H. This can be explained by the fact that smaller amounts of the drug particles induce kind of a ball bearing effect which reduces the friction and hence the maximum piston force. Both the influence of the solid content and the ball bearing

effect seem to balance each other at 5%, 10% and 15% drug loading. As can be seen, the same experimental setup was used for base-containing formulations. At 5% drug loading, a value similar to the one of the placebo was obtained: 21 kN. With increasing percentage amounts, the maximum piston force declines exponentially. This can be attributed to the fact that oxybutynin base melts during extrusion, that way reducing the viscosity of the material inside the barrel. At 100% of the API, it is likely to have piston forces close to 0 since the formulation is liquid then.

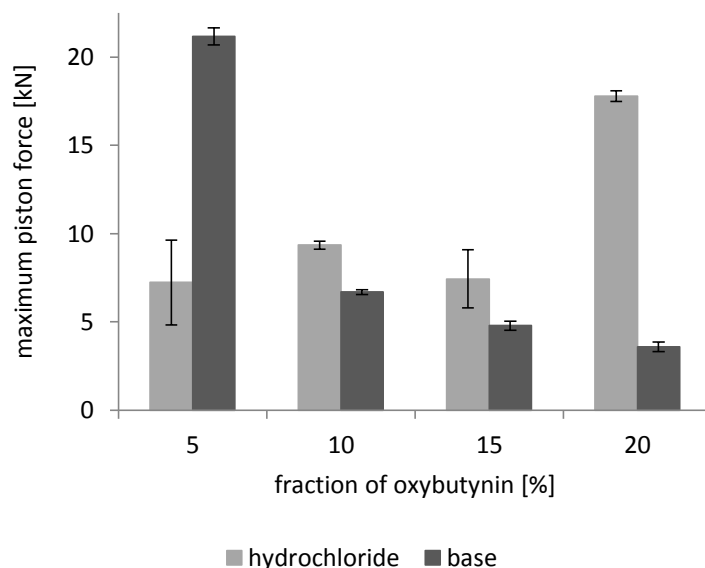


Figure 45 | Influence of the type of drug on the maximum piston force during the extrusion (standard program) of formulations consisting of RG 502 H and different fractions of oxybutynin (mean \pm standard deviation, $n = 2$).

In summary, the extrusion behavior of both drugs turned out to be completely different. This can primarily be ascribed to the fact that the base melts during manufacturing ($T_m = 56\text{ }^\circ\text{C} - 58\text{ }^\circ\text{C}$) [235] whereas the salt remains solid ($T_m = 124\text{ }^\circ\text{C} - 129\text{ }^\circ\text{C}$) [234]. As a consequence, two types of extrudates were obtained: almost transparent ones with a small diameter and white opaque ones with a larger diameter. Independent of the macroscopic appearance, the APIs were found to be homogeneously distributed. The determination of the polymer molecular weight and the glass transition temperature revealed that the base (slightly) accelerates the degradation of the matrix. Whether this has an impact on the release rates, can be seen in the following chapter.

1.2 *In vitro* release studies

Prior to the first comparative *in vitro* release studies, the saturation limits for oxybutynin hydrochloride and oxybutynin base in 0.1 M phosphate buffer pH 6.0 were determined. This is essential with regard to the sink conditions. It is recommended that the volume of the release medium is ten times greater than the volume at the saturation point of the drug [148]. For the hydrochloride that turned out to be easily soluble with $150.83 \text{ mg/mL} \pm 10.36 \text{ mg/mL}$, it is no problem to comply with these conditions. Given that the drug loading is 4 mg, a release medium of less than 300 μL would still fulfill the requirements. In contrast, more than 80 mL would be necessary for the release of the base which was found to be poorly soluble with $0.49 \text{ mg/mL} \pm 0.04 \text{ mg/mL}$. Although perfect sink conditions could not be guaranteed for both drugs, it was decided to work in a buffer volume of 10 mL. This can primarily be attributed to the quantification limit of the detection method. Studies on the sampling intervals and the buffer exchange evidenced that the release profiles for the base are not affected by non-compliance to the sink conditions (data not shown). Thus, the same static release model that was already successfully applied (for the determination of the hydrochloride) in the context of the process optimization was used for the base (☞ IV, 2.3). It is characterized by sampling intervals up to 4 d and a 10% buffer exchange.

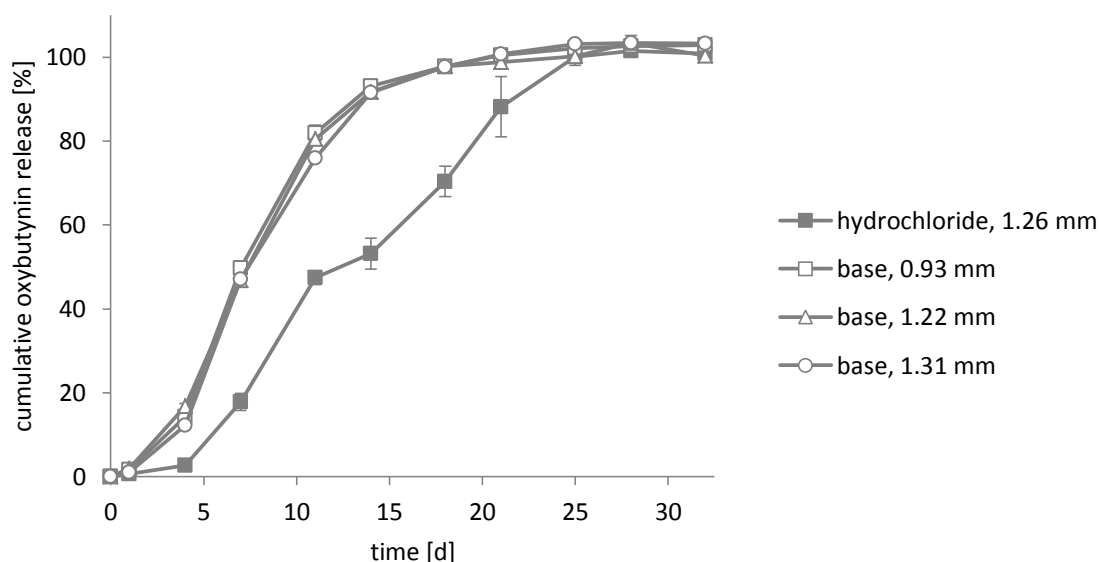


Figure 46 | *In vitro* drug release from implants consisting of 80% of RG 502 H and 20% of oxybutynin hydrochloride or oxybutynin base in 0.1 M phosphate buffer pH 6.0 at 37 °C. Influence of the implant diameter (mean \pm standard deviation, $n = 3$).

Figure 46 shows the cumulative release profiles of implants containing either oxybutynin hydrochloride or oxybutynin base in a matrix of RG 502 H. Different diameters were obtained by

varying the extrusion parameters. Both the 1.26 mm rods and the 0.93 mm rods were manufactured using the standard program at 75 °C. For the 1.22 mm rods, a reduced temperature of 65 °C was applied. Implants of 1.31 mm thickness resulted from an overload batch that was run with the optimized program at 55 °C. In this case, the extrusion temperature was below the melting temperature of the base. As demonstrated, independent of the implant diameter and the production parameters, the base is released faster than the hydrochloride. The lag phase is reduced to approximately 24 h, followed by a strong increase of the release rates. After 21 d, the drug release is completed.

Moreover, gamma-sterilized implants were investigated as well. Typically, sterilization is the last stage of the production process since the implants are intended for parenteral administration. The macroscopic appearance of the hydrochloride-loaded rods was found to remain unchanged whereas the base-loaded rods clearly changed color (☞ Figure 47). Yellowish, almost transparent strands were obtained post-sterilization. This suggests that the drug substance is somehow affected (the appearance of placebo strands is not influenced by the sterilization process).

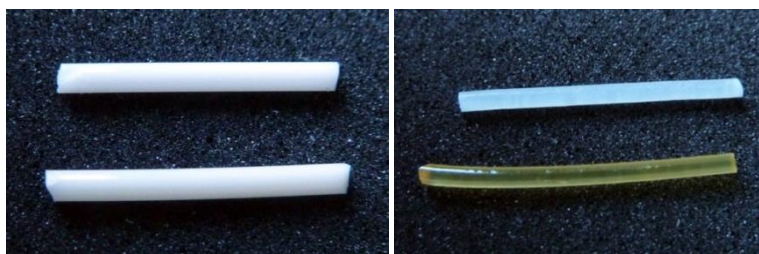


Figure 47 | Influence of gamma sterilization (top: non-sterilized, bottom: sterilized). **Left:** Implants consisting of 80% of RG 502 H and 20% of oxybutynin hydrochloride. **Right:** Implants consisting of 80% of RG 502 H and 20% of oxybutynin base.

As illustrated in Figure 48, the release curves of the sterilized implants are similar to the ones of the non-irradiated implants. The base is now released immediately from the beginning so that a lag phase cannot be detected any more. The initial release was determined to be $4.5\% \pm 0.2\%$ for sterilized rods whereas $1.7\% \pm 0.7\%$ were found for non-irradiated rods. Concerning the recovery of the APIs, it is important to notice that in both cases more than 5% of the drugs get lost after 32 d of incubation. This can be attributed to gamma-induced decomposition reactions, potentially in combination with the polymer matrix that is known to degrade upon irradiation [236].

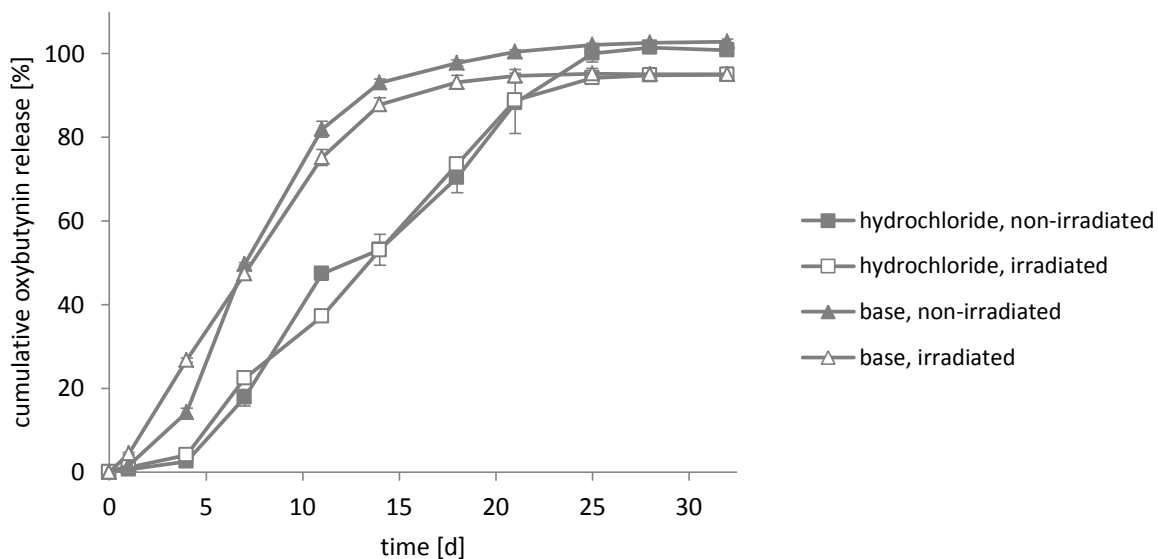


Figure 48 | *In vitro* drug release from implants consisting of 80% of RG 502 H and 20% of oxybutynin hydrochloride or oxybutynin base in 0.1 M phosphate buffer pH 6.0 at 37 °C. Influence of gamma sterilization (mean \pm standard deviation, n = 3).

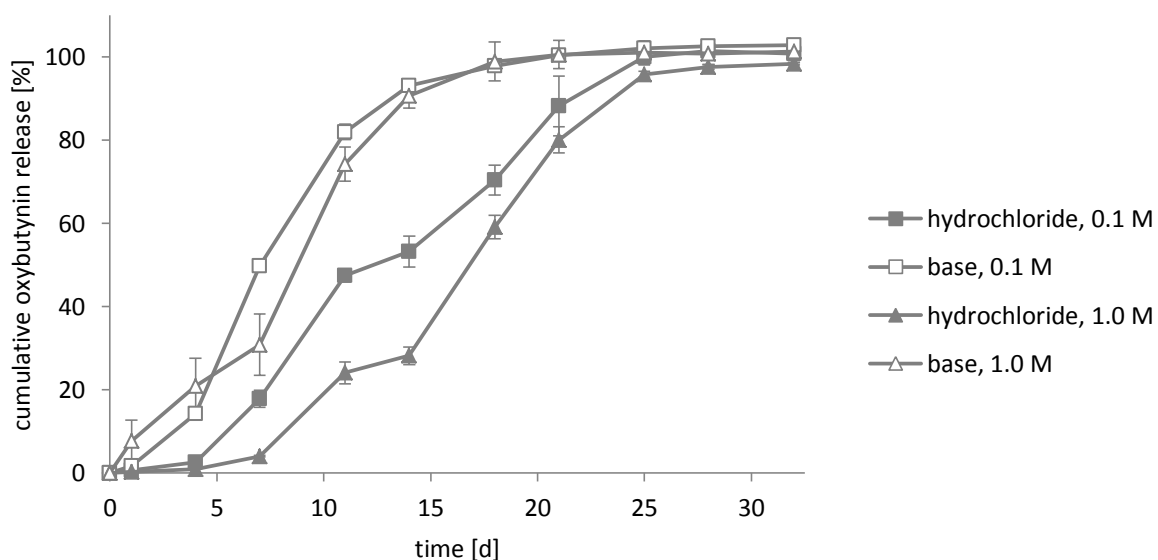


Figure 49 | *In vitro* drug release from implants consisting of 80% of RG 502 H and 20% of oxybutynin hydrochloride or oxybutynin base in phosphate buffer pH 6.0 at 37 °C. Influence of the molarity of the release medium (mean \pm standard deviation, n = 3).

In order to gain deeper insight into the differing release kinetics of the hydrochloride and the base, the release medium was changed to a molarity of 1.0 M. The idea was to increase the buffer capacity so that the pH values are stabilized and cannot be influenced by the APIs or the degradation products of the polymer. After 32 d of incubation, a pH value of 5.7 was measured for both drug substances.

This slight decrease from initially 6.0 was accepted. Figure 49 displays the release curves. For comparison purposes, the results obtained for the 0.1 M buffer are also shown. The release of oxybutynin hydrochloride decelerates with increasing molarity which is primarily due to an elongation of the lag phase. Comparable results were reported from Faisant et al. who worked with 5-fluorouracil-loaded PLGA microparticles. They explained that the decrease in the release rate might be attributable to the increase in the concentration of bases in the medium. Diffusion of these bases into the microparticles was suggested to suppress potentially occurring autocatalytic effects [237]. This effect might also play a role for the release of the base, especially in between 4 d and 7 d of incubation. Summarizing, changes in the pH are not responsible for the differing release behavior of the APIs. Although the release profiles changed at higher molarity, the release of the base was still faster in comparison to the hydrochloride.

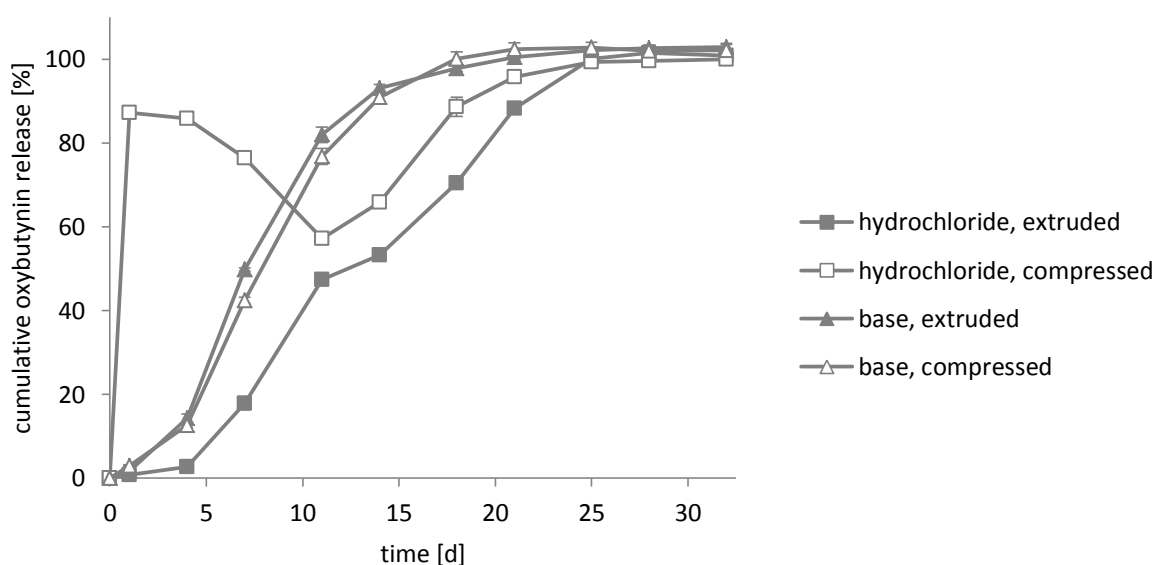


Figure 50 | *In vitro* drug release from implants consisting of 80% of RG 502 H and 20% of oxybutynin hydrochloride or oxybutynin base in 0.1 M phosphate buffer pH 6.0 at 37 °C. Influence of the manufacturing method (mean ± standard deviation, n = 3).

In a final step, the implant manufacturing technique was changed. Compressed implants were prepared by means of a hydraulic press. As this process is run at room temperature, two aspects have to be considered: on the one hand, oxybutynin base does not melt any more, and, on the other hand, the polymer remains as a solid. That way, it can be clarified whether the production conditions are responsible for the differing release profiles. The surface areas of the implants were calculated to be 49.6 mm² and 58.2 mm² for the hydrochloride- and base-containing extrudates and around 70 mm² for the disks. Independent of the geometry and the manufacturing process, the base

was observed to follow one and the same release profile resulting from an accelerated degradation of the matrix polymer (☞ Figure 50). In contrast, the initial release of the hydrochloride from the compressed implants is considerably high compared to the extrudates. More than 87% are released within the first 24 h. Since this effect is that pronounced, it cannot be ascribed alone to the increased surface area. Hence, oxybutynin hydrochloride needs to be processed at temperatures above the T_g of the polymer to obtain the characteristic multi-phase release curve. The API is then embedded in a close matrix of RG 502 H that controls the release behavior, mainly by degradation and erosion. In the case of the compressed implants, most of the drug particles seem to be easily accessible for hydration. The influence of the polymer is negligible in the beginning but becomes more and more important in the following days. As can be seen, the release rate is inverted starting from day 1, which is an indication on interactions between the drug and the polymer (☞ V, 4).

1.3 Studies on the release mechanism

Neither the implant diameter nor the release medium or the manufacturing process provided a sufficient explanation for the differing release profiles of oxybutynin hydrochloride and oxybutynin base (☞ V, 1.2). For this reason, detailed studies on the release mechanisms were carried out.

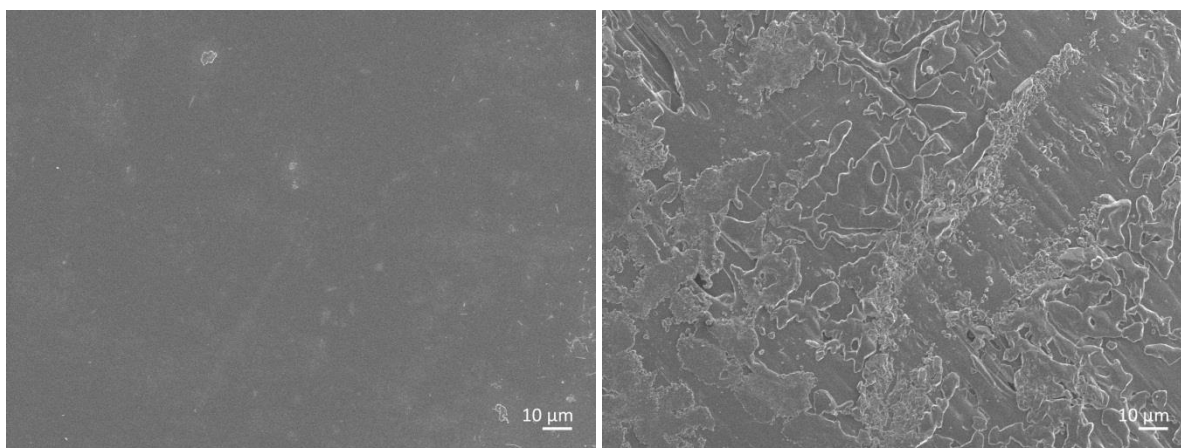


Figure 51 | Scanning electron microscopy. **Left:** Surface morphology of implants consisting of 80% of RG 502 H and 20% of oxybutynin hydrochloride. **Right:** Surface morphology of implants consisting of 80% of RG 502 H and 20% of oxybutynin base.

At first, the surface of the implants was investigated by scanning electron microscopy (☞ Figure 51). The morphology turned out to be different for both types of drug. The hydrochloride leads to a smooth surface whereas a rather rough surface is obtained for the base-containing implants. The latter can be associated with a greater specific surface area. After 1 d of incubation in

0.1 M phosphate buffer pH 6.0 at 37 °C, pores are formed at the surface of the base-loaded rods (☞ Figure 53). This contributes to faster release rates since it facilitates the diffusion of water into the implants. By implication, dissolved drug and soluble PLGA oligomers and monomers can easily be transported from the inner implant into the release medium. In contrast, the hydrochloride-loaded rods start to swell, thereby suppressing drug release from inside. The ripples on the surface result incidentally from the texture of the die orifice.

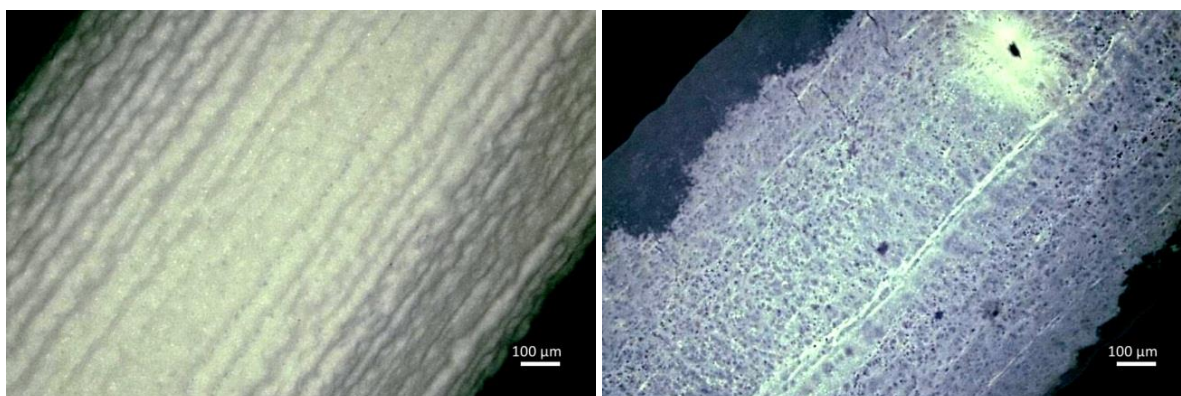


Figure 52 | Digital microscopy after 1 d of incubation in 0.1 M phosphate buffer pH 6.0 at 37 °C. **Left:** Surface morphology of implants consisting of 80% of RG 502 H and 20% of oxybutynin hydrochloride. **Right:** Surface morphology of implants consisting of 80% of RG 502 H and 20% of oxybutynin base.

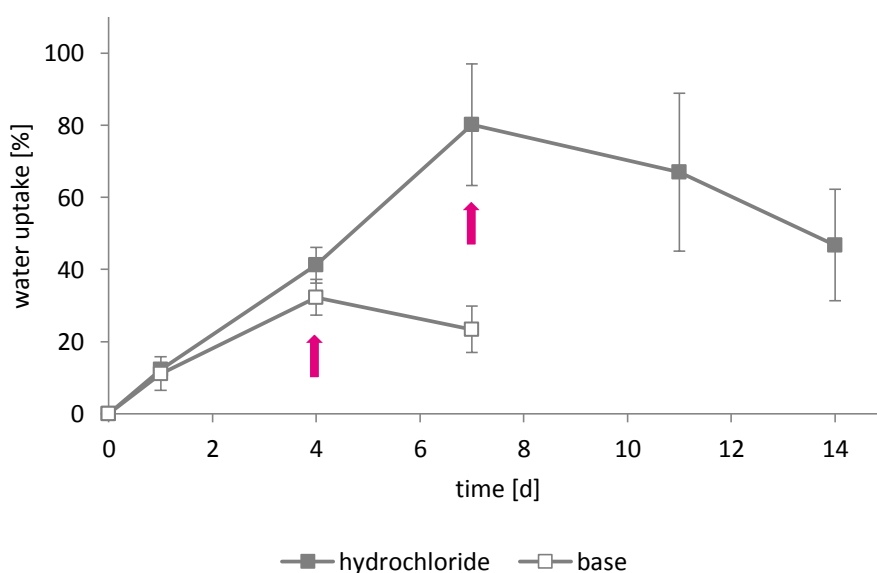


Figure 53 | Water uptake during the drug release from implants consisting of 80% of RG 502 H and 20% of oxybutynin hydrochloride or oxybutynin base in 0.1 M phosphate buffer pH 6.0 at 37 °C (mean \pm standard deviation, n = 3).

The water uptake referring to the dry implant mass was also studied. The results are illustrated in Figure 53. As can be seen, the base-containing rods reach a maximum value of $32.3\% \pm 5.0\%$ after 4 d of incubation in the release medium. Three days later, a maximum of $80.2\% \pm 16.8\%$ can be detected for the hydrochloride-containing rods. This is in good correlation with the results of the *in vitro* release tests (↪ V, 1.2). In the beginning, the water uptake increases, which is necessary to dissolve the API and to induce the hydrolytic degradation of the polymer. This process continues while the onset of erosion can be observed in an increase of the release rates. Thereafter, the water uptake decreases slightly. During this time, the drug release proceeds. Due to the fragility of the implant residues, the experiments had to be stopped after 7 d and 14 d, respectively. In general, the percentage water uptake is higher for hydrochloride-containing implants, which might be attributed to the good solubility of the API (↪ V, 1.2).

Apart from the water uptake, the mass loss referring to the initial implant weight was determined with the same experimental setup (↪ Figure 54). The shape of the curve that was calculated for the base is almost identical with the corresponding release profile (↪ V, 1.2). This indicates that the release is completely controlled by the degradation and erosion behavior of the polymer. Once more, the implant diameter turned out to have no influence. Concerning the hydrochloride, at least part of the API is released independent of the polymer, most probably by diffusion. This refers to the fact that the mass loss profile exhibits a more pronounced lag phase when compared to the corresponding release profile (↪ Figure 46).

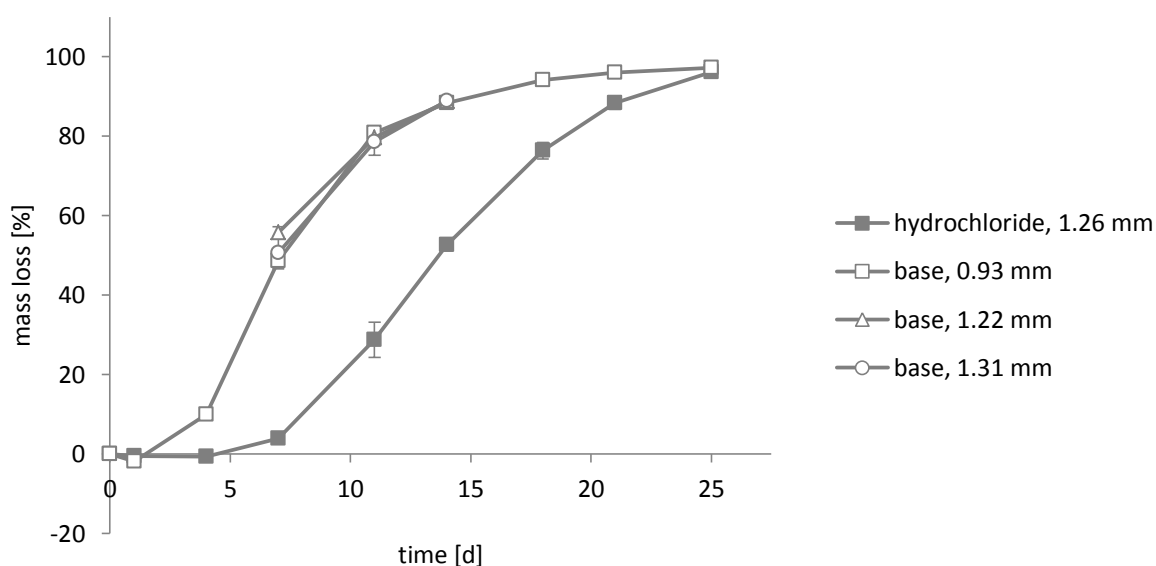


Figure 54 | Mass loss during the drug release from implants consisting of 80% of RG 502 H and 20% of oxybutynin hydrochloride or oxybutynin base in 0.1 M phosphate buffer pH 6.0 at 37 °C. Influence of the implant diameter (mean \pm standard deviation, $n = 3$).

Figure 55 presents the development of the pH values of the surrounding release medium. With increasing time of incubation, the pH decreases for both formulations. After 25 d, a minimum of 4.2 is reached. This can be ascribed to the degradation of the polymer and hence to the release of acidic degradation products [136, 238] (⇒ I, 2.3). As expected, the decrease referring to the base-containing implants starts earlier than for the hydrochloride-containing ones. When reflected over the x-axis, the pH curves are similar to the release curves (⇒ V, 1.2). Interestingly, the pH was found to depend on the implant diameters of the base-loaded rods. As can be seen, it drops earlier and even sharper for thinner implants. This is astonishing since both the release curves and the mass loss profiles are not affected. Thus, it might be argued that the acidic degradation products present in the release medium are of different molecular weight but of the same total mass. A plenty of small molecules is thought to decrease the pH to a greater extent than few large molecules. This suggests that thicker implants lead to larger degradation products. However, further investigations are necessary to clarify this issue.

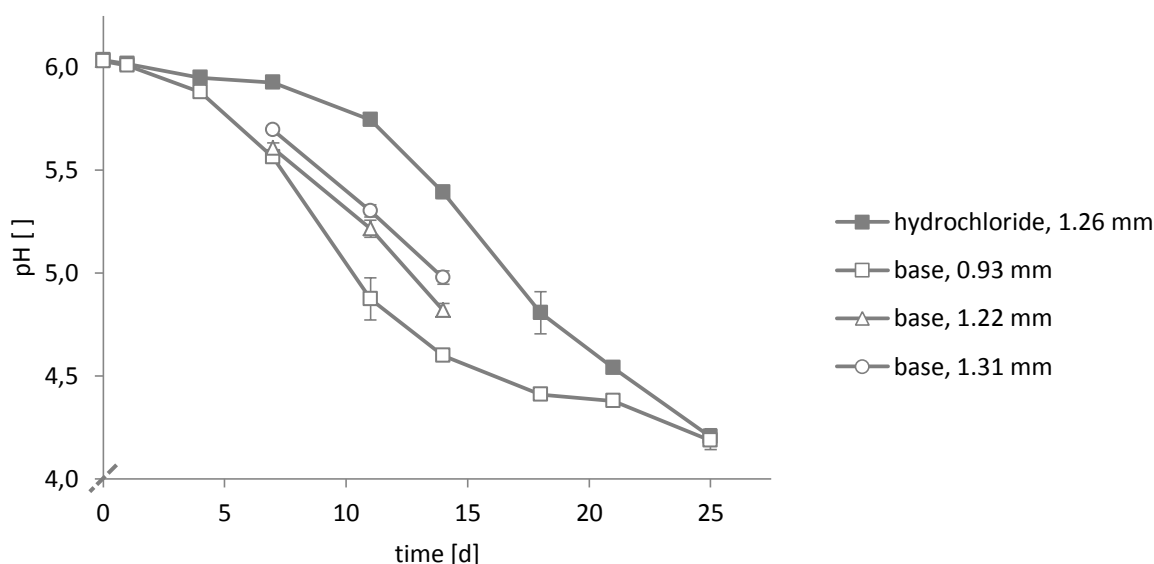


Figure 55 | pH values during the drug release from implants consisting of 80% of RG 502 H and 20% of oxybutynin hydrochloride or oxybutynin base in 0.1 M phosphate buffer pH 6.0 at 37 °C. Influence of the implant diameter (mean ± standard deviation, n = 3).

By means of size exclusion chromatography, the peak molecular weight of RG 502 H was determined during the release period (⇒ Figure 56). It is important to know that this method does not detect soluble degradation products. Consequently, the measured values refer to the non-eroded (residual) implants. As illustrated, polymer fragments with a peak molecular weight of approximately 1,000 g/mol represent the lower limit of detection. Smaller fragments are dissolved in the release

medium, and they are therefore excluded from the measurement. The molecular weight referring to the base-containing implants decreases drastically from 13,762 g/mol to 3,106 g/mol within the first 24 h of incubation. For the hydrochloride-containing implants, the degradation was shown to proceed more slowly. The molecular weight declines from initially 15,590 g/mol to 11,553 g/mol within the same period of time. In both cases, the degradation of the polymer is much faster than the release of oxybutynin (☞ V, 1.2) and the corresponding mass loss. It starts immediately from the beginning without any kind of lag phase. This indicates that the chain scission process sets in as soon as the implant comes in contact with water (☞ I, 2.3). The erosion that designates the loss of material owing to monomers and oligomers leaving the polymer follows a few days later [38]. Summarizing, the base seems to act as a catalyst for the degradation reaction of RG 502 H. Similar results were reported from Cha and Pitt who studied the influence of tertiary amines on the drug delivery from

INFO BOX #4

Weight average molecular weight and peak molecular weight - which one is more reliable?

In general, polymers cannot be characterized by a single molecular weight. Rather, a distribution of chain lengths is given [239]. This is the reason why different types of molecular weight are distinguished:

- ✓ Number average molecular weight: the M_n is the total weight of all the polymer molecules in a sample, divided by the number of polymer molecules.
- ✓ Weight average molecular weight: the M_w is based on the fact that a bigger molecule contains more of the total mass of the polymer sample than smaller molecules do [240].
- ✓ Peak molecular weight: the M_p is the molecular weight at the peak maximum.

The M_w is usually greater than the M_n . In literature, both values are used to describe the degradation behavior of poly(lactide-co-glycolide) [136, 216]. In this context, the M_p is rarely found, which might be attributed to the fact that it merely represents a single value of the complete molecular weight distribution. Hence, it is less reliable than the other values.

If possible, the weight average molecular weight was used in this thesis. However, during the release period, the peak of the polymer was sometimes observed to interfere with the peak of the API. As the peak maximum was not affected, it was exceptionally decided to work with the M_p .

polyester microspheres [241]. Further, Frank et al. showed that the base form of lidocaine has an accelerating effect on the matrix degradation of PLGA films [219]. Another example is given by Fitzgerald et al. who worked on polymer disks based on poly(lactide-co-glycolide). In contrast to the base, levamisole hydrochloride turned out to have a decelerating effect on the degradation of the matrix [226, 242].

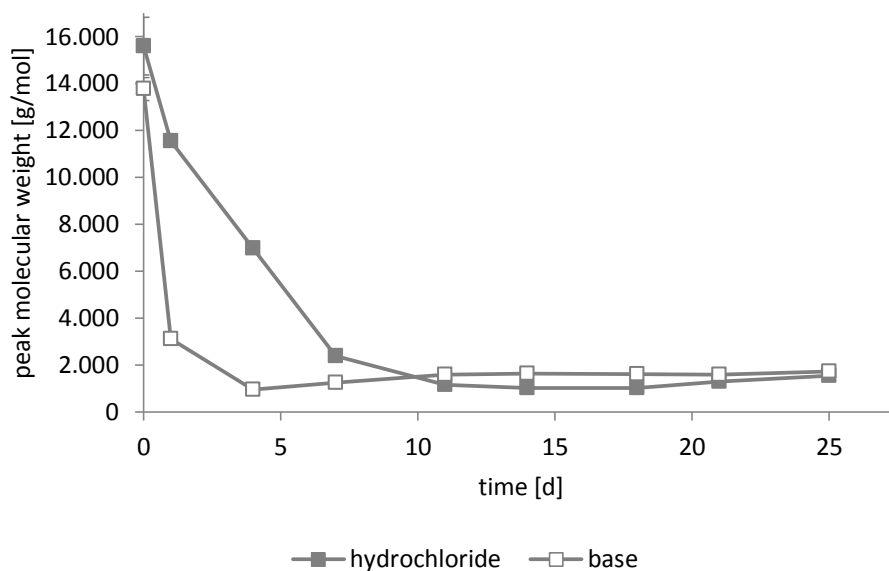


Figure 56 | Peak molecular weights of RG 502 H during the drug release from implants consisting of 80% of the polymer and 20% of oxybutynin hydrochloride or oxybutynin base in 0.1 M phosphate buffer pH 6.0 at 37 °C (mean \pm standard deviation, n = 3).

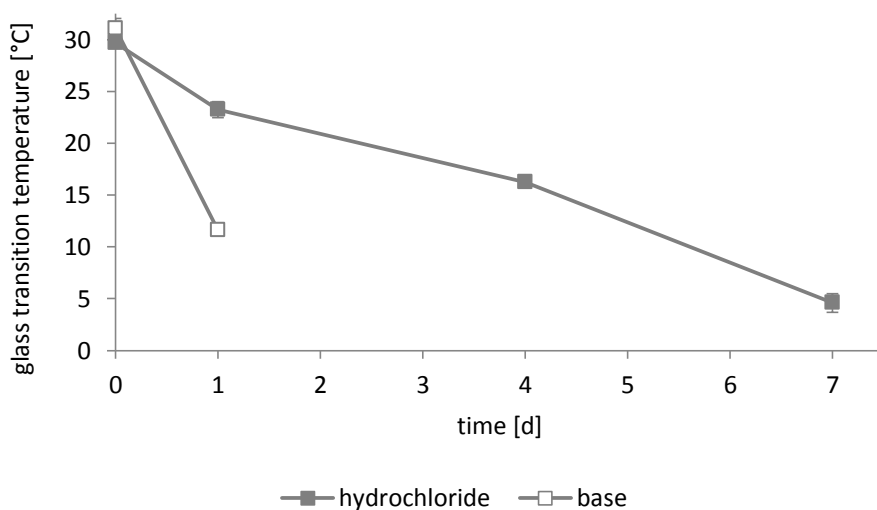


Figure 57 | Glass transition temperatures of RG 502 H during the drug release from implants consisting of 80% of the polymer and 20% of oxybutynin hydrochloride or oxybutynin base in 0.1 M phosphate buffer pH 6.0 at 37 °C (mean \pm standard deviation, n = 3).

The results obtained so far were confirmed by differential scanning calorimetry. As demonstrated in Figure 57, the glass transition temperatures of the polymer decrease over time. This effect is again more pronounced for the base-containing implants. Within the first 24 h, their T_g is reduced by 19.4 °C. In contrast, for the hydrochloride, a difference of 6.5 °C was measured. Since it is well-known that the glass transition temperature of PLGA is a function of the polymer molecular weight [136], this corresponds to the expectations. Due to the progressed degradation state of the implants, the experiments had to be stopped after 1 d for the base-loaded rods and after 7 d for the hydrochloride-loaded ones. It was no longer possible to transfer the sticky material into the DSC crucibles.

2 Influence of the type of polymer

As poly(lactide-co-glycolide) is available with different physical properties such as molecular weight, end-capping, or lactic to glycolic acid ratio (➔ I, 2.2), a broad range of release profiles and durations can be realized [34, 49]. The effect of different polymer types on the release from diverse PLGA-based drug delivery systems has already been investigated by research groups all over the world. Mollo and Corrigan, for example, prepared cylindrical amoxicillin-loaded disks and determined the influence of the molecular weight and the lactic to glycolic acid ratio [243]. The latter was also focused by Sung et al. who worked on nalbuphine-containing implants [218]. Trindade et al. analyzed the effects of the molecular weight and the end-capping on the release from bee venom-loaded microspheres [244]. In general, the following properties are known to result in a less hydrophobic polymer with increased rates of water absorption, hydrolysis, and erosion: low molecular weight, low lactic to glycolic acid ratio, and uncapped polymer end groups [245-248]. The choice of the type of poly(lactide-co-glycolide) is perhaps the most efficient tool for the modification of the release profiles [34].

In this thesis, the influence of the type of polymer was primarily investigated with the intention of getting further information on the differing release behavior of oxybutynin hydrochloride and oxybutynin base (➔ V, 1). It was of considerable interest to clarify whether the accelerating effect of the base is maintained when the matrix polymer is exchanged. Therefore, implants consisting of 20% of the API and 80% of RG 502, RG 503 H, or R 202 H were prepared according to the standard program. The extrusion temperature was adjusted to 75 °C for RG 502, 85 °C for RG 503 H, and 80 °C for R 202 H. Compared to RG 502 H, the polymers are characterized by the following properties:

- ✓ RG 502: end-capped with an ester group
- ✓ RG 503 H: higher molecular weight
- ✓ R 202 H: higher lactic to glycolic acid ratio (the polymer contains no glycolic acid units)

2.1 Insight into the manufacturing process

As illustrated in Figure 58, the type of polymer greatly influences the extrusion behavior. Formulations containing oxybutynin hydrochloride in combination with RG 503 H or R 202 H turned out not to be processible at 75 °C. Thus, the temperatures were adjusted to 85 °C and 80 °C. This is in good correlation with the physico-chemical properties of the polymers (➔ Table 2). Both RG 503 H and R 202 H are characterized by higher glass transition temperatures than RG 502 and RG 502 H. In addition, RG 503 H possesses the highest molecular weight of all polymers investigated. Interestingly,

base-containing formulations were found to be best extrudable (at 75 °C) when R 202 H was used instead of a copolymer. As this cannot be related to the polymer molecular weight or its T_g , it must be attributed to the drug substance. However, further investigations are necessary to clarify this issue. Concerning RG 502 H and RG 503 H, the maximum piston force for the base-containing formulations was shown to depend on the polymer properties. In this context, the chain mobility during extrusion might be a key issue. It is assumed that it increases with decreasing molecular weight and glass transition temperature, respectively [30]. Further, the rearrangement of the polymer chains seems to be facilitated by end-capped terminals. As can be seen, RG 502 can be processed at lower maximum piston forces than RG 502 H, independent of the type of drug. Expectably, the maximum piston force for the base-containing formulations is always below the one of the hydrochloride-containing formulations what is most probably accounted for by the different melting points of the APIs (the base melts upon manufacturing whereas the salt remains unchanged).

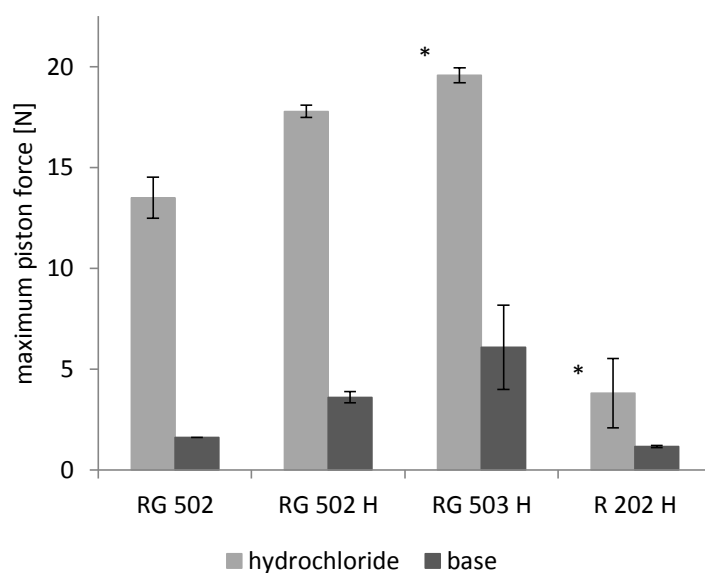


Figure 58 | Influence of the type of polymer on the maximum piston force during the extrusion (standard program at 75 °C) of formulations consisting of 80% of the polymer and 20% of oxybutynin hydrochloride or oxybutynin base (* formulations containing the hydrochloride required 85 °C for RG 503 H and 80 °C for R 202 H) (mean \pm standard deviation, $n = 2$).

The same trend can be observed for the implant diameters (\Rightarrow Figure 59). For example, $0.85 \text{ mm} \pm 0.28 \text{ mm}$ were measured for strands consisting of oxybutynin base in a matrix of RG 502. In contrast, comparable hydrochloride-loaded rods led to a thickness of $1.26 \pm 0.04 \text{ mm}$. This is consistent with the results obtained before and can be ascribed to the melting properties of the drug

molecules (↻ V, 1.1). RG 503 H constitutes an exception such that the diameter of the base-containing implants is far above the one of the die orifice. The corresponding standard deviation is quite low. This indicates that higher polymer molecular weights are capable of stabilizing the implant diameters, most probably by a reduction of the chain mobility.

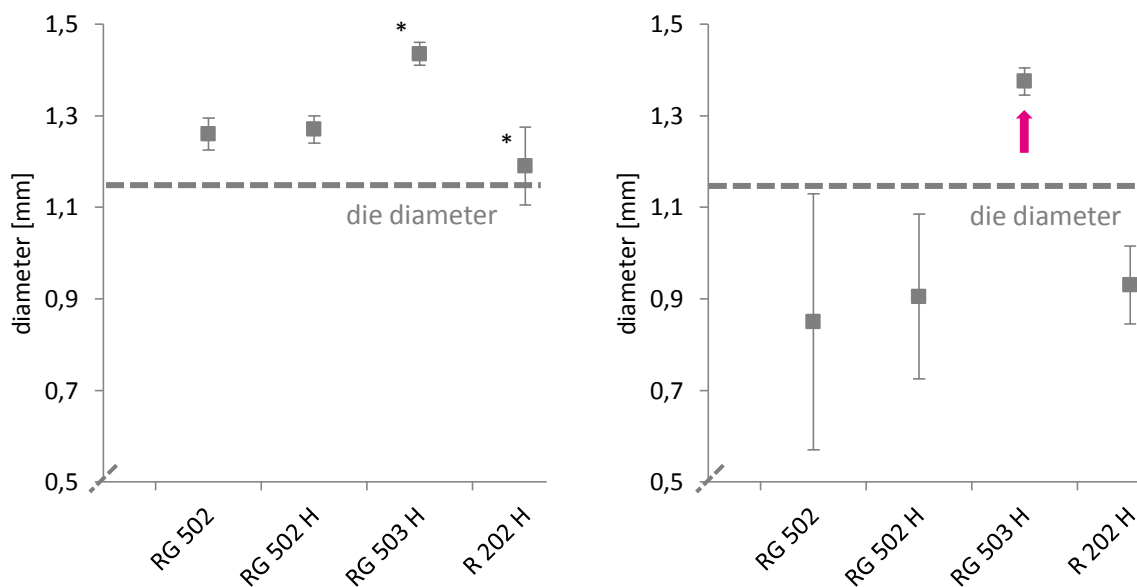


Figure 59 | Influence of the type of polymer on the implant diameter. The implants consisted of 80% of the polymer and 20% of oxybutynin. Extrusion was performed using the standard program at 75 °C (* 85 °C for RG 503 H and 80 °C for R 202 H; mean \pm standard deviation, n = 2). **Left:** Oxybutynin hydrochloride. **Right:** Oxybutynin base.

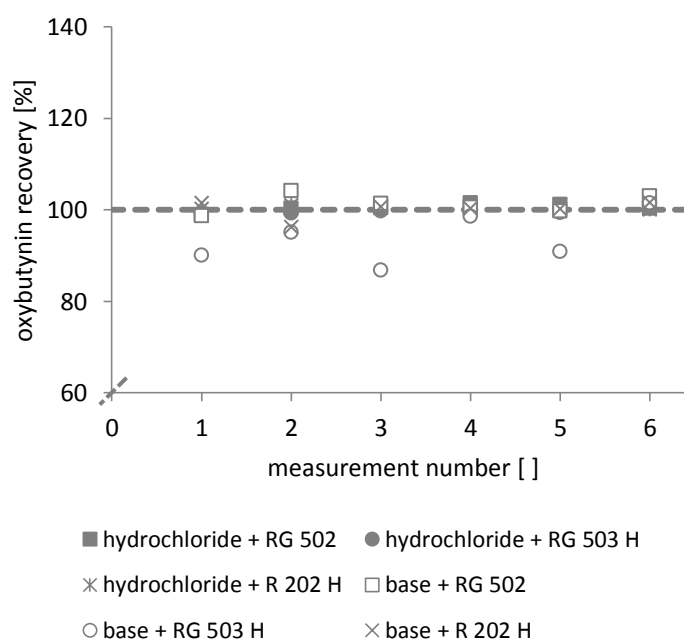


Figure 60 | Homogeneity of implants consisting of 80% of the polymer and 20% of oxybutynin hydrochloride or oxybutynin base (n = 6).

In a final step, the homogeneity of the implants was investigated. As displayed in Figure 60, the recovery of oxybutynin is around 100% for almost all combinations of API and polymer. Only for base-containing implants based on RG 503 H, a deviating value of $93.8\% \pm 5.6\%$ was obtained. The comparatively high standard deviation hints at homogeneity problems caused by demixing or even phase separation during the extrusion phase.

2.2 *In vitro* release studies

The results of the *in vitro* release studies mainly confirm what was expected from literature, both for oxybutynin hydrochloride and oxybutynin base. A matrix of pure poly(lactide) (R 202 H) was shown to considerably elongate the lag phase which is due to the hydrophobicity of the polymer. As can be seen, less than 2% of the hydrochloride and about 44% of the base are released after 25 d of incubation in 0.1 M phosphate buffer pH 6.0 at 37 °C. An increase of the molecular weight has a similar but less pronounced effect. End-capped RG 502 acts different with the hydrochloride and the base. Together with the latter, the corresponding release profile resembles the one of RG 502 H. Hence, the influence of the terminal groups on the base-catalyzed acceleration of the polymer degradation can be neglected (\Rightarrow V, 1.3). In contrast, together with the hydrochloride, the distinctive increase of the release rates is delayed by about 10 d. Independent of the type of polymer, the base is released faster than the hydrochloride.

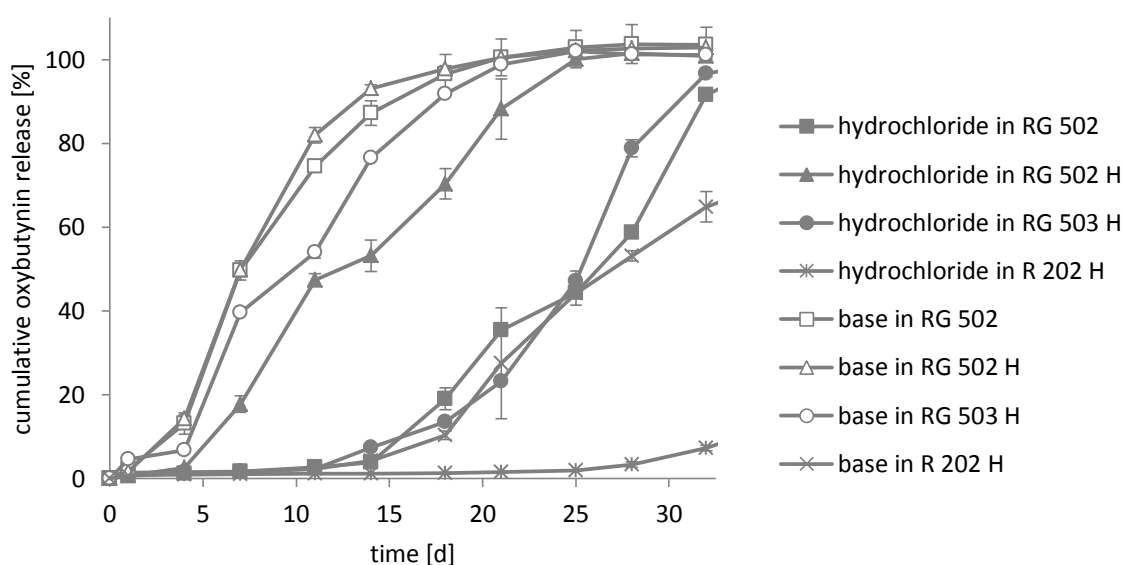


Figure 61 | *In vitro* drug release from implants consisting of 80% of the polymer and 20% of oxybutynin hydrochloride or oxybutynin base in 0.1 M phosphate buffer pH 6.0 at 37 °C (mean \pm standard deviation, $n = 3$).

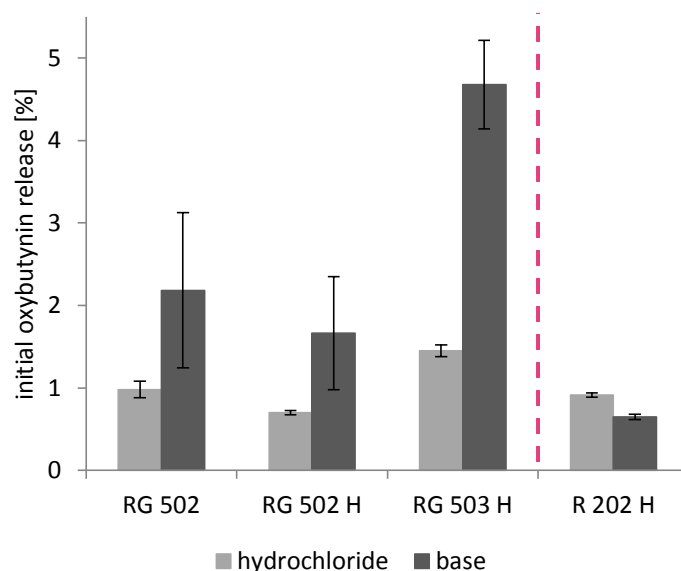


Figure 62 | Initial drug release from implants consisting of 80% of the polymer and 20% of oxybutynin hydrochloride or oxybutynin base in 0.1 M phosphate buffer pH 6.0 at 37 °C (mean \pm standard deviation, $n = 3$).

Figure 62 gives an overview of the initial burst which is defined as the percentage oxybutynin amount that is released within the first 24 h of incubation. With the exception of R 202 H-based rods, the initial release is greater for base-containing implants than for hydrochloride-containing ones. For the copolymers, it was observed to increase as follows: RG 502 H < RG 502 < RG 503 H. The same order is suggested for the hydrophobicity of the polymers. This is astonishing since RG 502 H was expected to have the highest initial release. Due to the acid end groups and the 'low' molecular weight, it is assumed to be more hydrophilic than the other polymers. The attraction of water and the dissolution of the API at the surface or in near-surface areas should be facilitated. However, this seems not to be correct. Fredenberg et al. who investigated the pore formation and pore closure in PLGA films provide a possible explanation. They found out that the pore-closing effect is more pronounced for less hydrophobic polymers. This is related to the mobility and flexibility of the polymer chains and their ability to mix with water. As the polymer chains diffuse easily, they are more likely to spread and cover pores [30]. That way, the initial release might be suppressed to a certain extent.

3 Development of innovative release strategies

It is common practice to control drug release from PLGA-based depot systems by using different polymer types. This approach usually leads to major changes in the release profiles (↻ V, 2.2). For instance, the lag phase might be drastically elongated or shortened when the polymer is changed. This problem might be overcome by using custom-made polymers or by blending different polymer types [249, 250]. With the intention to find another possibility that allows for precise controlling and fine-tuning of the release process, implants containing mixtures of oxybutynin hydrochloride and oxybutynin base were prepared. The idea was to create a delivery system that benefits from both the 'normal' delayed release of the hydrochloride and the base-catalyzed accelerated release (↻ V, 1.2). Thus, implants containing drug blends of different hydrochloride to base ratios were prepared. RG 502 and RG 502 H were exemplarily chosen as matrix materials. For all experiments, the ratio of drug to polymer remained unchanged at 1:4. The extrusions were run in accordance with the standard program at 75 °C (↻ IV, 1.1).

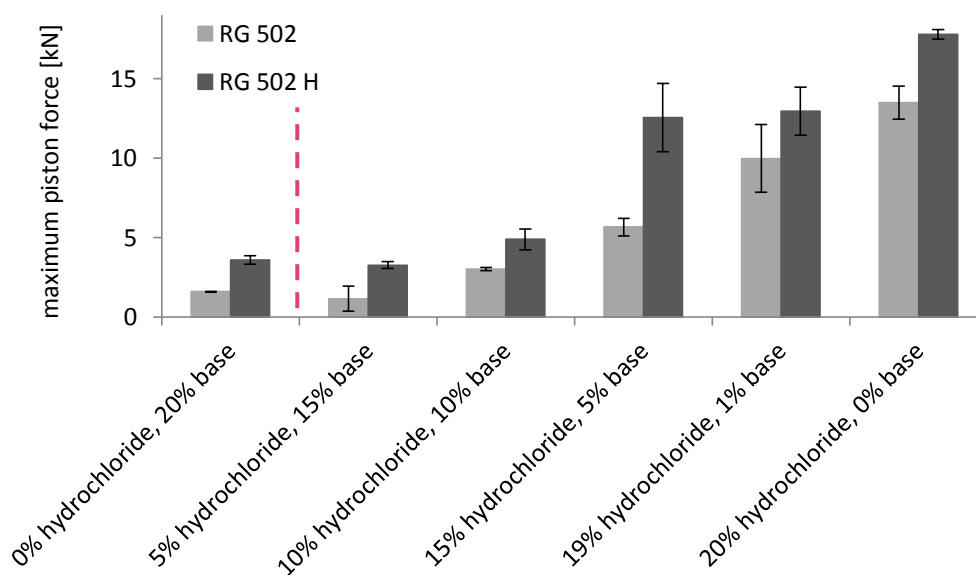


Figure 63 | Influence of different drug blends on the maximum piston force during the extrusion (standard program at 75 °C) of formulations consisting of 80% of RG 502 or RG 502 H and 20% of oxybutynin (mean ± standard deviation, n = 2).

Figure 63 shows the influence of the different drug blends on the maximum piston force. An increase of the latter can be observed with increasing hydrochloride content (from 5% to 20%) and is independent of the polymer type. The values obtained for RG 502 H are invariably greater than those for RG 502. Since the molecular weight and the glass transition temperature are equal for both polymers types (↻ Table 2), the end-capping must be responsible for the different extrudability.

When a mixture of 5% of the hydrochloride and 15% of the base is used instead of pure base, the maximum piston force is slightly decreased. In numbers, 1.2 kN and 3.3 kN are required instead of 1.6 kN and 3.6 kN for RG 502 and RG 502 H, respectively. This can probably be attributed to the ball bearing effect of the hydrochloride that was discussed earlier (☞ V, 1.1).

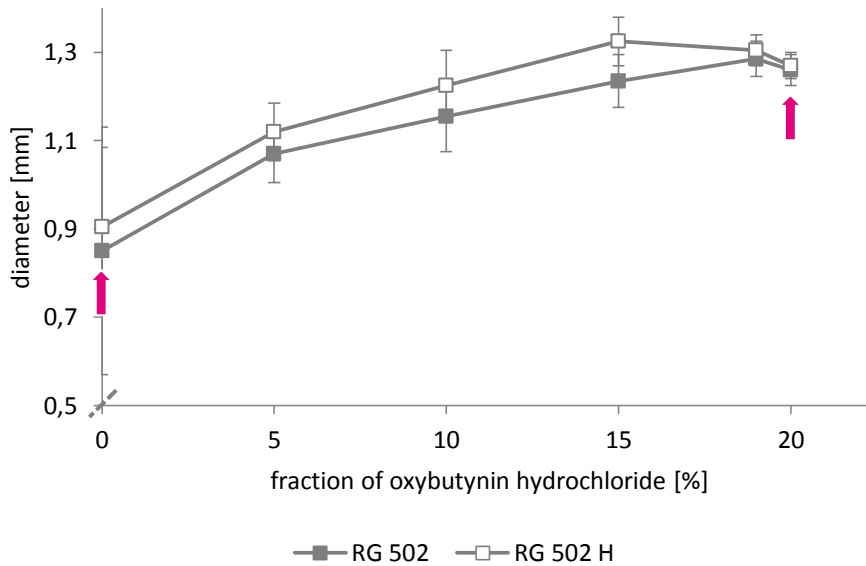


Figure 64 | Influence of different drug blends (fraction of oxybutynin hydrochloride + fraction of oxybutynin base = 20% of the total implant mass) on the implant diameter. The implants consisted of 80% of RG 502 or RG 502 H and 20% of oxybutynin. Extrusion was performed using the standard program at 75 °C (mean ± standard deviation, n = 2).

Figure 64 displays the development of the implant diameters with increasing amounts of oxybutynin hydrochloride in the drug blends. For the most part, a connection to the maximum piston force can be established. The diameters, for example, were found to be greater for implants based on RG 502 H instead of RG 502. In addition, the strand thickness increases with the hydrochloride content. An exception is only formed for the corner points which represent pure base and pure hydrochloride. In the beginning, when the hydrochloride to base ratio is increased from 0:1 to 1:3, the strand diameter increases as well although the maximum piston force turned out to slightly decrease. An inverse effect becomes obvious as soon as pure hydrochloride is used instead of a drug blend consisting of 19% of the salt and 1% of the base. The maximum piston force was shown to increase while the implant diameter became smaller. This phenomenon cannot be explained so far. Hence, it necessitates further investigations.

Figure 65 gives an overview of the *in vitro* release profiles that were obtained for the different drug blends. As can be seen, the combination of oxybutynin hydrochloride and oxybutynin base in one and

the same implant is an innovative tool for precisely controlling drug release from PLGA matrices. Even 1% of the base instead of the hydrochloride is enough to significantly alter the release characteristics. That way, every conceivable profile that ranges in between the limits given by the release of the pure drug substances can be realized. Dependent on the intended purpose, this might be much more effective than the replacement of the polymer. However, when the latter is combined with the use of different drug blends, a wide range of release profiles can be covered. The lag phase that refers to the release from RG 502-based systems, for example, can be shifted from 1 d to 14 d,

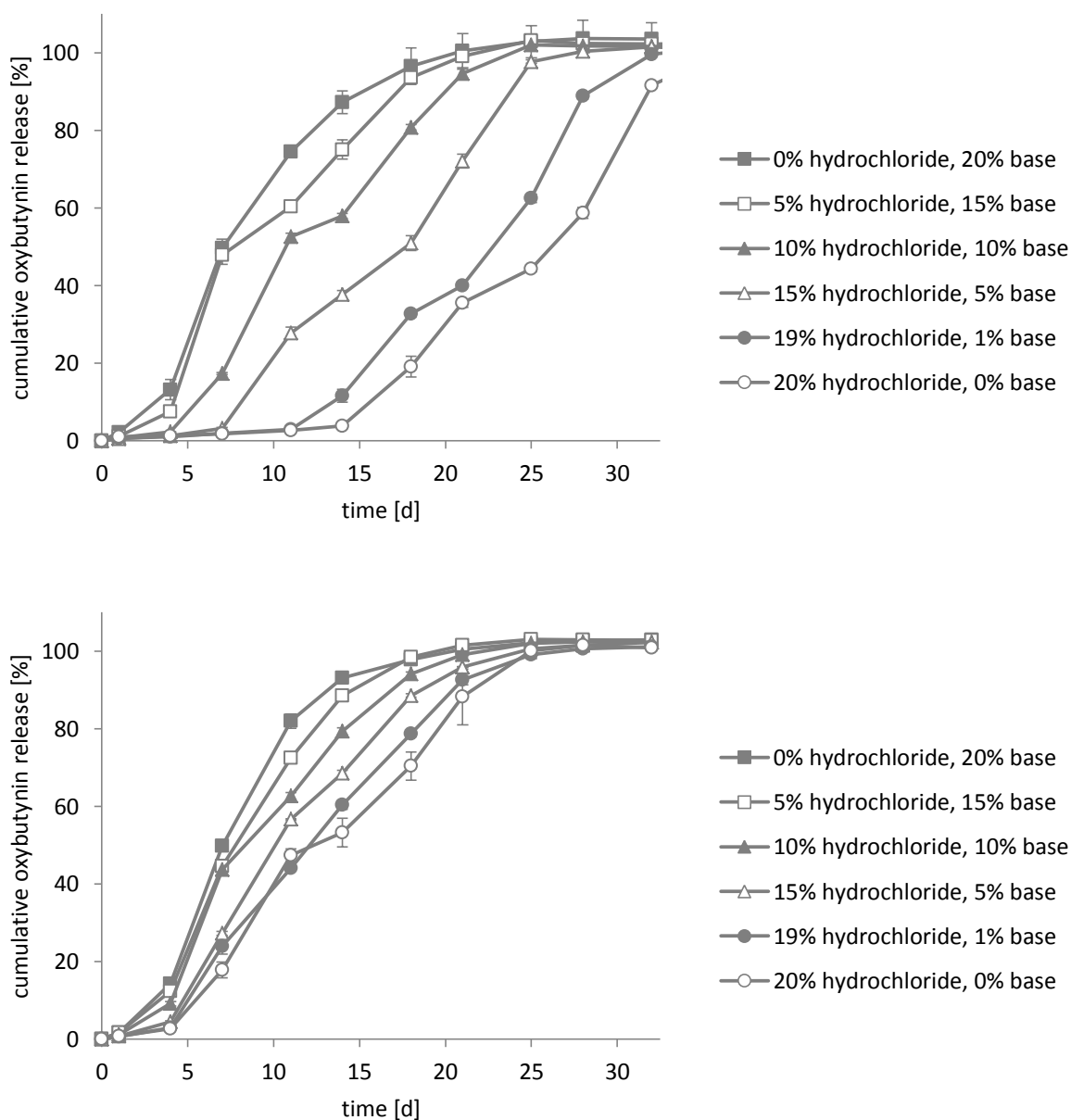


Figure 65 | *In vitro* drug release from implants consisting of 80% of the polymer and 20% of a drug blend made from oxybutynin hydrochloride and oxybutynin base in 0.1 M phosphate buffer pH 6.0 at 37 °C (mean \pm standard deviation, $n = 3$). **Top:** RG 502. **Bottom:** RG 502 H.

dependent on the composition of the drug blend. Higher hydrochloride to base ratios lead to more prolonged lag phases. Additionally, the increase of the release rates at the beginning of the erosion phase is more pronounced for implants with higher base contents. The drug release is finally completed between 21 d and 39 d (data not shown). For RG 502 H-based implants, similar results were found although the limits given by the pure drug substances were narrower.

If the release kinetics are compared to the results that were achieved for the maximum piston forces (➡ Figure 63), a correlation seems to be given. With increasing hydrochloride content, the maximum piston force increases as well. At the same time, the release becomes slower. This might be explained by the fact that the implants are of a higher density, that way decreasing the water uptake into the matrix. However, calculation of the rod densities revealed no significant differences. Implants consisting of 80% of RG 502 and 20% of oxybutynin base, for example, had a density of $1.32 \text{ mg/mm}^3 \pm 0.03 \text{ mg/mm}^3$ whereas $1.34 \text{ mg/mm}^3 \pm 0.01 \text{ mg/mm}^3$ were obtained for their salt-containing counterparts. This leads to the conclusion that the maximum piston force does not influence the release rates.

INFO BOX #5

How is it possible to determine the content of the hydrochloride and the base at the same time?

As soon as the drug substances are dissolved, it is no longer possible to distinguish between the hydrochloride and the base. This is the reason why one and the same HPLC method can be used for the determination of the concentration.

In this thesis, a standard curve referring to oxybutynin hydrochloride was prepared. By means of the molecular weights of both APIs, this line through the origin was translated to the corresponding base. That way, two factors - the slopes - were obtained that allowed for the conversion of the peak areas into the concentration of either the hydrochloride or the base.

When drug blends were investigated, it was necessary to convert these factors once more. For example, the correction factor for a 3:1 mixture of oxybutynin hydrochloride and oxybutynin base was calculated as follows: $\text{factor}_{\text{blend}} = 0.75 \cdot \text{factor}_{\text{hydrochloride}} + 0.25 \cdot \text{factor}_{\text{base}}$.

4 Investigations on the interaction of drug and polymer

Abnormalities in the *in vitro* release profiles, especially the absence of a burst release (☞ IV, 2.3) and the presence of negative release rates (☞ V, 1.2), were the motivation for investigating possible interactions between the drug molecules and the surrounding polymer matrix. Such interactions have already been reported in literature. For instance, Okada confirmed an ionic interaction between leuprorelin and poly(lactide-co-glycolide) in microspheres. He found out that the magnitude of this effect depends on the degree of degradation [251]. Jiang et al. studied the adsorption of lysozyme to the surface of blank PLGA microspheres. They explained that the protein disappearance from solution was most likely due to binding to the polymer rather than self-aggregation and precipitation [252]. Mollo and Corrigan investigated the release of amoxicillin from cylindrical compacts based on PLA and PLGA. They described an interaction between drug and polymer that was greater in systems with higher molecular weights and larger proportions of lactide [243]. Klose et al. noticed that the drug release from ibuprofen-loaded microparticles and films was always faster than from lidocaine-loaded systems. This was attributed to the fact that attractive ionic interactions between positively charged lidocaine molecules and negatively charged polymer end groups hindered drug diffusion [142].

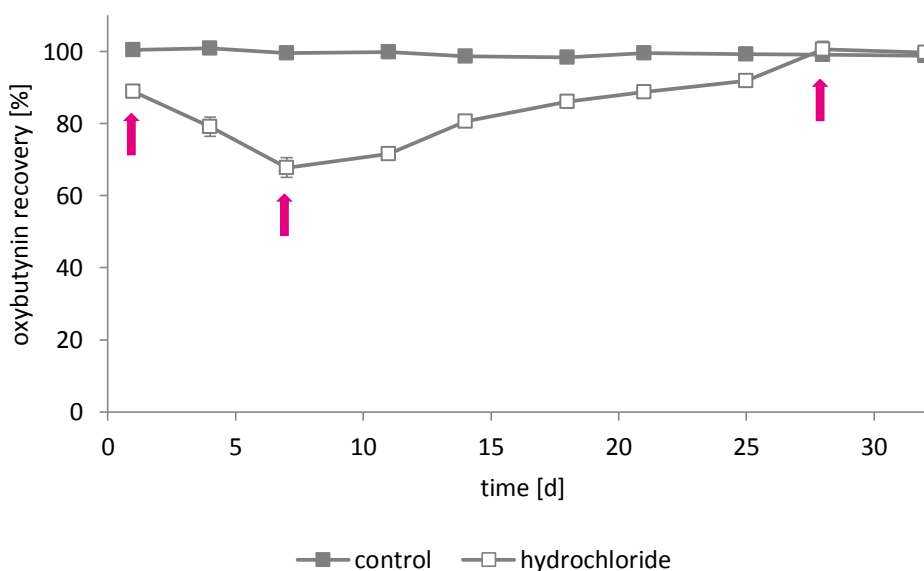


Figure 66 | Recovery of oxybutynin hydrochloride (0.4 mg/mL) in the presence of 16 mg of RG 502 H in 0.1 M phosphate buffer pH 6.0 at 37 °C (mean \pm standard deviation, n = 3).

Figure 66 shows the recovery of dissolved oxybutynin hydrochloride in the presence of ground RG 502 H over time. The amounts of drug and polymer were chosen with a view to reflecting the

composition of comparable implants. The samples were handled as for the *in vitro* release tests. In the absence of PLGA, the recovery of oxybutynin turned out to be constant at around 100%, even after 32 d of incubation at 37 °C. In contrast, when the polymer is present, the recovery decreases markedly. A minimum of 68% is obtained after 7 d. This means that up to 32% of the drug molecules interact with the degrading polymer, most probably by ionic attraction. Since oxybutynin is a weak base with a pK_a of 8.04 [253], its protonated form predominates in the release medium. PLGA as well as its degradation products exhibit negatively charged carboxyl end groups [142]. Thus, it is likely that dissolved drug molecules bind to insoluble polymer particles, that way avoiding detection via HPLC. This effect provides an explanation for the absence of the burst release. It is suggested that the drug particles at the surface or in near-surface areas are dissolved as soon as they come in contact with the release medium. At the same time, the polymer starts to degrade (☞ V, 1.3), thereby increasing the number of negatively charged end groups, which is the basis for the ionic attraction. As can be seen, the recovery of dissolved oxybutynin in the presence of blank PLGA particles is about 89% after 24 h of incubation. This indicates that the interaction plays a decisive role right from the beginning of the release period. Later, it is assumed to be responsible for declining or even negative release rates. PLGA erosion that is defined as loss of material [38] (☞ I, 2.3) usually starts when the oligomers become water-soluble at around 1100 Da [254]. As soon as this process is more dominant than the formation of further 'solid carboxyl groups' by hydrolysis, the recovery of oxybutynin increases again. It reaches approximately 100% after 28 d. This can be ascribed to the fact that the polymer is completely degraded and does not provide a negatively charged solid surface any more. Expectably, similar results were obtained for the base (data not shown).

The ionic nature of the drug/polymer interactions was confirmed by recovery studies at pH 3.0. At this low pH, it is supposed that the carboxyl terminals of poly(lactide-co-glycolide) and its degradation products are fully protonated. Hence, they are no longer available for an ionic interaction. After 24 h of incubation in 0.1 M phosphate buffer pH 3.0, the recovery of dissolved oxybutynin turned out to be the same as for the control samples without PLGA (data not shown). This indicates that the reaction between the drug molecules and the polymer was completely switched off. Longer incubation times could not be realized since oxybutynin tends to degrade upon storage at pH 3.0.

In addition, the recovery of dissolved oxybutynin in the presence of non-degraded and degraded placebo implants was investigated. For degradation, the rods were pretreated in 0.1 M phosphate buffer pH 6.0 for 10 d. The results are presented in Figure 67. Interestingly, full recovery is found for non-degraded implants after 24 h of incubation at pH 3.0 and pH 6.0. At a first glance, this is not

consistent with the results obtained before since no interactions occur at pH 6.0. However, it is important to keep in mind that the surface area of non-degraded (placebo) implants is much smaller than for the blank particles. Further, the implants are dense without any initial porosity. This is the reason why their degradation proceeds more slowly than the one of loose particles or drug-loaded implants. Subsequently, the number of negatively charged polymer end groups is limited. A remarkable interaction cannot be achieved. In contrast, when aged placebo implants are used, the recovery is reduced at pH 6.0. This can be attributed to an increased surface area which results from the progressive degradation of the polymer. As expected, these interactions are switched off when the pH is decreased to 3.0. PLGA and its degradation products are protonated then and do not attract positively charged drug molecules any more.

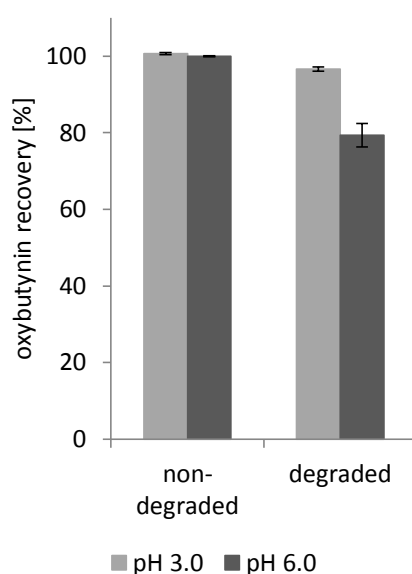


Figure 67 | Recovery of oxybutynin hydrochloride (0.4 mg/mL) in the presence of non-degraded and degraded placebo implants made from RG 502 H after 24 h of incubation in 0.1 M phosphate buffer pH 3.0 and pH 6.0 at 37 °C (mean \pm standard deviation, n = 3).

In order to ensure that the drug/polymer interaction depends on the surface area, the recovery in the presence of raw and ground RG 502 H was compared. Previously, the specific surface areas of the polymers were determined via BET measurements (↪ Figure 68). $1.91 \text{ m}^2/\text{g} \pm 0.07 \text{ m}^2/\text{g}$ were calculated for the raw material and $2.03 \text{ m}^2/\text{g} \pm 0.04 \text{ m}^2/\text{g}$ for the ground polymer. Although the difference between the values is low, a distinct effect on the recovery of dissolved oxybutynin can be observed (↪ Figure 69). After 24 h of incubation, 95% of the API are recovered in the presence of raw

RG 502 H. In contrast, 89% are found for the ground material. In this case, the interaction is more pronounced. A minimum of 68% is reached within 7 d. For the raw material, 11 d are necessary to achieve a minimum of 70%. Apparently, smaller-sized particles are prone to degrade faster, that way reducing the number of 'solid carboxyl groups'. As a consequence, the recovery increases earlier in time.

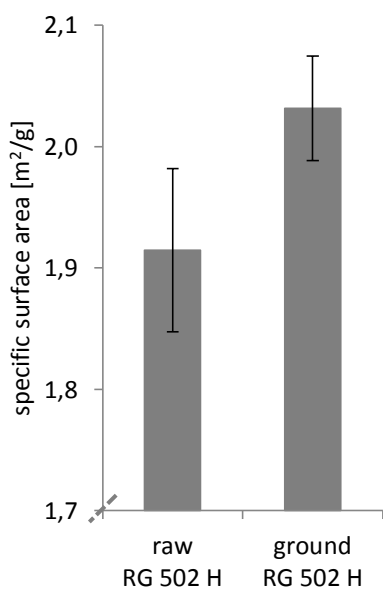


Figure 68 | Specific surface areas of raw and ground RG 502 H (mean \pm standard deviation, $n = 2$).

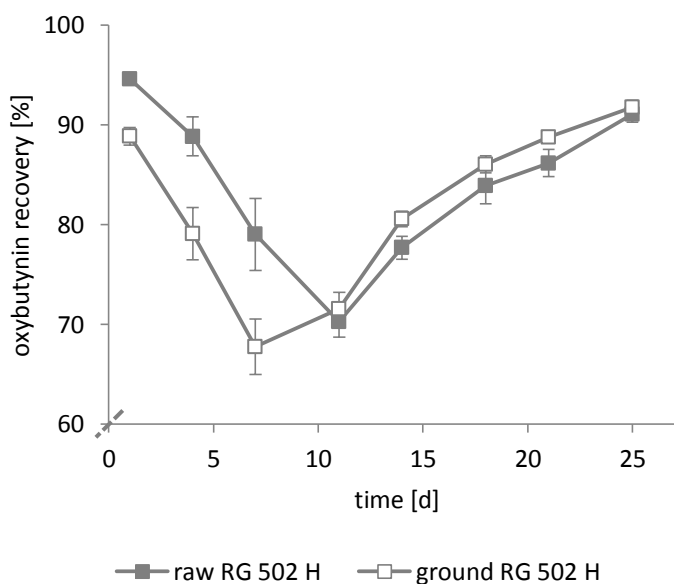


Figure 69 | Recovery of oxybutynin hydrochloride (0.4 mg/mL) in the presence of 16 mg of raw and ground RG 502 H in 0.1 M phosphate buffer pH 6.0 at 37 °C (mean \pm standard deviation, $n = 3$).

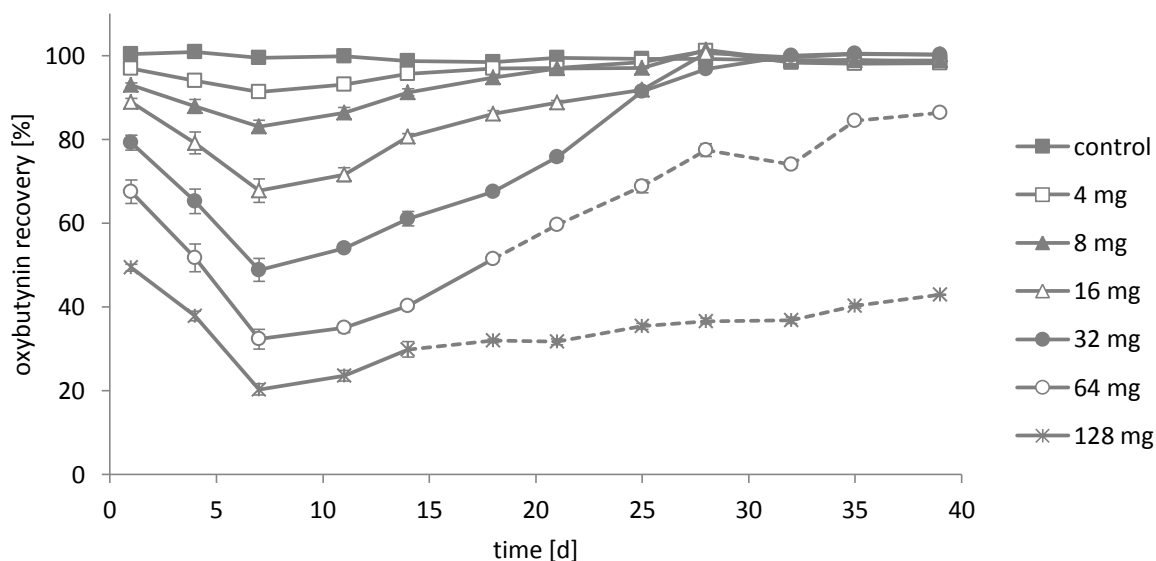


Figure 70 | Recovery of oxybutynin hydrochloride (0.4 mg/mL) in the presence of different amounts of RG 502 H in 0.1 M phosphate buffer pH 6.0 at 37 °C (mean \pm standard deviation, $n = 3$).

The influence of the available surface area was also studied by increasing the amount of RG 502 H while the concentration of oxybutynin in the release medium was kept constant at 0.4 mg/mL. For this experiment, ground polymer was used without exception. Figure 70 reveals that the degree of the drug/polymer interaction increases with increasing polymer mass. In other words, the size of the surface area and hence the number of carboxyl groups are decisive. In the presence of 128 mg of the polymer (which is the eightfold amount of what an implant contains) a minimum recovery of 20% can be measured after 7 d of incubation at pH 6.0. However, these samples were observed not to reach a recovery of 100% again. After 39 d, when PLGA is assumed to be completely degraded, about 57% of the API are still missing. This is due to the fact that oxybutynin starts to hydrolyze as well [255, 256]. The corresponding chromatograms show an upcoming peak at 3.6 min to 3.7 min that first appears after 18 d. The same holds true for an initial polymer mass of 64 mg. In this case, the 'degradation peak' is first detected after 21 d (data not shown). With a view to the pH values of the samples that were incubated for 39 d (☞ Figure 71), this effect can easily be explained. Values as low as 3.5 and 3.1 are obtained for 64 mg and 128 mg of RG 502 H. This can be ascribed to the degradation of the polymer during which acidic oligomers and monomers are formed [136] (☞ I, 2.3). The pK_a values for lactic and glycolic acid are 3.86 and 3.83, respectively [257]. In summary, the low pH of the release medium is thought to be responsible for the degradation of the API. When smaller amounts of the polymer are used, the pH drops to a minor degree, thus avoiding degradation of the drug molecules. As the buffer is able to neutralize the PLGA oligomers and monomers to a certain extent, the

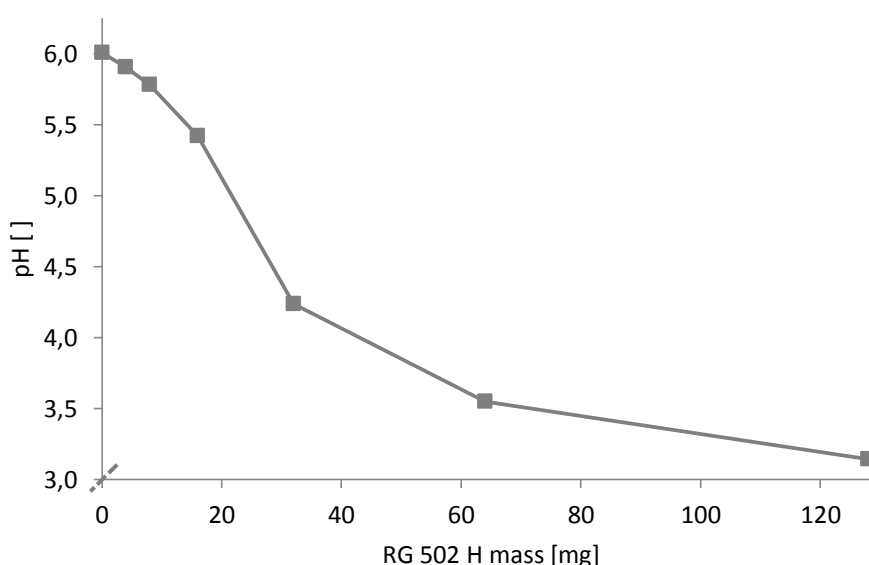


Figure 71 | pH values after 39 d of incubation of oxybutynin hydrochloride (0.4 mg/mL) in the presence of different amounts of RG 502 H in 0.1 M phosphate buffer pH 6.0 at 37 °C (mean \pm standard deviation, $n = 3$).

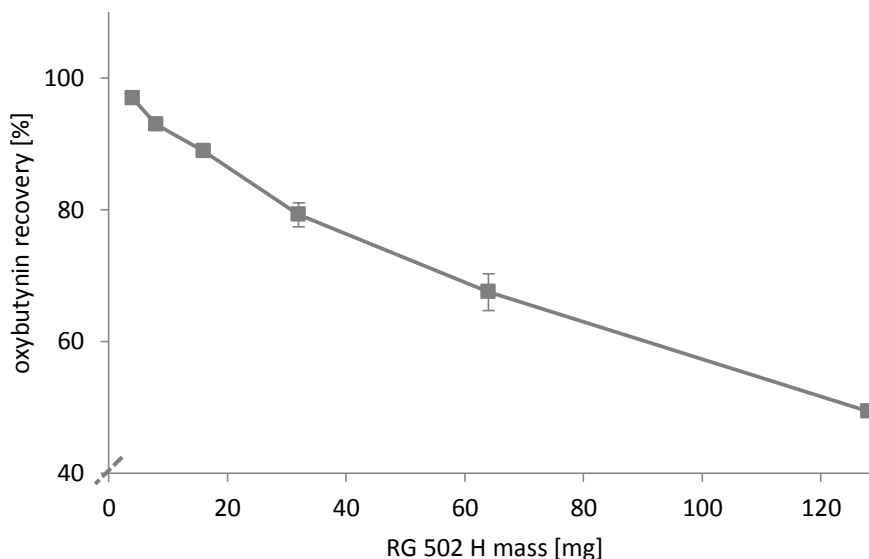


Figure 72 | Recovery of oxybutynin hydrochloride (0.4 mg/mL) in the presence of different amounts of RG 502 H after 24 h of incubation in 0.1 M phosphate buffer pH 6.0 at 37 °C (mean \pm standard deviation, $n = 3$).

pH values are more stable at smaller RG 502 H amounts. Since this issue is now clarified, the recovery of oxybutynin within the first 24 h of incubation is focused. As illustrated in Figure 72, the recovery does not decrease linearly with increasing polymer mass. The curve decreases more rapidly in the beginning and levels off at higher amounts of RG 502 H. This is attributable to the fact that the polymer particles tend to stick together. Agglomerates are formed, which leads to a decrease of the available surface area. This effect is of course more pronounced at higher polymer mass to volume ratios. As a consequence, the degree of the drug/polymer interaction is underachieved. Interestingly, similar curve shapes are obtained for the first 21 d of incubation (data not shown). Thereafter, the degradation of the polymer is so far advanced that no interactions can be detected any more. The recovery is around 100% then. It is important to mention that this is not true for the 64 mg and 128 mg samples that were shown to induce degradation of the API.

In a final step, the recovery was investigated in the presence of different poly(lactide-co-glycolide) and poly(lactide) types. All polymers were used as received. Condensate RG 50:50 is semisolid at room temperature whereas all other types are more or less fine powders. This is the reason why the resulting graphs that are displayed in Figure 73 have to be evaluated from a qualitative point of view. As already discussed, the available surface area considerably influences the extent of the drug/polymer interaction. So, the absolute recoveries as well as the time intervals that are necessary

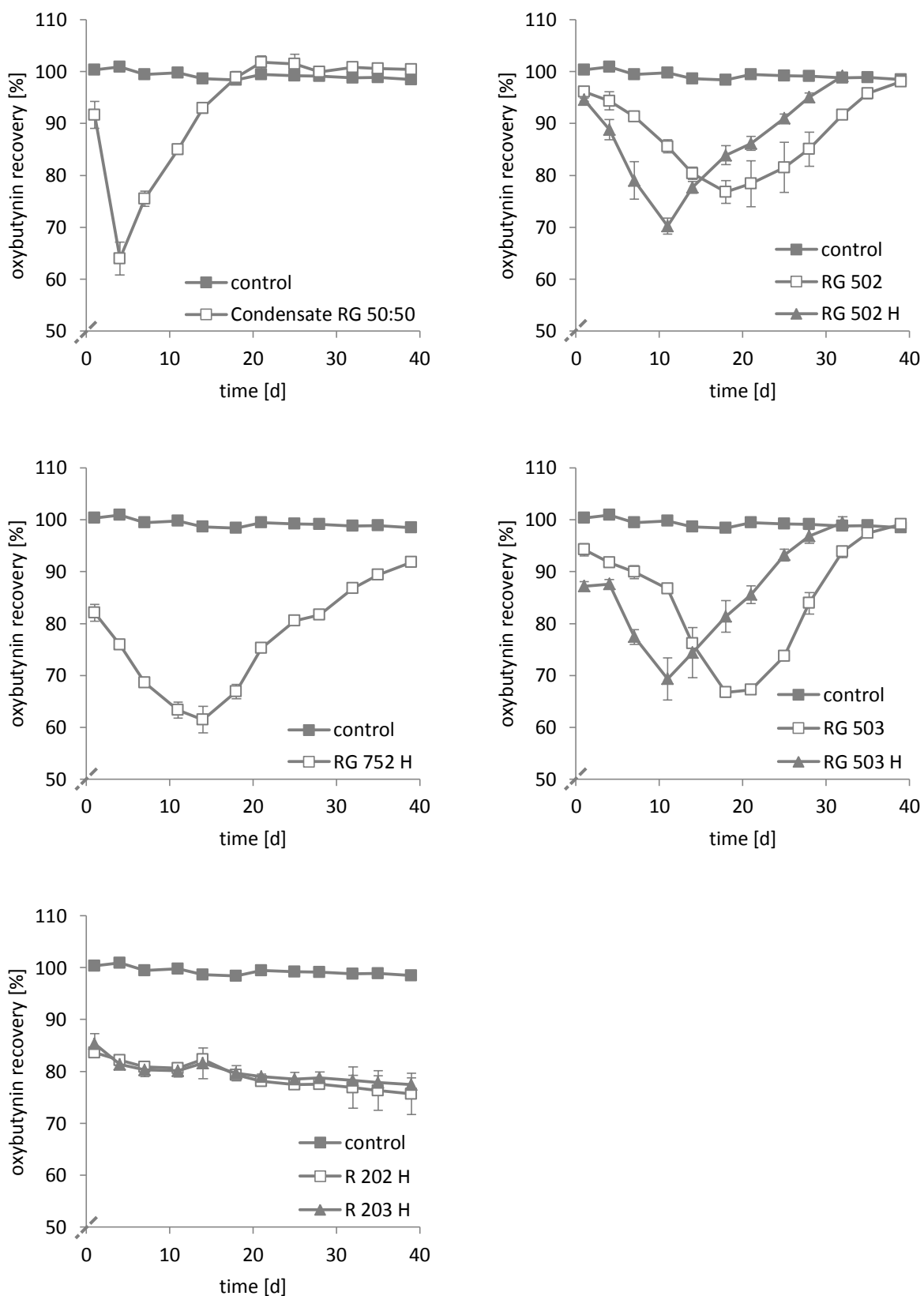


Figure 73 | Recovery of oxybutynin hydrochloride (0.4 mg/mL) in the presence of 16 mg of different polymers in 0.1 M phosphate buffer pH 6.0 at 37 °C (mean ± standard deviation, n = 3). **Top left:** Condensate RG 50:50. **Top right:** RG 502 and RG 502 H. **Center left:** RG 752 H. **Center right:** RG 503 and RG 503 H. **Bottom:** R 202 H and R 203 H.

to reach the minimum recovery cannot be compared one-to-one. Despite that, the results clearly demonstrate that the interaction depends on the type of polymer, more precisely on its degradation and erosion properties. R 202 H and R 203 H, for example, are characterized by a lactic to glycolic acid ratio of 1:0. Both polymers count among the group of poly(lactides). As they are more hydrophobic than the copolymers, the rates of water adsorption, hydrolysis, and erosion are considerably decreased [34]. This becomes apparent in the corresponding recovery profiles. Even after 39 d of incubation, the minimum recovery was not reached. It is unlikely that this effect is only caused by the particle size and the surface area, respectively. The same holds true for Condensate RG 50:50 which is a low molecular weight polymer with a T_g around 30 °C (☞ III, 1.2). Since it is semisolid at room temperature, the surface area that is available for drug/polymer interactions is assumed to be reduced to a minimum. In spite of that, a strong interaction can be observed after 4 d of incubation. This is in good agreement with the polymer properties that indicate a fast degradation. Additionally, the recovery of oxybutynin in the presence of RG 502, RG 502 H, RG 503, RG 503 H, and RG 752 H was analyzed. Once again, most of the recovery profiles can be related to the physico-chemical properties of the polymers. Especially the effect of the end-capping stands out. It renders the polymers more hydrophobic, thus delaying the onset of erosion [258] (☞ I, 2.2 and III, 2.3). The same was thought to occur at higher molecular weights. However, this is not confirmed by the recovery studies. For instance, the curves referring to RG 502 H and RG 503 H are similar. This results most probably from the fact that the RG 503 H particles are smaller in size. Hence, the surface area is greater, which might compensate the retarding effect of the molecular weight. This hypothesis is supported by the results from the *in vitro* release tests (☞ V, 2.2) that give evidence of an elongated lag phase.

5 Summary

The intention of this chapter was to gain deeper insight into the mechanisms that are responsible for the release of oxybutynin from PLGA-based implants. As these delivery systems consist of only two components - the drug substance and the polymer, it is suggested that the resulting release profiles can easily be predicted and controlled. However, the reverse is true. Diffusion and degradation/erosion which are commonly considered as main release mechanisms might be influenced by a variety of factors such as polymer/drug interactions, drug/drug interactions, water absorption, pore formation, pore closure, drug dissolution, dissolution of PLGA oligomers and monomers inside the matrix, pH changes, or changes in the polymer chain mobility [136] (☞ I, 2.3). Detailed knowledge of these processes is necessary to be able to develop innovative delivery systems with predictable release rates.

At first, the release of oxybutynin hydrochloride and oxybutynin base from RG 502 H-based implants was studied. Although the rods were prepared with the same manufacturing technique, their appearance turned out to be completely different. The hydrochloride led to opaque white strands whereas the base resulted in almost transparent milky strands. By comparison, the diameters were much smaller for the base-containing implants. However, this was not decisive for the resulting release profiles. Independent of the implant thickness, the base was shown to considerably accelerate drug release. This was confirmed by investigations on the water uptake, the pH of the release medium, the polymer molecular weight, and its glass transition temperature. Additionally, changes in the surface morphology were analyzed by scanning electron microscopy and digital microscopy. After 24 h of incubation in the release buffer, pores were only formed in the presence of the base. The hydrochloride-containing implants were observed to swell. This is in good correlation with the results obtained for the *in vitro* release tests. Studies on the mass loss finally revealed that the degradation and erosion behavior of the polymer is the determining factor for the release of the base. Diffusional processes, in contrast, were found not to play a major role. It was thus concluded that the accelerating effect can thoroughly be attributed to the base-catalyzed hydrolysis of the polymer chains. Interestingly, together with the base, the extrusion temperature could be lowered to 65 °C using the standard program and 60 °C using the optimized program in combination with a two-holed die.

In a next step, the influence of the type of polymer was determined. For that, implants consisting of oxybutynin hydrochloride or oxybutynin base in a matrix of RG 502, RG 502 H, RG 503 H, or R 202 H were manufactured. As expected, the release profiles could be correlated to the typical polymer properties. An increase in the lactic to glycolic acid ratio, for example, led to a substantial elongation

of the lag phase. A similar, but less pronounced effect was detectable for higher molecular weight polymers. Together with the hydrochloride, end-capped polymers also delayed the characteristic increase of the release rates, which usually points to the onset of erosion. This effect could not be observed for implants containing the base. Hence, it can be summarized that the base-catalyzed degradation of the polymer is independent of the terminal alkyl ester groups.

On the basis of the previous experiments, drug delivery systems with an innovative release strategy were developed. The combination of oxybutynin hydrochloride and oxybutynin base in one and the same implant allowed for precisely controlling drug release. The depot was shown to benefit from both the 'normal' delayed release of the hydrochloride and the base-catalyzed accelerated release. That way, every desired profile that ranges in between the limits given by the release of the pure drug substances can be realized. When the polymer is additionally changed, still more possibilities are available.

As a last point, the interaction between the drug molecules and the polymer chains was investigated. Recovery studies in which dissolved oxybutynin was incubated in the presence of blank polymer particles revealed that the interaction is of an ionic nature and that it strongly depends on the degradation and erosion behavior of the polymer. It was assumed that positively charged oxybutynin molecules are attracted by the negatively charged polymer chains. During the degradation of the polymer, the number of negatively charged carboxyl terminals increases, thus decreasing the recovery of oxybutynin in the release medium. As soon as the PLGA oligomers and monomers become water-soluble, this process is inverted. Consequently, the recoveries were found to increase again.

Chapter VI | Lipids as innovative excipients

This chapter focusses on lipids as innovative excipients in the manufacturing of implants based on poly(lactide-co-glycolide). It first presents the outcome of a lipid screening including triglycerides, hydrogenated cocoglycerides, monoglycerides, acetylated glycerides, macroglycerides, and phosphatidylcholines. Influences on the production processes, the mechanical properties, the release profiles, and the drug/polymer interactions are discussed. On the basis of these results, promising candidates for a reduction of the extrusion temperature are identified and further investigated. Detailed studies on heterogeneous implants that are characterized by a core-shell structure complete this chapter.

1 Lipid screening

A huge number of publications referring either to lipid implants [4, 6, 51-53, 169] or PLGA-based implants [198, 218, 221, 224, 259, 260] is available. However, hybrid implants combining both types of matrix have not been reported so far. In the field of particulate drug delivery systems, it is not unusual to find both excipients in the same formulation. For instance, Meng et al. studied the effect of medium-chain triglycerides on the release behavior of recombinant human endostatin encapsulated in PLGA microspheres [261]. Mu and Feng worked on paclitaxel-loaded PLGA-based microspheres for which phosphatidylcholine was used as emulsifier to increase the encapsulation efficiency [262]. Another example is given by Xie et al. who introduced PLGA as polymeric emulsifier for the preparation of hydrophilic protein-loaded solid lipid nanoparticles [263].

In this thesis, a variety of lipids was screened in order to identify promising candidates for an optimization of the manufacturing process towards lower temperatures. It was assumed that lipid excipients might act as lubricants or binders, that way reducing the piston force during extrusion. High potential was seen in lipids with low melting points such as hydrogenated cocoglycerides, acetylated glycerides, macroglycerides, or phosphatidylcholines. Despite that, lipids with higher melting points as for example triglycerides or monoglycerides were additionally investigated. Formulations consisting of 70% of RG 502 H, 20% oxybutynin hydrochloride and 10% of the lipid were extruded using the standard program at 75 °C (☞ IV, 1). This temperature is above the melting temperature of all lipids.

1.1 Insight into the manufacturing process

Figure 74 displays the influence of the different lipids on the manufacturing process. As can be seen, a large number of these excipients is able to substantially reduce the maximum piston force. The monoglyceride Imwitor 960 P (F) and the acetylated glycerides Dynacet 211 P and Dynacet 212 P turned out to be best performing. For the latter, the maximum piston forces were even smaller than 1 kN. The macroglycerides Gelucire 44/14 and Gelucire 50/13 were also promising candidates

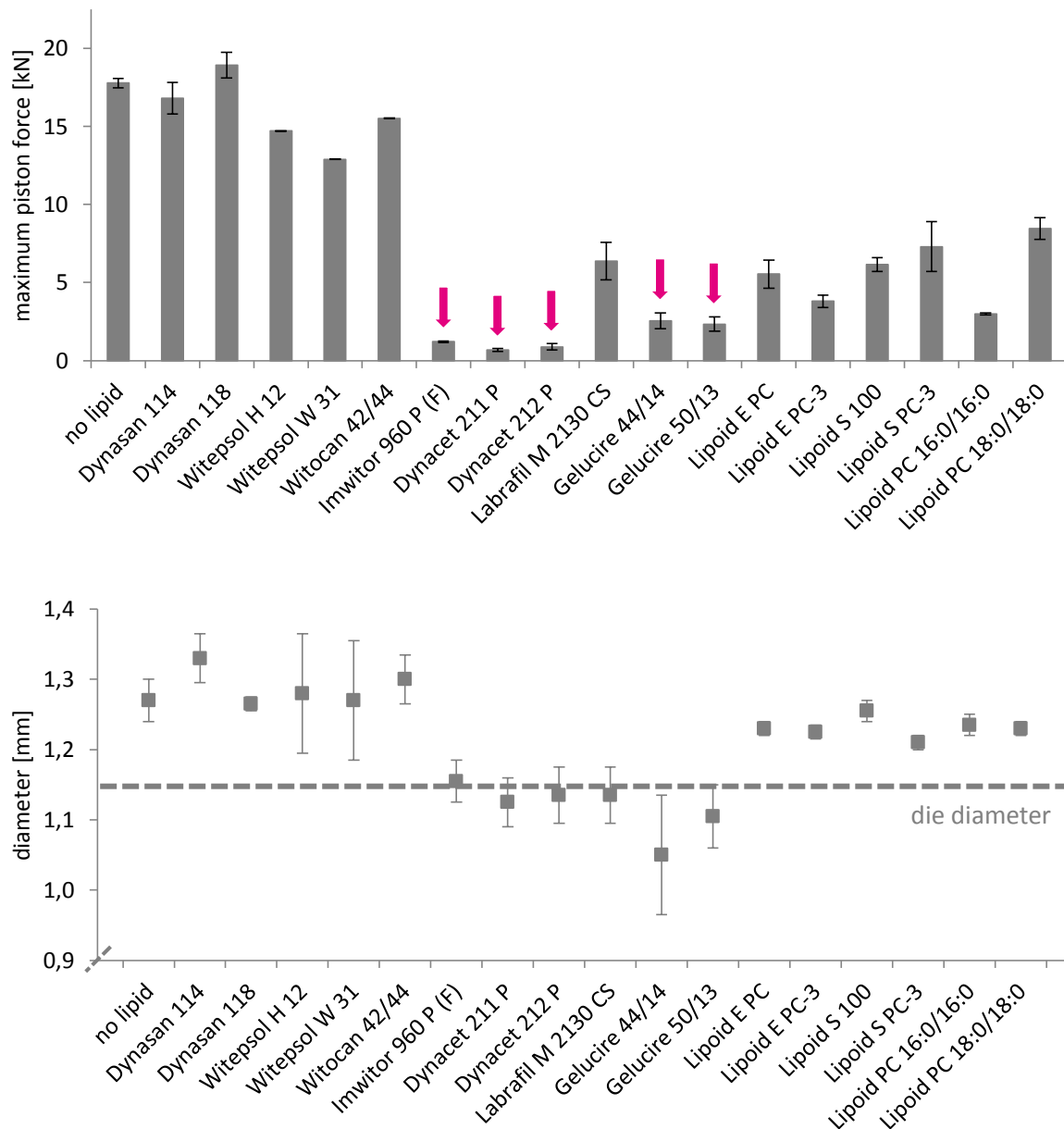


Figure 74 | Influence of the type of lipid. The implants consisted of 70% of RG 502 H, 20% of oxybutynin hydrochloride, and 10% of the lipid. Extrusion was performed using the standard program at 75 °C. For comparison purposes, a formulation with RG 502 H instead of the lipid was investigated as well (mean ± standard deviation, n = 2). **Top:** Influence on the maximum piston force. **Bottom:** Influence on the implant diameter.

with maximum values in between 2 kN and 3 kN. The addition of the phosphatidylcholines Lipoid E PC, Lipoid E PC-3, Lipoid S 100, Lipoid S PC-3, Lipoid PC 16:0/16:0, and Lipoid PC 18:0/18:0 led to values in the range of 3 kN to 9 kN. In contrast, the effect of the hydrogenated cocoglycerides Witepsol H 12, Witepsol W 31, and Witocan 42/44 was much less pronounced with values greater than 12 kN. With regard to the process optimization, the triglycerides Dynasan 114 and Dynasan 118 did not provide any advantages compared to the standard formulation without lipid. This can be related to their hydrophobicity. The excipients are saturated fats derived from myristic acid and stearic acid, respectively. The hydrophobicity of the cocoglycerides which comprise a mixture of tri-, di-, and monoglycerides of saturated C10 to C18 fatty acids is similar. For both groups, phase separation processes were observed during extrusion. As opposed to this, the extrudability of all other lipids was unproblematic. These excipients, namely the monoglycerides, the acetylated glycerides, the macroglycerides, and the phosphatidylcholines are characterized by a lower hydrophobicity which is primarily caused by their amphiphilic nature. Most of the lipids are used as emulsifying agents.

Figure 74 additionally presents the implant diameters. A one-to-one correlation to the maximum piston forces is not possible although higher diameters were monitored in the presence of the most hydrophobic lipids. With the exception of the Gelucire types, the monoglycerides, the acetylated glycerides and the macroglycerides led to an implant thickness in the range of the diameter of the die orifice. The corresponding standard deviations are comparable to the lipid-free formulation. The best results were obtained for the phosphatidylcholines which seem to stabilize the extrusion process such that thinning of the strands is reduced to a minimum (☞ IV, 1.1). The resulting standard deviations are comparatively low with maximum 0.02 mm for Lipoid S 100.

1.2 Determination of mechanical properties

The mechanical properties of the implants were determined using an EZ Test 500 N. As illustrated in Figure 75, the extrudate is fixed in a custom-made holder so that the uncovered part is exactly 0.4 cm. A link chain which is connected to the measuring cell is attached to the middle of the implant. It is raised at a constant speed of 10 mm/min for maximum 60 s until the implant is broken or completely deformed. The tensile strength is calculated as force per unit area whereby the latter refers to the implant cross section.

As demonstrated in Figure 76, extrudates containing one of the Gelucire types are considerably stretched upon applying force. Distances of $0.88 \text{ mm} \pm 0.05 \text{ mm}$ and $1.36 \text{ mm} \pm 0.13 \text{ mm}$ were

measured for Gelucire 44/14 and Gelucire 50/13, respectively. This means that the breaking resistance was maintained for more than 5 s and 8 s. In contrast, all other implants were broken within at most 2 s. Thus, two types of extrudates can be distinguished - sharply breaking ones and highly deforming ones. The latter cannot be administered by means of a hypodermic needle but they might be of interest for the oral surgery or for related application fields.

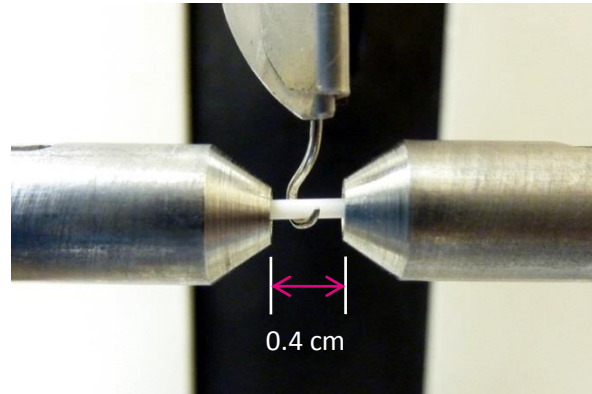


Figure 75 | Determination of the mechanical properties using an EZ test 500 N.

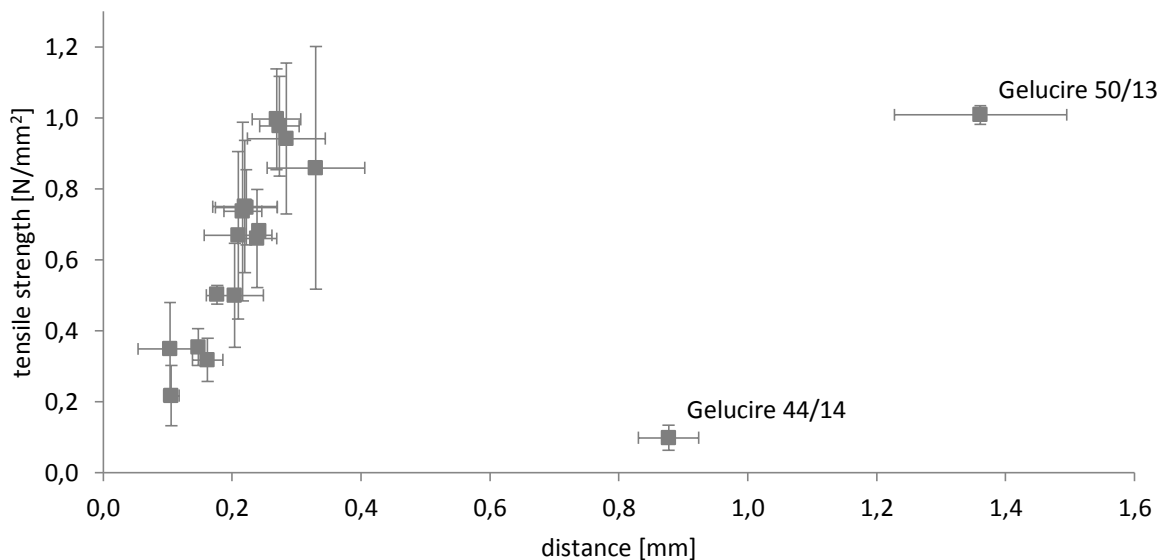


Figure 76 | Tensile strength of implants consisting of 70% of RG 502 H, 20% of oxybutynin hydrochloride, and 10% of the lipid. The cluster on the left side refers to implants containing Dynasan 114, Dynasan 118, Witepsol H 12, Witepsol W 31, Witocan 42/44, Imwitor 960 P (F), Dynacet 211 P, Dynacet 212 P, Labrafil M 2130 CS, Lipoid E PC, Lipoid E PC-3, Lipoid S 100, Lipoid S PC-3, Lipoid PC 16:0/16:0, Lipoid PC 18:0/18:0, or RG 502 H instead of the lipid (mean \pm standard deviation, n = 3).

The corresponding absolute values for the tensile strength are shown in Figure 77. For the lipid-free formulation, a value of $0.94 \text{ N/mm}^2 \pm 0.21 \text{ N/mm}^2$ was determined. Similar results were obtained for implants containing Gelucire 50/13, Lipoid S PC-3 and Lipoid PC 18:0/18:0. The other phosphatidylcholines as well as the triglycerides and Witocan 42/44 led to values in the range of 0.66 N/mm^2 to 0.86 N/mm^2 . For the remaining lipids, a tensile strength of maximum 0.50 N/mm^2 was calculated. It is a debatable point whether such implants can still be injected subcutaneously. The force that has to be applied via the metal plunger is not to be underestimated. However, further investigations are necessary to clarify this point.

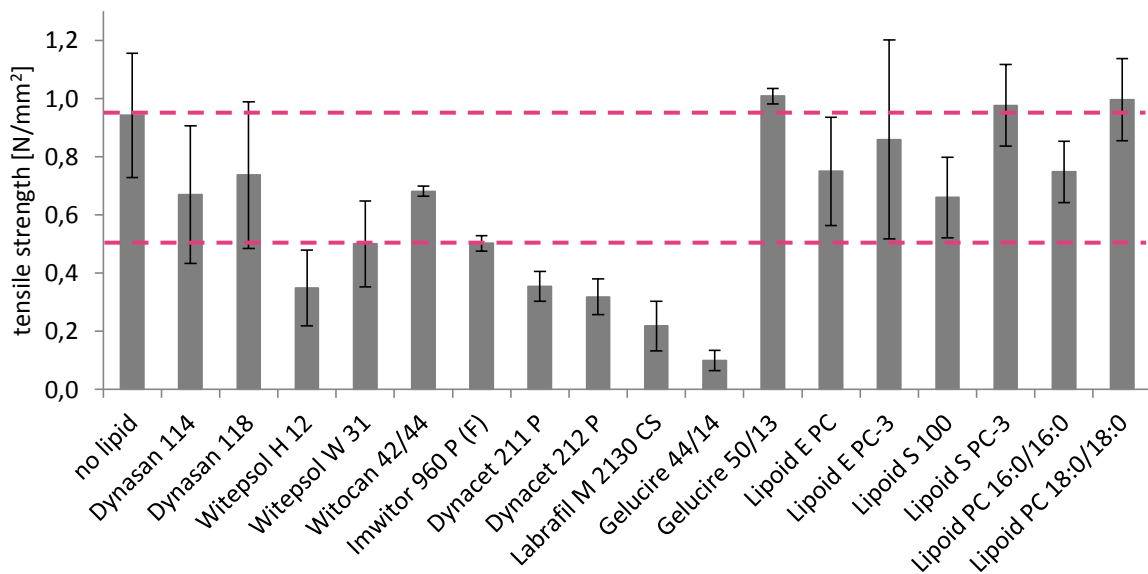


Figure 77 | Tensile strength of implants consisting of 70% of RG 502 H, 20% of oxybutynin hydrochloride, and 10% of the lipid. For comparison purposes, a formulation with RG 502 H instead of the lipid was investigated as well (mean \pm standard deviation, $n = 3$).

1.3 *In vitro* release studies

Besides the investigations on the manufacturing process and the mechanical properties, *in vitro* release tests were carried out in order to assess the influence of the different lipids on the release profiles. First of all, the focus was on the initial release which refers to the first 24 h of incubation in 0.1 M phosphate buffer pH 6.0 at 37°C (➔ Figure 78). For implants containing Imwitor 960 P (F), a burst release of more than 55% was detected. As this excipient is insoluble in water and does not melt during the release tests, it is unlikely that it acts as pore-forming agent, that way facilitating the intrusion of the buffer and the dissolution of the API. Possibly, it affects the extrusion process such that the polymer is hindered to form a dense matrix around the drug particles. So, the latter are

immediately washed out, thereby forming a porous network which accelerates further diffusion of the API molecules. Of course, such release characteristics are unworthy of discussion since they differ greatly from the aim of a prolonged release with constant release rates or a profile that is similar to the one of the standard formulation without lipid. By way of comparison, the latter starts with a release of $0.70\% \pm 0.03\%$. In general, an initial release up to 5% was regarded as acceptable for further studies. According to this, Dynasan 114, Witepsol H 12, Witepsol W 31, Witocan 42/44, Dynacet 211 P, Labrafil M 2130 CS, Lipoid E PC, Lipoid S 100, and Lipoid PC 16:0/16:0 were identified as promising candidates.

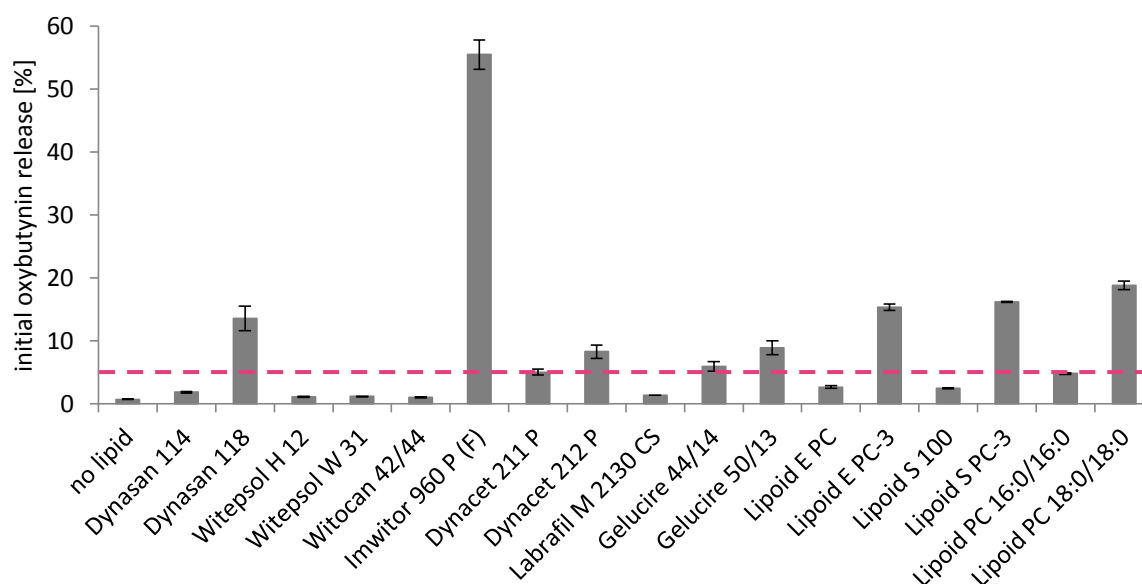


Figure 78 | Initial drug release from implants consisting of 70% of RG 502 H, 20% of oxybutynin hydrochloride, and 10% of the lipid in 0.1 M phosphate buffer pH 6.0 at 37 °C. For comparison purposes, a formulation with RG 502 H instead of the lipid was investigated as well (mean \pm standard deviation, n = 3).

However, the complete release profiles that are depicted in Figure 79 reveal that not every candidate is that auspicious. Dynasan 114, for example, induces a strong increase of the release rates beginning after 1 d of incubation. The same holds true for Witocan 42/44. The other hydrogenated cocoglycerides were shown to have almost no influence on the release profiles. This is advantageous but plays a tangential role since the corresponding maximum piston forces are in the range of the lipid-free formulation. Potential towards a process optimization could not be found. In contrast, both the maximum piston forces and the release profiles were encouraging for the acetylated glycerides. Compared to the standard formulation without lipid, the lag phases were observed to be slightly prolonged, followed by an erosion phase during which the cumulative release increases almost

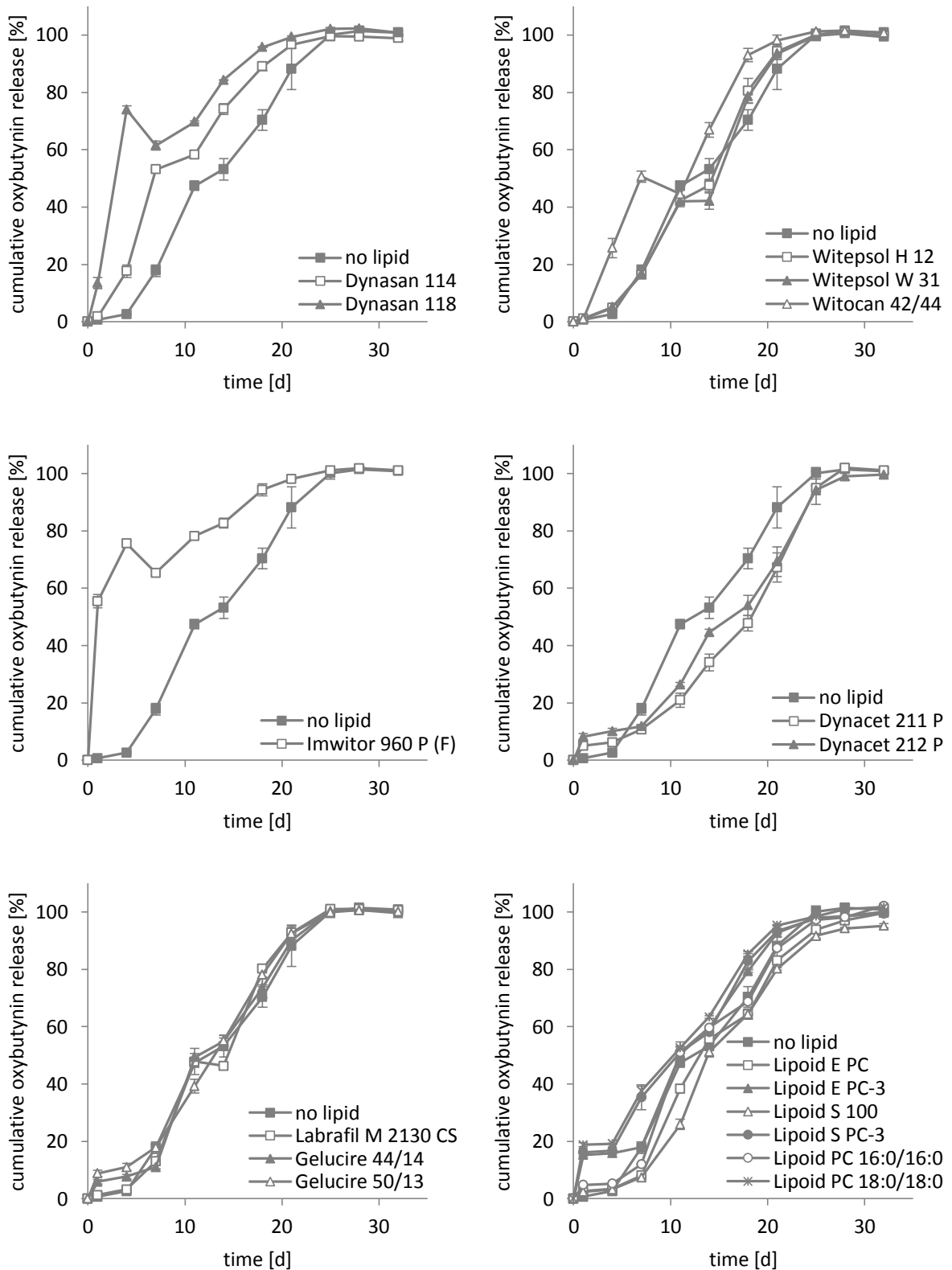


Figure 79 | *In vitro* drug release from implants consisting of 70% of RG 502 H, 20% of oxybutynin hydrochloride, and 10% of the lipid in 0.1 M phosphate buffer pH 6.0 at 37 °C. For comparison purposes, a formulation with RG 502 H instead of the lipid was investigated as well (mean \pm standard deviation, $n = 3$). **Top left:** Dynasan 114 and Dynasan 118. **Top right:** Witepsol H 12, Witepsol W 31, and Witocan 42/44. **Center left:** Imwitor 960 P (F). **Center right:** Dynacet 211 P and Dynacet 212 P. **Bottom left:** Labrafil M 2130 CS, Gelucire 44/14, and Gelucire 50/13. **Bottom right:** Lipoid E PC, Lipoid E PC-3, Lipoid S 100, Lipoid S PC-3, Lipoid PC 16:0/16:0, and Lipoid PC 18:0/18:0.

linearly. Dynacet 211 P was finally chosen for further investigations (☞ VI, 2.1). Interestingly, the addition of macroglycerides did not significantly change the release profiles. Although the initial release was slightly increased for Gelucire 50/13, the lipid was the second candidate that was chosen for more profound studies (☞ VI, 2.2). This is primarily due to its ability of reducing the maximum piston force. Further, the mechanical properties are much better than for Gelucire 44/14. The last group of lipids is represented by the phosphatidylcholines. Depending on their fatty acid composition, the release profiles are more or less affected. Despite that, the shape of all curves resembles the one of the standard formulation. Even though attractive candidates such as Lipoid E PC-3 or Lipoid PC 16:0/16:0 could be identified, they were not used for further investigations. This can be attributed to the fact the lipids turned rancid upon incubation in the release buffer.

INFO BOX #6

How can negative release rates be explained?

This thesis provides a variety of examples for negative release rates. On the one hand, this phenomenon can be ascribed to the release method which works with a 10% buffer exchange instead of a complete one. On the other hand, interactions between the positively charged oxybutynin molecules and the negatively charged polymer chains are responsible (☞ V, 4). As the extent of the ionic interaction increases while the polymer degrades, more and more of the drug molecules are bound to the PLGA degradation products. Hence, less oxybutynin is recovered in the surrounding buffer. The release curve levels off or it even declines.

For unknown APIs, this approach is advisable since possible drug/polymer interactions are detected much faster than in the case of 'traditional' release methods.

1.4 Investigations on the interaction of lipid and polymer

For the sake of completeness, it was investigated whether the interaction between oxybutynin and RG 502 H is influenced by the addition of lipids (☞ V, 4). As usual, 10 mL of a 0.4 mg/mL solution of oxybutynin in 0.1 M phosphate buffer pH 6.0 were incubated together with 14 mg of RG 502 H. 2 mg and 14 mg of a representative lipid were added, respectively. The smaller amount refers to the composition of the implants whereas the higher amount was intended to gain scientific knowledge. All lipids were used as received. Figure 80 summarizes the results. Obviously, Wittepsol H 12,

Dynacet 211 P, and Lipoid S 100 are able to affect the recovery of oxybutynin. At 2 mg, this effect is much less pronounced than at 14 mg. This suggests that the additional interaction with the lipid does not substantially influence the release profiles (➡ VI, 1.3). In general, the interaction with Lipoid S 100 has to be distinguished from the one with Witepsol H 12 or Dynacet 211 P. When 14 mg of the excipients are added, the latter leads to a distinct decrease of the initial recovery. After 24 h of incubation, 66% and 73% of the API are recovered in the presence of the cocoglyceride and the

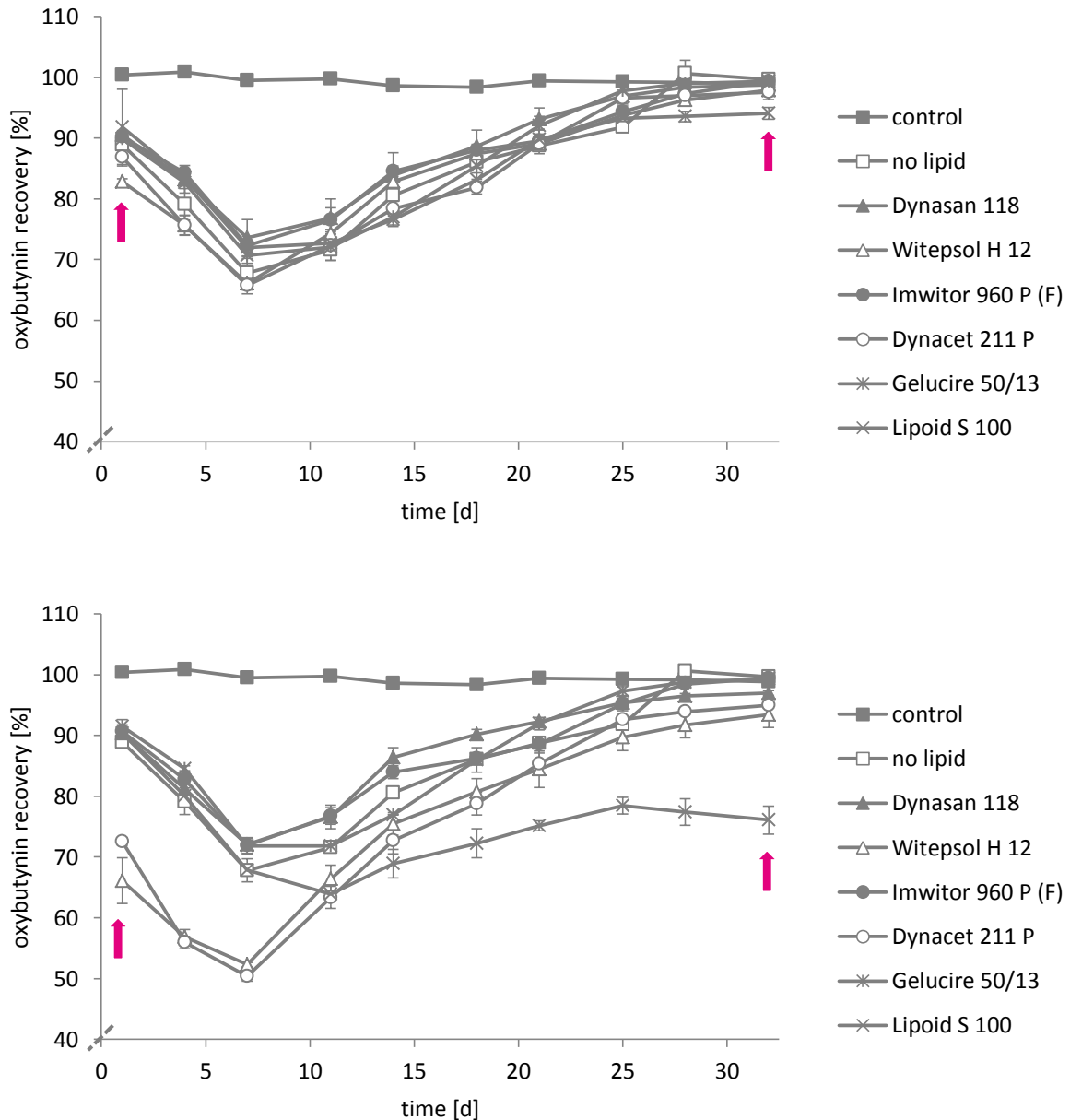


Figure 80 | Recovery of oxybutynin hydrochloride (0.4 mg/mL) in the presence of 14 mg of RG 502 H and a certain amount of the lipid in 0.1 M phosphate buffer pH 6.0 at 37 °C (mean \pm standard deviation, $n = 3$). **Top:** 2 mg of the lipid. **Bottom:** 14 mg of the lipid.

acetylated glyceride. By way of comparison, 89% are found for the lipid-free samples. In the following days, the recovery further decreases. This can be ascribed to the degradation of the polymer which was previously shown to increase the extent of interaction (⊖ V, 4). As soon as the PLGA oligomers and monomers become soluble, the recovery increases again. After 32 d, values of 93% and 95% are obtained for samples containing Witepsol H 12 and Dynacet 211 P, respectively. For the samples without lipid, 100% of oxybutynin can be detected. This indicates that the affinity of the oxybutynin molecules to the polymer and its degradation products is greater than to the lipids. It is assumed that the importance of the drug/lipid interaction decreases with increasing extent of PLGA degradation. Accordingly, at the end of the erosion phase, only 7% and 5% of oxybutynin remain in the drug/lipid interaction. Interestingly, this effect is independent of the state of aggregation of the lipid. Witepsol H 12 melts during incubation at 37 °C while Dynacet 211 P stays solid. Both lipids were observed not to degrade during the recovery studies. In order to ensure that the drug/lipid interaction is an independent process, the incubation tests were repeated without PLGA. That way, pH changes of the release buffer and the influence of the negatively charged degradation products are switched off. Figure 81 reveals that the recovery of oxybutynin clearly decreases in the first 4 d of incubation. After 24 h, values of 79% and 82% are found in the presence of Witepsol H 12 and Dynacet 211 P. As expected, this is more than together with RG 502 H. When the percentage amounts of interacting oxybutynin are calculated, it becomes clear that a lipid/polymer interaction can be excluded. For example, 21% of the API was shown to interact with pure Witepsol H 12. If the polymer is added, this value increases to 34%. The presence of blank polymer particles alone leads to

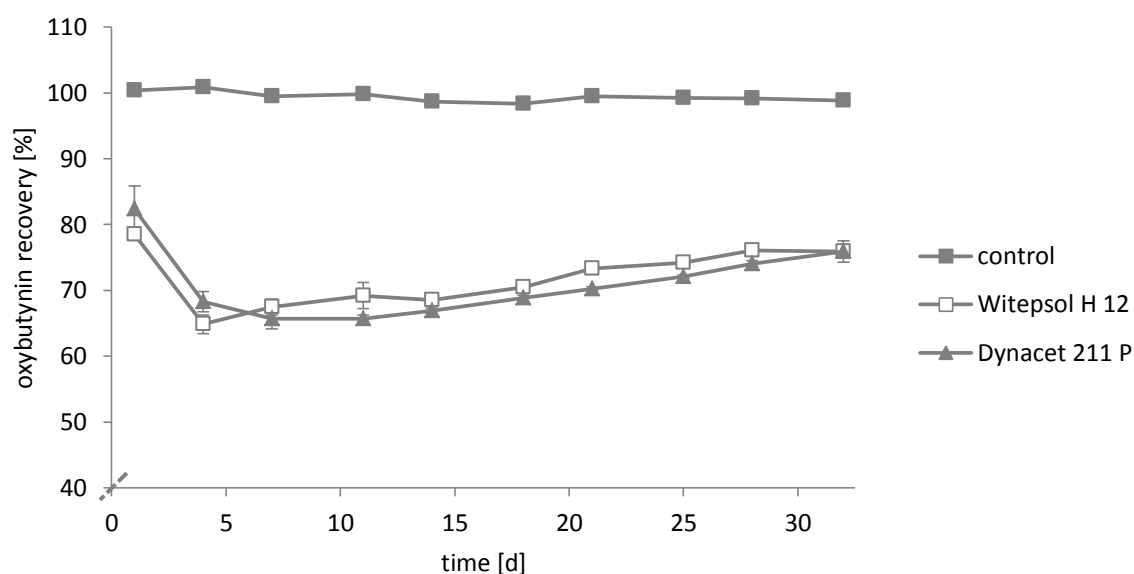


Figure 81 | Recovery of oxybutynin hydrochloride (0.4 mg/mL) in the presence of 14 mg of the lipid in 0.1 M phosphate buffer pH 6.0 at 37 °C (mean ± standard deviation, n = 3).

a value of 11%. Thus, it can be concluded that the drug/polymer interaction and the drug/lipid interaction can simply be added to result in the total interaction. The same holds true for Dynacet 211 P. For both lipids, the recovery slightly increases after the minimum was reached. This is due to the fact that the lipid which is withdrawn during sampling is not replaced. It might be speculated that otherwise the recoveries would remain at a constant value. If this is also considered for the results displayed in Figure 80, the real values after 32 d of incubation in the presence of the lipids and the polymer would be expected to be a little lower.

In contrast, the effect of Lipoid S 100 is completely different. It starts to interfere after 7 d and results in comparatively low recoveries. In the end of the test period, 24% of the oxybutynin molecules are still thought to interact with the lipid. This is presumably attributable to the fact that the phosphatidylcholines turn rancid upon incubation in the release buffer.

2 Homogeneous implants

As already mentioned, some of the lipids that were included in the screening approach were observed to induce phase separation processes during extrusion (⇒ VI, 1.1). The resulting implants were defined as heterogeneous implants, which refers to their core-shell structure. Consequently, the other implants were classified as homogeneous implants. It is important to keep in mind that this term describes the extrudability and the appearance of the extrudates. It does not necessarily imply that the API is homogeneously distributed in the polymer matrix.

2.1 Dynacet 211 P as excipient

In the lipid screening, Dynacet 211 P was identified as promising candidate for the reduction of the extrusion temperature (⇒ VI, 1). Therefore, different amounts were added to the standard formulation such that PLGA was partially replaced. The drug loading with either oxybutynin hydrochloride or oxybutynin base remained unchanged at 20%. For the implant manufacturing, the standard program was used at different temperatures (⇒ IV, 1.1). As the optimized program was specially geared to lipid-free formulations, it was not applied (⇒ VI, 2.2).

2.1.1 Influence on the manufacturing process

Figure 82 gives an overview of the maximum piston forces resulting from the extrusion of different Dynacet 211 P-containing formulations loaded with oxybutynin hydrochloride. As can be seen, the addition of the lipid strongly influences the extrudability. With increasing amount of the acetylated glyceride, the maximum force decreases, that way allowing for the reduction of the process temperature. More precisely, if 5%, 10%, 15%, and 20% of the lipid are used, the temperature can be reduced to 70 °C, 55 °C, 50 °C, and 40 °C, respectively. Compared to the lipid-free formulation, this is a difference up to 35 °C. Interestingly, the shapes of the depicted curves are similar, particularly in the case of higher amounts of Dynacet 211 P. When the temperature is reduced from 75 °C to 65 °C, a slight increase of the maximum piston forces can be observed. This is followed by a strong increase and results in a plateau in between 60 °C and 55 °C. Thereafter, the maximum piston forces increase again until an overload is induced at 25 kN. It is astonishing that these observations can neither be related to the melting behavior of the lipid nor to the softening behavior of PLGA. The glass transition temperature of the latter was found to be lowered in the presence of Dynacet 211 P (⇒ Figure 83). For instance, the addition of 10% of the lipid led to a T_g of $22.7\text{ °C} \pm 0.2\text{ °C}$. This indicates that the

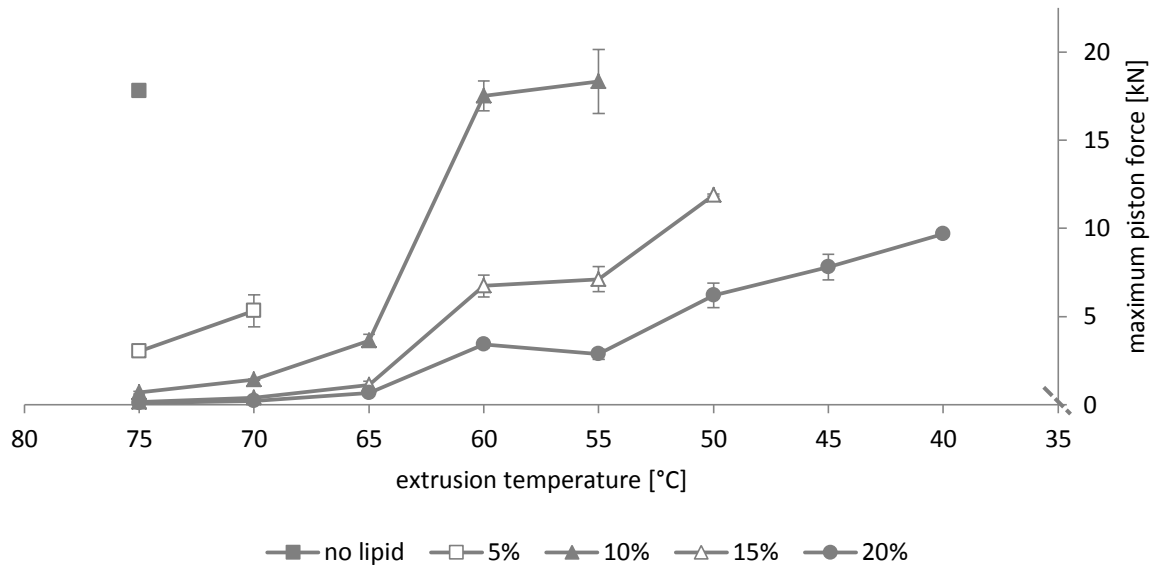


Figure 82 | Influence of the temperature on the maximum piston force during the extrusion (standard program) of formulations consisting of RG 502 H, 20% of oxybutynin hydrochloride, and different fractions of Dynacet 211 P (mean \pm standard deviation, $n = 2$).

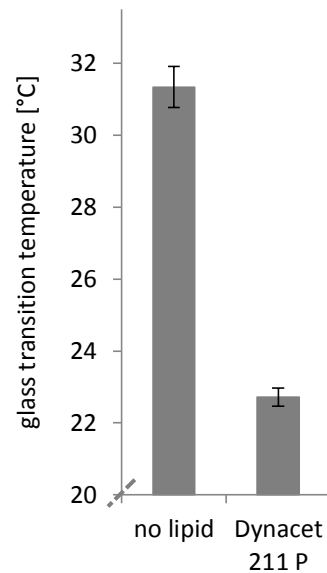


Figure 83 | Glass transition temperature of RG 502 H in implants consisting of 80% of the polymer and 20% of oxybutynin hydrochloride or 70% of the polymer, 20% of oxybutynin hydrochloride, and 10% of Dynacet 211 P (mean \pm standard deviation, $n = 3$).

acetylated glyceride acts as a plasticizer for the polymer. Especially higher concentrations of the lipid were shown to decrease the implant stability. This is due to the fact that the T_g of RG 502 H is then in the range of the room temperature or even below. Thus, it was decided to store all extrudates at 2 °C to 8 °C.

The implant diameters that were obtained for the different formulations are displayed in Figure 84. As soon as only 5% of Dynacet 211 P are added, the diameter decreases considerably. Extrusion at 75 °C leads to a value of $1.17 \text{ mm} \pm 0.03 \text{ mm}$ while $1.27 \pm 0.03 \text{ mm}$ can be detected for the lipid-free formulation. With increasing amount of the lipid, this effect becomes less pronounced. Hence, a thickness of $1.11 \text{ mm} \pm 0.05 \text{ mm}$ is found for the 20% formulation. Similar to the curves of the maximum piston force, the implant diameters increase until a temperature of 60 °C is reached. The following plateau phase is reflected by slightly decreasing values. Thereafter, both the maximum piston forces and the diameters increase again. However, temperatures lower than 50 °C induce decreasing values for the formulation containing 20% of the acetylated glyceride. It might be speculated that this is closely linked to the melting behavior of the lipid which is characterized by a T_m of 41 °C to 47 °C (☞ III, 1.3.4). So, it can be assumed that the excipient remains (at least partially) solid at 45 °C and 40 °C.

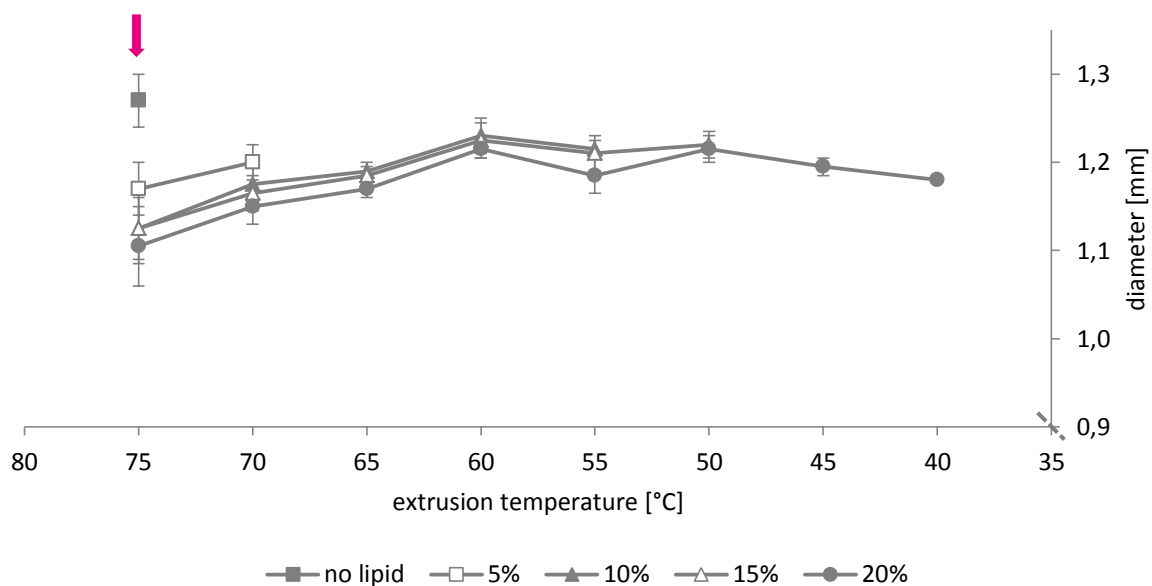


Figure 84 | Influence of the temperature on the implant diameter. The implants consisted of RG 502 H, 20% of oxybutynin hydrochloride, and different fractions of Dynacet 211 P. Extrusion was performed using the standard program (mean \pm standard deviation, $n = 2$).

Next, the fluctuations of the implant diameters were investigated using the example of the 20% formulation again (☞ Figure 85). Apparently, the standard deviations can substantially be optimized

when the extrusion temperature is reduced. At 40 °C, thinning of the strand is completely avoided (⇒ IV, 1.1), thus resulting in a constant thickness of $1.18 \text{ mm} \pm 0.00 \text{ mm}$. For the temperatures in between 65 °C and 45 °C, similar standard deviations were obtained with 0.01 mm and 0.02 mm. In this range, a clear trend cannot be observed which might be ascribed to the low number of experiments. However, if the extrusion at 75 °C is compared to the one at 40 °C, a tremendous difference shows up. In former case, a zigzag curve is monitored for the implant diameters whereas the latter leads to a straight line.

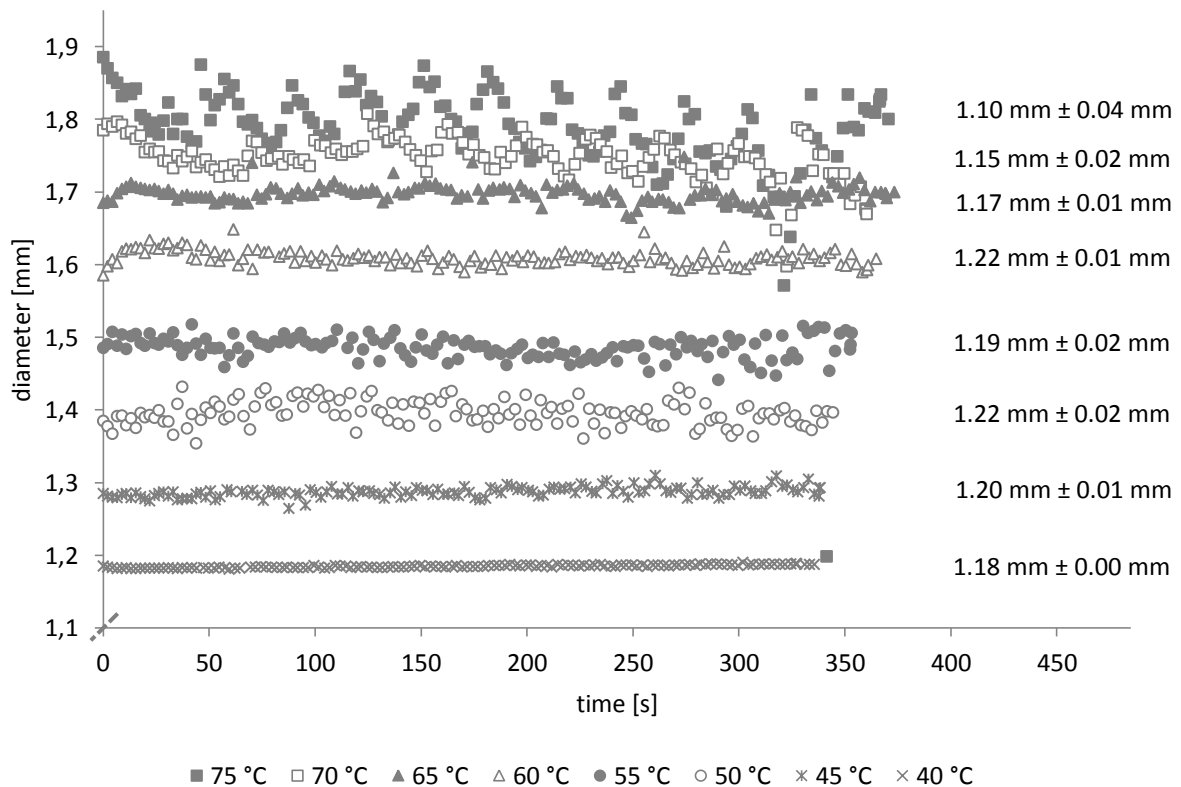


Figure 85 | Influence of the temperature on the implant diameter. The implants consisted of 60% of RG 502 H, 20% of oxybutynin hydrochloride, and 20% of Dynacet 211 P. Extrusion was performed using the standard program (n = 1).

In addition, the influence of Dynacet 211 P on the reduction of the fill levels during the first extrusion phases was studied. The results are presented in Figure 86. If increasing amounts of the lipid are added, thereby replacing the polymer, two effects can be noticed: on the one hand, the fill levels inside the barrel increase during the compression phase, and on the other hand, they decrease during the heating phases. The latter can be explained by the fact that the amount of RG 502 H which is responsible for the loss of volume is reduced (⇒ IV, 1.1). As a consequence, the fill level reduction declines almost linearly from initially 33.0% for the lipid-free formulation to 3.4% for the 20% formulation. For comparison purposes, lipid-based implants without poly(lactide-co-glycolide) were

prepared. Independent of the formulation, the fill levels remained unchanged during the heating phases. In contrast, during the compression phase that is run at room temperature, comparatively high values were obtained for the fill level reduction. This means that the lipids are more compressible than the polymer, providing that both materials are solid. As soon as the lipidic excipient is molten, it cannot be further compressed. Coming back to Figure 86, this is the reason why the fill level reduction increases during the compression phase with increasing amounts of Dynacet 211 P. Regarding the overall fill level reduction which includes the first three extrusion phases, it becomes apparent that the values substantially decrease with increasing fractions of the lipid (data not shown). This indicates that the percentage effect of the polymer is much higher than the one of the lipid.

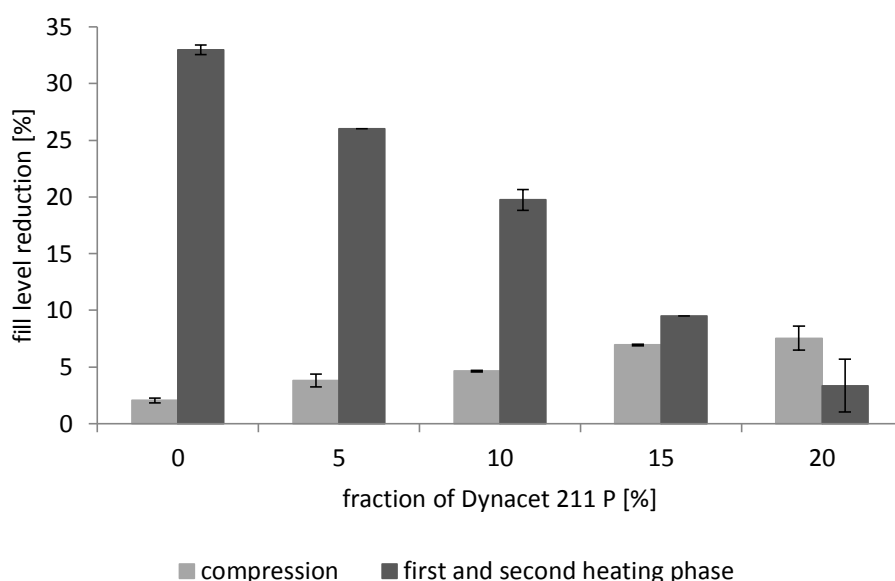


Figure 86 | Influence of the fraction of Dynacet 211 P on the fill level reduction during the extrusion (standard program at 75 °C) of formulations consisting of RG 502 H, 20% of oxybutynin hydrochloride, and different fractions of the lipid (mean \pm standard deviation, $n = 2$).

Aside from the hydrochloride-containing implants, base-containing implants were additionally prepared and analyzed. The minimum extrusion temperature was only determined for the formulation with 10% of the acetylated glyceride and turned out to be 55 °C. This is the same value that was already obtained for the hydrochloride. Concerning the optimization of the extrusion process towards lower temperatures, the base proved to be no longer superior to the salt (considerable differences were found in the absence of the lipid) (\Rightarrow V, 1.1). The corresponding maximum piston force was determined to be $11 \text{ kN} \pm 1 \text{ kN}$, and the implant diameter was $1.28 \text{ mm} \pm 0.05 \text{ mm}$. The standard deviation of the latter points to phase separation processes which

were confirmed by the results of the homogeneity tests. As can be seen in Figure 87, the recovery of the base strongly fluctuates around the 100% value. Implants with 93.2% of the intended drug loading as well as implants with 114.8% originate from one and the same batch. In contrast, the recovery of the hydrochloride is very good with $100.3\% \pm 0.6\%$. It can be assumed that this API is homogeneously distributed in the polymer matrix.

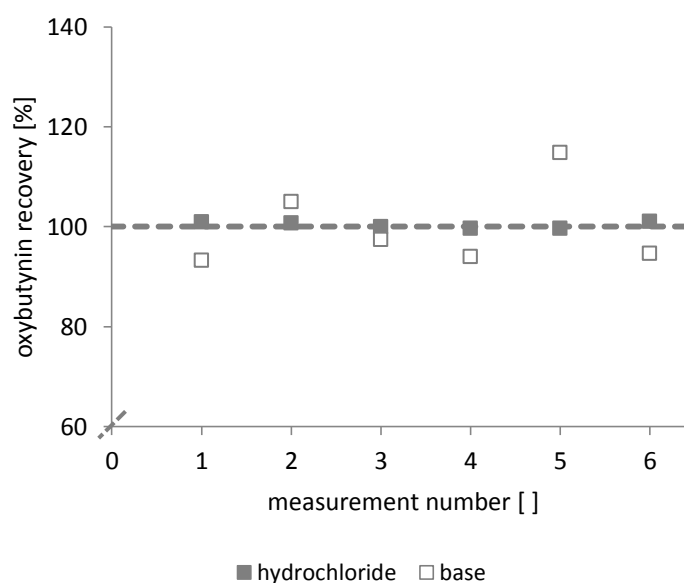


Figure 87 | Homogeneity of implants consisting of 70% of RG 502 H, 20% of oxybutynin hydrochloride or oxybutynin base, and 10% of Dynacet 211 P. Extrusion was performed using the standard program at 55 °C (n = 6).

2.1.2 *In vitro* release studies

In order to get further information on the potential use of Dynacet 211 P as plasticizer for the extrusion of PLGA-based implants, the *in vitro* release was investigated for the 10% formulations. As demonstrated in Figure 88, the release profiles for the hydrochloride are considerably affected if the temperature is reduced. The initial release increases drastically from $5.0\% \pm 0.4\%$ at 75 °C to $68.8\% \pm 0.6\%$ at 55 °C. Of course, such high values have to be avoided since they do not agree with the expectations on a sustained drug delivery system. Only the curve of the 70 °C extrusion is almost congruent with the one of the 75 °C extrusion. However, a distinct process optimization cannot be achieved that way. When the base is embedded instead of the salt, extrusion at 55 °C leads to a suppression of the initial release by about 44% to $25.1\% \pm 1.0\%$. This indicates that the base is at least partially retained by the lipid, presumably by hydrophobic interactions. It is not unlikely that the API and the acetylated glyceride form kind of a solid solution. Despite that, this effect is not

pronounced enough to result in a desirable release. Furthermore, the time for the complete depletion of the depot is reached earlier than in the case of the hydrochloride. For these reasons, alternative manufacturing strategies were developed (⇨ VI, 2.1.4).

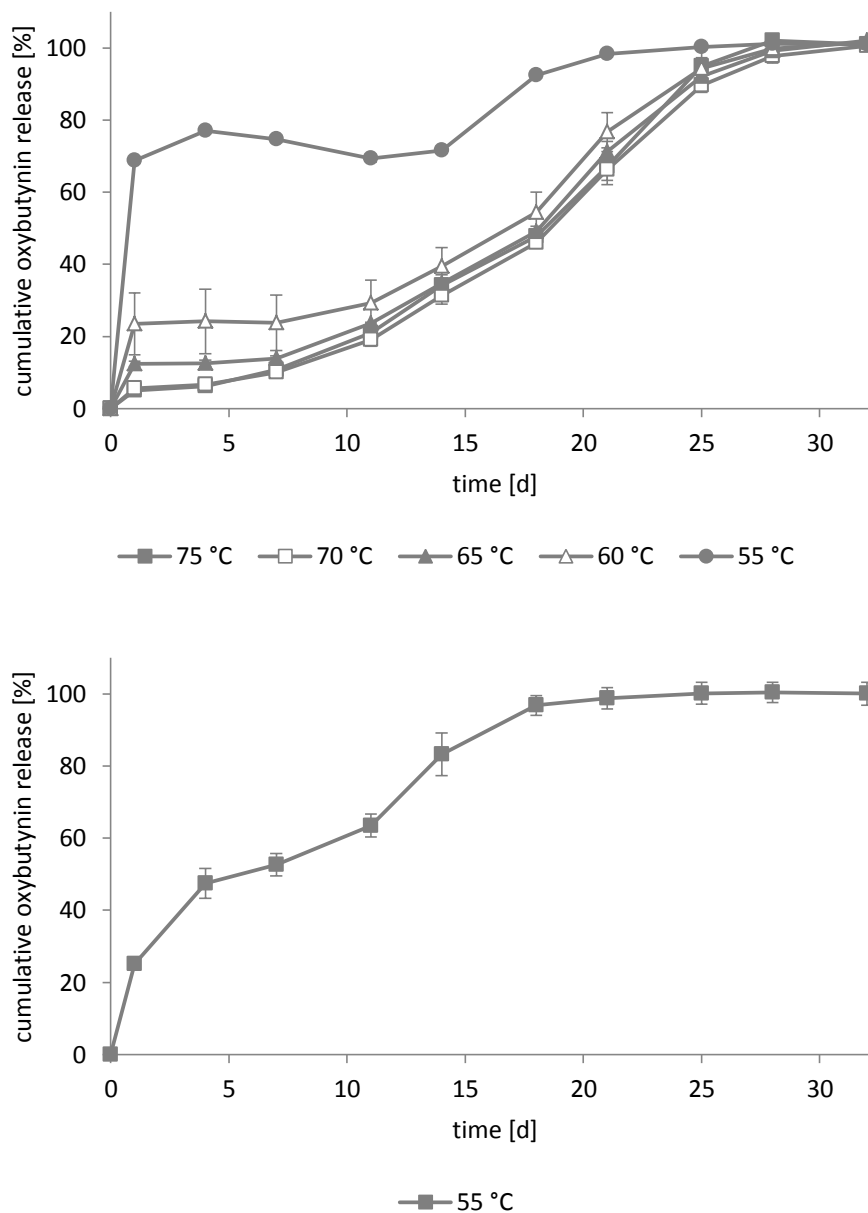


Figure 88 | *In vitro* drug release from implants consisting of 70% of RG 502 H, 20% of oxybutynin, and 10% of Dynacet 211 P in 0.1 M phosphate buffer pH 6.0 at 37 °C. Influence of the extrusion temperature (mean \pm standard deviation, $n = 3$). **Top:** Oxybutynin hydrochloride. **Bottom:** Oxybutynin base.

2.1.3 Studies on the release mechanism

Studies on the release mechanism were carried out with the intention to get deeper insight into the single release profiles. PLGA-based implants with 20% of oxybutynin hydrochloride and 10% of Dynacet 211 P manufactured at 75 °C and 55 °C were focused since their initial releases differed widely (⇒ VI, 2.1.2). Additionally, comparable base-containing implants extruded at 55 °C were investigated because of their API-retaining ability. The shift in the pH values during the incubation in 0.1 M phosphate buffer pH 6.0 at 37 °C is displayed in Figure 89. Independent of the drug substance and the process temperature, all curves are approximately equal. After 21 d, a minimum pH of 4.6 to 4.7 is reached, which can be ascribed to the degradation of the polymer. In an independent experiment, the lipid was shown not to have an effect on the pH. Interestingly, the base-catalyzed acceleration of the chain scission process (⇒ V, 1.3) disappears as soon as Dynacet 211 P is added. This supports the hypothesis of hydrophobic interactions between the lipid and the base. It is important not to confuse such interactions with the ones that were previously described, and according to which the recovery of dissolved oxybutynin was found to be reduced in the presence of the acetylated glyceride (⇒ VI, 1.4).

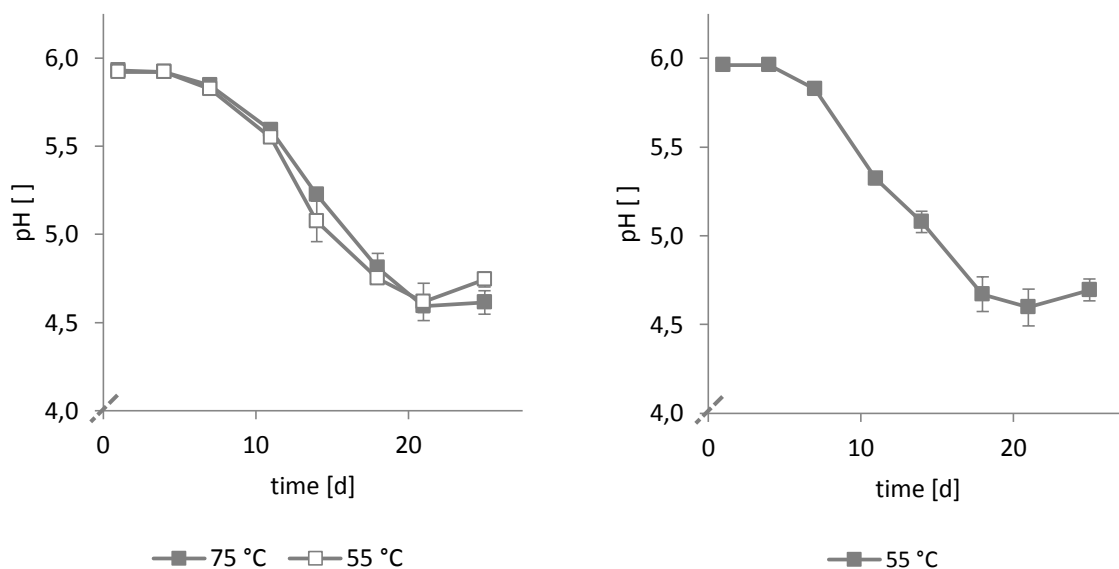


Figure 89 | pH values during the drug release from implants consisting of 70% of RG 502 H, 20% of oxybutynin, and 10% of Dynacet 211 P in 0.1 M phosphate buffer pH 6.0 at 37 °C. Influence of the extrusion temperature (mean \pm standard deviation, n = 3). **Left:** Oxybutynin hydrochloride. **Right:** Oxybutynin base.

The investigations on the mass loss were helpful to find an explanation for the comparatively high initial release rates of the hydrochloride-containing implants that were extruded at temperatures below 70 °C (⇒ Figure 90). For the extrudates manufactured at 55 °C, a burst release of about 69%

and a mass loss of more than 23% were detected. Converted to the absolute masses, this means that 2.75 mg of the API are released within the first 24 h while 4.70 mg of the total implant mass are lost during the same time. As opposed to this, values of 0.20 mg and 0.84 mg were obtained for implants extruded at 75 °C. Since Dynacet 211 P was shown not to degrade during the incubation time (this is confirmed by mass losses of about 90% after 32 d), the differences between both extrusion temperatures can be ascribed only to the polymer. Accordingly, 1.95 mg and 0.64 mg of RG 502 H are released together with the drug substance. As the pH values are not affected, it can be assumed that mainly larger insoluble PLGA particles are set free in the former case. Thus, it can be concluded that extrusion temperatures of at least 70 °C are necessary to completely encapsulate the drug molecules in a dense coherent matrix. It is suggested that otherwise the API and the matrix molecules are more or less loosely bound so that the disintegration of the implant is facilitated. Despite that, the following release is controlled by the degradation of the polymer. Beginning after 4 d of incubation, the mass loss profiles resemble each other, independent of the manufacturing temperature. If the base is incorporated instead of the hydrochloride, the initial mass loss is much smaller with about 5%. This is in good correlation with the release data. Hence, the mass loss within the first four days is entirely attributable to the diffusional release of the base. Thereafter, the polymer and its degradation products are released as well. When both mass loss curves - the one of the hydrochloride and the one of the base - are corrected for the API release, two equivalent curves are obtained (data not shown). This proves once more that the base-catalyzed acceleration of the

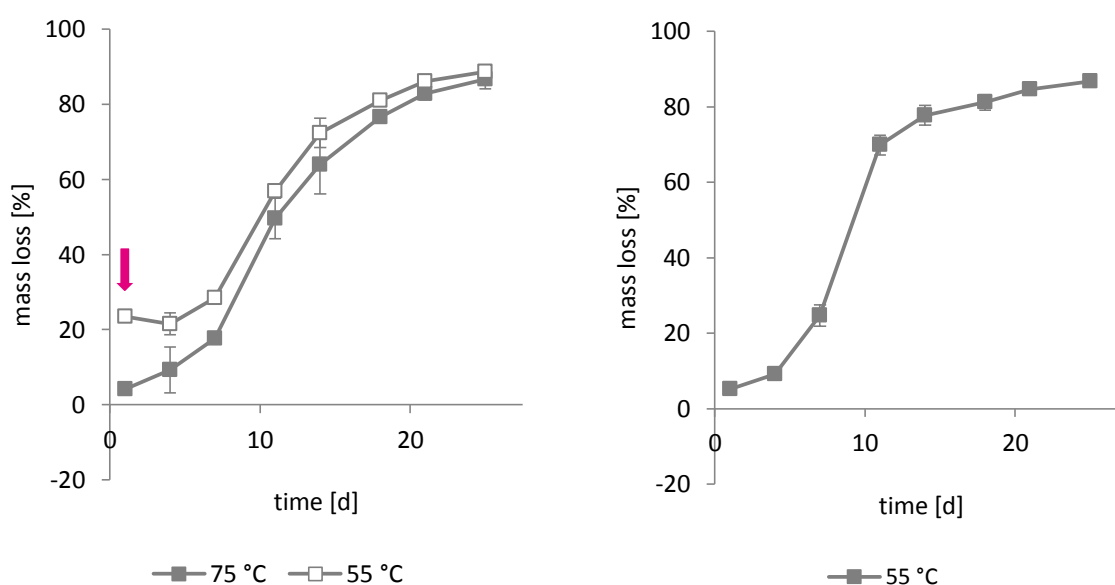


Figure 90 | Mass loss during the drug release from implants consisting of 70% of RG 502 H, 20% of oxybutynin, and 10% of Dynacet 211 P in 0.1 M phosphate buffer pH 6.0 at 37 °C. Influence of the extrusion temperature (mean \pm standard deviation, n = 3). **Left:** Oxybutynin hydrochloride. **Right:** Oxybutynin base.

polymer degradation (☞ V, 1.3) is suppressed in the presence of the acetylated glyceride. For the release of other bases, this principle might also be relevant. The addition of the lipid simply allows for decelerating the degradation of the polymer, that way possibly elongating the release period.

The previous findings concerning the initial mass loss were confirmed by scanning electron microscopy. Figure 91 shows the surface morphology of implants consisting of 70% of RG 502 H, 20% of oxybutynin hydrochloride, and 10% of Dynacet 211 P that were extruded at 75 °C and 55 °C. Expectably, the surface is much smoother in the former case. Even the cavities that can be seen are characterized by a closed surface. In contrast, implants that were manufactured at 55 °C have a wrinkled, platelet-shaped surface with larger cavities. This is in good agreement with the suggestion that the matrix excipients are rather loosely bound than fused together. In addition, the densities of the implants were calculated. $1.32 \text{ mg/mm}^3 \pm 0.02 \text{ mg/mm}^3$ and $1.14 \text{ mg/mm}^3 \pm 0.04 \text{ mg/mm}^3$ were obtained for 75 °C and 55 °C, respectively. This supports once more the aforementioned hypothesis.

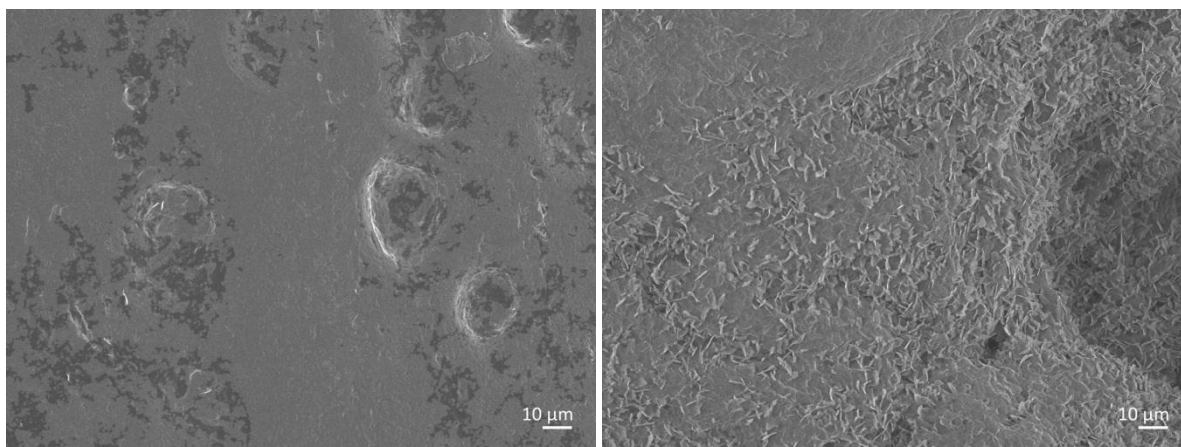


Figure 91 | Scanning electron microscopy. Surface morphology of implants consisting of 70% of RG 502 H, 20% of oxybutynin hydrochloride, and 10% of Dynacet 211 P. **Left:** Extruded at 75 °C. **Right:** Extruded at 55 °C.

2.1.4 Alternative manufacturing strategies

For the hydrochloride-containing 10% formulation, alternative manufacturing strategies were developed with the aim of suppressing the burst release and - at the same time - reducing the extrusion temperature to a minimum. In the first three attempts, the API and the polymer were subjected to one of the following pretreatments:

✓ **Heptane dispersion**

Oxybutynin hydrochloride and RG 502 H were dispersed in heptane. The solvent was allowed to evaporate, and the resulting particles were dried to constant weight.

✓ **Solvent casting**

Oxybutynin hydrochloride and RG 502 H were dissolved in a suitable solvent, for example acetonitrile. Aliquots of 50 μL were pipetted onto a synthetic foil. The solvent was allowed to evaporate, and the resulting platelets were dried to constant weight (➡ Figure 92).

✓ **Compression**

Oxybutynin hydrochloride and RG 502 H were ground using the cryogenic mill. The mixture was then compressed to a pellet (➡ Figure 92).



Figure 92 | Pretreatment of RG 502 H and oxybutynin hydrochloride. **Left:** Platelets produced by solvent casting. **Right:** Pellet produced by compression.

Dynacet 211 P was then added, and the formulations were subjected to cryogenic grinding.

In contrast, the lipid was added from the beginning for the other two attempts:

✓ **Threefold grinding**

Oxybutynin hydrochloride, RG 502 H, and Dynacet 211 P were ground three times in a row using the cryogenic mill.

✓ **Double extrusion**

Oxybutynin hydrochloride, RG 502 H, and Dynacet 211 P were ground and extruded twice in a row at the same conditions.

All formulations were extruded with the standard program at a temperature of 55 °C. The corresponding piston forces are displayed in Figure 93. As can be seen, the pretreatment method greatly influences the curves. In the case of implants that were extruded twice, the piston forces during the second manufacturing cycle were shown to be higher than during the first one. Formulations that were ground three times resulted in values comparable to the formulation without pretreatment. When ‘compression’ or ‘heptane dispersion’ were applied, a reduction of the piston forces could be observed. Values in the range of 7 kN to 8 kN were obtained. ‘Solvent casting’ turned out to be the best-performing method with a maximum smaller than 3 kN. Regarding further optimization of the process towards lower extrusion temperatures, this is promising. However, the results of the *in vitro* release tests have to be taken into account before a decision is made. Concerning the implant diameters, all pretreatment methods were found to have no negative impact. The values ranged in between 1.20 mm and 1.24 mm with a standard deviation of maximum 0.02 mm. A correlation to the piston forces is not given.

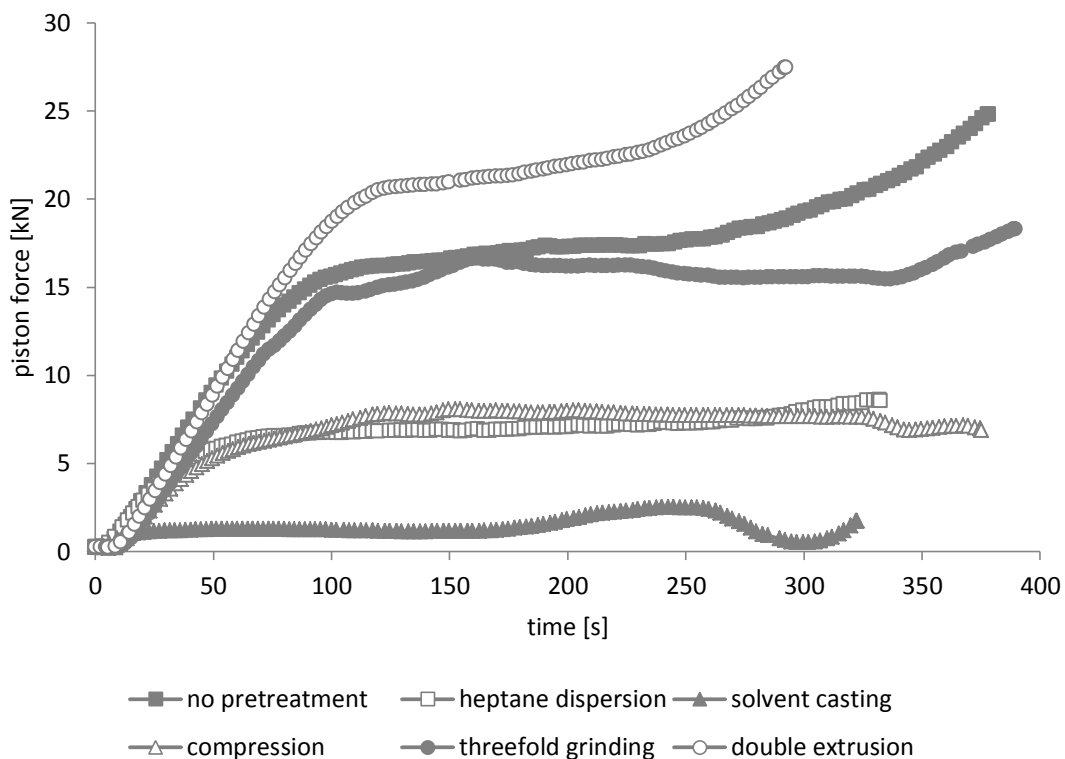


Figure 93 | Influence of the pretreatment method on the piston force during the extrusion (standard program at 55 °C) of formulations consisting of 70% of RG 502 H, 20% of oxybutynin hydrochloride, and 10% of Dynacet 211 P.

The release profiles that are depicted in Figure 94 reveal a strong influence of the pretreatment method. Especially the initial bursts are affected. As demonstrated, the ‘heptane dispersion’ is not suitable to optimize the release characteristics. The corresponding curve resembles the one of the implants that were manufactured without pretreatment. This is not astonishing since heptane is a non-solvent for both the drug substance and the polymer. A tight physical linkage of the particles cannot be achieved. In contrast, all other methods were shown to substantially reduce the burst release. For ‘threefold grinding’ and ‘double extrusion’, values around 35% were measured. ‘Compression’ leads to a value of approximately 21%, and ‘solvent casting’ was found to be the most efficient method with an initial release of less than 5%. In the latter case, it can be assumed that the drug molecules are surrounded by a dense matrix of poly(lactide-co-glycolide) before the lipid is added. Thus, the encapsulation step that is commonly part of the extrusion process is anticipated. The following drug release is primarily controlled by the degradation and erosion behavior of the polymer. After 7 d of incubation, a considerable increase of the release rates was registered. This does not occur for implants that were produced at extrusion temperatures of minimum 70 °C (⇒ VI, 2.1.2). Despite that, the approach was promising enough to be further investigated.

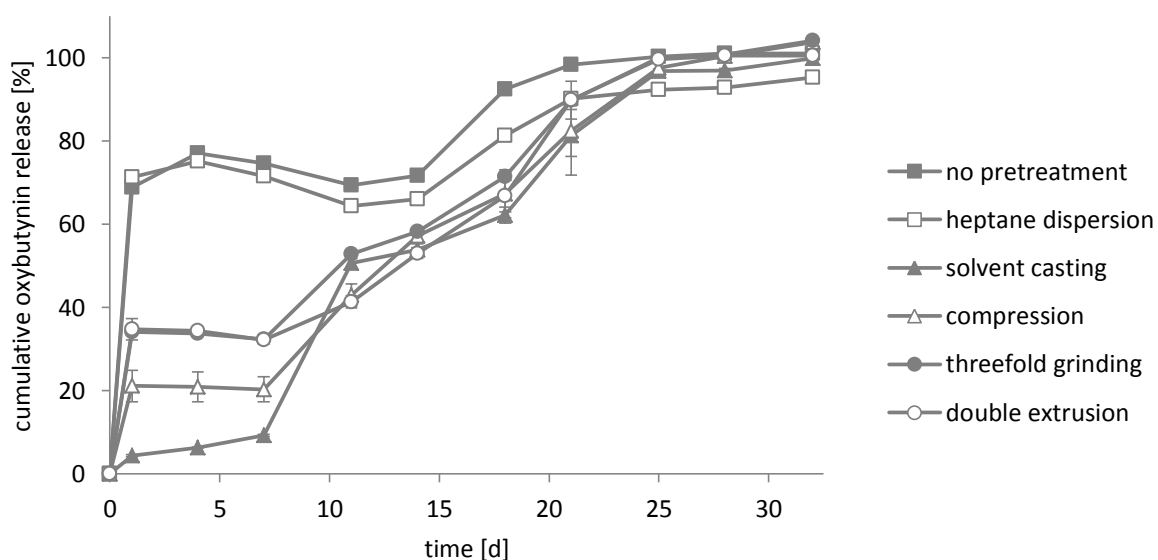


Figure 94 | *In vitro* drug release from implants consisting of 70% of RG 502 H, 20% of oxybutynin hydrochloride, and 10% of Dynacet 211 P in 0.1 M phosphate buffer pH 6.0 at 37 °C. Extrusion was performed using the standard program at 55 °C. Influence of the pretreatment method (mean ± standard deviation, n = 3).

At first, it was studied whether the process temperature could further be reduced. Extrusion at 40 °C was shown to be unproblematic with a maximum piston force of less than 6 kN. Lower temperatures were not tested since the Rheograph 25 E II requires at least 5 °C more than the room temperature

for a precise control. However, it is easily conceivable that extrusion at room temperature can be realized for the future. As it is probable that the residual solvents are responsible for this behavior, their contents were determined by gas chromatography. Up to that point, acetonitrile was the only solvent that was used. The results are displayed in Figure 95. The percentage values refer to the implant mass. Obviously, extrusion at 55 °C and 50 °C leads to an acetonitrile content of about 1.0% while temperatures of 45 °C and 40 °C result in values smaller than 0.8%. This is not logical since higher temperatures were expected to decrease the solvent content to a greater extent. With a view to the production of the single batches, this phenomenon can be explained. The 55 °C batch and the 50 °C batch were prepared from one and the same formulation. The same holds true for the 45 °C batch and the 40 °C batch. This indicates that the acetonitrile content depends rather on the pretreatment method than on the process temperature. For future productions, it is absolutely necessary to enhance the reproducibility of the platelet manufacturing, most probably by changing the drying technique. For comparison purposes, formulations without Dynacet 211 P but with the same drug to polymer ratio were investigated. The maximum piston forces were relatively high with more than 5 kN for the 55 °C extrusion and approximately 23 kN for the 50 °C extrusion. Production temperatures of 45 °C or below were not possible. This indicates that the residual acetonitrile content and the presence of the lipid are unavoidable for extrusion temperatures as low as 40 °C. Both excipients are assumed to act synergistically as a plasticizer for the polymer. Regarding this

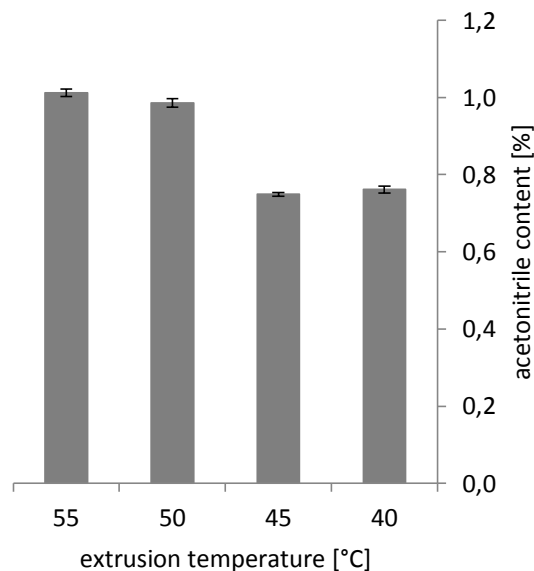


Figure 95 | Acetonitrile content of implants consisting of 70% of RG 502 H, 20% of oxybutynin hydrochloride, and 10% of Dynacet 211 P. Extrusion was performed using the standard program at different temperatures (mean \pm standard deviation, $n = 3$).

topic, interesting studies were undertaken by Mauriac and Marion who applied for a patent on the use of ethanol as a plasticizer for PLGA. According to their invention, pure polymer particles are ground and mixed with ethanol. Heating is applied in order to obtain a viscous gel which is then dried and milled to a fine powder. Optionally, the product is mixed with additional PLGA. In a last step, the material is extruded and ground again. It is finally used for the manufacturing of implants containing thermosensitive APIs. Extrusion temperatures ranging from 40 °C to 70 °C can be realized that way [264]. The approach that was developed in this thesis provides an alternative but demands further optimization. If possible, the solvent should be replaced by a less toxic one. Aside from acetonitrile, acetone, dimethyl sulfoxide, and ethyl acetate have already been tested. According to the ICH guideline for residual solvents, these liquids belong to the 'solvents with low toxic potential' for which amounts of 50 mg per day are recognized as acceptable [265]. From a technical point of view, acetone was the most promising candidate since its vapor pressure is much higher than for the other solvents. In spite of that, none of the liquids was superior to acetonitrile which is most probably attributable to the drying technique that was applied.

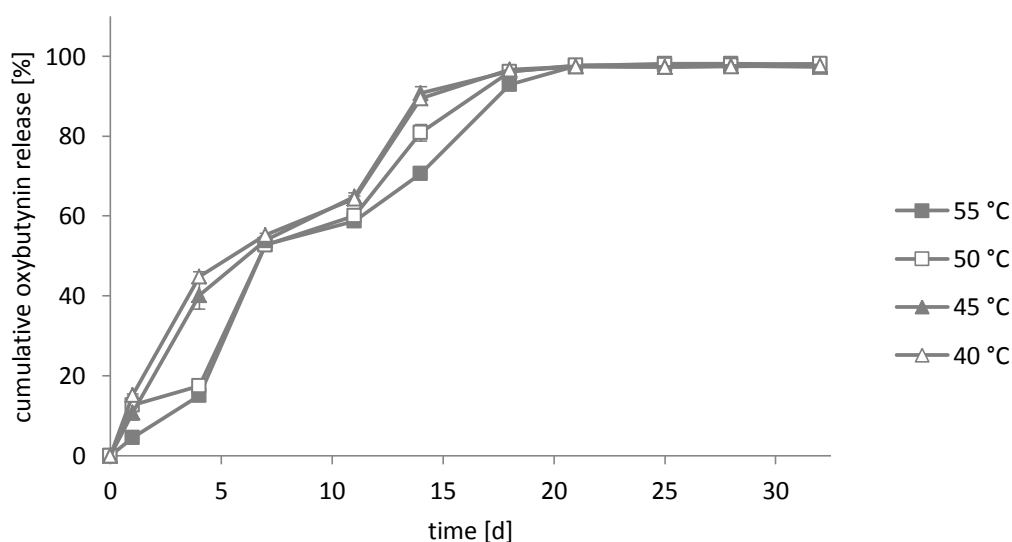


Figure 96 | *In vitro* drug release from implants consisting of 70% of RG 502 H, 20% of oxybutynin hydrochloride, and 10% of Dynacet 211 P in 0.1 M phosphate buffer pH 6.0 at 37 °C. Extrusion was performed using the standard program. Influence of the temperature (mean \pm standard deviation, $n = 3$).

The *in vitro* release profiles referring to the acetonitrile-containing implants are shown in Figure 96. With the previous results in mind, the curves can be distinguished in two groups. The first one is connected to a residual solvent content of about 1.0% and results in kind of a lag phase that ends after 4 d of incubation. The second one refers to a residual solvent content of approximately 0.8%

and leads to an elimination of the lag phase. Assuming that the process temperature plays no role, it might be speculated that the duration of the lag phase is mainly controlled by the acetonitrile content. If more of the solvent is incorporated, the lag phase seems to be elongated. This might be due to a delay in the water uptake. However, further investigations are necessary to clarify this issue.

In summary, all of the investigated pretreatment methods have to be approached with skepticism. For future applications, the 'solvent casting' turned out to be the most promising one. In the best case, the desired release profile can be realized by adjusting the residual solvent content. Extrusion temperatures as low as 40 °C can be reached.

2.2 Gelucire 50/13 as excipient

Gelucire 50/13 was the second excipient that was identified in the lipid screening (☞ VI, 1). Due to comparatively low maximum piston forces and acceptable initial release rates, it was thought to have the potential for the optimization of the extrusion process towards lower temperatures. Thus, analogous to the experiments with Dynacet 211 P, the polymer was partially replaced by the macroglyceride. The drug loading with oxybutynin hydrochloride or oxybutynin base remained unchanged at 20%. All extrusions were run with the standard program at different temperatures (☞ IV, 1.1).

2.2.1 Influence on the manufacturing process

Figure 97 gives information on the maximum piston forces resulting from the extrusion of hydrochloride-containing formulations with up to 20% of Gelucire 50/13. If possible, the process temperatures were revised downwards. That way, minimum temperatures of 70 °C, 65 °C, 60 °C, and 55 °C were obtained for the 5%, 10%, 15%, and 20% formulation. With increasing amounts of the macroglyceride, the temperature range in which relatively low maximum piston forces are attained is elongated. Thereafter, a strong increase can be observed which rapidly induces an overload (☞ IV, 1.1). Interestingly, this behavior can neither be correlated to the drop point of the lipid nor to the glass transition temperature of the polymer.

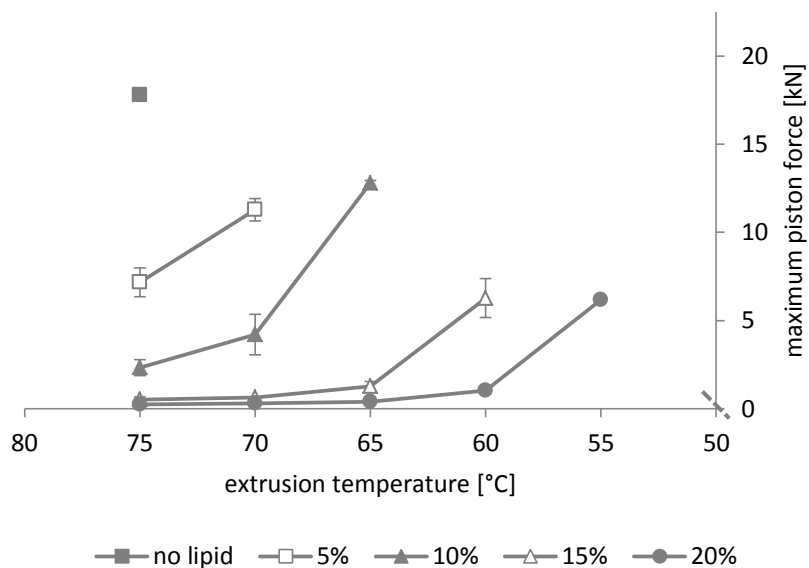


Figure 97 | Influence of the temperature on the maximum piston force during the extrusion (standard program) of formulations consisting of RG 502 H, 20% of oxybutynin hydrochloride, and different fractions of Gelucire 50/13 (mean \pm standard deviation, n = 2).

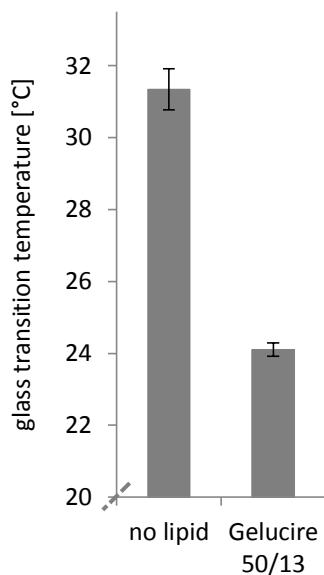


Figure 98 | Glass transition temperature of RG 502 H in implants consisting of 80% of the polymer and 20% of oxybutynin hydrochloride or 70% of the polymer, 20% of oxybutynin hydrochloride, and 10% of Gelucire 50/13 (mean \pm standard deviation, n = 3).

In the following, implants consisting of 70% of RG 502 H, 20% of oxybutynin hydrochloride, and 10% of Gelucire 50/13 were subjected to DSC measurements. As depicted in Figure 98, the presence of the lipid considerably decreases the glass transition temperature of the polymer. $24.1\text{ }^{\circ}\text{C} \pm 0.2\text{ }^{\circ}\text{C}$ were measured whereas $31.3\text{ }^{\circ}\text{C} \pm 0.6\text{ }^{\circ}\text{C}$ were detected for the lipid-free formulation. Apparently, the macroglyceride acts as a plasticizer for RG 502 H. This is probably the reason why the implants were less stable at room temperature. Especially at higher fractions of the lipid, they became sticky and could be deformed easily. This was also confirmed by the determination of the mechanical properties (↪ VI, 1.2). As a consequence, it was decided to store the extrudates at $2\text{ }^{\circ}\text{C}$ to $8\text{ }^{\circ}\text{C}$.

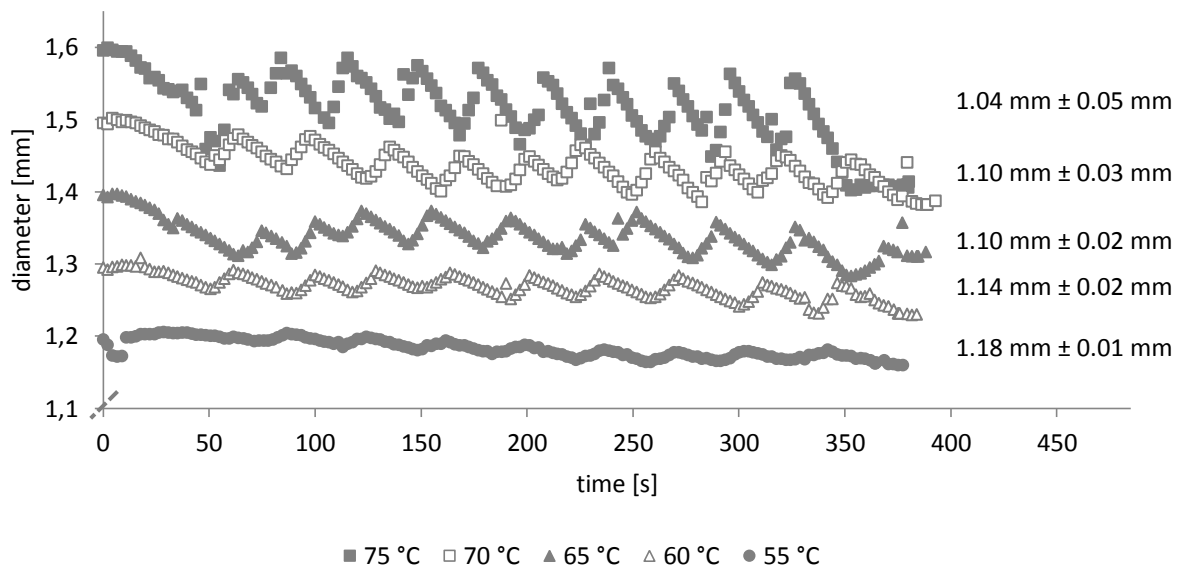


Figure 99 | Influence of the temperature on the implant diameter. The implants consisted of 70% of RG 502 H, 20% of oxybutynin hydrochloride, and 20% of Gelucire 50/13. Extrusion was performed using the standard program.

Similar to the maximum piston forces, the implant diameters were observed to increase with decreasing process temperature. The results for the 20% formulation are exemplarily displayed in Figure 99. The increase is neither linear nor directly proportional to the maximum piston forces. It starts at $1.04\text{ mm} \pm 0.05\text{ mm}$ for the $75\text{ }^{\circ}\text{C}$ extrusion and ends at $1.18\text{ mm} \pm 0.01\text{ mm}$ for the $55\text{ }^{\circ}\text{C}$ extrusion. The corresponding standard deviations are clearly optimized when the temperature is reduced. The zigzag characteristic disappears almost completely. This indicates that thinning of the strands fails to materialize (↪ IV, 1.1).

The reduction of the fill levels during the compression phase and the heating phases was almost identical as for the addition of Dynacet 211 P (↪ IV, 2.1.1). For this reason, the discussion is not repeated at this point.

Next, the 10% formulation was focused with oxybutynin base instead of the hydrochloride. The development of the piston forces at different temperatures is presented in Figure 100. Remarkably, two types of curves are obtained - plateau-shaped ones and zigzag-shaped ones. The latter are only available for extrusions at 60 °C whereas the former are found at temperatures above and below. In this case, the maximum piston force increases with decreasing temperature. At 45 °C, the manufacturing process is stopped due to an overload. This can be ascribed to the increasing viscosity of the material inside the barrel. However, by means of the lipid, it is possible to extrude at temperatures below the melting point of the API. For the 60 °C extrusion, fluctuations in between 6 kN and 13 kN are monitored. This indicates that the strand leaves the die in a stop-and-go manner. Although this effect was shown to be reproducible, an explanation cannot be provided so far. Anyway, the corresponding implant diameter was comparatively high with $1.24 \text{ mm} \pm 0.03 \text{ mm}$. For the manufacturing at 65 °C, 55 °C, and 50 °C, values ranging from 1.19 mm to 1.21 mm were detected. Once more, the thickness increased with decreasing temperature, and the standard deviations became better.

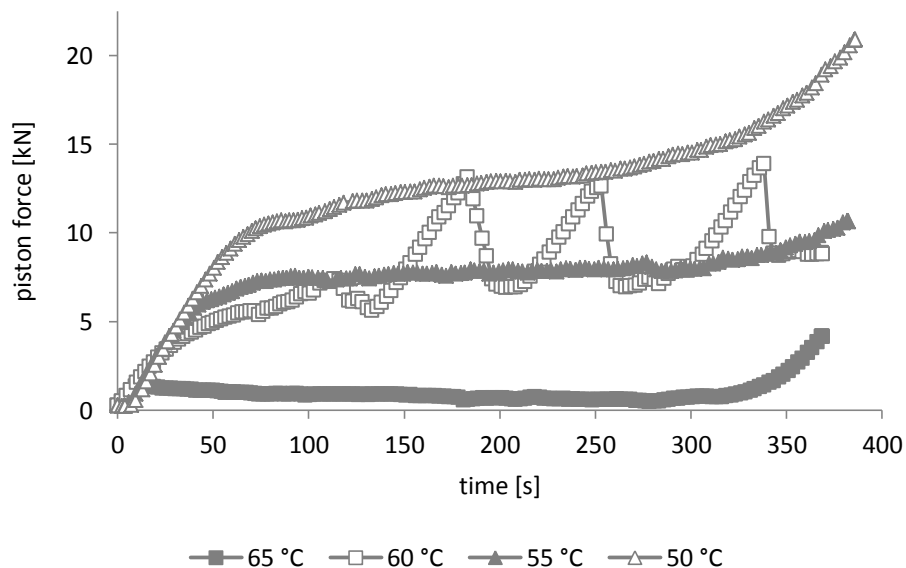


Figure 100 | Influence of the temperature on the piston force during the extrusion (standard program) of formulations consisting of 70% of RG 502 H, 20% of oxybutynin base, and 10% of Gelucire 50/13.

Finally, the distribution of the drug particles inside the polymer/lipid matrix was investigated by recovery studies (☞ Figure 101). At the lowest possible extrusion temperature, the hydrochloride was determined to be homogeneously distributed with a recovery close to 100% and a relatively small standard deviation. The same holds true for the base-containing implants that were extruded

at 55 °C and 50 °C, respectively. In contrast, higher extrusion temperatures lead to an enormous increase of the standard deviations. For extrudates that were prepared at 60 °C and 65 °C, values of 7.9% and 16.0% were obtained. This can be related to the melting temperature of the API. As long as the drug particles remain solid (below 56 °C to 58 °C [235]), homogeneous strands can be extruded. The other way around, when the base becomes liquid, demixing can be observed. The fluctuating piston forces at 60 °C might be regarded as first indicator for such processes. At higher temperatures, the softening of the polymer has to be taken into account. This might explain the absence of the zigzag characteristics at 65 °C.

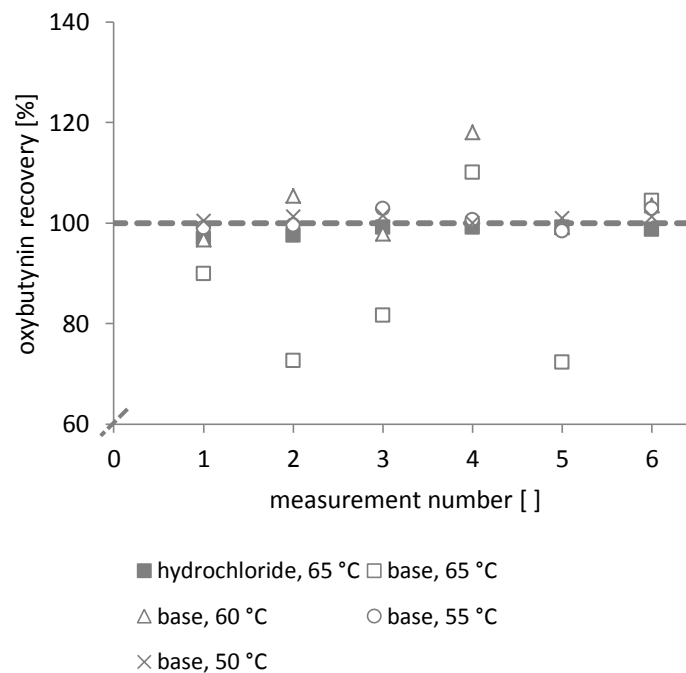


Figure 101 | Homogeneity of implants consisting of 70% of RG 502 H, 20% of oxybutynin hydrochloride or oxybutynin base, and 10% of Gelucire 50/13. Influence of the temperature (n = 6).

2.2.2 *In vitro* release studies

Figure 102 illustrates the *in vitro* release profiles of PLGA-based implants containing 20% of oxybutynin hydrochloride or oxybutynin base and 10% of Gelucire 50/13. As usual, the tests were performed in 0.1 M phosphate buffer pH 6.0 at 37 °C. Comparable to the lipid-free implants, the base was found to be released faster than the corresponding salt (☞ V, 1.2). Complete recovery of the API takes 21 d whereas the hydrochloride requires minimum 25 d. This indicates that the macroglyceride is not able to prevent the base-catalyzed acceleration of the chain scission

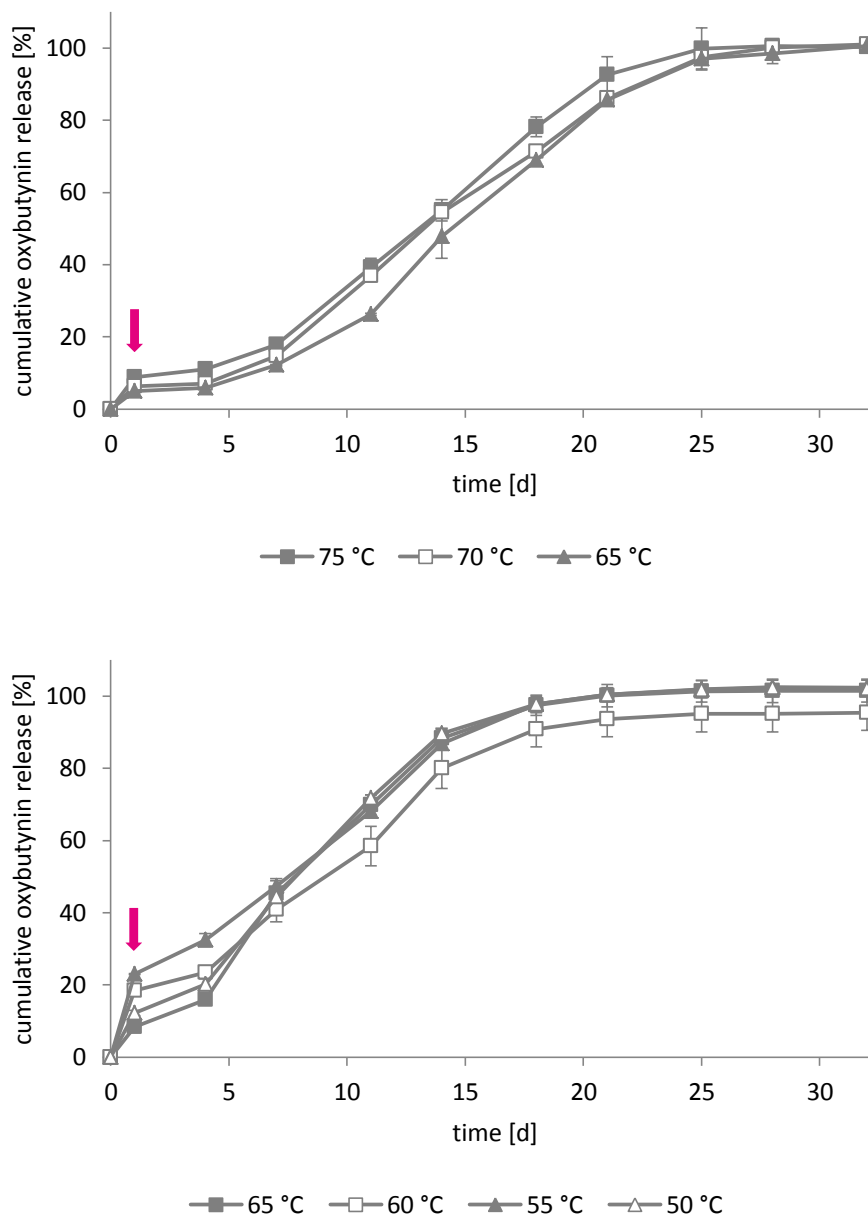


Figure 102 | *In vitro* drug release from implants consisting of 70% of RG 502 H, 20% of oxybutynin, and 10% of Gelucire 50/13 in 0.1 M phosphate buffer pH 6.0 at 37 °C. Influence of the temperature (mean \pm standard deviation, $n = 3$). **Top:** Oxybutynin hydrochloride. **Bottom:** Oxybutynin base.

process (\Rightarrow V, 1.3). For this reason, the release mechanisms in the presence of Dynacet 211 P (\Rightarrow VI, 2.1.2 and VI, 2.1.3) and Gelucire 50/13 have to be strictly distinguished from each other. Figure 102 reveals that the initial release of the salt decreases with decreasing process temperature. At 75 °C and 65 °C, values of $8.9\% \pm 1.1\%$ and $4.9\% \pm 0.1\%$ are obtained, respectively. This trend is favorable since two aims can be achieved at the same time: the reduction of the extrusion temperature and the suppression of the burst release. After a short lag phase of about 3 d to 7 d, the curves start to

increase almost linearly, which is desirable as well. The only disadvantage of this delivery system is the minimum temperature of 65 °C. Compared to the standard formulation, an improvement of maximum 10 °C can be realized. For future applications, it is recommended to optimize the extrusion process as described previously (☞ IV, 2, 3). When the base is embedded instead of the hydrochloride, temperatures as low as 50 °C can be reached. The lag phase is shortened to maximum 4 d, and the erosion phase is characterized by higher release rates. The initial burst causes confusion since it increases in the following order: 65 °C < 50 °C < 60 °C < 55 °C. For a detailed consideration, it is necessary to distinguish between extrusions that were run above and below the melting temperature of the API. This leads to the following revised rankings: 65 °C < 60 °C and 50 °C < 55 °C. The former might possibly be related to the fact that the encapsulation of the drug particles is more efficient at higher temperatures. As a consequence, the burst release declines. Since the extrudates were shown to be highly inhomogeneous (☞ VI, 2.2.1), these results have to be treated with caution. In contrast, the base is homogeneously distributed in implants that were manufactured at 55 °C and 50 °C. For such extrudates, the order of the initial release is exactly the opposite. With decreasing process temperature, the burst release decreases as well. This is the same as was already found for the hydrochloride-containing implants.

2.2.3 Studies on the release mechanism

In order to identify the mechanisms that are responsible for the single release profiles, studies on the pH, the mass loss, and the surface morphology of the Gelucire 50/13-containing implants were carried out. At first, it was determined whether the pH is influenced by the lipid. Even after 32 d of incubation, no differences could be detected. Thus, changes in the pH can totally be ascribed to the degradation and erosion behavior of the polymer. Figure 103 displays the pH profiles of rods containing either the hydrochloride or the base. For each type of drug, the starting temperature and the lowest possible extrusion temperature are depicted. As expected, the curves of the base decrease faster than those of the salt. After 11 d of incubation, a difference of more than 0.2 pH units is available. This can be explained by the base-induced acceleration of the polymer hydrolysis that has already been discussed for the lipid-free implants (☞ V, 1.3). Concerning the hydrochloride-loaded rods, a slight difference in the pH curves can be seen: the one referring to the 75 °C extrusion declines earlier than the one of the 65 °C extrusion. This is in good correlation with the release data which show a marginally delayed release for the implants that were manufactured at 65 °C (☞ VI, 2.2.2). Thus, it might be summarized that the degradation of RG 502 H slows down as soon as the

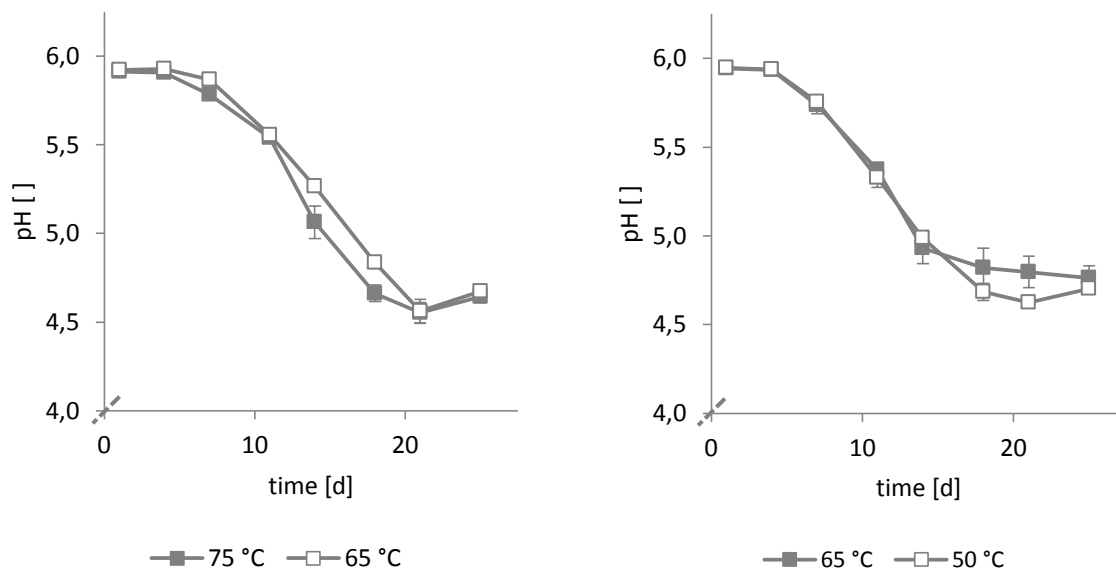


Figure 103 | pH values during the drug release from implants consisting of 70% of RG 502 H, 20% of oxybutynin, and 10% of Gelucire 50/13 in 0.1 M phosphate buffer pH 6.0 at 37 °C. Influence of the temperature (mean \pm standard deviation, n = 3). **Left:** Oxybutynin hydrochloride. **Right:** Oxybutynin base.

manufacturing temperature is reduced. Assuming that the heating stress during the extrusion is responsible for the initial reduction of the polymer molecular weight (☞ IV, 1.2), such a development seems to be conclusive. However, for Dynacet 211 P-containing extrudates, this effect could not be observed (☞ VI, 2.1.3). If the hydrochloride is finally replaced by the base, independent of the process temperature, almost identical pH values are obtained during the first 14 d of incubation. Thereafter, the pH referring to the 50 °C extrusion declines to a greater extent than the one referring to the 65 °C extrusion. This is astonishing and cannot be explained so far, most notably because of the release profiles that closely resemble each other.

The results of the mass loss experiments are illustrated in Figure 104. Independent of the type of drug and the extrusion temperature, more than 90% of the initial implant mass are lost after 25 d of incubation in the release medium. Since this includes at least parts of the lipid, Gelucire 50/13 is thought to degrade as well. With regard to the subcutaneous application of such delivery systems, this is of course desirable. However, the evaluation of the mass loss profiles is now complicated. It cannot be distinguished between the erosion of the polymer and the one of the lipid any more. In spite of that, it is obvious that the mass loss of the base-containing implants proceeds much faster than the one of the hydrochloride-loaded ones. Comparable to the lipid-free implants, the release of the base seems to be mainly controlled by the degradation of the matrix (☞ V, 1.3). With the

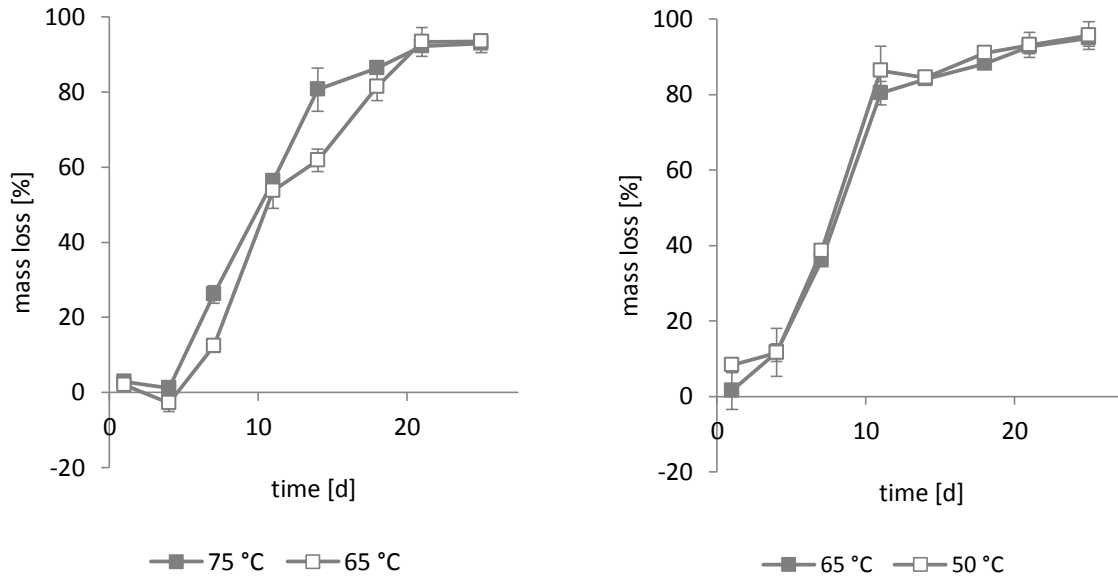


Figure 104 | Mass loss during the drug release from implants consisting of 70% of RG 502 H, 20% of oxybutynin, and 10% of Gelucire 50/13 in 0.1 M phosphate buffer pH 6.0 at 37 °C. Influence of the temperature (mean \pm standard deviation, $n = 3$). **Left:** Oxybutynin hydrochloride. **Right:** Oxybutynin base.

exception of the initial values, the shapes of the release profiles and the mass loss profiles were found to be similar at both temperatures. The initial release of the extrudates that were manufactured at 65 °C is completely controlled by the diffusion of the API. The mass loss reflects exactly the amount of oxybutynin in the release medium. In contrast, the burst release of implants that were produced at 50 °C follows the degradation of the matrix. In this case, the drug particles remain solid during the manufacturing whereas they melt at 65 °C. That way, the mechanisms that are responsible for the release within the first 24 h can be easily controlled - as long as Gelucire 50/13 is present. When the hydrochloride is used instead of the base, diffusional processes and, to a much smaller extent, the degradation of the matrix seem to determine the release within the first 4 d. Thereafter, the erosion of the matrix predominates. As can be seen, the mass loss increases faster for the 75 °C extrusion. This is in good agreement with the results of the pH measurements and the release profiles (⇒ VI, 2.2.2).

In addition, the surface morphology of the implants was investigated by scanning electron microscopy (⇒ Figure 105). The surfaces of the salt-containing rods turned out to be smooth, covered with a number of rhombic crystals. The latter were only observed for formulations containing the hydrochloride in combination with Gelucire 50/13. With decreasing process temperature, the size of the crystals increases. At the same time, their total number is reduced. Assuming that the crystals originate from the drug substance, the different initial releases can be

explained. For the implants that were extruded at 75 °C, larger parts of the surface area are covered by the rhombuses. As soon as the extrudates get in contact with the release buffer, these crystals might be dissolved and - at least partially - be released. As previously shown, dissolved drug molecules are prone to be retained by drug/polymer interactions (☞ V, 4). This is presumably the reason why the initial bursts are comparatively low with less than 9%. At lower process temperatures, fewer crystals are available, thus further reducing the release within the first 24 h. If the salt is replaced by the base, the rhombuses disappear. A rough surface is obtained which becomes even more wrinkled and porous when the manufacturing temperature is reduced. This is also confirmed by the implant density that was calculated to be $1.26 \text{ mg/mm}^3 \pm 0.02 \text{ mg/mm}^3$ for the 65 °C extrudates and $1.18 \text{ mg/mm}^3 \pm 0.02 \text{ mg/mm}^3$ for the 50 °C extrudates. For the latter, the intrusion of water and the transport of dissolved API and PLGA degradation products is facilitated. However, it remains unclear why the burst release is considerably higher for implants that were produced at 55 °C. As can be seen, the 65 °C rods are much denser, which might possibly result from the fact that both the lipid and the drug particles melt during extrusion. For the 60 °C rods, similar

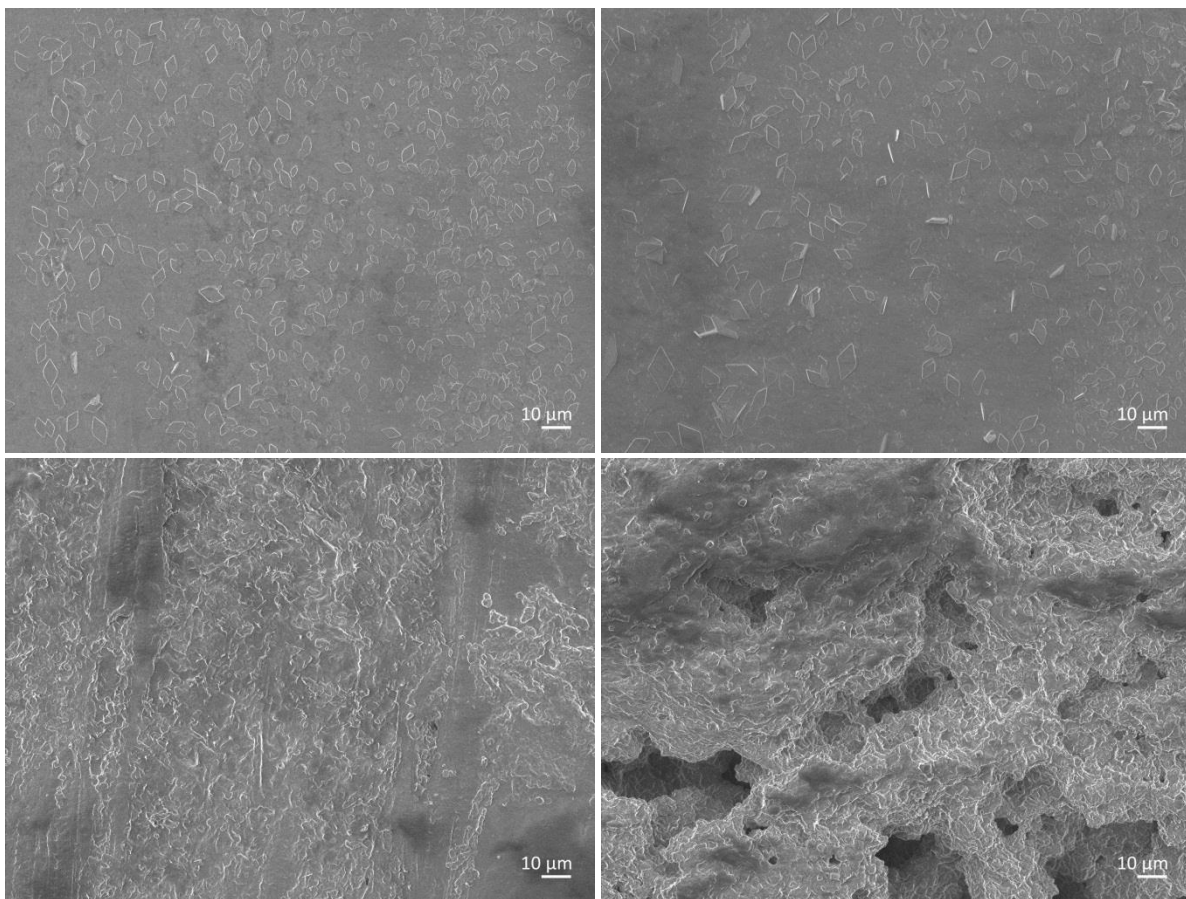


Figure 105 | Scanning electron microscopy. Surface morphology of implants consisting of 70% of RG 502 H, 20% of oxybutynin, and 10% of Gelucire 50/13. **Top left:** Oxybutynin hydrochloride, extruded at 75 °C. **Top right:** Oxybutynin hydrochloride, extruded at 65 °C. **Bottom left:** Oxybutynin base, extruded at 65 °C. **Bottom right:** Oxybutynin base, extruded at 50 °C.

SEM pictures were taken (data not shown). This indicates that the different initial releases can rather be ascribed to the more efficient encapsulation of the API at higher temperatures than to differences in the surface morphology.

3 Heterogeneous implants - core-shell implants

As described before, the lipid screening generated to two types of implants: homogeneous ones that could be extruded without any problems and heterogeneous ones of which the manufacturing was complicated by phase separation processes (➔ VI, 1.1, 2). According to their special structure, the latter were defined as core-shell implants (➔ Figure 106). They result from formulations consisting of poly(lactide-co-glycolide) and up to 20% of highly hydrophobic lipids (without emulsifying properties) such as triglycerides or hydrogenated cocoglycerides. The addition of up to 20% of oxybutynin hydrochloride or oxybutynin base was shown to be unproblematic. The extrusions were carried out using the standard program at 75 °C. This temperature ensures complete melting of the lipids. Such productions were found to yield in quite high maximum piston forces so that the lipids were not categorized as promising candidates for the process optimization. However, the corresponding release profiles resembled the one of the lipid-free formulation. This is the reason why further investigations with a special focus on the release characteristics were started.

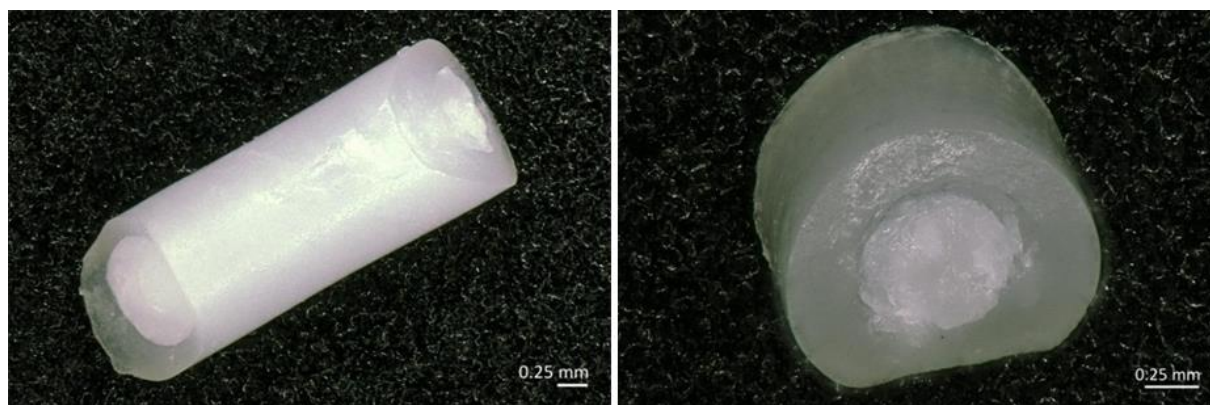


Figure 106 | Digital microscopy of core-shell-structured placebo implants consisting of 80% of RG 502 H and 20% of Witocan 42/44.

3.1 Influence on the manufacturing process

During the preliminary stages, placebo extrudates consisting of RG 502 H and different amounts of Witepsol H 12 were manufactured. Figure 107 presents their macroscopic appearance. From left to right, the amount of the lipid increases from 5% to 20%. As can be seen, the strands are almost transparent or white dotted post-extrusion. The size of these dots increases with increasing lipid content. After cooling, all strands become completely white. The same occurs after storage at room temperature for several days. A consistent core-shell structure was obtained for extrudates containing 10% and 15% of the hydrogenated glyceride, respectively. At 5%, the inner structure of

the implants was mainly homogenous. In contrast, at 20%, the molten lipid formed droplets at the exit of the die which solidified at the surface of the strands. This led to strongly fluctuating implant diameters.

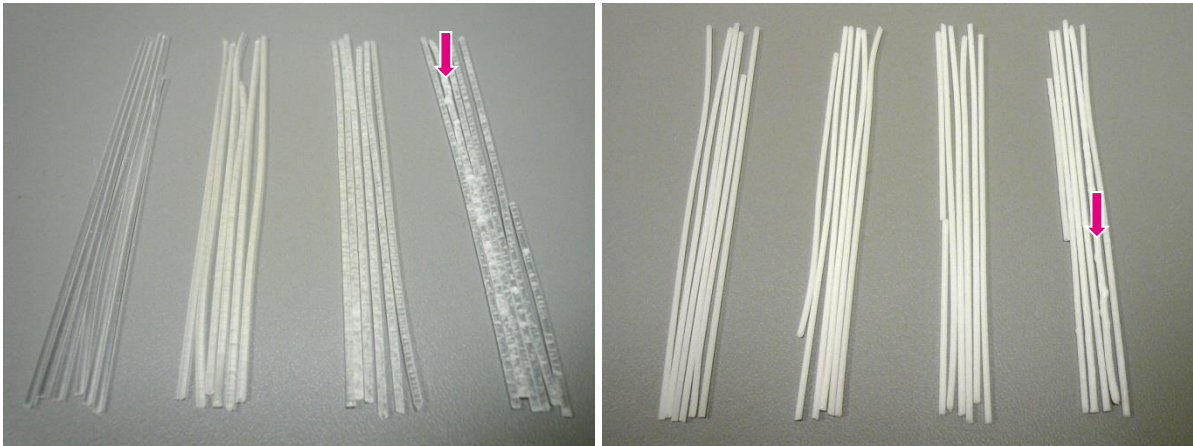


Figure 107 | Macroscopic appearance of placebo implant strands consisting of RG 502 H and 5%, 10%, 15%, or 20% of Witepsol H 12. **Left:** Post-extrusion. **Right:** After cooling at 2 °C to 8 °C.

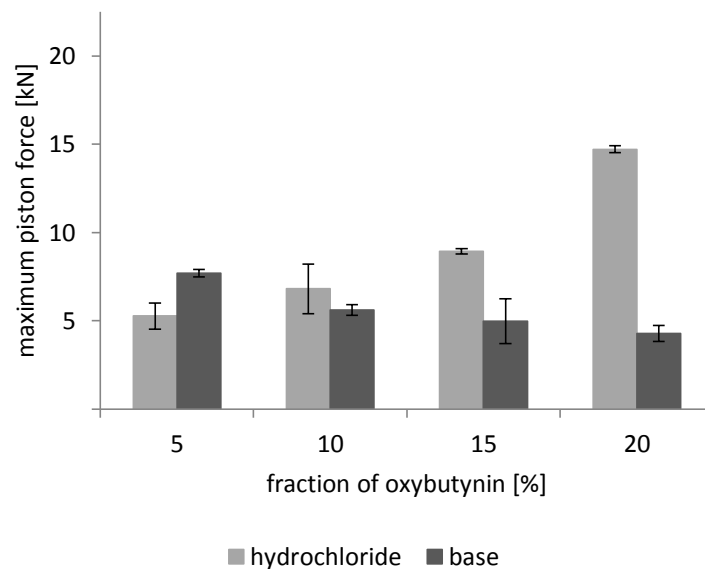


Figure 108 | Influence of the type of drug on the maximum piston force during the extrusion (standard program at 75 °C) of formulations consisting of RG 502 H, 10% of Witepsol H 12, and different fractions of oxybutynin (mean \pm standard deviation, $n = 2$).

For the following studies, it was decided to work with the 10% formulation. Oxybutynin hydrochloride or oxybutynin base were added in 5% steps. The resulting maximum piston forces are illustrated in Figure 108. Similar to the lipid-free formulations, the values were found to increase with

increasing salt and decreasing base concentration (☞ V, 1.1). This can be attributed to the fact that the hydrochloride stays solid during extrusion while the base melts. Hence, the viscosity of the implant material increases in the former case whereas it decreases in the latter. Interestingly, most of the values turned out to be smaller than for the formulations without lipid. 15 kN instead of 18 kN were, for example, measured for the formulations containing 20% of the salt. The highest reduction was attained for the formulations with 5% of the base. The maximum piston force decreased from initially 21 kN to less than 8 kN (☞ Figure 45). This is presumably due to the lubricating effect of the lipid. The ball bearing effect that was discussed earlier for the salt-containing formulations (☞ V, 1.1) seems to disappear in the presence of Witepsol H 12. Placebo implants consisting of 90% of RG 502 H and 10% of the lipid require a maximum piston force of less than 5 kN.

Table 10 | Influence of the fraction of oxybutynin on the implant diameter. The implants consisted of RG 502 H, 10% of Witepsol H 12, and different amounts of the drug. Extrusion was performed using the standard program at 75 °C (mean ± standard deviation, n = 2).

drug loading [%]	oxybutynin hydrochloride	oxybutynin base
5	1.35 mm ± 0.08 mm	1.42 mm ± 0.09 mm
10	1.37 mm ± 0.06 mm	1.37 mm ± 0.09 mm
15	1.38 mm ± 0.05 mm	1.42 mm ± 0.13 mm
20	1.28 mm ± 0.09 mm	1.38 mm ± 0.14 mm

The corresponding implant diameters are shown in Table 10. Independent from the type of drug, the values attract attention since they are relatively high. Although a 1.15 mm die was used, mean thicknesses ranging from 1.28 mm to 1.42 mm were monitored. This is distinctive of extrudates containing hydrophobic non-emulsifying lipids such as triglycerides or hydrogenated cocoglycerides (☞ VI, 1.1). In the presence of these excipients, the expansion of the implant material at the exit of the die was observed to be much more pronounced than in the case of amphiphilic additives. Obviously, a correlation of the diameters to the maximum piston forces is not given. The standard deviations are comparatively high with 0.05 mm to 0.09 mm for the salt-loaded rods and 0.09 mm to 0.14 mm for the base-loaded ones. This is a strong indicator for the occurrence of phase separation processes. The base which is known to melt during extrusion at 75 °C [235] leads to larger fluctuations in the strand thickness than the hydrochloride. It is assumed that the solid drug particles are able to suppress the demixing to a certain extent so that an optimum loading can be identified. For Witepsol H 12 in combination with oxybutynin hydrochloride, this value was detected to be 15%.

Interestingly, the determination of the homogeneity (☞ Figure 109) revealed that the salt form of the API is homogeneously distributed in the polymer/lipid matrix. Independent of the drug loading, recoveries around 100% were measured for all samples. The standard deviations were extremely

small with maximum 1.0% for the 15% loading. This is astonishing since the demixing of the implant material inside the barrel was thought to be indicative for an inhomogeneous distribution of the drug particles. The latter was only obtained for base-containing formulations. As illustrated, the corresponding recoveries strongly fluctuate. For example, values of 78.6% and 131.7% were attained for implants of one and the same batch consisting of 75% of RG 502 H, 15% of oxybutynin base, and 10% of Witepsol H 12. This results in a standard deviation of 19.7% (n = 6). Although the standard deviations became better with decreasing amounts of the drug, values comparable to the ones of the

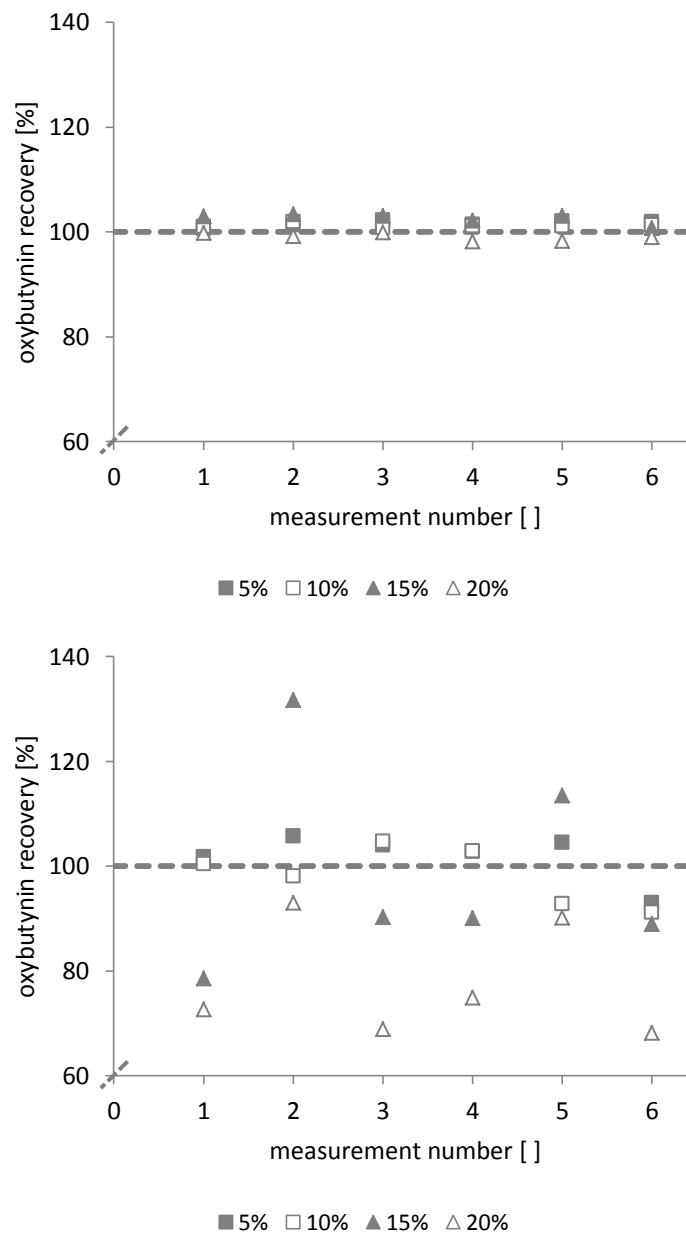


Figure 109 | Homogeneity of implants consisting of RG 502 H, 10% of Witepsol H 12, and different fractions of oxybutynin (n = 6). **Top:** Oxybutynin hydrochloride. **Bottom:** Oxybutynin base.

hydrochloride could not be reached. This is the reason why salt-containing implants were focused in the following.

In summary, it can be concluded that core-shell-structured implants can be manufactured by means of a simple one-step extrusion method. The use of special equipment that allows for the co-extrusion of the matrix materials is not necessary. Dependent of the physico-chemical properties of the incorporated drug, a homogeneous distribution can be achieved. With oxybutynin hydrochloride, for example, perfectly homogeneous two-phase extrudates can be prepared.

3.2 Investigations on the structure

In order to find out whether the polymer or the lipid forms the core (or the shell), thin placebo cross sections were subjected to thermo-optical analysis. As an example, implants consisting of 80% of RG 502 H and 20% of Witocan 42/44 were chosen. The results are depicted in Figure 110. The melting range of the hydrogenated cocoglyceride is 42 °C to 44 °C (☞ III, 1.3.2) while the glass transition temperature of the polymer ranges between 42 °C and 46 °C (☞ III, 1.2). In spite of the overlap, both excipients can be easily distinguished from each other. In independent experiments (data not shown), the lipid was observed to melt rapidly. It turned transparent within seconds. In contrast,

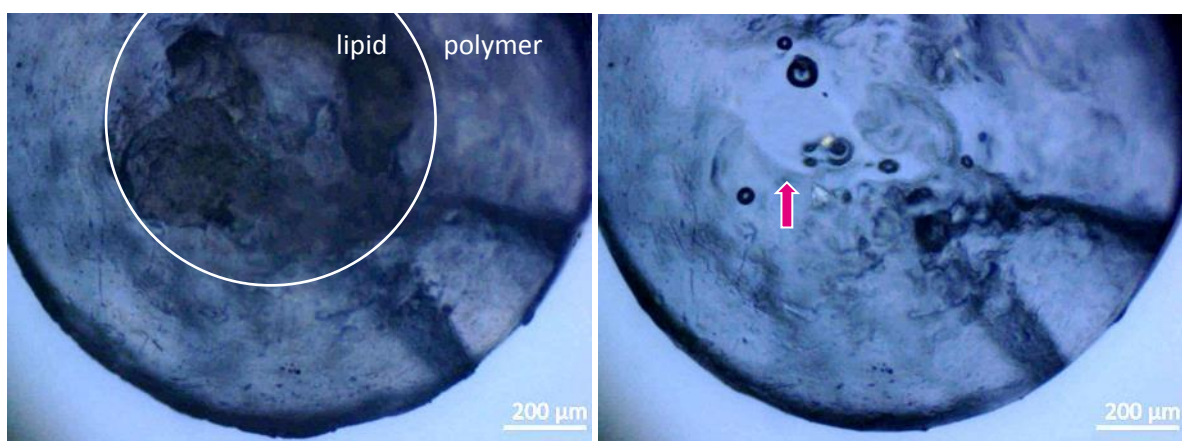


Figure 110 | Thermo-optical analysis of a cross section of an implant consisting of 80% of RG 502 H and 20% of Witocan 42/44. **Left:** 42.0 °C. **Right:** 46.0 °C.

PLGA remained opaque although its T_g was clearly exceeded. Consequently, thermo-optical analysis was the method of choice for the investigations on the implant structure. Up to a temperature of 42 °C, the microscopic appearance of the cross sections was almost unchanged. A dark core was surrounded by a shade lighter shell. As soon as the T_m range of the lipid was reached, the core started to melt. At 46 °C, larger transparent areas could be recognized in the inner implant. This indicates

that the phase separation during the manufacturing process leads to extrudates with a lipidic core and a polymeric shell.

With the objective to clarify if incorporated drug molecules tend towards agglomeration in one of the phases, staining experiments with methylene blue and Sudan red G as model substances were performed. Less than 0.05% of these dyes were added to placebo formulations consisting of 87.5% of RG 502 H and 12.5% of Witepsol H 12. It was assumed that methylene blue which is water-soluble colors the less hydrophobic shell while Sudan red G which is lipophilic dissolves in the more hydrophobic core. However, Figure 111 reveals that this is not true. Both dyes are homogeneously distributed over the complete implant cross section. This might be ascribed to the fact that the hydrophobicity of the lipid and the one of the surrounding polymer are not different enough. Thus, an agglomeration in the core or the shell does not occur. Regarding conventional APIs that are commonly used in much higher concentrations, it is not expected that the demixing of the matrix materials has an influence on the distribution of the drug molecules. It might possibly make a difference if the API melts during extrusion (as oxybutynin base does). This was neither the case for methylene blue nor for Sudan red G.



Figure 111 | Macroscopic appearance of implants consisting of 87.5% of RG 502 H, 12.5% of Witepsol H 12, and less than 0.05% of methylene blue or Sudan red G.

3.3 *In vitro* release studies

In vitro release tests were carried out in 0.1 M phosphate buffer pH 6.0 at 37 °C. The focus was on oxybutynin hydrochloride-containing core-shell-structured implants which are characterized by a homogeneous API distribution (☞ VI, 3.1). The drug loading varied from 5% to 20%. Witepsol H 12, a hydrogenated cocoglyceride, was used in a concentration of 10%, that way guaranteeing phase separation during the manufacturing process. Formulations with RG 502 H instead of the lipid were

investigated as well. Thus, monolithic and core-shell implants can be compared directly. Since the release mechanisms from polymeric and lipidic matrices are known not to be equal [4, 6, 34] (☞ I, 2.3 and I, 3.2), the release profiles from both types of extrudates were assumed to differ from each other. However, the opposite turned out to be true. As shown in Figure 112, the curves are almost identical. Independent of the API concentration, the addition of the lipid and hence the formation of the core-shell structure does not affect the release characteristics. This is astonishing since at least part of the drug particles are supposed to be located in the inner implant which is comprised of the

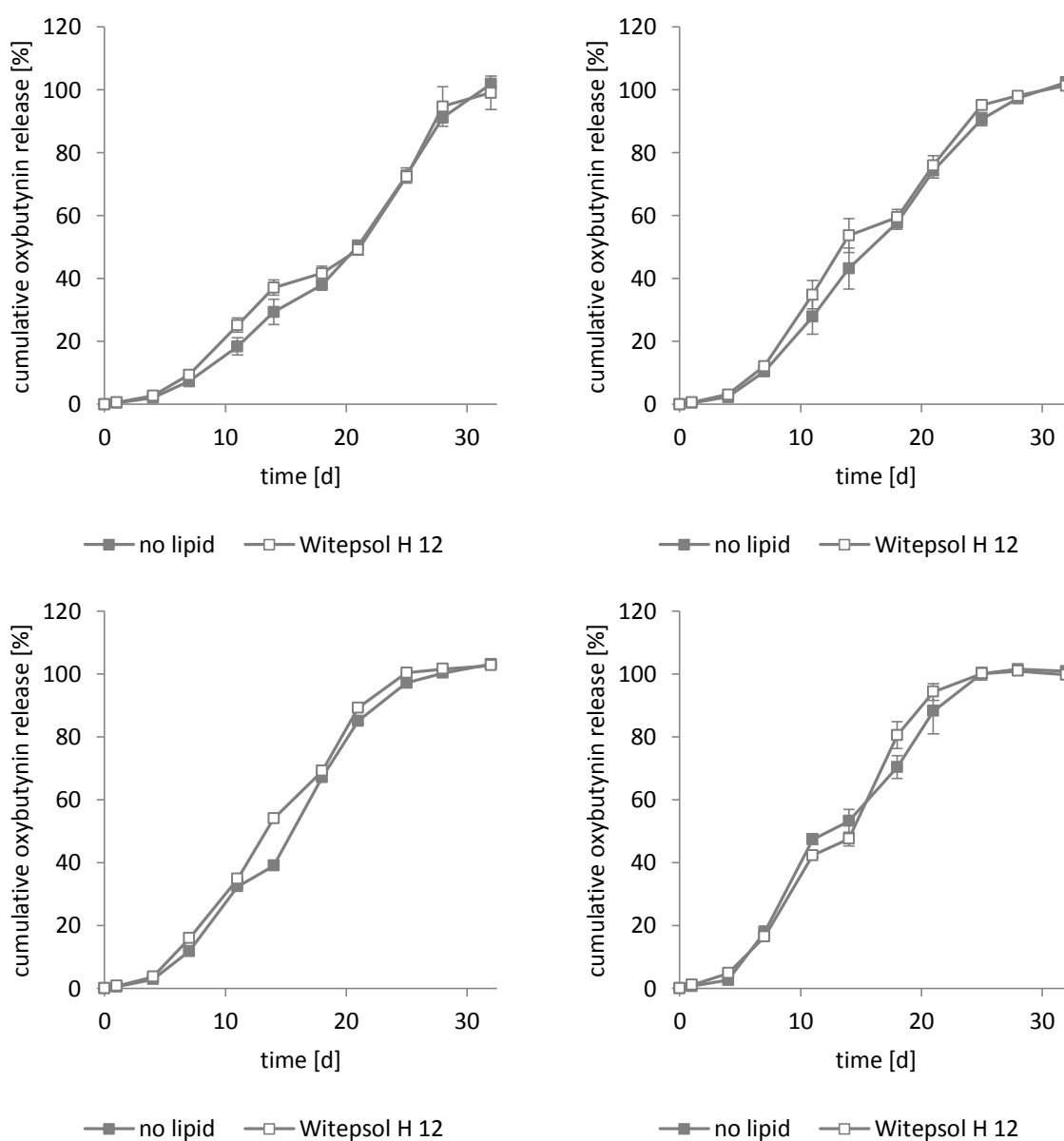


Figure 112 | *In vitro* drug release from implants consisting of RG 502 H, 10% of Witepsol H 12, and different fractions of oxybutynin hydrochloride in 0.1 M phosphate buffer pH 6.0 at 37 °C. For comparison purposes, formulations with RG 502 H instead of the lipid were investigated as well (mean \pm standard deviation, n = 3). **Top left:** 5% of the drug. **Top right:** 10% of the drug. **Bottom left:** 15% of the drug. **Bottom right:** 20% of the drug.

cocoglyceride and surrounded by a dense matrix of RG 502 H (➔ VI, 3.2). Most probably, drug release from such systems can be explained as follows: the composition of the outer shell (that makes up the largest part of the extrudate) is similar to the one of the lipid-free implants. Therefore, the release of the API will primarily be controlled by the erosion of the polymer. The drug molecules that are embedded in the inner lipodic core will be released by diffusion. If this process is at least as fast as the degradation of the PLGA shell, it is likely that the influence of the lipid will not be reflected in the resulting release profiles. Of course, this mechanism has to be ascribed to the comparatively high drug loadings. Further investigations are absolutely necessary to clarify whether the release profiles change when much smaller amounts of the API are embedded. It would also be of interest to work with highly lipophilic and less soluble drugs that form a solid solution with the core material.

Figure 112 further reveals that the release rates increase with increasing drug loading. For the lipid-free formulations, this was already expected from literature. Ramchandani and Robinson, for example, investigated the *in vitro* release of ciprofloxacin from PLGA-based implants [198]. The drug loadings varied between 10% and 50%. Interestingly, it was found that the characteristic biphasic release profile turned into a monophasic one at 35% and 50%. This is indicative for an overlapping of the initial diffusive phase and the erosion phase, and it results in a continuous release that can be described by a square root-time relationship. At lower concentrations, namely at 10% and 20%, multiphasic release profiles were obtained. This is in good agreement with the results of this work and also holds true for the core-shell implants.

3.4 Studies on the release mechanism

In a final step, studies on the release mechanism were accomplished. Figure 113 displays the pH changes within the first 25 d of incubation - both for lipid-free and Witepsol H 12-containing implants. The drug loading remained unchanged at 20%. As the pH is only dependent on the polymer and its degradation products, it was expected to decrease to a greater extent for the formulation without lipid and hence more PLGA. This was confirmed by a difference of 0.2 pH units at the end of the release period. Remarkably, the pH values referring to the core-shell implants start to decrease earlier and more linear than the ones of the lipid-free formulations. This might possibly be attributed to the fact that the addition of the cocoglyceride reduces the overall density of the extrudates from initially $1.35 \text{ mg/mm}^3 \pm 0.01 \text{ mg/mm}^3$ to $1.26 \text{ mg/mm}^3 \pm 0.04 \text{ mg/mm}^3$. Due to the demixing process, it is assumed that not only the core but also the shell is affected. Thus, the intrusion of water will be facilitated, and the polymer chains will hydrolyze earlier in time.

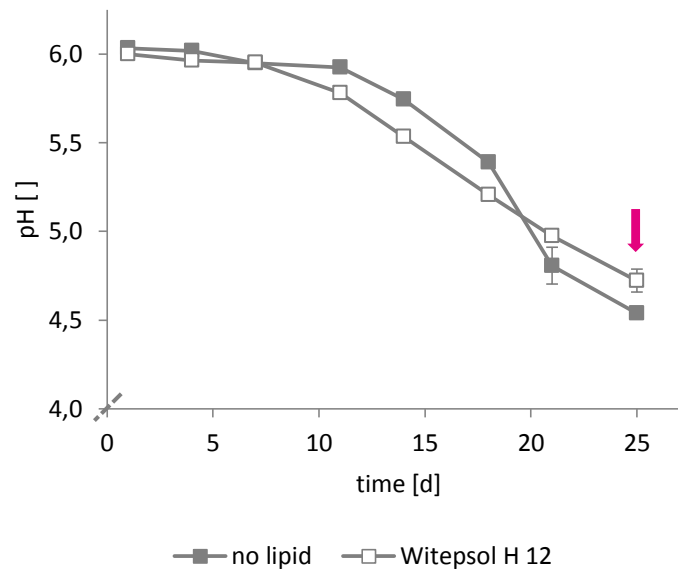


Figure 113 | pH values during the drug release from implants consisting of 70% of RG 502 H, 20% of oxybutynin hydrochloride, and 10% of Witepsol H 12 in 0.1 M phosphate buffer pH 6.0 at 37 °C. For comparison purposes, formulations with RG 502 H instead of the lipid were investigated as well (mean \pm standard deviation, n = 3).

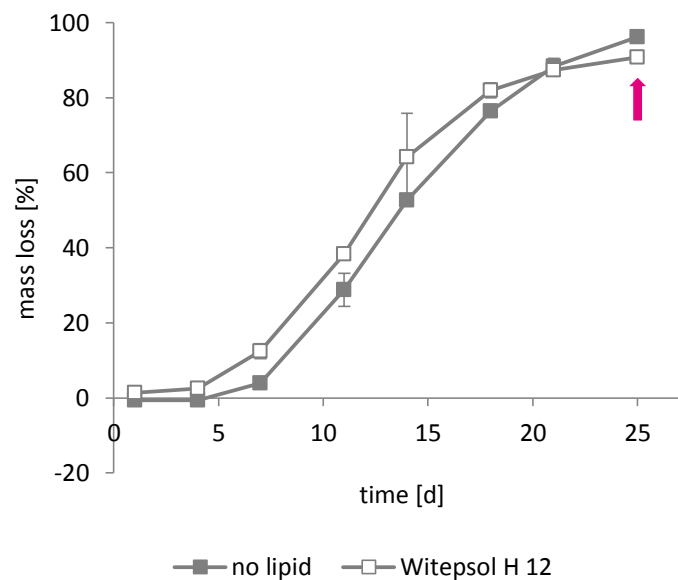


Figure 114 | Mass loss during the drug release from implants consisting of 70% of RG 502 H, 20% of oxybutynin hydrochloride, and 10% of Witepsol H 12 in 0.1 M phosphate buffer pH 6.0 at 37 °C. For comparison purposes, formulations with RG 502 H instead of the lipid were investigated as well (mean \pm standard deviation, n = 3).

The same explanation might be applied for the investigations on the mass loss of which the results are depicted in Figure 114. During the first 4 d, the weight of the implants without lipid remained

unchanged, followed by a strong decrease which was shown to proceed until a mass loss of 96% was reached after 25 d. In contrast, for the core-shell implants, a mass loss of 1% and 2% could already be detected after 1 d and 4 d of incubation. Thereafter, the weight loss increased slightly faster than for the lipid-free extrudates. Between 7 d and 14 d, the slope of both curves was found to be almost identical. However, in the end, the mass loss of the Witepsol H 12-containing implants was not more than 91%. At this point in time, 100% of the API were released (⇒ VI, 3.3).

At last, the macroscopic appearance of both types of extrudates was evaluated. Pictures were taken after 1 d, 4 d, 7 d, 11 d, and 14 d of incubation in 0.1 M phosphate buffer pH 6.0 at 37 °C (⇒ Figure 115). As can be seen, the addition of the cocoglyceride substantially changed the implant morphology during the degradation process. The lipid-free rods lengthened, became barbell-shaped, and adapted their form to the walls of the vessel. In the later stages, when transparency and porosity drastically increased, the implants were observed to shrink. Finally, beads were formed. As opposed to this, the core-shell implants maintained their shape over the complete release period. They grew shorter but increased in diameter. After 7 d in the release medium, the rods began to turn transparent, and white dots appeared inside. It is presumed that these dots stem from the Witepsol H 12 core.

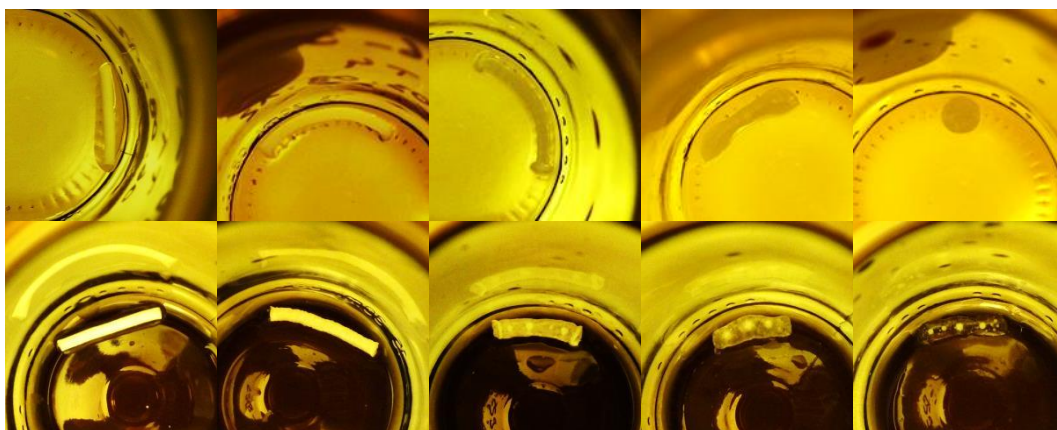


Figure 115 | Macroscopic appearance after 1 d, 4 d, 7 d, 11 d, and 14 d of incubation in 0.1 M phosphate buffer pH 6.0 at 37 °C. Extrusion was performed using the standard program at 75 °C. **Top:** The implants consisted of 80% of RG 502 H and 20% of oxybutynin hydrochloride. **Bottom:** The implants consisted of 70% of RG 502 H, 20% of oxybutynin hydrochloride, and 10% of Witepsol H 12.

In summary, the studies on the release mechanism revealed smaller differences between the ‘traditional’ lipid-free and the core-shell-structured extrudates. However, the release profiles were found to be almost congruent. It seems that the degradation of the polymer which obviously starts earlier in the rods containing the cocoglyceride does not affect the release rates. In order to clarify this issue, further investigations on the drug/polymer and drug/lipid interactions which might retain

the API would be necessary. Nevertheless, it can be stated that diffusional and erosional processes are involved in the release mechanism for both types of implants.

4 Summary

In this chapter, lipids were investigated as innovative excipients for the manufacturing of biodegradable PLGA-based implants. With the aim of reducing the process temperature to a minimum, a variety of lipids was screened (at 75 °C): triglycerides, hydrogenated cocoglycerides, monoglycerides, acetylated glycerides, macroglycerides, and phosphatidylcholines. Dynacet 211 P and Gelucire 50/13 were identified as most promising candidates. Formulations consisting of 70% of RG 502 H, 20% of oxybutynin hydrochloride, and 10% of the acetylated glyceride or the macroglyceride led to maximum piston forces smaller than 3 kN. Compared to the lipid-free standard formulation, this is an optimization of about 15 kN. Concerning the release profiles, the addition of the lipids was observed to slightly increase the initial burst. However, the measured values were far below 10%, and they were hence acceptable. For implants containing Dynacet 211 P, the subsequent release was characterized by an elongation of the lag phase. In contrast, the release from implants containing Gelucire 50/13 was hardly affected. In addition, the extrudates were analyzed for their mechanical properties. In the case of the acetylated glyceride, the strands were categorized as sharply breaking ones whereas the macroglyceride resulted in highly deforming strands. As both types come along with advantages and disadvantages, these properties were excluded as decision criterion. In a final step, studies on the interaction between drug and lipid were carried out. Interestingly, it was found that such interactions occur for Dynacet 211 P but not for Gelucire 50/13.

The following investigations were intended to determine the smallest possible extrusion temperature and its impact on the release behavior. The acetylated glyceride was focused first. An addition of only 10% enabled implant manufacturing at 55 °C. The lipid was shown to act as a plasticizer, that way considerably reducing the T_g of the polymer. In terms of the release profiles, a major drawback emerged: with decreasing process temperatures, the initial releases increased substantially. Approximately 69% of the hydrochloride were released within the first 24 h from rods extruded at 55 °C. It was concluded that temperatures of at least 70 °C are necessary to completely encapsulate the drug molecules in a dense coherent matrix. Otherwise, the disintegration of the implants will be facilitated by more or less loosely bound particles of the API and the matrix materials. This is the reason why alternative manufacturing techniques such as heptane dispersion, double extrusion, or solvent casting were developed. The latter which is a pretreatment method for the API and the polymer was the most auspicious one. With this strategy, the burst release could successfully be lowered, and an extrusion temperature of 40 °C could be realized.

When oxybutynin base was embedded instead of the hydrochloride, the lowest possible manufacturing temperature was 55 °C. Interestingly, the initial release was found to be much smaller than for the salt-containing formulations. This led to the assumption that Dynacet 211 P possesses a drug-retaining ability which is most probably caused by hydrophobic interactions. At the same time, the base-catalyzed acceleration of the chain scission process that was previously reported for the release from lipid-free implants was switched off. Independent of the type of drug, the lipid was observed not to undergo degradation during the release period. With regard to future applications, this might be a crucial factor.

As opposed to this, implants containing 10% of Gelucire 50/13 were completely dissolved after 32 d of incubation in the release buffer. This indicates that both the polymer and the lipid are subjected to degradation processes. The smallest possible temperature that could be reached for the manufacturing of such extrudates was 65 °C for the hydrochloride and 50 °C for the base. Once more, this was attributed to the plasticizing effect of the lipid. The corresponding release profiles were comparable to the ones of the lipid-free formulations and therefore quite promising, especially for the salt form of the API. The addition of the macroglyceride was shown to have no influence on the accelerating effect of the base. Thus, the latter was released considerably faster than the hydrochloride. The degradation and erosion of the polymer turned out to be the prevalent release mechanism. However, diffusional processes were also of importance - in particular for base-containing rods that were manufactured at higher temperatures and for salt-containing extrudates.

Dynacet 211 P and Gelucire 50/13 share the characteristics that they are more amphiphilic than, for instance, triglycerides or hydrogenated cocoglycerides. This is the reason why phase separation processes were not observed during the manufacturing of implants with up to 20% of these lipids. In contrast, highly hydrophobic lipids were found to induce demixing. As a consequence, extrudates with a lipidic core and a polymeric shell were formed. If 5% to 20% of oxybutynin hydrochloride were embedded, a homogeneous distribution of the API was obtained. Interestingly, the release behavior was not affected by the core-shell structure of the implants. The curves were almost identical to the ones referring to the lipid-free formulations although the corresponding release mechanisms were shown to slightly differ.

In summary, this chapter emphasized the relevance of different lipids as innovative excipients for the manufacturing of PLGA-based implants. As the addition of amphiphilic lipids provides the possibility

to substantially reduce the process temperature, the extrusion technology might become more and more interesting for the increasing market of thermosensitive drugs such as biopharmaceuticals.

Chapter VII | Final summary

As its title implies, this thesis deals with industrial ram extrusion as innovative tool for the development of biodegradable sustained release implants. More precisely, injectable rods based on a matrix of poly(lactide-co-glycolide) are focused. For extrusion, temperatures far above the glass transition temperature of the polymer usually have to be applied [200]. Otherwise, the material does not soften enough and cannot be forced through the die. By implication, this means that the manufacturing technique is restricted to temperature-resistant APIs only. Thus, it was the main objective of this work to reduce the extrusion temperature to a minimum so that thermosensitive drugs such as biopharmaceuticals could be processed as well. Importantly, the classic sustained release profiles had to be maintained.

Chapter I serves as introduction. First, it gives an overview of parenteral controlled release systems in general. The historical background is highlighted, beginning in the early 1960s with Folkman and his silicone rubber tubing [10, 12, 13]. Nowadays, more than 50 years later, a variety of different dosage forms has become commercially available, among those implants, micro-, and nanoparticles. Each of these systems is briefly described. Next, the copolymer PLGA is introduced against the background of answering the question whether it is a magic (matrix) material or not. Emphasis is put on its synthesis which allows for producing a number of polymers with different physico-chemical properties and its degradation and erosion behavior that mainly controls drug release. In addition, the current market situation is presented. In the third place, insight into lipids as alternative matrix materials is given. Pros and cons are balanced with polymer-based systems in mind. Finally, the most important implant manufacturing techniques are listed.

Chapter II summarizes the aims of this thesis.

Chapter III outlines the materials and methods that were used within the scope of this work.

Chapter IV is the first chapter of the results and discussion part, and it mainly contains information on the optimization of the conventional extrusion process by means of a factorial design of experiments. With the aim of reducing the manufacturing temperature to a minimum, the influence of seven factors on the maximum piston force (that relates inversely to the temperature) was investigated. The applied Rechtschaffner design required a total of 39 runs. As a consequence, it allowed for calculating a prediction plot with non-significant model terms as constants. On this basis, an optimum parameter set was identified. The extrusion temperature for the standard formulation

consisting of 80% of RG 502 H and 20% of oxybutynin hydrochloride could successfully be lowered from initially 75 °C to 65 °C. Another 10 °C could be saved when the two-holed die was replaced by a four-holed one. By shortening the cutting interval, the standard deviation of the strand diameter was observed to be reduced to a minimum. Furthermore, an up-scaling of the batch size to the fourfold amount could be realized without any restrictions. Independent of all interventions, either concerning the extrusion program or the die geometry, the resulting release profiles remained unaffected. In summary, it was proven that the manufacturing temperature can simply be shifted towards lower values by specifically adjusting the process parameters and/or by properly choosing the die geometry. So, it is not necessarily the formulation that has to be changed.

Chapter V is about the mechanisms controlling drug release and focusses on the influence of the type of drug and the type of polymer. In a first attempt, implants containing either oxybutynin hydrochloride or oxybutynin base in a matrix of RG 502 H were prepared. Although the manufacturing technique was the same for both formulations, great differences could be observed. The extrudability and the release kinetics were tremendously affected. The former was reflected in the fact that the base-containing mixtures could be processed at 65 °C with the standard program (and at 60 °C with the optimized program in combination with a two-holed die) whereas at least 75 °C were necessary for the salt-containing mixtures. The latter became apparent during the *in vitro* release tests where the implants with the base were found to degrade much faster, which consequently resulted in an accelerated drug release. Investigations on the surface morphology, the water uptake, the mass loss, the pH of the release medium, the polymer molecular weight, and its glass transition temperature revealed that the base acts as a catalyst for the hydrolysis of the PLGA chains. In other words, the degradation and erosion behavior of the polymer proved to be the determining factor for the release of this API.

Moreover, the effect of different matrices - altogether made from poly(lactide-co-glycolide) or even pure poly(lactide) - was studied. RG 502 H that had been used by then was replaced by RG 502, RG 503 H, and R 202 H, respectively. As expected, the release profiles turned out to be strongly related to the polymer properties. The lag phase, for example, increased with increasing molecular weight or lactic to glycolic acid ratio. Regarding the extrudability, none of the matrix materials led to a remarkable reduction of the maximum piston force. Hence, they did not qualify for a process optimization towards lower extrusion temperatures.

With the outstanding release properties of oxybutynin base in mind, drug delivery systems with an innovative release strategy were developed. The idea was to combine both the 'slow' salt form and

the 'fast' base form of the API in one and the same implant. It was successfully shown that the release could be precisely controlled that way. If the polymer was additionally changed, almost every desired release profile could be achieved.

In order to get deeper insight into possibly occurring drug/polymer interactions, recovery studies in which dissolved oxybutynin was incubated in the presence of blank PLGA were carried out. Ionic interactions between positively charged drug molecules and negatively charged polymer chains could be detected. It was concluded that such interactions depend on the progress of polymer degradation and erosion.

Chapter VI introduces lipids as innovative excipients for the manufacturing of biodegradable implants based on poly(lactide-co-glycolide). It starts with the presentation of a lipid screening that was run with the intention of identifying promising candidates for a reduction of the maximum piston force and hence the extrusion temperature. Triglycerides, hydrogenated cocoglycerides, monoglycerides, acetylated glycerides, macrogolglycerides, and phosphatidylcholines were investigated. Among those, Dynacet 211 P and Gelucire 50/13 were best performing. If only 10% of the polymer in the implant formulation with oxybutynin hydrochloride were replaced by one of the lipids, maximum piston forces smaller than 3 kN could be achieved. For comparison, lipid-free formulations required around 18 kN. Since both initial and further drug release were still acceptable, the determination of the smallest possible process temperature and its impact on the release behavior were focused.

First, the influence of the acetylated glyceride was studied. In the presence of the salt form of the API, extrusion temperatures as low as 55 °C could be realized. The lipid was found to act as a plasticizer, that way reducing the glass transition temperature of the polymer. However, the major drawback of this approach were the resulting release data. The initial release which refers to the first 24 h increased drastically with decreasing process temperature. This was the reason why alternative manufacturing techniques were finally developed. 'Solvent casting' turned out to be the most efficient one. It might be described as pretreatment method that is intended to embed the drug particles in a dense matrix of PLGA before the lipid is added. In this manner, the burst release can drastically be lowered, and extrusion temperatures down to 40 °C can be achieved.

For the base, the smallest possible process temperature was also determined to be 55 °C. Investigations on the *in vitro* release and the mechanisms behind suggested that the API is retained by the lipid, presumably by hydrophobic interactions. Anyhow, the base-catalyzed acceleration of the

chain scission process of the polymer was shown to be switched off. Independent of the type of drug, the lipid was observed not to degrade during the release period.

In contrast, the macroglyceride completely dissolved within this timeframe. The addition of Gelucire 50/13 allowed for extrusion temperatures of 65 °C for oxybutynin hydrochloride and 50 °C for the corresponding base. Once more, this effect could be ascribed to the plasticizing effect of the lipid. Since the release profiles were comparable to the ones of the lipid-free implants, the macroglyceride qualified as interesting candidate for future applications.

Both Dynacet 211 P and Gelucire 50/13 are considered to be rather amphiphilic. For this reason, demixing of the single components upon extrusion could not be observed - even if 20% of the lipid were added. As opposed to this, highly hydrophobic lipids such as triglycerides or hydrogenated cocoglycerides induced phase separation. Implants with a lipidic core and a polymeric shell were formed. Independent from the drug loading that ranged between 5% and 20%, the release behavior was not affected. This great advantage was regrettably accompanied by the fact that the extrusion temperature could not be optimized for these formulations.

In conclusion, the main objective of this thesis could be achieved by different ways:

- ✓ Using an optimized parameter set together with the 'right' die
- ✓ Choosing the 'right' type of drug (and polymer)
- ✓ Adding amphiphilic lipids to the implant formulation

Of course, each of these methods has its own advantages and limitations, especially concerning the release properties. However, all of them were successfully shown to result in a reduction of the manufacturing temperature. This opens industrial ram extrusion to a variety of less stable thermosensitive drugs.

SUPPLEMENT

Table 11 | Rechtschaffner design calculated for seven variable extrusion parameters (pink) and response of the maximum piston force.

experiment number	run order	piston force/compression phase [N]	piston force/heating phases [N]	time/compression phase [min]	time/first heating phase [min]	time/second heating phase [min]	piston speed [mm/s]	temperature [°C]	maximum piston force [N]
1	7	1000	125	2	10	10	0.0025	75	2502.5
2	23	1000	500	20	20	20	0.0125	90	562.8
3	6	4000	125	20	20	20	0.0125	90	614.2
4	29	4000	500	2	20	20	0.0125	90	736.7
5	39	4000	500	20	10	20	0.0125	90	759.3
6	11	4000	500	20	20	10	0.0125	90	709.0
7	10	4000	500	20	20	20	0.0025	90	149.7
8	20	4000	500	20	20	20	0.0125	75	9279.7
9	8	4000	500	2	10	10	0.0025	75	2474.0
10	5	4000	125	20	10	10	0.0025	75	2489.5
11	12	4000	125	2	20	10	0.0025	75	1903.7
12	38	4000	125	2	10	20	0.0025	75	1877.2
13	13	4000	125	2	10	10	0.0125	75	9924.6
14	25	4000	125	2	10	10	0.0025	90	336.7
15	9	1000	500	20	10	10	0.0025	75	2778.1
16	14	1000	500	2	20	10	0.0025	75	1756.8
17	21	1000	500	2	10	20	0.0025	75	1997.6
18	33	1000	500	2	10	10	0.0125	75	13197.2
19	24	1000	500	2	10	10	0.0025	90	333.1
20	37	1000	125	20	20	10	0.0025	75	1877.7
21	2	1000	125	20	10	20	0.0025	75	2009.1
22	26	1000	125	20	10	10	0.0125	75	13883.1
23	3	1000	125	20	10	10	0.0025	90	337.3

experiment number	run order	piston force/compression phase [N]	piston force/heating phases [N]	time/compression phase [min]	time/first heating phase [min]	time/second heating phase [min]	piston speed [mm/s]	temperature [°C]	maximum piston force [N]
24	19	1000	125	2	20	20	0.0025	75	2071.1
25	32	1000	125	2	20	10	0.0125	75	10457.4
26	36	1000	125	2	20	10	0.0025	90	185.0
27	4	1000	125	2	10	20	0.0125	75	8930.3
28	35	1000	125	2	10	20	0.0025	90	208.0
29	16	1000	125	2	10	10	0.0125	90	1045.0
30	27	4000	312.5	11	15	15	0.0075	82.5	1378.5
31	31	2500	500	11	15	15	0.0075	82.5	1461.5
32	28	2500	312.5	20	15	15	0.0075	82.5	1470.2
33	22	2500	312.5	11	20	15	0.0075	82.5	1403.5
34	30	2500	312.5	11	15	20	0.0075	82.5	1703.5
35	18	2500	312.5	11	15	15	0.0125	82.5	2553.2
36	17	2500	312.5	11	15	15	0.0075	90	477.2
37	15	2500	312.5	11	15	15	0.0075	82.5	1407.8
38	34	2500	312.5	11	15	15	0.0075	82.5	1649.6
39	1	2500	312.5	11	15	15	0.0075	82.5	1537.1

REFERENCES

1. Smith, K.L., Schimpf, M.E. and Thompson, K.E., *Bioerodible polymers for delivery of macromolecules*. *Advanced Drug Delivery Reviews*, 1990. **4**(3): p. 343-357.
2. Hutchinson, F.G. and Furr, B.J.A., *Biodegradable carriers for the sustained release of polypeptides*. *Trends in Biotechnology*, 1987. **5**(4): p. 102-106.
3. Hutchinson, F.G. and Furr, B.J.A., *Biodegradable polymer systems for the sustained release of polypeptides*. *Journal of Controlled Release*, 1990. **13**(2-3): p. 279-294.
4. Guse, C., Könnings, S., Kreye, F., Siepmann, F., Göpferich, A. and Siepmann, J., *Drug release from lipid-based implants: Elucidation of the underlying mass transport mechanisms*. *International Journal of Pharmaceutics*, 2006. **314**(2): p. 137-144.
5. Mohl, S. and Winter, G., *Continuous release of rh-interferon α -2a from triglyceride matrices*. *Journal of Controlled Release*, 2004. **97**(1): p. 67-78.
6. Kreye, F., Siepmann, F. and Siepmann, J., *Drug release mechanisms of compressed lipid implants*. *International Journal of Pharmaceutics*, 2011. **404**(1-2): p. 27-35.
7. Langer, R.S. and Peppas, N.A., *Present and future applications of biomaterials in controlled drug delivery systems*. *Biomaterials*, 1981. **2**(4): p. 201-214.
8. Athanasiou, K.A., Niederauer, G.G. and Agrawal, C.M., *Sterilization, toxicity, biocompatibility and clinical applications of polylactic acid/ polyglycolic acid copolymers*. *Biomaterials*, 1996. **17**(2): p. 93-102.
9. Martinez, M., Rathbone, M., Burgess, D. and Huynh, M., *In vitro and in vivo considerations associated with parenteral sustained release products: A review based upon information presented and points expressed at the 2007 Controlled Release Society Annual Meeting*. *Journal of Controlled Release*, 2008. **129**(2): p. 79-87.
10. Hoffman, A.S., *The origins and evolution of "controlled" drug delivery systems*. *Journal of Controlled Release*, 2008. **132**(3): p. 153-163.
11. Folkman, J., Long, D.M. and Rosenbaum, R., *Silicone rubber: a new diffusion property useful for general anesthesia*. *Science*, 1966. **154**(3745): p. 148-149.
12. Folkman, J. and Long, D.M., *The use of silicone rubber as a carrier for prolonged drug therapy*. *Journal of Surgical Research*, 1964. **4**(3): p. 139-142.
13. Folkman, J., *How the field of controlled-release technology began, and its central role in the development of angiogenesis research*. *Biomaterials*, 1990. **11**(9): p. 615-618.
14. Langer, R. and Folkman, J., *Polymers for the sustained release of proteins and other macromolecules*. *Nature*, 1976. **263**: p. 797-800.
15. Jain, R.A., *The manufacturing techniques of various drug loaded biodegradable poly(lactide-co-glycolide) (PLGA) devices*. *Biomaterials*, 2000. **21**(23): p. 2475-2490.
16. Zhang, Y., Chan, H.F. and Leong, K.W., *Advanced materials and processing for drug delivery: The past and the future*. *Advanced Drug Delivery Reviews*, 2013. **65**(1): p. 104-120.
17. <http://www.mims.com/resources/drugs/Malaysia/pic/Zoladex%20depot%20inj%203.6%20mg6d00617c-6323-44d0-a782-9faa0009503a.GIF>, 27th January 2014.
18. Könnings, S., Berié, A., Tessmar, J., Blunk, T. and Göpferich, A., *Influence of wettability and surface activity on release behavior of hydrophilic substances from lipid matrices*. *Journal of Controlled Release*, 2007. **119**(2): p. 173-181.

19. Walsh, G., *Biopharmaceuticals: recent approvals and likely directions*. Trends in Biotechnology, 2005. **23**(11): p. 553-558.
20. Pavlou, A.K. and Reichert, J.M., *Recombinant protein therapeutics - success rates, market trends and values to 2010*. Nature Biotechnology, 2004. **22**(12): p. 1513-1519.
21. Iyer, S.S., Barr, W.H. and Karnes, H.T., *Profiling in vitro drug release from subcutaneous implants: a review of current status and potential implications on drug product development*. Biopharmaceutics & Drug Disposition, 2006. **27**(4): p. 157-170.
22. Shah, N.H., Railkar, A.S., Chen, F.C., Tarantino, R., Kumar, S., Murjani, M., Palmer, D., Infeld, M.H. and Malick, A.W., *A biodegradable injectable implant for delivering micro and macromolecules using poly (lactic-co-glycolic) acid (PLGA) copolymers*. Journal of Controlled Release, 1993. **27**(2): p. 139-147.
23. Adams, K. and Beal, M.W., *Implanon: A review of the literature with recommendations for clinical management*. Journal of Midwifery & Women's Health, 2009. **54**(2): p. 142-149.
24. *Long-acting Reversible Contraception: the Effective and Appropriate Use of Long-acting Reversible Contraception*, 2005, NICE Clinical Guidelines: London.
25. Mitchell, H., *Goserelin ('Zoladex') - offering patients more choice in early breast cancer*. European Journal of Oncology Nursing, 2004. **8**: p. 95-103.
26. Metz, R., Namer, M., Adenis, L., Audhuy, B., Bugat, R., Colombel, P., Couette, J., Grise, P., Khater, R., LePorz, B., Levin, G., Marti, P., Mauriac, M., Rouxel, A. and Tetelboum, R., *Zoladex: Endocrine effects, efficacy and safety in advanced prostate cancer. A French cooperative study*. European Journal of Cancer and Clinical Oncology, 1987. **23**(8): p. 1245.
27. Takahashi, M., Onishi, H. and Machida, Y., *Development of implant tablet for a week-long sustained release*. Journal of Controlled Release, 2004. **100**(1): p. 63-74.
28. Dorta, M.J., Santoveña, A., Llabrés, M. and Fariña, J.B., *Potential applications of PLGA film-implants in modulating in vitro drugs release*. International Journal of Pharmaceutics, 2002. **248**(1-2): p. 149-156.
29. *Fundamentals and Applications of Controlled Release Drug Delivery*. Advances in Delivery Science and Technology, Siepmann, J., Siegel, R.A. and Rathbone, M.J., editors. 2012.
30. Fredenberg, S., Wahlgren, M., Reslow, M. and Axelsson, A., *Pore formation and pore closure in poly(D,L-lactide-co-glycolide) films*. Journal of Controlled Release, 2011. **150**(2): p. 142-149.
31. Webber, W.L., Lago, F., Thanos, C. and Mathiowitz, E., *Characterization of soluble, salt-loaded, degradable PLGA films and their release of tetracycline*. Journal of Biomedical Materials Research, 1998. **41**(1): p. 18-29.
32. Matsumoto, A., Matsukawa, Y., Suzuki, T. and Yoshino, H., *Drug release characteristics of multi-reservoir type microspheres with poly(DL-lactide-co-glycolide) and poly(DL-lactide)*. Journal of Controlled Release, 2005. **106**(1-2): p. 172-180.
33. Batycky, R.P., Hanes, J., Langer, R. and Edwards, D.A., *A theoretical model of erosion and macromolecular drug release from biodegrading microspheres*. Journal of Pharmaceutical Sciences, 1997. **86**(12): p. 1464-1477.
34. Fredenberg, S., Wahlgren, M., Reslow, M. and Axelsson, A., *The mechanisms of drug release in poly(lactic-co-glycolic acid)-based drug delivery systems - A review*. International Journal of Pharmaceutics, 2011. **415**(1-2): p. 34-52.

35. Wang, J., Wang, B.M. and Schwendeman, S.P., *Characterization of the initial burst release of a model peptide from poly(D,L-lactide-co-glycolide) microspheres*. Journal of Controlled Release, 2002. **82**(2-3): p. 289-307.
36. Sax, G. and Winter, G., *Mechanistic studies on the release of lysozyme from twin-screw extruded lipid implants*. Journal of Controlled Release, 2012. **163**(2): p. 187-194.
37. Shah, S.S., Cha, Y. and Pitt, C.G., *Poly (glycolic acid-co-DL-lactic acid): diffusion or degradation controlled drug delivery?* Journal of Controlled Release, 1992. **18**(3): p. 261-270.
38. Göpferich, A., *Mechanisms of polymer degradation and erosion*. Biomaterials, 1996. **17**(2): p. 103-114.
39. Nair, L.S. and Laurencin, C.T., *Biodegradable polymers as biomaterials*. Progress in Polymer Science, 2007. **32**(8-9): p. 762-798.
40. Katti, D.S., Lakshmi, S., Langer, R. and Laurencin, C.T., *Toxicity, biodegradation and elimination of polyanhydrides*. Advanced Drug Delivery Reviews, 2002. **54**(7): p. 933-961.
41. Wischke, C. and Schwendeman, S.P., *Principles of encapsulating hydrophobic drugs in PLA/PLGA microparticles*. International Journal of Pharmaceutics, 2008. **364**(2): p. 298-327.
42. Raman, C., Berklund, C., Kim, K. and Pack, D.W., *Modeling small-molecule release from PLG microspheres: effects of polymer degradation and nonuniform drug distribution*. Journal of Controlled Release, 2005. **103**(1): p. 149-158.
43. Karlsson, O.J., Stubbs, J.M., Karlsson, L.E. and Sundberg, D.C., *Estimating diffusion coefficients for small molecules in polymers and polymer solutions*. Polymer, 2001. **42**(11): p. 4915-4923.
44. Brunner, A., Mäder, K. and Göpferich, A., *pH and osmotic pressure inside biodegradable microspheres during erosion*. Pharmaceutical Research, 1999. **16**(6): p. 847-853.
45. Fredenberg, S., Jönsson, M., Laakso, T., Wahlgren, M., Reslow, M. and Axelsson, A., *Development of mass transport resistance in poly(lactide-co-glycolide) films and particles - A mechanistic study*. International Journal of Pharmaceutics, 2011. **409**(1-2): p. 194-202.
46. Langer, R., *New methods of drug delivery*. Science, 1990. **249**(4976): p. 1527-1533.
47. Göpferich, A., *Erosion of composite polymer matrices*. Biomaterials, 1997. **18**(5): p. 397-403.
48. Hiremath, J.G., Khamar, N.S., Palavalli, S.G., Rudani, C.G., Aitha, R. and Mura, P., *Paclitaxel loaded carrier based biodegradable polymeric implants: Preparation and in vitro characterization*. Saudi Pharmaceutical Journal, 2013. **21**(1): p. 85-91.
49. Makadia, H.K. and Siegel, S.J., *Poly lactic-co-glycolic acid (PLGA) as biodegradable controlled drug delivery carrier*. Polymers, 2011. **3**(3): p. 1377-1397.
50. Almeida, A., Brabant, L., Siepmann, F., De Beer, T., Bouquet, W., van Hoorebeke, L., Siepmann, J., Remon, J.P. and Vervaet, C., *Sustained release from hot-melt extruded matrices based on ethylene vinyl acetate and polyethylene oxide*. European Journal of Pharmaceutics and Biopharmaceutics, 2012. **82**(3): p. 526-533.
51. Appel, B., Maschke, A., Weiser, B., Sarhan, H., Englert, C., Angele, P., Blunk, T. and Göpferich, A., *Lipidic implants for controlled release of bioactive insulin: Effects on cartilage engineered in vitro*. International Journal of Pharmaceutics, 2006. **314**(2): p. 170-178.
52. Schulze, S. and Winter, G., *Lipid extrudates as novel sustained release systems for pharmaceutical proteins*. Journal of Controlled Release, 2009. **134**(3): p. 177-185.

53. Kreye, F., Siepmann, F., Willart, J.F., Descamps, M. and Siepmann, J., *Drug release mechanisms of cast lipid implants*. European Journal of Pharmaceutics and Biopharmaceutics, 2011. **78**(3): p. 394-400.
54. Thakur, R.R.S., McMillan, H.L. and Jones, D.S., *Solvent induced phase inversion-based in situ forming controlled release drug delivery implants*. Journal of Controlled Release, 2014. **176**: p. 8-23.
55. Packhäuser, C.B., Schnieders, J., Oster, C.G. and Kissel, T., *In situ forming parenteral drug delivery systems: an overview*. European Journal of Pharmaceutics and Biopharmaceutics, 2004. **58**(2): p. 445-455.
56. Kempe, S. and Mäder, K., *In situ forming implants - an attractive formulation principle for parenteral depot formulations*. Journal of Controlled Release, 2012. **161**(2): p. 668-679.
57. Santhosh, K.J., Voruganti, S., Raju, T., Aravind, G. and Ravindra, B.D.S., *Formulation and development of in situ implants of cytarabine*. International Journal of Pharmacy and Pharmaceutical Sciences, 2012. **4**: p. 412-420.
58. Sartor, O., *Eligard: leuprolide acetate in a novel sustained-release delivery system*. Urology, 2003. **61**(2): p. 25-31.
59. Dong, W.Y., Körber, M., López Esguerra, V. and Bodmeier, R., *Stability of poly(D,L-lactide-co-glycolide) and leuprolide acetate in in-situ forming drug delivery systems*. Journal of Controlled Release, 2006. **115**(2): p. 158-167.
60. Körber, M., *Bioabbaubare in-situ Systeme*, in *Moderne Arzneiformen & Pharmazeutische Technologie*, Keck, C.M. and Müller, R.H., editors. 2012.
61. Padalkar, A.N., Shahi, S.R. and Thube, M.W., *Microparticles: an approach for betterment of drug delivery system*. International Journal of Pharma Research and Development, 2012. **3**(1): p. 99-115.
62. Veldhuis, G., Gironès, M. and Bingham, D., *Monodisperse microspheres for parenteral drug delivery*. Drug Delivery Technology, 2009. **9**(1).
63. Patel, R.M., *Parenteral suspension: an overview*. International Journal of Current Pharmaceutical Research, 2010. **2**(3): p. 4-13.
64. Hu, Z., Liu, Y., Yuan, W., Wu, F., Su, J. and Jin, T., *Effect of bases with different solubility on the release behavior of risperidone loaded PLGA microspheres*. Colloids and Surfaces B: Biointerfaces, 2011. **86**(1): p. 206-211.
65. Eerdeken, M., van Hove, I., Remmerie, B. and Mannaert, E., *Pharmacokinetics and tolerability of long-acting risperidone in schizophrenia*. Schizophrenia Research, 2004. **70**(1): p. 91-100.
66. Ereshefsky, L. and Mannaert, E., *Pharmacokinetic profile and clinical efficacy of long-acting risperidone: potential benefits of combining an atypical antipsychotic and a new delivery system*. Drugs in R&D, 2005. **6**(3): p. 129-137.
67. Jalil, R. and Nixon, J.R., *Biodegradable poly(lactic acid) and poly(lactide-co-glycolide) microcapsules: problems associated with preparative techniques and release properties*. Journal of Microencapsulation, 1990. **7**(3): p. 297-325.
68. Arshady, R., *Preparation of biodegradable microspheres and microcapsules: 2. Polylactides and related polyesters*. Journal of Controlled Release, 1991. **17**(1): p. 1-21.
69. Kim, K. and Pack, D.W., *Microspheres for drug delivery*, in *Biological and Biomedical Nanotechnology*, Ferrari, M., Lee, A.P. and Lee, J., editors. 2006. p. 19-50.

70. Singh, M.N., Hemant, K.S., Ram, M. and Shivakumar, H.G., *Microencapsulation: A promising technique for controlled drug delivery*. Research in Pharmaceutical Sciences, 2010. **5**(2): p. 65-77.
71. De Jong, W.H. and Borm, P.J., *Drug delivery and nanoparticles: Applications and hazards*. International Journal of Nanomedicine, 2008. **3**(2): p. 133-149.
72. Jokerst, J.V., Lobovkina, T., Zare, R.N. and Gambhir, S.S., *Nanoparticle PEGylation for imaging and therapy*. Nanomedicine, 2011. **6**(4): p. 715-728.
73. Prabhakar, U., Maeda, H., Jain, R.K., Sevick-Muraca, E.M., Zamboni, W., Farokhzad, O.C., Barry, S.T., Gabizon, A., Grodzinski, P. and Blakey, D.C., *Challenges and key considerations of the enhanced permeability and retention effect for nanomedicine drug delivery in oncology*. Cancer Research, 2013. **73**(8): p. 2412-2417.
74. Saha, K., Kim, S.T., Yan, B., Miranda, O.R., Alfonso, F.S., Shlosman, D. and Rotello, V.M., *Surface functionality of nanoparticles determines cellular uptake mechanisms in mammalian cells*. Small, 2013. **9**(2): p. 300-305.
75. Koo, O.M., Rubinstein, I. and Onyuksel, H., *Role of nanotechnology in targeted drug delivery and imaging: a concise review*. Nanomedicine: Nanotechnology, Biology and Medicine, 2005. **1**(3): p. 193-212.
76. Sirsi, S.R. and Borden, M.A., *State-of-the-art materials for ultrasound-triggered drug delivery*. Advanced Drug Delivery Reviews, 2013.
77. Kulkarni, P.R., Yadav, J.D. and Vaidya, K.A., *Liposomes: a novel drug delivery system*. International Journal of Current Pharmaceutical Research, 2011. **3**(2): p. 10-18.
78. Samad, A., Sultana, Y. and Aqil, M., *Liposomal drug delivery systems: an update review*. Current Drug Delivery, 2007. **4**(4): p. 297-305.
79. Taylor, K.M.G., Taylor, G., Kellaway, I.W. and Stevens, J., *Drug entrapment and release from multilamellar and reverse-phase evaporation liposomes*. International Journal of Pharmaceutics, 1990. **58**(1): p. 49-55.
80. Justo, O.R. and Moraes, Â.M., *Analysis of process parameters on the characteristics of liposomes prepared by ethanol injection with a view to process scale-up: Effect of temperature and batch volume*. Chemical Engineering Research and Design, 2011. **89**(6): p. 785-792.
81. Barnadas-Rodríguez, R. and Sabés, M., *Factors involved in the production of liposomes with a high-pressure homogenizer*. International Journal of Pharmaceutics, 2001. **213**(1-2): p. 175-186.
82. Seynhaeve, A.L.B., Dicheva, B.M., Hoving, S., Koning, G.A. and ten Hagen, T.L.M., *Intact Doxil is taken up intracellularly and released doxorubicin sequesters in the lysosome: Evaluated by in vitro/in vivo live cell imaging*. Journal of Controlled Release, 2013. **172**(1): p. 330-340.
83. Chang, H.-I. and Yeh, M.-K., *Clinical development of liposome-based drugs: formulation, characterization, and therapeutic efficacy*. International Journal of Nanomedicine, 2012. **7**: p. 49-60.
84. Ta, T. and Porter, T.M., *Thermosensitive liposomes for localized delivery and triggered release of chemotherapy*. Journal of Controlled Release, 2013. **169**(1-2): p. 112-125.
85. Liu, X. and Huang, G., *Formation strategies, mechanism of intracellular delivery and potential clinical applications of pH-sensitive liposomes*. Asian Journal of Pharmaceutical Sciences, 2013. **8**(6): p. 319-328.

86. Xu, W., Ling, P. and Zhang, T., *Polymeric micelles, a promising drug delivery system to enhance bioavailability of poorly water-soluble drugs*. Journal of Drug Delivery, 2013.
87. Riess, G., *Micellization of block copolymers*. Progress in Polymer Science, 2003. **28**(7): p. 1107-1170.
88. Jones, M.-C. and Leroux, J.-C., *Polymeric micelles - a new generation of colloidal drug carriers*. European Journal of Pharmaceutics and Biopharmaceutics, 1999. **48**(2): p. 101-111.
89. van Butsele, K., Sibret, P., Fustin, C.A., Gohy, J.F., Passirani, C., Benoit, J.P., Jérôme, R. and Jérôme, C., *Synthesis and pH-dependent micellization of diblock copolymer mixtures*. Journal of Colloid and Interface Science, 2009. **329**(2): p. 235-243.
90. Taillefer, J., Jones, M.C., Brasseur, N., van Lier, J.E. and Leroux, J.C., *Preparation and characterization of pH-responsive polymeric micelles for the delivery of photosensitizing anticancer drugs*. Journal of Pharmaceutical Sciences, 2000. **89**(1): p. 52-62.
91. Sezgin, Z., Yüksel, N. and Baykara, T., *Preparation and characterization of polymeric micelles for solubilization of poorly soluble anticancer drugs*. European Journal of Pharmaceutics and Biopharmaceutics, 2006. **64**(3): p. 261-268.
92. Kwon, G.S., *Polymeric micelles for delivery of poorly water-soluble compounds*. Critical Reviews in Therapeutic Drug Carrier Systems, 2003. **20**(5): p. 357-403.
93. Lavasanifar, A., Samuel, J. and Kwon, G.S., *Poly(ethylene oxide)-block-poly(L-amino acid) micelles for drug delivery*. Advanced Drug Delivery Reviews, 2002. **54**(2): p. 169-190.
94. Liu, Y., Wang, W., Yang, J., Zhou, C. and Sun, J., *pH-sensitive polymeric micelles triggered drug release for extracellular and intracellular drug targeting delivery*. Asian Journal of Pharmaceutical Sciences, 2013. **8**(3): p. 159-167.
95. Liu, T.-Y., Liu, K.-H., Liu, D.-M., Chen, S.-Y. and Chen, I.-W., *Temperature-sensitive nanocapsules for controlled drug release caused by magnetically triggered structural disruption*. Advanced Functional Materials, 2009. **19**(4): p. 616-623.
96. Dand, N.M., Patel, P.B., Ayre, A.P. and Kadam, V.J., *Polymeric micelles as a drug carrier for tumor targeting*. Chronicles of Young Scientists, 2013. **4**(2): p. 94-101.
97. Weng Larsen, S. and Larsen, C., *Critical factors influencing the in vivo performance of long-acting lipophilic solutions - impact on in vitro release method design*. The AAPS Journal, 2009. **11**(4): p. 762-770.
98. Chien, Y.W., *Long-acting parenteral drug formulations*. Journal of Parenteral Science and Technology, 1981. **35**(3): p. 106-139.
99. Zuidema, J., Kadir, F., Titulaer, H.A.C. and Oussoren, C., *Release and absorption rates of intramuscularly and subcutaneously injected pharmaceuticals (II)*. International Journal of Pharmaceutics, 1994. **105**(3): p. 189-207.
100. Benson, H.A. and Pranker, R.J., *Optimisation of drug delivery 6: modified-release parenterals*. Australian Journal of Hospital Pharmacy, 1998. **28**(2): p. 99-104.
101. Sudhakar, M., Kancharla, R. and Rao, V.U., *A review on sustained release injectable depot drug delivery systems*. PHARMANEST, 2013. **4**(2): p. 142-158.
102. Rutz, A., *Ölige Suspensionen als parenterale Depotsysteme für rekombinante Proteine*. Dissertation der Fakultät für Chemie und Pharmazie der Ludwig-Maximilians-Universität München, 2007.
103. <http://www.rote-liste.de/Online/jumpsearch>, 1st February 2014.

104. Luo, J.P., Hubbard, J.W. and Midha, K.K., *The roles of depot injection sites and proximal lymph nodes in the presystemic absorption of fluphenazine decanoate and fluphenazine: ex vivo experiments in rats*. *Pharmaceutical Research*, 1998. **15**(9): p. 1485-1489.
105. Matsunaga, Y., Nambu, K., Oh-e, Y., Miyazaki, H. and Hashimoto, M., *Absorption of intramuscularly administered [¹⁴C]haloperidol decanoate in rats*. *European Journal of Drug Metabolism and Pharmacokinetics*, 1987. **12**(3): p. 175-181.
106. Oh-e, Y., Miyazaki, H., Matsunaga, Y. and Hashimoto, M., *Pharmacokinetics of haloperidol decanoate in rats*. *Journal of Pharmacobiodynamics*, 1991. **14**(11): p. 615-622.
107. Huang, Y., Hubbard, J.W. and Midha, K.K., *The role of the lymphatic system in the presystemic absorption of fluphenazine after intramuscular administration of fluphenazine decanoate in rats*. *European Journal of Pharmaceutical Sciences*, 1995. **3**(1): p. 15-20.
108. Armstrong, N.A. and James, K.C., *Drug release from lipid-based dosage forms. I*. *International Journal of Pharmaceutics*, 1980. **6**(3-4): p. 185-193.
109. James, K.C., Nicholls, P.J. and Roberts, M., *Biological half-lives of [⁴⁻¹⁴C]testosterone and some of its esters after injection into the rat*. *Journal of Pharmacy and Pharmacology*, 1969. **21**(1): p. 24-27.
110. Al-Hindawi, M.K., James, K.C. and Nicholls, P.J., *Influence of solvent on the availability of testosterone propionate from oily, intramuscular injections in the rat*. *Journal of Pharmacy and Pharmacology*, 1987. **39**(2): p. 90-95.
111. Akers, M.J., Fites, A.L. and Robison, R.L., *Formulation design and development of parenteral suspensions*. *Journal of Parenteral Science and Technology*, 1987. **41**(3): p. 88-96.
112. *Materials in Biology and Medicine*. Green Chemistry and Chemical Engineering, Lee, S. and Henthorn, D., editors. 2012: CRC Press.
113. Maurus, P.B. and Kaeding, C.C., *Bioabsorbable implant material review*. *Operative Techniques in Sports Medicine*, 2004. **12**(3): p. 158-160.
114. Qian, J., Xu, W., Yong, X., Jin, X. and Zhang, W., *Fabrication and in vitro biocompatibility of biomorphic PLGA/nHA composite scaffolds for bone tissue engineering*. *Materials Science and Engineering: C*, 2014. **36**: p. 95-101.
115. Vozi, G., Flaim, C.J., Bianchi, F., Ahluwalia, A. and Bhatia, S., *Microfabricated PLGA scaffolds: a comparative study for application to tissue engineering*. *Materials Science and Engineering: C*, 2002. **20**(1-2): p. 43-47.
116. Yang, S., Chen, Y., Gu, K., Dash, A., Sayre, C.L., Davies, N.M. and Ho, E.A., *Novel intravaginal nanomedicine for the targeted delivery of saquinavir to CD4+ immune cells*. *International Journal of Nanomedicine*, 2013. **8**: p. 2847-2858.
117. Vert, M., Li, S. and Garreau, H., *New insights on the degradation of bioresorbable polymeric devices based on lactic and glycolic acids*. *Clinical Materials*, 1992. **10**(1-2): p. 3-8.
118. Allison, S.D., *Effect of structural relaxation on the preparation and drug release behavior of poly(lactic-co-glycolic)acid microparticle drug delivery systems*. *Journal of Pharmaceutical Sciences*, 2008. **97**(6): p. 2022-2035.
119. Mundargi, R.C., Babu, V.R., Rangaswamy, V., Patel, P. and Aminabhavi, T.M., *Nano/micro technologies for delivering macromolecular therapeutics using poly(D,L-lactide-co-glycolide) and its derivatives*. *Journal of Controlled Release*, 2008. **125**(3): p. 193-209.

120. Mohamed, F. and van der Walle, C.F., *Engineering biodegradable polyester particles with specific drug targeting and drug release properties*. Journal of Pharmaceutical Sciences, 2008. **97**(1): p. 71-87.
121. Singh Kaur, M.A., *Poly(DL-lactide-co-glycolide) 50:50 - hydrophilic polymer blends: hydrolysis, bioadhesion and drug release characterization*. Dissertation of the Graduate College of the University of Iowa, 2008.
122. Mank, R., Rafler, G. and Nerlich, B., *Parenterale Depotarzneiformen auf der Basis von biologisch abbaubaren Polymeren*. Pharmazie, 1991. **46**: p. 9-18.
123. Wise, D.L., Fellmann, T.D., Sanderson, J.E. and Wentworth, R.L., *Drug Carriers in Biology and Medicine*. Academic Press, Gregoriadis, G., editor. 1979, New York.
124. Völkel, C., *Einfluss von Polymereigenschaften auf pharmazeutisch-technologische und biopharmazeutische Eigenschaften von gepressten und in situ geformten Implantaten*. Dissertation der Mathematisch-Naturwissenschaftlich-Technischen Fakultät der Martin-Luther-Universität Halle-Wittenberg, 2003.
125. Södergård, A. and Stolt, M., *Properties of lactic acid based polymers and their correlation with composition*. Progress in Polymer Science, 2002. **27**(6): p. 1123-1163.
126. Zhou, S., Deng, X., Li, X., Jia, W. and Liu, L., *Synthesis and characterization of biodegradable low molecular weight aliphatic polyesters and their use in protein-delivery systems*. Journal of Applied Polymer Science, 2004. **91**(3): p. 1848-1856.
127. Astete, C.E. and Sabliov, C.M., *Synthesis and characterization of PLGA nanoparticles*. Journal of Biomaterials Science, Polymer Edition, 2006. **17**(3): p. 247-289.
128. Wang, N., Wu, X.S., Li, C. and Feng, M.F., *Synthesis, characterization, biodegradation, and drug delivery application of biodegradable lactic/glycolic acid polymers: I. Synthesis and characterization*. Journal of Biomaterials Science, Polymer Edition, 2000. **11**(3): p. 301-318.
129. Kricheldorf, H.R., Boettcher, C. and Tönnies, K.-U., *Polylactones: 23. Polymerization of racemic and meso D,L-lactide with various organotin catalysts - stereochemical aspects*. Polymer, 1992. **33**(13): p. 2817-2824.
130. Qian, H., Wohl, A.R., Crow, J.T., Macosko, C.W. and Hoyer, T.R., *A strategy for control of "random" copolymerization of lactide and glycolide: Application to synthesis of PEG-b-PLGA block polymers having narrow dispersity*. Macromolecules, 2011. **44**(18): p. 7132-7140.
131. Albertsson, A.C. and Srivastava, R.K., *Recent developments in enzyme-catalyzed ring-opening polymerization*. Advanced Drug Delivery Reviews, 2008. **60**(9): p. 1077-1093.
132. Asandei, A.D., Erkey, C., Burgess, D.J., Saquing, C., Saha, G. and Zolnik, B.S., *Preparation of drug delivery biodegradable PLGA nanocomposites and foams by supercritical CO₂ expanded ring opening polymerization and by rapid expansion from CHClF₂ supercritical solutions*. MRS Proceedings, 2004. **845**.
133. Kitchell, J.P. and Wise, D.L., *Poly(lactic/glycolic acid) biodegradable drug-polymer matrix systems*. Methods in Enzymology, 1985. **112**: p. 436-448.
134. Wu, X.S., *Synthesis and properties of biodegradable lactic/glycolic acid polymers*, in *Encyclopedic Handbook of Biomaterials and Bioengineering, Part A: Materials*, Wise, D.L., Trantolo, D.J., Altobelli, D.E. and Yaszemski, M.J., editors. 1995, Marcel Dekker: New York. p. 1015-1054.
135. [http://www.resomer.com/product/biodegradable-polymers/en/applications-products/products/pages/default.aspx#Controlled release](http://www.resomer.com/product/biodegradable-polymers/en/applications-products/products/pages/default.aspx#Controlled%20release), 2nd March 2014.

136. Vey, E., Roger, C., Meehan, L., Booth, J., Claybourn, M., Miller, A.F. and Saiani, A., *Degradation mechanism of poly(lactic-co-glycolic) acid block copolymer cast films in phosphate buffer solution*. *Polymer Degradation and Stability*, 2008. **93**(10): p. 1869-1876.
137. Young, R.J. and Lovell, P.A., *Introduction to Polymers*. 1991, London: CRC Press.
138. Gunatillake, P., Mayadunne, R. and Adhikari, R., *Recent developments in biodegradable synthetic polymers*. *Biotechnology Annual Review*, 2006. **12**: p. 301-347.
139. Miller, R.A., Brady, J.M. and Cutright, D.E., *Degradation rates of oral resorbable implants (polylactates and polyglycolates): rate modification with changes in PLA/PGA copolymer ratios*. *Journal of Biomedical Materials Research*, 1977. **11**(5): p. 711-719.
140. Gilding, D.K. and Reed, A.M., *Biodegradable polymers for use in surgery - poly(glycolic)/poly(lactic acid) homo- and copolymers: 1*. *Polymer*, 1979. **20**(12): p. 1459-1464.
141. Loo, S.C.J., Ooi, C.P., Wee, S.H.E. and Boey, Y.C.F., *Effect of isothermal annealing on the hydrolytic degradation rate of poly(lactide-co-glycolide) (PLGA)*. *Biomaterials*, 2005. **26**(16): p. 2827-2833.
142. Klose, D., Siepmann, F., Elkharraz, K. and Siepmann, J., *PLGA-based drug delivery systems: Importance of the type of drug and device geometry*. *International Journal of Pharmaceutics*, 2008. **354**(1-2): p. 95-103.
143. Uhrich, K.E., Cannizzaro, S.M., Langer, R.S. and Shakesheff, K.M., *Polymeric systems for controlled drug release*. *Chemical Reviews*, 1999. **99**(11): p. 3181-3198.
144. Wu, X.S. and Wang, N., *Synthesis, characterization, biodegradation, and drug delivery application of biodegradable lactic/glycolic acid polymers. Part II: biodegradation*. *Journal of Biomaterials Science, Polymer Edition*, 2001. **12**(1): p. 21-34.
145. Regnier-Delplace, C., Thillaye du Boullay, O., Siepmann, F., Martin-Vaca, B., Degrave, N., Demonchaux, P., Jentzer, O., Bourissou, D. and Siepmann, J., *PLGA microparticles with zero-order release of the labile anti-Parkinson drug apomorphine*. *International Journal of Pharmaceutics*, 2013. **443**(1-2): p. 68-79.
146. Huang, X. and Brazel, C.S., *On the importance and mechanisms of burst release in matrix-controlled drug delivery systems*. *Journal of Controlled Release*, 2001. **73**(2-3): p. 121-136.
147. von Burkersroda, F., Schedl, L. and Göpferich, A., *Why degradable polymers undergo surface erosion or bulk erosion*. *Biomaterials*, 2002. **23**(21): p. 4221-4231.
148. Klose, D., Delplace, C. and Siepmann, J., *Unintended potential impact of perfect sink conditions on PLGA degradation in microparticles*. *International Journal of Pharmaceutics*, 2011. **404**(1-2): p. 75-82.
149. Ulery, B.D., Nair, L.S. and Laurencin, C.T., *Biomedical applications of biodegradable polymers*. *Journal of Polymer Science Part B: Polymer Physics*, 2011. **49**(12): p. 832-864.
150. Göpferich, A., *Polymer bulk erosion*. *Macromolecules*, 1997. **30**(9): p. 2598-2604.
151. Göpferich, A. and Langer, R., *Modeling of polymer erosion in three dimensions: Rotationally symmetric devices*. *AIChE Journal*, 1995. **41**(10): p. 2292-2299.
152. Li, L. and Schwendeman, S.P., *Mapping neutral microclimate pH in PLGA microspheres*. *Journal of Controlled Release*, 2005. **101**(1-3): p. 163-173.
153. Li, S. and McCarthy, S., *Further investigations on the hydrolytic degradation of poly (DL-lactide)*. *Biomaterials*, 1999. **20**(1): p. 35-44.

154. Anderson, J.M., *Biological responses to materials*. Annual Review of Materials Research, 2001. **31**: p. 81-110.
155. Tice, T.R. and Tabibi, E.S., *Parenteral drug delivery: injectables*, in *Treatise on Controlled Drug Delivery: Fundamentals, Optimization, Applications*, Kydonieus, A., editor. 1991, Marcel Dekker: New York. p. 315-339.
156. Anderson, J.M. and Shive, M.S., *Biodegradation and biocompatibility of PLA and PLGA microspheres*. Advanced Drug Delivery Reviews, 1997. **28**(1): p. 5-24.
157. Anderson, J.M., Rodriguez, A. and Chang, D.T., *Foreign body reaction to biomaterials*. Seminars in Immunology, 2008. **20**(2): p. 86-100.
158. Yoon, S.J., Kim, S.H., Ha, H.J., Ko, Y.K., So, J.W., Kim, M.S., Yang, Y.I., Khang, G., Rhee, J.M. and Lee, H.B., *Reduction of inflammatory reaction of poly(D,L-lactic-co-glycolic acid) using demineralized bone particles*. Tissue Engineering Part A, 2008. **14**(4): p. 539-547.
159. http://www.accessdata.fda.gov/drugsatfda_docs/label/2007/021731s005,021488s010,021379s010,021343s015lbl.pdf, 23rd February 2014.
160. Fahy, E., Subramaniam, S., Brown, H.A., Glass, C.K., Merrill, A.H., Murphy, R.C., Raetz, C.R., Russell, D.W., Seyama, Y., Shaw, W., Shimizu, T., Spener, F., van Meer, G., VanNieuwenhze, M.S., White, S.H., Witztum, J.L. and Dennis, E.A., *A comprehensive classification system for lipids*. Journal of Lipid Research, 2005. **46**(5): p. 839-861.
161. *Oxford Dictionary of Biochemistry and Molecular Biology*. 2nd edition, Cammack, R., Atwood, T., Campbell, P., Parish, H. and Smith, A., editors. 2000, Oxford: Oxford University Press.
162. <http://dwb.unl.edu/Teacher/NSF/C10/C10Links/mills.edu/RESEARCH/FUTURES/JOHNB/structurefunction/724.html>, 22nd March 2014.
163. Schwab, M., Sax, G., Schulze, S. and Winter, G., *Studies on the lipase induced degradation of lipid based drug delivery systems*. Journal of Controlled Release, 2009. **140**(1): p. 27-33.
164. Sullivan, M.F., Ruemmler, P.S. and Kalkwarf, D.R., *Sustained administration of cyclazocine for antagonism of morphine*. Drug and Alcohol Dependence, 1976. **1**(6): p. 415-428.
165. Joseph, A.A., Hill, J.L., Patel, J., Patel, S. and Kincl, F.A., *Sustained-release hormonal preparations XV: release of progesterone from cholesterol pellets in vivo*. Journal of Pharmaceutical Sciences, 1977. **66**(4): p. 490-493.
166. Fu, K., Klibanov, A.M. and Langer, R., *Protein stability in controlled-release systems*. Nature Biotechnology, 2000. **18**(1): p. 24-25.
167. Pérez, C., Castellanos, I.J., Costantino, H.R., Al-Azzam, W. and Griebenow, K., *Recent trends in stabilizing protein structure upon encapsulation and release from bioerodible polymers*. Journal of Pharmacy and Pharmacology, 2002. **54**(3): p. 301-313.
168. Jorgensen, L., Moeller, E.H., van de Weert, M., Nielsen, H.M. and Frokjaer, S., *Preparing and evaluating delivery systems for proteins*. European Journal of Pharmaceutical Sciences, 2006. **29**(3-4): p. 174-182.
169. Könnings, S., Sapin, A., Blunk, T., Menei, P. and Göpferich, A., *Towards controlled release of BDNF - Manufacturing strategies for protein-loaded lipid implants and biocompatibility evaluation in the brain*. Journal of Controlled Release, 2007. **119**(2): p. 163-172.
170. Maschke, A., Becker, C., Eyrich, D., Kiermaier, J., Blunk, T. and Göpferich, A., *Development of a spray congealing process for the preparation of insulin-loaded lipid microparticles and characterization thereof*. European Journal of Pharmaceutics and Biopharmaceutics, 2007. **65**(2): p. 175-187.

171. Herrmann, S., Winter, G., Mohl, S., Siepmann, F. and Siepmann, J., *Mechanisms controlling protein release from lipidic implants: Effects of PEG addition*. Journal of Controlled Release, 2007. **118**(2): p. 161-168.
172. Sinha, V.R. and Trehan, A., *Biodegradable microspheres for protein delivery*. Journal of Controlled Release, 2003. **90**(3): p. 261-280.
173. Guse, C., Könnings, S., Maschke, A., Hacker, M., Becker, C., Schreiner, S., Blunk, T., Spruss, T. and Göpferich, A., *Biocompatibility and erosion behavior of implants made of triglycerides and blends with cholesterol and phospholipids*. International Journal of Pharmaceutics, 2006. **314**(2): p. 153-160.
174. Herrmann, S., *Lipidic implants for pharmaceutical proteins: mechanisms of release and development of extruded devices*. Dissertation der Fakultät für Chemie und Pharmazie der Ludwig-Maximilians-Universität München, 2007.
175. Lucke, A. and Göpferich, A., *Acylation of peptides by lactic acid solutions*. European Journal of Pharmaceutics and Biopharmaceutics, 2003. **55**(1): p. 27-33.
176. Zhu, G., Mallery, S.R. and Schwendeman, S.P., *Stabilization of proteins encapsulated in injectable poly (lactide- co-glycolide)*. Nature Biotechnology, 2000. **18**(1): p. 52-57.
177. Zhu, G. and Schwendeman, S.P., *Stabilization of proteins encapsulated in cylindrical poly(lactide-co-glycolide) implants: mechanism of stabilization by basic additives*. Pharmaceutical Research, 2000. **17**(3): p. 351-357.
178. Giteau, A., Venier-Julienne, M.C., Aubert-Pouëssel, A. and Benoit, J.P., *How to achieve sustained and complete protein release from PLGA-based microparticles?* International Journal of Pharmaceutics, 2008. **350**(1-2): p. 14-26.
179. Ghalanbor, Z., Körber, M. and Bodmeier, R., *Improved lysozyme stability and release properties of poly(lactide-co-glycolide) implants prepared by hot-melt extrusion*. Pharmaceutical Research, 2010. **27**(2): p. 371-379.
180. *Design of Organic Solids*, Weber, E., Aoyama, Y., Caira, M.R., Desiraju, G.R., Glusker, J.P., Hamilton, A.D., Meléndez, R.E. and Nangia, A., editors. Vol. 198. 1998: Springer-Verlag.
181. Sato, K., Ueno, S. and Yano, J., *Molecular interactions and kinetic properties of fats*. Progress in Lipid Research, 1999. **38**(1): p. 91-116.
182. Threlfall, T., *Structural and thermodynamic explanations of Ostwald's rule*. Organic Process Research & Development, 2003. **7**(6): p. 1017-1027.
183. Eldem, T., Speiser, P. and Hincal, A., *Optimization of spray-dried and -congealed lipid micropellets and characterization of their surface morphology by scanning electron microscopy*. Pharmaceutical Research, 1991. **8**(1): p. 47-54.
184. Sax, G.L., *Twin-screw extruded lipid implants for controlled protein drug delivery*. Dissertation der Fakultät für Chemie und Pharmazie der Ludwig-Maximilians-Universität München, 2012.
185. Siegel, R.A., Kost, J. and Langer, R., *Mechanistic studies of macromolecular drug release from macroporous polymers. I. Experiments and preliminary theory concerning completeness of drug release*. Journal of Controlled Release, 1989. **8**(3): p. 223-236.
186. Sax, G., Feil, F., Schulze, S., Jung, C., Bräuchle, C. and Winter, G., *Release pathways of interferon $\alpha 2a$ molecules from lipid twin screw extrudates revealed by single molecule fluorescence microscopy*. Journal of Controlled Release, 2012. **162**(2): p. 295-302.

187. Siepmann, F., Herrmann, S., Winter, G. and Siepmann, J., *A novel mathematical model quantifying drug release from lipid implants*. Journal of Controlled Release, 2008. **128**(3): p. 233-240.
188. Herrmann, S., Mohl, S., Siepmann, F., Siepmann, J. and Winter, G., *New insight into the role of polyethylene glycol acting as protein release modifier in lipidic implants*. Pharmaceutical Research, 2007. **24**(8): p. 1527-1537.
189. Mohl, S., *The development of a sustained and controlled release device for pharmaceutical proteins based on lipid implants*. Dissertation der Fakultät für Chemie und Pharmazie der Ludwig-Maximilians-Universität München, 2004.
190. Vogelhuber, W., Magni, E., Gazzaniga, A. and Göpferich, A., *Monolithic glyceryl trimyristate matrices for parenteral drug release applications*. European Journal of Pharmaceutics and Biopharmaceutics, 2003. **55**(1): p. 133-138.
191. Vogelhuber, W., Magni, E., Mouro, M., Spruss, T., Guse, C., Gazzaniga, A. and Göpferich, A., *Monolithic triglyceride matrices: a controlled-release system for proteins*. Pharmaceutical Development and Technology, 2003. **8**(1): p. 71-79.
192. Schwab, M., Kessler, B., Wolf, E., Jordan, G., Mohl, S. and Winter, G., *Correlation of in vivo and in vitro release data for rh-INF α lipid implants*. European Journal of Pharmaceutics and Biopharmaceutics, 2008. **70**(2): p. 690-694.
193. Khan, M.Z.I., Tucker, I.G. and Opdebeeck, J.P., *Cholesterol and lecithin implants for sustained release of antigen: release and erosion in vitro, and antibody response in mice*. International Journal of Pharmaceutics, 1991. **76**(1-2): p. 161-170.
194. Allababidi, S. and Shah, J.C., *Efficacy and pharmacokinetics of site-specific cefazolin delivery using biodegradable implants in the prevention of post-operative wound infections*. Pharmaceutical Research, 1998. **15**(2): p. 325-333.
195. Sax, G., Kessler, B., Wolf, E. and Winter, G., *In-vivo biodegradation of extruded lipid implants in rabbits*. Journal of Controlled Release, 2012. **163**(2): p. 195-202.
196. Reithmeier, H., Herrmann, J. and Göpferich, A., *Lipid microparticles as a parenteral controlled release device for peptides*. Journal of Controlled Release, 2001. **73**(2-3): p. 339-350.
197. Könnings, S., Garcion, E., Faisant, N., Menei, P., Benoit, J.P. and Göpferich, A., *In vitro investigation of lipid implants as a controlled release system for interleukin-18*. International Journal of Pharmaceutics, 2006. **314**(2): p. 145-152.
198. Ramchandani, M. and Robinson, D., *In vitro and in vivo release of ciprofloxacin from PLGA 50:50 implants*. Journal of Controlled Release, 1998. **54**(2): p. 167-175.
199. Santoveña, A., Álvarez-Lorenzo, C., Llabrés, M., Concheiro, A. and Fariña, J.B., *hGH release from directly compressed hGH-PLGA biodegradable implantable tablets: Influence of physicochemical factors*. European Polymer Journal, 2009. **45**(10): p. 2830-2838.
200. Crowley, M.M., Zhang, F., Repka, M.A., Thumma, S., Upadhye, S.B., Battu, S.K., McGinity, J.W. and Martin, C., *Pharmaceutical applications of hot-melt extrusion: part I*. Drug Development and Industrial Pharmacy, 2007. **33**(9): p. 909-926.
201. Williams, M., Tian, Y., Jones, D.S. and Andrews, G.P., *Hot-melt extrusion technology: optimizing drug delivery*. European Industrial Pharmacy, 2010(7): p. 7-10.
202. DiNunzio, J.C., Martin, C. and Zhang, F., *Melt extrusion - Shaping drug delivery in the 21st century*. Pharmaceutical Technology, 2010: p. 31-37.

203. Breitenbach, J., *Melt extrusion: from process to drug delivery technology*. European Journal of Pharmaceutics and Biopharmaceutics, 2002. **54**(2): p. 107-117.
204. Madan, S. and Madan, S., *Hot melt extrusion and its pharmaceutical applications*. Asian Journal of Pharmaceutical Sciences, 2012. **7**(2): p. 123-133
205. Repka, M.A., Battu, S.K., Upadhye, S.B., Thumma, S., Crowley, M.M., Zhang, F., Martin, C. and McGinity, J.W., *Pharmaceutical applications of hot-melt extrusion: Part II*. Drug Development and Industrial Pharmacy, 2007. **33**(10): p. 1043-1057.
206. Breitenbach, J., *Feste Lösungen durch Schmelzextrusion - ein integriertes Herstellkonzept*. Pharmazie in unserer Zeit, 2000. **29**(1): p. 46-49.
207. Rothen-Weinhold, A., Besseghir, K., Vuaridel, E., Sublet, E., Oudry, N., Kubel, F. and Gurny, R., *Injection-molding versus extrusion as manufacturing technique for the preparation of biodegradable implants*. European Journal of Pharmaceutics and Biopharmaceutics, 1999. **48**(2): p. 113-121.
208. Singhal, S., Lohar, V.K. and Arora, V., *Hot melt extrusion technique*. WebmedCentral, 2011. **2**(1): p. 1-20.
209. Chokshi, R. and Zia, H., *Hot-melt extrusion technique: a review*. Iranian Journal of Pharmaceutical Research, 2004. **3**: p. 3-16.
210. Pahl, M.H., *Dynamische Mischer für hochviskose Flüssigkeiten, Mischen von Kunststoffen*. 1983, Düsseldorf: VDI-Verlag.
211. Ghalanbor, Z., Körber, M. and Bodmeier, R., *Protein release from poly(lactide-co-glycolide) implants prepared by hot-melt extrusion: Thioester formation as a reason for incomplete release*. International Journal of Pharmaceutics, 2012. **438**(1-2): p. 302-306.
212. Todd, R.H., Allen, D.K. and Alting, L., *Manufacturing Processes Reference Guide*. 1994: Industrial Press.
213. Zema, L., Loreti, G., Melocchi, A., Maroni, A. and Gazzaniga, A., *Injection molding and its application to drug delivery*. Journal of Controlled Release, 2012. **159**(3): p. 324-331.
214. *Injection and Compression Molding Fundamentals*, Isayev, A.I., editor. 1987, New York: Marcel Dekker.
215. *Polymeric Biomaterials*. 2nd edition, Dumitriu, S., editor. 2002, New York: Marcel Dekker.
216. Witt, C., Mäder, K. and Kissel, T., *The degradation, swelling and erosion properties of biodegradable implants prepared by extrusion or compression moulding of poly(lactide-co-glycolide) and ABA triblock copolymers*. Biomaterials, 2000. **21**(9): p. 931-938.
217. Santoveña, A., Álvarez-Lorenzo, C., Concheiro, A., Llabrés, M. and Fariña, J.B., *Rheological properties of PLGA film-based implants: correlation with polymer degradation and SPf66 antimalaric synthetic peptide release*. Biomaterials, 2004. **25**(5): p. 925-931.
218. Sung, K.C., Han, R.-Y., Hu, O.Y.P. and Hsu, L.-R., *Controlled release of nalbuphine prodrugs from biodegradable polymeric matrices: influence of prodrug hydrophilicity and polymer composition*. International Journal of Pharmaceutics, 1998. **172**(1-2): p. 17-25.
219. Frank, A., Rath, S.K. and Venkatraman, S.S., *Controlled release from bioerodible polymers: effect of drug type and polymer composition*. Journal of Controlled Release, 2005. **102**(2): p. 333-344.

220. Wang, C.K., Wang, W.Y., Meyer, R.F., Liang, Y., Winey, K.I. and Siegel, S.J., *A rapid method for creating drug implants: translating laboratory-based methods into a scalable manufacturing process*. Journal of Biomedical Materials Research Part B: Applied Biomaterials, 2010. **93**(2): p. 562-572.
221. Bhardwaj, R. and Blanchard, J., *In vitro characterization and in vivo release profile of a poly (D,L-lactide-co-glycolide)-based implant delivery system for the α -MSH analog, melanotan-I*. International Journal of Pharmaceutics, 1998. **170**(1): p. 109-117.
222. Schiffter, H.A., *The delivery of drugs - Peptides and proteins*, in *Comprehensive Biotechnology*. 2nd edition, Moo-Young, M., editor. 2011, Academic Press: Burlington. p. 587-604.
223. http://www.goettfert.com/index.php?option=com_content&view=article&id=125:rheograph-25e&catid=33:produktdetails&Itemid=154, 23rd June 2013.
224. Rothen-Weinhold, A., Besseghir, K. and Gurny, R., *Analysis of the influence of polymer characteristics and core loading on the in vivo release of a somatostatin analogue*. European Journal of Pharmaceutical Sciences, 1997. **5**(6): p. 303-313.
225. Blasi, P., D'Souza, S.S., Selmin, F. and DeLuca, P.P., *Plasticizing effect of water on poly(lactide-co-glycolide)*. Journal of Controlled Release, 2005. **108**(1): p. 1-9.
226. Fitzgerald, J.F. and Corrigan, O.I., *Investigation of the mechanisms governing the release of levamisole from poly-lactide-co-glycolide delivery systems*. Journal of Controlled Release, 1996. **42**(2): p. 125-132.
227. Reil, M., *Systematische Prozessoptimierung unter Einsatz der statistischen Versuchsplanung (DoE)*. TechnoPharm, 2012. **2**(6): p. 414-419.
228. Qu, X., *Statistical properties of Rechtschaffner designs*. Journal of Statistical Planning and Inference, 2007. **137**(7): p. 2156-2164.
229. MODDE 9, software, Umetrics, Umeå, Sweden.
230. Wan, J. and Rickman, C., *The durability of intravesical oxybutynin solutions over time*. The Journal of Urology, 2007. **178**(4): p. 1768-1770.
231. Rabin, C., Liang, Y., Ehrlichman, R.S., Budhian, A., Metzger, K.L., Majewski-Tiedeken, C., Winey, K.I. and Siegel, S.J., *In vitro and in vivo demonstration of risperidone implants in mice*. Schizophrenia Research, 2008. **98**(1-3): p. 66-78.
232. Siegel, S.J., Kahn, J.B., Metzger, K., Winey, K.I., Werner, K. and Dan, N., *Effect of drug type on the degradation rate of PLGA matrices*. European Journal of Pharmaceutics and Biopharmaceutics, 2006. **64**(3): p. 287-293.
233. Miyajima, M., Koshika, A., Okada, J., Kusai, A. and Ikeda, M., *The effects of drug physico-chemical properties on release from copoly (lactic/glycolic acid) matrix*. International Journal of Pharmaceutics, 1998. **169**(2): p. 255-263.
234. http://worldaccount.basf.com/wa/NAFTA~es_MX/Catalog/Pharma/doc4/BASF/PRD/30274613/Material%20Safety%20Data%20Sheet-US-EN.pdf?title=&asset_type=msds/pdf&language=EN&validArea=US&urn=urn:documentum:ProductBase_EU:09007af8800d1cab.pdf, 24th July 2013.
235. http://worldaccount.basf.com/wa/NAFTA~en_US/Catalog/Pharma/doc4/BASF/PRD/30274707/.pdf?title=&asset_type=msds/pdf&language=EN&validArea=US&urn=urn:documentum:ProductBase_EU:09007af8800d76af.pdf, 24th July 2013.

236. Volland, C., Wolff, M. and Kissel, T., *The influence of terminal gamma-sterilization on captopril containing poly(D,L-lactide-co-glycolide) microspheres*. Journal of Controlled Release, 1994. **31**(3): p. 293-305.
237. Faisant, N., Akiki, J., Siepmann, F., Benoit, J.P. and Siepmann, J., *Effects of the type of release medium on drug release from PLGA-based microparticles: Experiment and theory*. International Journal of Pharmaceutics, 2006. **314**(2): p. 189-197.
238. Agrawal, C.M. and Athanasiou, K.A., *Technique to control pH in vicinity of biodegrading PLA-PGA implants*. Journal of Biomedical Materials Research, 1997. **38**(2): p. 105-114.
239. Meunier, D.M., *Molecular weight determinations*, in *Handbook of Instrumental Techniques for Analytical Chemistry*, Settle, F.A., editor. 1997, Prentice Hall PTR. p. 853-866.
240. <http://pslc.ws/macrog/weight.htm>, 27th July 2013.
241. Cha, Y. and Pitt, C.G., *The acceleration of degradation-controlled drug delivery from polyester microspheres*. Journal of Controlled Release, 1989. **8**(3): p. 259-265.
242. Gallagher, K.M. and Corrigan, O.I., *Mechanistic aspects of the release of levamisole hydrochloride from biodegradable polymers*. Journal of Controlled Release, 2000. **69**(2): p. 261-272.
243. Mollo, A.R. and Corrigan, O.I., *Effect of poly-hydroxy aliphatic ester polymer type on amoxicillin release from cylindrical compacts*. International Journal of Pharmaceutics, 2003. **268**(1-2): p. 71-79.
244. Trindade, R.A., Kiyohara, P.K., de Araujo, P.S. and Bueno da Costa, M.H., *PLGA microspheres containing bee venom proteins for preventive immunotherapy*. International Journal of Pharmaceutics, 2012. **423**(1): p. 124-133.
245. Husmann, M., Schenderlein, S., Lück, M., Lindner, H. and Kleinebudde, P., *Polymer erosion in PLGA microparticles produced by phase separation method*. International Journal of Pharmaceutics, 2002. **242**(1-2): p. 277-280.
246. Tracy, M.A., Ward, K.L., Firouzabadian, L., Wang, Y., Dong, N., Qian, R. and Zhang, Y., *Factors affecting the degradation rate of poly(lactide-co-glycolide) microspheres in vivo and in vitro*. Biomaterials, 1999. **20**(11): p. 1057-1062.
247. Lu, L., Garcia, C.A. and Mikos, A.G., *In vitro degradation of thin poly(DL-lactic-co-glycolic acid) films*. Journal of Biomedical Materials Research, 1999. **46**(2): p. 236-244.
248. Zilberman, M. and Grinberg, O., *HRP-loaded bioresorbable microspheres: effect of copolymer composition and molecular weight on microstructure and release profile*. Journal of Biomaterials Applications, 2008. **22**(5): p. 391-407.
249. Blanco-Príeto, M.J., Campanero, M.A., Besseghir, K., Heimgatner, F. and Gander, B., *Importance of single or blended polymer types for controlled in vitro release and plasma levels of a somatostatin analogue entrapped in PLA/PLGA microspheres*. Journal of Controlled Release, 2004. **96**(3): p. 437-448.
250. Duvvuri, S., Gaurav Janoria, K. and Mitra, A.K., *Effect of polymer blending on the release of ganciclovir from PLGA microspheres*. Pharmaceutical Research, 2006. **23**(1): p. 215-223.
251. Okada, H., *One- and three-month release injectable microspheres of the LH-RH superagonist leuprorelin acetate*. Advanced Drug Delivery Reviews, 1997. **28**(1): p. 43-70.
252. Jiang, G., Woo, B.H., Kang, F., Singh, J. and DeLuca, P.P., *Assessment of protein release kinetics, stability and protein polymer interaction of lysozyme encapsulated poly(D,L-lactide-co-glycolide) microspheres*. Journal of Controlled Release, 2002. **79**(1-3): p. 137-145.

253. *The Merck Index: An Encyclopedia of Chemicals, Drugs, and Biologicals*, O'Neil, M.J., Heckelman, P.E., Koch, C.B., Roman, K.J., Kenny, C.M. and D'Arecca, M.R., editors. 2006: Wiley.
254. Park, T.G., Lu, W. and Crotts, G., *Importance of in vitro experimental conditions on protein release kinetics, stability and polymer degradation in protein encapsulated poly (D,L-lactic acid-co-glycolic acid) microspheres*. *Journal of Controlled Release*, 1995. **33**(2): p. 211-222.
255. El-Gindy, A., *High performance liquid chromatographic determination of oxeladin citrate and oxybutynin hydrochloride and their degradation products*. *Il Farmaco*, 2005. **60**(8): p. 689-699.
256. Wagieh, N.E., Hegazy, M.A., Abdelkawy, M. and Abdelaleem, E.A., *Quantitative determination of oxybutynin hydrochloride by spectrophotometry, chemometry and HPTLC in presence of its degradation product and additives in different pharmaceutical dosage forms*. *Talanta*, 2010. **80**(5): p. 2007-2015.
257. Houchin, M.L., Neuenswander, S.A. and Topp, E.M., *Effect of excipients on PLGA film degradation and the stability of an incorporated peptide*. *Journal of Controlled Release*, 2007. **117**(3): p. 413-420.
258. Samadi, N., Abbadessa, A., Di Stefano, A., van Nostrum, C.F., Vermonden, T., Rahimian, S., Teunissen, E.A., van Steenberghe, M.J., Amidi, M. and Hennink, W.E., *The effect of lauryl capping group on protein release and degradation of poly(D,L-lactic-co-glycolic acid) particles*. *Journal of Controlled Release*, 2013. **172**(2): p. 436-443.
259. Schliecker, G., Schmidt, C., Fuchs, S., Ehinger, A., Sandow, J. and Kissel, T., *In vitro and in vivo correlation of busserelin release from biodegradable implants using statistical moment analysis*. *Journal of Controlled Release*, 2004. **94**(1): p. 25-37.
260. Ramchandani, M., Pankaskie, M. and Robinson, D., *The influence of manufacturing procedure on the degradation of poly(lactide-co-glycolide) 85:15 and 50:50 implants*. *Journal of Controlled Release*, 1997. **43**(2-3): p. 161-173.
261. Meng, B., Li, L., Hua, S., Wang, Q., Liu, C., Xu, X. and Yin, X., *Effect of medium-chain triglycerides on the release behavior of Endostar® encapsulated PLGA microspheres*. *International Journal of Pharmaceutics*, 2010. **397**(1-2): p. 136-143.
262. Mu, L. and Feng, S.S., *Fabrication, characterization and in vitro release of paclitaxel (Taxol®) loaded poly (lactic-co-glycolic acid) microspheres prepared by spray drying technique with lipid/cholesterol emulsifiers*. *Journal of Controlled Release*, 2001. **76**(3): p. 239-254.
263. Xie, S., Wang, S., Zhao, B., Han, C., Wang, M. and Zhou, W., *Effect of PLGA as a polymeric emulsifier on preparation of hydrophilic protein-loaded solid lipid nanoparticles*. *Colloids and Surfaces B: Biointerfaces*, 2008. **67**(2): p. 199-204.
264. Mauriac, P. and Marion, P., *Use of ethanol as plasticizer for preparing subcutaneous implants containing thermolabile active principles dispersed in a PLGA matrix*. United States Patent Application Publication, US 2006/0171987 A1, 2006: p. 1-5.
265. *ICH Topic Q3C (R4), Impurities: Guideline for Residual Solvents*, 2009, International Conference on Harmonisation of Technical Requirements for Registration of Pharmaceuticals for Human Use.

CURRICULUM VITAE

Martina Sprengholz

born on the 7th of July 1984 in Eggenfelden, Germany

- | | |
|-----------------------|---|
| since Dec 2012 | Project manager in the group 'Tableting management' at Aenova, Tittmoning |
| June 2009 - July 2014 | PhD thesis 'Industrial Ram Extrusion as Innovative Tool for the Development of Biodegradable Sustained Release Implants' at the Department of Pharmacy, Pharmaceutical Technology and Biopharmaceutics, Ludwig-Maximilians-University, Munich in cooperation with Acino, Miesbach

Supervisors: Prof. Dr. Gerhard Winter (LMU)
Dr. Heiko Spilgies, Dr. Sabine Hauck,
Dr. Nicoline Vermeulen (all Acino) |
| Mar 2009 | Master's degree |
| Sept 2008 - Feb 2009 | Master's thesis 'Accelerated <i>In Vitro</i> Goserelin Release from Biodegradable Parenteral Poly(D,L-lactic-co-glycolic acid) Implants' the Department of Pharmacy, Pharmaceutical Technology and Biopharmaceutics, Ludwig-Maximilians-University, Munich in cooperation with Acino, Miesbach

Supervisors: Prof. Dr. Gerhard Winter (LMU)
Dr. Heiko Spilgies, Dr. Thomas Beckert (both Acino) |
| Aug 2007 | Bachelor's degree |
| Mar 2007 - June 2007 | Bachelor's thesis 'Medikamente von tschechischen "Vietnamesenmärkten" - Originale oder Fälschungen?' at the Department of Pharmacy, Pharmaceutical Chemistry, Ludwig-Maximilians-University, Munich

Supervisor: Prof. Dr. Franz Bracher |
| Oct 2004 - Mar 2009 | Studies in Pharmaceutical Sciences at the Ludwig-Maximilians-University, Munich |
| June 2004 | 'Abitur', higher education entrance qualification |
| Sept 1995 - June 2004 | Secondary school 'Gymnasium Waldkraiburg', Waldkraiburg |
| Sept 1991 - July 1995 | Elementary school 'an der Graslitzer Straße', Waldkraiburg |